

Evaluating the Potential of Continuous Processes for Monoclonal Antibodies: Economic, Environmental and Operational Feasibility

A Thesis submitted to University College London for the degree of
Doctor of Engineering (EngD) in Biochemical Engineering and
Bioprocess Leadership

By

James Edward Pollock, MEng (Hons)

The Advanced Centre for Biochemical Engineering

Department of Biochemical Engineering

UCL

Torrington Place

London

WC1E 7JE

September 2013

I, *James Edward Pollock* confirm that the work presented in this thesis is my own. Where information has been derived from other sources, I confirm that this has been indicated in the thesis.

*To my loving wife, the thesis widow,
who kept her sense of humour when I had lost mine.*

Abstract

The next generation of monoclonal antibody (mAb) therapies are under increasing pressure from healthcare providers to offer cost effective treatments in the face of intensified competition from rival manufacturers and the looming loss of patent exclusivity for a number of blockbusters. To remain competitive in such a challenging environment companies are looking to reduce R&D and manufacturing costs by improving their manufacturing platform processes whilst maintaining flexibility and product quality. As a result companies are now exploring whether they should choose conventional batch technologies or invest in novel continuous technologies, which may lead to lower production costs. This thesis explores the creation of a dynamic tool as part of a decision-support framework that is capable of simulating and optimising continuous monoclonal antibody manufacturing strategies to assist decision-making in this challenging environment.

The decision-support framework is able to tackle the complex problem domain found in biopharmaceutical manufacturing, through holistic technology evaluations employing deterministic discrete-event simulation, Monte Carlo simulation and multi-attribute decision-making techniques. The hierarchical nature of the framework (including a unique sixth hierarchical layer; sub-batches) made it possible to simulate multiple continuous manufacturing scenarios on a number of levels of detail, ranging from high-level process performance metrics to low-level ancillary task estimates. The framework is therefore capable of capturing the impact of future titres, multiple scales of operation and key decisional drivers on manufacturing strategies linking multiple continuous unit operations (perfusion cell culture & semi-continuous chromatography).

The work in this thesis demonstrates that the framework is a powerful test bed for assessing the potential of novel continuous technologies and manufacturing strategies, via integrated techno-economic evaluations that take proof-of-concept experimental evaluations to complete life-cycle performance evaluations.

Acknowledgements

This thesis would not have been possible without the support and encourage of a few individuals. I would first like to express my gratitude to my supervisor Dr Suzanne Farid for her insightful advice and whose maddening attention to detail drove me to finally learn to punctuate prose.

I would also like to thank my industrial supervisor Dr Sa Ho (Pfizer R&D Global Biologics, MA, USA) for his consistently positive and supportive attitude.

I particularly want to thank my supervisors for giving me the opportunity to spend six months of my study at Pfizer in Boston, an experience I will never forget. I also wish to extend my thanks to Dr Glen Bolton for his expert advice and welcome to his team that made my stay in Boston so enjoyable.

Finical support from the Engineering and Physical Sciences Research Council (EPSRC) and Pfizer Inc., is gratefully acknowledged.

Contents

Abstract	4
Acknowledgements	5
Contents	6
List of Tables	11
List of figures	13
Abbreviations	21
1 Introduction	23
1.1 Biopharmaceutical Drug Development	24
1.1.1 Economics & Success of Development	27
1.1.2 Future Development Paradigms	29
1.2 Biopharmaceutical Manufacture	31
1.2.1 Capital Investment	33
1.2.2 Cost of Goods	36
1.2.3 Environmental Sustainability	38
1.3 Monoclonal Antibodies	40
1.3.1 Structure.....	40
1.3.2 Application of Monoclonal Antibodies	43
1.4 Manufacture of Monoclonal Antibodies	46
1.4.1 Current platform processes	46
1.4.2 Future platform processes	48
1.4.3 Continuous unit operations	52
1.4.3.1 Perfusion	53
1.4.3.1.2 Semi-continuous chromatography	56
1.5 Computational Decision Making Tools	59
1.5.1 Process Simulations Tools for the Biotech Industry	62
1.5.2 Risk Modelling	66
1.5.3 Multiple Criteria Decision Analysis	68
1.5.4 Modelling of Continuous Processes	70
1.6 Aims & Organisation of Thesis	71
2 Materials & Methods	74
2.1 Decision-Support Framework	75
2.1.1 Domain Description	75
2.1.2 Scope of Framework	77
2.1.3 Requirement Specification & Software Selection	79
2.1.4 Tool Implementation.....	83
2.1.4.1 Modelling Approach	83
2.1.4.2 Database Structure.....	87

2.1.4.3	Discrete-Event Simulation Tool	88
2.1.4.3.1	Model Structure	89
2.1.4.3.2	Unit Operation Model Structure	91
2.1.4.3.2.1	Sub-task Routing	94
2.1.4.3.2.2	Resource Allocation	97
2.1.4.3.3	Ancillary Model Operations	98
2.1.4.3.4	Process Models	99
2.1.4.3.4.1	Fermentation	101
2.1.4.3.4.1.1	Fed-batch Cell Culture	101
2.1.4.3.4.1.2	Perfusion Cell Culture	106
2.1.4.3.4.2	Centrifugation	110
2.1.4.3.4.3	Chromatography	111
2.1.4.3.4.3.1	Batch Chromatography	111
2.1.4.3.4.3.2	Continuous Chromatography	114
2.1.4.3.4.4	Viral Inactivation	116
2.1.4.3.4.5	Membrane Filtration	117
2.1.4.3.4.5.1	Depth Filtration	117
2.1.4.3.4.5.2	Viral Retention Filtration	118
2.1.4.3.4.5.3	Concentration and Diafiltration	118
2.1.4.3.5	Optimisation Protocols	120
2.1.4.3.6	Cost Models	123
2.1.4.3.6.1	Fixed Capital Investment	124
2.1.4.3.6.2	Cost Of Goods	126
2.1.4.3.7	Environmental models	127
2.1.4.3.8	Risk Modelling	128
2.1.5	Multi-Attribute Decision Making	130
2.1.6	Data Collection	132
2.2	Chromatography Experimental Protocols	132
2.2.1	Materials	132
2.2.1.1	Chemicals	132
2.2.1.2	Harvested Cell Culture Material	132
2.2.2	Chromatography	133
2.2.2.1	ÄKTA FPLC System	133
2.2.2.2	Periodic Counter Current Chromatography System	134
2.2.3	Analytical Techniques	135
2.2.3.1	NanoDrop Concentration Measurements	135
2.2.3.2	Protein A HPLC	136
2.2.3.3	CEX HPLC	137
2.2.3.4	SEC HPLC	138
2.2.3.5	Batch Uptake	139
2.2.3.6	Isotherms	139
2.2.3.7	Scanning Electron Microscope	140
2.3	Conclusions	141
3	Fed-batch & Perfusion Culture	143

3.1	Introduction	143
3.2	Methods	144
3.2.1	Fermentation	144
3.2.2	Multi-attribute Decision-Making	148
3.2.3	Case Study	149
3.2.4	Assumptions	150
3.2.4.1	Monte Carlo Assumptions	154
3.3	Results and Discussion	156
3.3.1	Deterministic Cost Comparison	156
3.3.1.1	COG/g Comparison Across Scales	156
3.3.1.2	Key Economic Metrics Across Scales and Titres	160
3.3.2	Stochastic Cost Comparison	164
3.3.2.1	Expected Scenario Outputs	164
3.3.3	Multi-attribute Decision Making	167
3.3.3.1	Environmental Impact Analysis	167
3.3.3.2	Qualitative Operational Benefits	168
3.3.3.3	Overall Aggregate Strategy Scores	169
3.4	Conclusions	171
4	Batch & Semi-Continuous Chromatography	172
4.1	Introduction	172
4.2	Methods	173
4.2.1	Three and Four Column Periodic Counter Current Chromatography	173
4.2.2	Switch Time and Optimisation Calculation	175
4.2.3	Wash Step Optimisation	179
4.2.4	Resin Reuse Study	179
4.2.5	Decisional Tool	180
4.2.6	Case Study & Assumptions	181
4.3	Results and Discussion	183
4.3.1	Verification of Optimisation Strategy for Semi-Continuous Chromatography	183
4.3.2	Wash Step Evaluation	187
4.3.3	Economic Impact of Semi-Continuous Chromatography	188
4.3.4	Impact of Resin Reuse	192
4.3.4.1	Resin Reuse Study	192
4.3.4.1.1	Resin Characterisation	196
4.3.4.2	Variable Binding Capacity Study	201
4.3.5	Retrofitting Costs	204
4.4	Conclusions	205
5	Integrated Continuous Processing	207
5.1	Introduction	207

5.2	Methods	208
5.2.1	Visualising an Integrated Continuous Process	208
5.2.2	Decisional Tool	211
5.2.3	Multi-Attribute Decision-Making	213
5.2.4	Case Study Assumptions	214
5.3	Results and Discussion	217
5.3.1	Impact of Development Phase on Cost Drivers	218
5.3.2	Impact of Company Size on Indirect Costs	221
5.3.3	Batch versus Continuous COG/g Comparison	221
5.3.4	Key Economic Metrics Across Company Size and Manufacturing Scale	224
5.3.5	Multi-Attribute Decision-Making	230
5.3.5.1	Environmental Impact Analysis	230
5.3.5.2	Operational Risk Analysis	232
5.3.5.3	Overall Aggregate Strategy Scores	233
5.4	Conclusion	236
6	Process Validation: Principles & Practices	237
6.1	A Paradigm Shift in Process Validation	237
6.2	Validation Concerns for Continuous Processes	241
7	Conclusions & Future Work	244
7.1	Overall Conclusions	244
7.2	Future Work	249
8	References	252
9	Appendices	261
9.1	Chapter 2 Appendix	261
9.1.1	Tables	261
9.1.2	Equations	266
9.1.2.1	Centrifugation	266
9.1.2.2	Depth Filtration	266
9.1.2.3	Viral Retention Filtration	266
9.1.2.4	Concentration and Diafiltration	266
9.1.2.5	Chromatography	267
9.1.2.6	Viral Inactivation	267
9.2	Chapter 3 Appendix	268
9.2.1	Tables	268
9.2.2	Figures	271
9.3	Chapter 4 Appendix	273
9.3.1	Tables	273
9.3.2	Figures	277

9.4 Chapter 5 Appendix	279
9.4.1 Tables	279
9.5 Papers by the Author.....	282

List of Tables

Table 1.1. Stages of Biopharmaceutical Development.....	26
Table 1.2. Probabilities of Success for Clinical Phase Transition.....	27
Table 1.3. Overview of Biopharmaceutical Manufacturing Operations.....	32
Table 1.4. Benchmarks for Antibody Manufacturing Facilities.....	34
Table 1.5. MAb suffix nomenclature based on source and target	42
Table 1.6. Monoclonal antibodies approved or in review in the EU or US....	43
Table 1.7. Current perfusion cell culture manufacturing strategies.....	54
Table 1.8. Current commercial use of semi-continuous chromatography	59
Table 1.9. Summary of functionality and capabilities of common biopharmaceutical simulation tools.....	66
Table 2.1. Requirements specification for the simulation tool	80
Table 2.2. Key outputs from the unit operation process models.....	100
Table 2.3. Biopharmaceutical facilities capital investment factors and corresponding “Lang” factors.....	125
Table 3.1. Cell integral and product concentration calculations for the fed- batch, spin-filter and ATF processes	147
Table 3.2. Attribute grouping and ranking Economic and environmental scores (low = best, high = worst), operational scores (3 = best, 9 = worst)	148
Table 3.3. Key assumptions for the fed-batch, spin-filter and ATF processes	153
Table 3.4. Monte Carlo assumptions	155
Table 3.5. E-Factor scores for water and consumable consumption.....	168
Table 4.1. Case Study Assumptions.....	182
Table 4.2. Protein Pool Product Quality.....	186
Table 4.3. Equilibrium Constants for the Resin Samples	199
Table 5.1. Mode of operation for key stages of the alternate strategies.....	211
Table 5.2. Attribute grouping and ranking for each company scale.....	214
Table 5.3. Key assumptions for alternate manufacturing strategies.....	216
Table 5.4. Number of drug candidates per company scale scenario.....	217
Table 5.5. Effect of company size on indirect cost per gram for the base case scenario at the PoC (4kg) manufacturing scale	221

Table 5.6. E factor scores for alternate manufacturing strategies	231
Table 5.7. Batch risk for alternate manufacturing strategies	233
Table 6.1. Validation stages and expected activities	239
Table A2.1. Block Types Employed Within the Simulation Framework	261
Table A2.2. Equipment size, cost and exponential scaling coefficients.....	263
Table A2.3. Consumables costs	264
Table A2.4. Raw material costs	265
Table A2.5. Consumable unit masses	265
Table A3.1. Uncompleted qualitative factor questionnaire	268
Table A3.2. Completed qualitative factor questionnaire – Respondent #1 .	269
Table A3.3. Completed qualitative factor questionnaire – Respondent #2 .	269
Table A3.4. Completed qualitative factor questionnaire – Respondent #3 .	270
Table A3.5. A comparison of the key economic metrics.....	270
Table A4.1. Scenario Equipment Scales.....	273
Table A4.2. Batch Uptake Experimental Data for the New Resin Sample .	274
Table A4.3. Batch Uptake Experimental Data for the Cycled Resin Sample	274
Table A4.4. Batch Uptake Experimental Data for the NaOH Cycled Resin Sample.....	275
Table A4.5. Isotherm Experimental Data for the New Resin Sample	275
Table A4.6. Isotherm Experimental Data for the Cycled Resin Sample	276
Table A4.7. Isotherm Experimental Data for the NaOH Cycled Resin Sample	276
Table A5.1. Scenario Equipment Scales.....	279

List of Figures

- Figure 1.1.** A comparison of the differences between (a) the traditional development paradigm and (b) quick win, fail fast paradigm. The alternative paradigm demonstrates the use of proof-of-concept (PoC) to reduce the number of expensive late-stage R&D failures. The savings are re-invested in drug discovery generating more drug candidates to feed into the PoC model, this referred to as the “R&D sweet spot”. FED, first efficacy dose; FHD, first human dose; PD, product decision. Adapted from Paul et al, 2010. 30
- Figure 1.2.** Typical cost trends seen as scale increases for a) total cost of goods per gram (COG/g); b) material, labour and indirect costs; c) upstream and downstream operating costs. Adapted from Farid 2009. 37
- Figure 1.3.** General Structure of IgG monoclonal antibody, highlighting the key structural properties including the antigen binding fragment (Fab), crystallisable fragment (Fc), light chain (L), heavy chain (H), constant regions (C) and variable regions (V)..... 41
- Figure 1.4.** Typical manufacturing processes for a) Cohn-based IgG platform and b) typical recombinant mAb platform. UFDF, ultrafiltration/diafiltration..... 48
- Figure 1.5.** Emerging two-column recombinant mAb manufacturing platforms. UFDF, ultrafiltration/diafiltration. 51
- Figure 1.6.** Key constraints and uncertainties in biopharmaceutical drug development. Sourced from Farid, 2012. 60
- Figure 2.1.** Overview of simulation tool structure highlighting key communication directionality and content with respect to key inputs and outputs. ODBC; open data base connectivity.....82
- Figure 2.2.** UML class diagram representing the main classes and associations in the framework. Each block represents a class (e.g. Suite), with attributes (e.g. SuiteID, Description etc.) and procedures (e.g. CalcUtilisation). Lines symbolise the associations and number the multiplicity between the classes. An unfilled triangle and a solid line represent a generalised relationship (e.g. Chromatography is a type of Unit Operation), with an unfilled diamond and a solid line as a aggregated relationship (e.g.one Process Sequence is made of Unit Operations) and a dashed line as an associated class (e.g. FilterSizeDF exists for a particular Unit Operation and Filter). 85

Figure 2.3. Core structure of the simulation engine. USP, upstream processing; DSP, downstream processing; UOp, unit operation.....	89
Figure 2.4. The structure of an Equipment block, where the solid line show the items path and the dotted line the lines of communication between blocks and resource managers. Blocks that can delay the items are marked with `D` .	93
Figure 2.5. Overview of the sub-tasks used in a bind and elute chromatographic unit operation demonstrating the Task Cycling routing methodology. Highlighted sub-tasks show vessel manager interactions.	95
Figure 2.6. Overview of the sub-tasks used in a continuous perfusion unit operation demonstrating the Sub-task Cycling routing methodology. Highlighted sub-tasks show vessel manager interactions, where <i>Inoculate</i> triggers the draining of the N-1 reactor and <i>Bag</i> triggers the filling of the harvest vessel.....	97
Figure 2.7. Fed-batch fermentation cell culture growth profiles of four fermentation runs a) tracking the viable cell density (x) and resultant product titre (+), and b) with fitted viable cell density (bold black line) and estimated product titres (bold dashed line), with key growth regions highlighted.	102
Figure 2.8. Continuous perfusion fermentation cell culture growth profile for viable cell density (black line), estimated product titre (dashed line) and perfusion rate (dotted line), with key growth regions highlighted. The growth profiles shown were derived from discussions with Morten Munk, Christoffer Bro and Jacob Jensen (CMC biologics, Copenhagen, Denmark) and based on valid fermentation data.....	107
Figure 2.9. Protein breakthrough curve for a column operated in bind & elute mode, highlighting A) the dynamic binding capacity used in manufacturing (90% of 1% breakthrough), B) the point of breakthrough (1% breakthrough), C) 10% breakthrough and D) resin saturation.	111
Figure 2.10. Schedule of the loading (grey) and non-loading (white) processes for the batch, 3-column periodic counter current chromatography system and the simulations interpretation of the periodic counter current chromatography system.	115
Figure 2.11. Schematic of 4-column PCC system (copyright GE Healthcare).	134
Figure 2.12. Calibration curve for the NanoDrop 2000 for the serial dilution of bulk drug substance.....	135

Figure 2.13. Calibration curve comparing Protein A HPLC peak area to known concentrations of BDS.....	136
Figure 2.14. Example chromatographic profile of a cation exchange HPLC run for a purified IgG1 sample, denoting the acidic, designated and basic species of the sample.....	137
Figure 2.15. Example chromatographic profile of SEC HPLC run for a purified IgG1 sample, denoting the HMW, Monomeric and basic LMW of the sample.	138
Figure 3.1. Perfusion fermentation cell culture growth profiles for a) spin-filter perfusion cell culture and b) alternating tangential flow perfusion cell culture, where viable cell density (black line), estimated product titre (dashed line) and perfusion rate (dotted line) are highlighted alongside the key growth regions.....	145
Figure 3.2. Case study process sequences and suite configuration for (a) the fed-batch (FB), (b) the spin-filter (SPIN) and (c) the alternating tangential flow (ATF) process. CC = cell culture, Cent = centrifugation, DepF = depth filtration, UF = ultrafiltration, ProA = Protein A chromatography, VI = virus inactivation, Pool = daily perfusate volume pooling, CEX = cation exchange chromatography, UFDF = ultrafiltration/diafiltration, AEX = anion exchange chromatography, VRF = virus retention filtration.....	151
Figure 3.3. A comparison of the cost of goods per gram on a category basis for labour costs (black), direct material costs (light grey), and indirect costs (dark grey) between the fed-batch process (FB), the spin-filter process (SPIN) and the alternating tangential flow process (ATF) over a range of scales of production for an equivalent fed-batch titre of 5 g/L, where the percentage difference is relative to the fed-batch process. The embedded table highlights the materials cost per gram for the production strategies. The optimal sizing strategy for each process is indicated in the boxes above each bar highlighting the number and scale of bioreactor(s) (solid box) and the column diameter for the Protein A chromatography step (dashed box) across a range of scales of production.....	157
Figure 3.4. A comparison of cost of goods per gram with a detailed breakdown of material costs on a category basis for (a) the fed-batch process, (b) the spin-filter process, (c) the alternating tangential flow process and (d) the concept fed-batch SUB process, for a 500 kg/yr scale of production and an equivalent fed-batch titre of 5 g/L. The COG/g values for each process are also indicated in \$/g.....	159

- Figure 3.5.** Contour plot showing the impact of scale of production and titre on the percentage difference in COG/g relative to the fed-batch process for (a) the spin-filter perfusion process and (b) the alternating tangential flow (ATF) perfusion process. The processes are resized for each combination of scales of production and titres. 161
- Figure 3.6.** Contour plot showing the impact of the ATF system's viable cell density at different scales of production and titres on the percentage difference in COG/g relative to the fed-batch process for (a) 20 million cells/mL, (b) 30 million cells/mL, (c) 40 million cells/mL, and (d) 50 million cells/mL. The fed-batch system was assumed to achieve a maximum viable cell density of 10 million cells/mL. The processes are resized for each combination of scale of production and titre. 163
- Figure 3.7.** Frequency distribution plots depicting the expected process outputs under manufacturing uncertainty for (a) the expected annual kilogram output, (b) the expected cost of goods per gram, and (c) the number of fed-batch culture failures, for a 500 kg/year scale of production and equivalent fed-batch titre of 5 g/L. 166
- Figure 3.8.** Sensitivity plots showing the effect of the economic attribute combination ratio (R_1) on the overall aggregate scores when (a) the operational attribute combination ratio is constant and (b) the environmental attribute combination ratio is constant. For the fed-batch (solid line), spin-filter (dashed line), and ATF (dotted line) processes, for 500 kg/year scale of production and equivalent titre of 5 g/L. 170
- Figure 4.1.** 4C-PCC process description (a) column 1 HCCF loading, (b) column 1 flush and column 2 loading, (c) column 2 loading and column 1 wash & elution, (d) column 2 flush, column 3 loading and column 1 strip, (e) column 3 loading, column 2 wash & elution and column 1 regeneration & equilibration..... 174
- Figure 4.2.** The effect of residence time on (a) the protein breakthrough (BT) profile from a 2.77 mg/ml load concentration with a residence time of 14.3 minutes (21 cm/hr) (Blue), 6.5 minutes (45 cm/hr) (Green), 5 minutes (60 cm/hr) (Red), 3 minutes (100 cm/hr) (Purple) and (b) the relationship between the amount of unbound protein in the flowthrough (FT) of the column being loaded to 100% BT (x) and the maximum protein challenge the FT column can capture (protein challenge at 1% BT) (+), resulting in either protein loss or retention. 176
- Figure 4.3.** Flow-sheet detailing a systematic design approach to optimise the performance of a 3-column or 4-column periodic counter-current chromatographic process, with example input and output variables for a completed verification run..... 178

- Figure 4.4.** Schedule of the loading (grey) and non-loading (white) processes for the batch, 3-column periodic counter current chromatography system and the simulations interpretation of the periodic counter current chromatography system. 181
- Figure 4.5.** UV profiles for the 3-column PCC verification runs (column 1; red, column 2; green & column 3; blue). (a) A 3-column PCC run loaded with 2g/L HCCF at 0.15 ml/min with a residence time of 6.5 minutes, including system ramp-down. (b) A detailed plot of a 3-column PCC run loaded with 0.9 mg/ml HCCF at 0.33 ml/min with a residence time of 3 minutes, detailing column 1 (red) in the FT position with column 3 in the loading position (blue), before switching to the loading position. Point A highlights when column 1 enters the FT position, capturing any unbound protein from column 3. The increase in UV signal at point B highlights the loss of unbound protein, before column 1 switches to the load position at point C. Column 1 loading ends at point D and the non-loading steps start..... 184
- Figure 4.6.** The impact of salt molarity of the high salt wash step on percentage loss of bound protein for a 100% breakthrough challenged column, for a minimally (3 cycles) cycled protein A resin. 188
- Figure 4.7.** A comparison of direct cost per gram highlighting the protein A cost (black) to the other direct costs (grey) between the standard batch process (STD) and the 3-column (3C-PCC) and 4-column periodic counter-current chromatographic (4C-PCC) process over a range of scales of production for the low titre scenario, where the percentage difference is relative to the standard batch process. The embedded table highlights the percentage contribution of the protein A resin towards the total direct costs. The optimal sizing strategy for each process is indicated in the boxes above each bar highlighting the number and scale of columns (solid box) and the number of system cycles (dashed box) across a range of scales of production. 190
- Figure 4.8.** The effect of cycle number on (a) binding capacity for standard batch process (40 mg/ml of protein load challenge per cycle)(black circles) and 100% break-through study (~110 mg/ml of protein load challenge per cycle)(crosses), (b) the percentage of the challenge load in the flow-through for the standard batch process. 193
- Figure 4.9.** Elution peak pH for 100% breakthrough cycle study versus cycle number..... 194
- Figure 4.10.** Breakthrough profiles on MabSelect resin in the 100% BT cycle study for resin used for 20 cycles (red), 40 cycles (green), 60 cycles (yellow), 80 cycles (light blue) and 100 cycles (purple). The increase in

A280 for the breakthrough at cycle 60 (yellow) was caused by an air bubble in the UV monitor.	195
Figure 4.11. Batch uptake curves of 2.6 mg/ml mAb by new (Solid line), cycled (dotted line) and NaOH cycled (dashed line) MabSelect resin samples during batch experiments. (Feed to resin volume ratio 45:1).	197
Figure 4.12. Adsorption isotherms for the new (solid line), cycled (dotted line) and NaOH cycled (dashed line) resin samples. The experimental data points were fitted with the Langmuir isotherm.	198
Figure 4.13. Scanning electron microscopy images of the new (1), NaOH cycled (2) and cycled (3) resin samples at (A) x250 and (B) x40,000.	200
Figure 4.14. The effect of batch number for the Commercial scale of manufacture utilising the 3C-PCC system for (a) dynamic binding capacity (solid line) and resulting harvest hold time (dashed line) with respect to the maximum allowable harvest hold time (dotted line). (b) The product pool volume (dashed line) and resulting bulk drug substance yield (solid line) when constrained by the maximum vessel volume (dotted line).	203
Figure 5.1. Downstream process scheduling for a) the base case process sequence, b) the continuous to batch process sequence and c) the continuous process sequence. Protein A chromatography; VI, viral inactivation; AEX, anion exchange chromatography; VRF, viral retention filtration; UFDF, ultrafiltration/diafiltration.....	210
Figure 5.2. Continuous flow between two unit operations in a discrete event environment. UOp, Unit Operation.	212
Figure 5.3. Direct cost of goods category breakdown across the different manufacturing scales required for each development phase for the base case scenario a) direct cost per product per phase and b) direct cost per gram. Categories: labour costs (grey dashed line), QCQA batch release costs (grey solid line), chromatographic resin costs (black solid line), fermentation media (black dotted line) and single use components and buffers (black dashed line).....	219
Figure 5.4. Direct (black dashed line) and indirect (black line) cost of goods per gram across the different manufacturing scales required for each development phase for the base case scenario.	220
Figure 5.5. A comparison of the direct costs per gram for the base case (B) and continuous (C) strategy on a category basis for material costs (black), labour costs (light grey), QCQA batch release costs (dark grey) and indirect costs (white), between the different manufacturing scales for	

the base case scenario. The embedded table highlights the percentage cost contribution for the key direct cost categories..... 223

Figure 5.6. Contour plots showing the impact of manufacturing scale and manufacturing strategies on the percentage difference in cost of goods per gram relative to the base case scenario for a) the large-sized company, b) the medium-sized company and c) the small-sized company. (Pre-Clinical, 1 x 0.5kg; PoC, 1 x 4kg; Phase III, 4 x 10kg; Commercial, 20 x 10kg)..... 225

Figure 5.7. Contour plots showing the impact of manufacturing scale and manufacturing strategies on a) the most economically attractive manufacturing strategies for each scenario and b) the resulting cost per launch for all company sizes relative to the base case manufacturing strategy. (Pre-Clinical, 1 x 0.5kg; PoC, 1 x 4kg; Phase III, 4 x 10kg; Commercial, 20 x 10kg)..... 227

Figure 5.8. A comparison of cost of goods per gram with a detailed breakdown of material costs on a category basis for a) the base case, b) FB-CB, c) ATF-CB, d) FB-CC, e) ATF-CC scenario for a Phase III clinical batch in a medium-sized company. 229

Figure 5.9. Sensitivity plots portraying the effect of the economic attribute combination ratio (R_1) in the overall aggregate scores when the environmental combination rate is constant, for a) the large-sized company, b) medium-sized company and c) small-sized company, for the base case (solid black line), FB-CB (grey dashed line), ATF-CB (grey dotted line), FB-CC (black dashed line) and ATF-CC (black dotted line). 235

Figure 6.1. Validation activities throughout a products lifecycle. Adpated from Scott 2011..... 241

Figure A3.1. Sensitivity plots showing the effect of the economic attribute combination ratio (R_1) on the overall aggregate scores when (a) the operational attribute combination ratio is constant and (b) the environmental attribute combination ratio is constant. For the fed-batch (solid line), spin-filter (dashed line), and ATF (dotted line) processes, for 100 kg/year scale of production and equivalent titre of 5 g/L. 271

Figure A3.2. Sensitivity plots showing the effect of the economic attribute combination ratio (R_1) on the overall aggregate scores when (a) the operational attribute combination ratio is constant and (b) the environmental attribute combination ratio is constant. For the fed-batch (solid line), spin-filter (dashed line), and ATF (dotted line) processes, for 1000 kg/year scale of production and equivalent titre of 5 g/L. 272

Figure A4.1. Langmuir regression plots for the new resin sample.....	277
Figure A4.2. Langmuir regression plots for the cycled resin sample	277
Figure A4.3. Langmuir regression plots for the NaOH cycled resin sample	278
Figure A5.1. Sensitivity plots portraying the effect of the economic attribute combination ratio (R1) in the overall aggregate scores when the environmental combination rate is constant, for a) the large-sized company, b) medium-sized company and c) small-sized company, for the base case (solid black line), FB-CB (grey dashed line), ATF-CB (grey dotted line), FB-CC (black dashed line) and ATF-CC (black dotted line).	281

Abbreviations

AEX	Anion-Exchange Chromatography
ATF	Alternating Tangential Flow perfusion cell culture
ATF-CB	ATF perfusion, Continuous capture and Batch polishing
ATF-CC	ATF perfusion, Continuous capture and Continuous polishing
B&E	Bind and Elute
BDS	Bulk Drug Substance
BLA	Biological Licensure application
CDR	Complementarity-Determining Regions
CEX	Cation-Exchange Chromatography
CFR	Code of Federal Regulations
cGMP	current Good Manufacturing Practices
CIP	Cleaning-in-Place
CMO	Contract Manufacturing Organisation
COG	Cost of Goods
COG/g	Cost of Goods per gram
CPP	Critical Process Parameters
CPV	Continuous Process Verification
CQA	Critical Quality Attributes
CV	Column Volumes
DC	Drug Candidate
DSP	Downstream Processing
EB	Environment Burden
EMA	European Medicines Agency
Fab	Antigen Binding Fragment
FB	Fed-Batch cell culture
FB-CB	Fed-Batch, Continuous capture and Batch polishing
FB-CC	Fed-Batch, Continuous capture and Continuous polishing
Fc	Crystallisable Fragment
FCI	Fixed Capital Investment
FDA	United States Food and Drug Administration
FT	Flow Through

FTE	Full Time Equivalent
HCCF	Harvested Cell Culture Fluid
HCP	Host Cell Proteins
HIC	Hydrophobic Interaction Chromatography
HMW	High Molecular Weight species
HPLC	High Performance Liquid Chromatography
ICH	International Conference on Harmonisation Technical Requirements for Registration of Pharmaceuticals for Human Use
IgG	Immunoglobulin G
IND	Investigational New Drug application
LMW	Low Molecular Weight species
mAb	Monoclonal Antibody
MADM	Multi-Attribute Decision-Making
MCDM	Multi-Criteria Decision-Making
MODM	Multi-Objective Decision-Making
ODBC	Open Data Base Connectivity
PCC	Periodic Counter Current chromatography
PoC	Proof-of-Concept
PoS	Probability-of-Success
PPQ	Process Performance Qualification
QbD	Quality by Design
QCQA	Quality Control and Quality Assurance
R&D	Research and Development
SEC	Size Exclusion Chromatography
SEM	Scanning Electron Microscopy
SIP	Sterilising-in-Place
SPIN	Spin-Filter perfusion cell culture
SQL	Structured Query Language
UFDF	Ultrafiltration/Diafiltration
UML	Unified Modelling Language
USP	Upstream Processing
VBA	Visual Basic for Applications
VRF	Virus Retention Filtration

1 Introduction

Over 20 therapeutic monoclonal antibodies (mAb) have been approved to date accounting for 35% of the therapeutic market (Aggarwal 2011; Wang et al. 2009), with the top-selling eight mAbs accounting for greater than \$18 billion in annual revenue in the US (Aggarwal 2011; Yamane-Ohnuki and Satoh 2009). In addition, there are approximately 300 antibodies in clinical development increasing at an annual rate of 18% since 2004 (PhRMA 2004; PhRMA 2006; PhRMA 2008; PhRMA 2011) and with expected clinical success rates of 11-17% a significant number will make it market (DiMasi et al. 2010; Kelley 2009; Paul et al. 2010; Reichart 2009; Strohl 2009). Furthermore, ten licensed recombinant antibodies will lose patent exclusivity over the next eight years. In this climate of increasing competition and lower reimbursement levels, improving research and development (R&D) productivity whilst reducing manufacturing costs is a major challenge for the biopharmaceutical industry (DiMasi et al. 2010; Farid 2009a; Morgan et al. 2011; O'Hagan and Farkas 2009; Paul et al. 2010).

In the effort to reduce R&D and manufacturing costs biopharmaceutical manufacturers are looking to improve their manufacturing platform processes whilst maintaining flexibility and product quality (DiMasi et al. 2010; Farid 2009a; Morgan et al. 2011; O'Hagan and Farkas 2009; Paul et al. 2010). However, the development and manufacture of biopharmaceutical drugs is a highly complex endeavour that is heavily regulated (DiMasi et al. 2010; Paul et al. 2010). This has stimulated controversial discussions within the industry on the best choice of mAb production technologies (Kelley 2009; Kelley 2007). Companies are now asking whether they should choose conventional batch technologies or invest in novel continuous technologies, which may lead to lower production costs. These questions demonstrate that there is a significant opportunity for a decisional framework capable of comparing the new continuous technologies to existing platform technologies and guiding decision makers towards effective technology evaluations. Consequently, the aim of this thesis is the development of a decisional tool that is capable of

simulating and optimising continuous mAb manufacturing processes in this challenging environment.

This introductory chapter provides an overview of this challenging environment, by exploring the published literature on drug development, manufacturing norms and alternatives, the use of computational frameworks and the techniques they employ. **Section 1.1** provides an overview of the economics, success rates and on-going paradigm shift in clinical trial strategy being experienced currently in biopharmaceutical drug development. **Section 1.2** explores biopharmaceutical manufacturing, providing an insight into the current technologies being employed and the resulting economic and environmental impacts of biopharmaceutical manufacturing processes. **Sections 1.3 & 1.4** focuses on mAbs as therapeutic drugs and reviews the current state of mAb manufacturing combined with an overview of future mAb manufacturing processes. There is an overview of computational simulation tools and the techniques they employ when simulating and evaluating biopharmaceutical manufacturing processes in **Section 1.5**. Finally, in **Section 1.6** the aims and organisation of the thesis are presented.

1.1 Biopharmaceutical Drug Development

Biopharmaceuticals are medical drugs produced by biotechnology processes. Examples include recombinant vaccines (attenuated or killed viral bodies, toxins or surface proteins), nucleic acids (DNA, RNA or antisense oligonucleotides) and recombinant proteins. Recombinant proteins are the leading category of biopharmaceuticals (Aggarwal 2011) and include hormones (e.g. Insulin for diabetes), growth factors (e.g. erythropoietin for anaemia), cytokines (e.g. Interferon beta-1a for multiple sclerosis), therapeutic enzymes (e.g. beta-glucoerebrosidase for Gaucher disease), blood factors (e.g. r.Factor VIII for haemophilia) and monoclonal antibodies (e.g. infliximab for Crohn's disease etc.). This thesis takes a particular interest in monoclonal antibodies (mAbs); the development of which follows the same path as other biopharmaceuticals, including several stages of

clinical testing before approval.

The development of a biopharmaceutical is a lengthy and expensive process that involves three distinct phases of development from drug discovery to clinical testing and eventual approval. Drug discovery can be broken down into four phases: target identification, target validation (Target-to-hit), lead identification (hit-to-lead) and lead optimisation (Bogdan and Villiger 2010; Paul et al. 2010). During target identification both the healthy and pathological states are compared to allow possible drug targets to be found. Once a target has been found its biochemical functions are assessed in a disease model; this is created from either cultured human cells or an animal model (usually mouse). After the identification of multiple promising targets and the successful creation of a disease model, the chosen targets are validated; the most promising targets are then selected for further development. These promising targets feed into the lead identification phase where large libraries of molecules are screened. The molecules that show specificity for the target and exhibit the desired changes are selected (leads). The leads are then optimised; this is where an attempt is made to improve the activity of the lead without compromising safety and bioavailability, which are tracked by in vivo and in vitro studies.

Once the optimal lead (drug candidate) is selected it then enters the clinical testing phase of development, which is designed to test the safety, biological activity and effectiveness of the drug candidate (DC). Pre-clinical testing is the last stage prior to human testing and therefore the principle aim of the study is to assess if the DC is safe to administer to humans. To start human clinical trials an investigational new drug application (IND) must be submitted to the FDA. The IND details all the experimental results from drug discovery; the chemical structure of the DC; how it is thought to work in the body; any toxicity findings from pre-clinical studies and how the DC is manufactured (PhRMA 2011). **Table 1.1** illustrates how the principle aim of Phase I clinical trials are to establish the safety of the DC in humans; this is achieved by studying the DCs safety profile and the safe dosage range. These studies also address the bioavailability of the DC by monitoring its

biochemical and physiological effects on the healthy test population. Phase II studies use a patient test population; these are divided into two streams of studies, with IIa studies designed to define dosage and IIb designed to prove effectiveness. The goal of Phase II trials is to show the proof-of-concept of the DC i.e. showing that it is effective in treating the target indication (Bogdan and Villiger 2010). If the DC is successful it progresses to Phase III clinical trials. Phase III trials encompass a large patient test population, the aim of which is to confirm effectiveness, establish the correct dosage and disclose any side effects seen. Following the completion of all three phases of clinical trials the company files a biological licence application (BLA). The FDA or EMEA reviews the data and decides if it will grant the company marketing approval, ask for further clinical trials or even refuse marketing approval. After approval a company is required to submit periodic reports focusing on continued product quality and any adverse side effects reported. In some cases a company may have to carry out further clinical studies (Phase IV) that evaluate the long-term effects of the DC.

Table 1.1. Stages of Biopharmaceutical Development

	Discovery & Pre-clinical	Clinical Trials		
		Phase I	Phase II	Phase III
Test Population	Laboratory and animal studies	20 to 100 healthy volunteers	100 to 500 patient volunteers	1000 to 5000 patient volunteers
Purpose	Assess safety and biological activity	Determine safety and dosage	Evaluate effectiveness and define dosage	Confirm effectiveness, dosage and monitor any adverse reactions

1.1.1 Economics & Success of Development

The average capitalised and risk-adjusted R&D cost to bring a new biopharmaceutical to market has recently been estimated to be between \$1.2-1.8 billion (DiMasi and Grabowski 2007; Paul et al. 2010). The substantial development cost can be attributed to the high attrition rate of new drug candidates from preclinical discovery to BLA submission and launch. Estimated success rates of 11-17% mean that 6-9 DCs must enter Phase I clinical trials to generate a single successful launch (DiMasi et al. 2010; Paul et al. 2010; Reichart 2009). This translates into an average cash outlay of approximately \$210 million (\$170 - \$250 million) per drug as it proceeds from preclinical development to launch (DiMasi and Grabowski 2007; Paul et al. 2010). **Table 1.2** highlights how the highest level of attrition occurs at the transition of the DC from Phase II to Phase III trials; this is when the DC must prove efficacy before being enrolled in expensive Phase III trials. The resulting successful DCs have to recover the cost of the failed DC projects, with the majority of which have incurred Phase I and Phase II clinical trial costs.

Table 1.2. Probabilities of Success for Clinical Phase Transition

	DiMasi et al, 2010	Paul et al, 2010	Reichert, 2009	Nelson et al, 2010	
Drug Candidate Categories	Biotech ¹	Biotech	Humanised mAbs ²	Humanised mAbs ³	Human mAbs ⁴
Phase I-II	64%	54%	80%	80%	89%
Phase II-III	39%	34%	46%	47%	51%
Phase III-BLA	66%	70%	80%	86%	75%
BLA-Launch	100%	91%	100%	100%	100%
Overall success	16%	12%	29%	32%	33%

¹ Phase success rates from 1999 to 2004

² Phase success rates from 1997 to 2008

³ Phase success rates from 1997 to 2008 (n = 133)

⁴ Phase success rates from 1997 to 2008 (n = 131)

Probabilities of success (PoS) play a key role in determining how companies allocate resources; for example resources are more likely to be directed towards development programs deemed to have a higher chance of success. **Table 1.2** highlights the PoS for general biopharmaceuticals alongside humanised and human mAbs. Both exhibit the same high attrition rates between Phase II and Phase III transitions, however, nearly half of all humanised and human mAbs (46-51%) will move onto Phase III studies compared to just over a third of general biopharmaceuticals (34-39%). A significant majority of humanised and human mAbs (80-89%) also demonstrate a superior Phase I to Phase II transition success compared to general biopharmaceuticals (54-64%). The higher PoS shown for humanised and human mAbs is due to their highly specific nature and reduced likelihood of generating an adverse immune response. This in turn leads to improved safety (Phase I success) and efficacy (Phase II success) profiles compared to other biopharmaceuticals.

The high success rates shown have made companies more likely to champion mAb drug candidates over other biopharmaceuticals. Today mAbs and Fc fusion proteins account for 35% of the therapeutic market (Strohl 2009) and this is likely to increase significantly, with approximately 300 candidates currently under development (PhRMA 2011). This trend demonstrates a common approach by companies to de-risk their candidate pipeline in an attempt to reduce development costs by having to recuperate fewer failed DCs. However, numerous studies have demonstrated that development costs have been trending upwards significantly over the last couple of decades (DiMasi et al. 2010; DiMasi et al. 2003; Morgan et al. 2011). The principle factors routinely identified as primary drivers of development costs are the risk and time involved in drug development. Real development times have remained relatively stable during the last two decades, but the 'time costs' associated with development are increasing above inflation as clinical trials become larger and more complex, demanding increased investment of resources (DiMasi et al. 2010; Paul et al. 2010).

1.1.2 Future Development Paradigms

Over a decade ago the increase in R&D costs was shown to be occurring at a significantly higher rate in comparison to the number of new approvals (DiMasi et al. 2003). The overall R&D productivity, as measured by IND & BLA applications per dollar invested, has declined 21% annually in the ensuing time period (O'Hagan and Farkas 2009). Biopharmaceutical companies are now struggling to make the same level of returns on invested capital previously seen for new DC development; due to a drop from 9% in 1995-2000 to only 4% in capital returns today (O'Hagan and Farkas 2009). In addition, ten licensed recombinant antibodies will lose patent exclusivity over the next eight years. This will affect the amount of capital these companies have at their disposal to invest. In this climate, improving research and development (R&D) productivity whilst reducing R&D costs is a major challenge facing the biopharmaceutical industry. This has led to some questioning the business model of larger biopharma, with many even predicting its imminent demise (O'Hagan and Farkas 2009; Paul et al. 2010).

Efforts are being made to improve R&D productivity by the biopharmaceutical companies, including experimenting with new R&D organisations, partnerships and technologies (O'Hagan and Farkas 2009). However, most companies are still employing the traditional R&D paradigm, using the scale-more tactic, hoping the number of "shots on goal" will translate into more successful launches (O'Hagan and Farkas 2009; Paul et al. 2010). An alternative paradigm gathering support employs the scale-more tactic, but attempts to reduce the incurred development costs caused by failed DCs.

Current R&D costs are dominated by clinical expenditure, which typically accounts for 70% of the \$210 million R&D cost per successful DC (Bogdan and Villiger 2010; DiMasi and Grabowski 2007; Paul et al. 2010). Therefore, approximately \$145 million can be attributed to clinical activities, with a further \$65 million spent on process development and manufacturing. The quick win, fail fast development paradigm targets a reduction in the clinical expenditure by reducing uncertainty from the expensive later development

stages (Phase II & III) through the establishment of proof-of-concept (PoC) (Cartwright et al. 2010; Paul et al. 2010). Where proof-of-concept is defined as “The earliest point in the drug development process at which the weight of evidence suggests that it is reasonably likely that the key attributes for success are present and the key causes of failure are absent” (Cartwright et al. 2010).

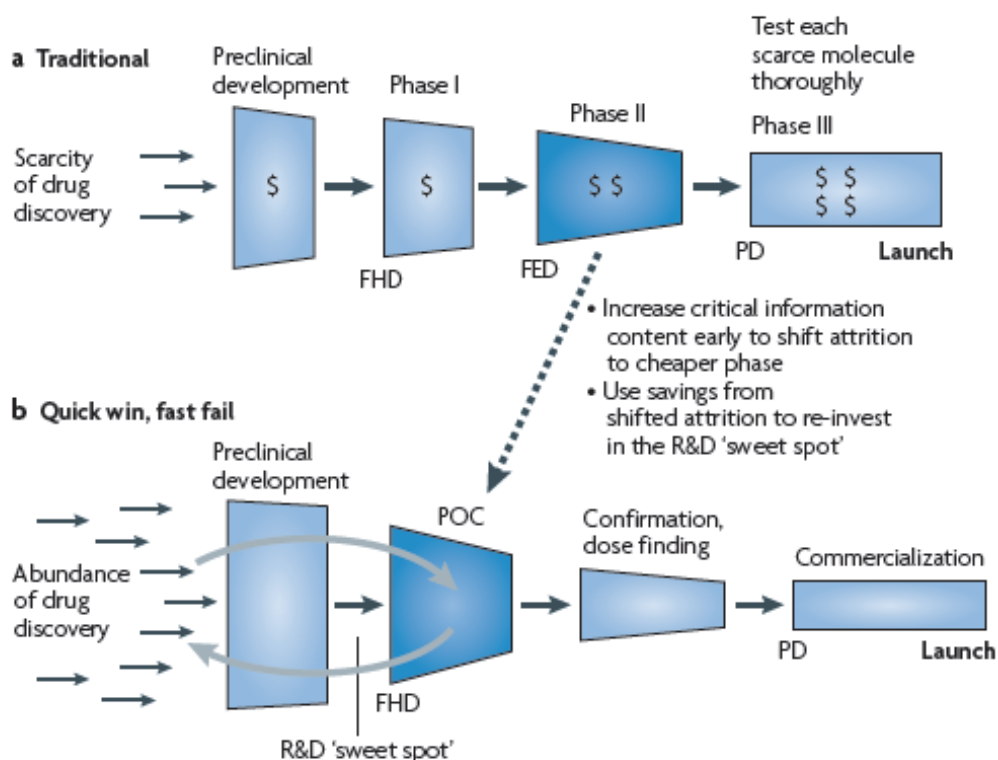


Figure 1.1. A comparison of the differences between (a) the traditional development paradigm and (b) quick win, fail fast paradigm. The alternative paradigm demonstrates the use of proof-of-concept (PoC) to reduce the number of expensive late-stage R&D failures. The savings are re-invested in drug discovery generating more drug candidates to feed into the PoC model, this referred to as the “R&D sweet spot”. FED, first efficacy dose; FHD, first human dose; PD, product decision. Adapted from Paul et al, 2010.

Figure 1.1 highlights the key difference between the traditional R&D paradigm (**Figure 1.a**) and the quick win, fail fast paradigm (**Figure 1.b**). In this alternative paradigm the early development stages (Phase I & IIa) are designed to include the ability to monitor the efficacy, safety and differentiation of the DC, allowing the termination of ineffective DCs as early as possible and therefore reducing the incurred development costs for the successful DCs (Cartwright et al. 2010; Paul et al. 2010). This approach reduces the number of DCs progressing to Phase II & III, but the ones that do progress have a much higher PoS and Launch. The reduction in resource investment into late-stage development (Phase III & IV) for just one product has been estimated to be sufficient to fund the early-development of almost 10 Phase 1 DCs (Paul et al. 2010). The paradigm's two pronged approach to increase R&D productivity, by killing-off DCs destined to fail early-on and invest the resulting saved resources into further lead development, is projected to offer a 28% reduction in the cost in bringing a new DC to market (Paul et al. 2010).

1.2 Biopharmaceutical Manufacture

Manufacturing processes for biopharmaceuticals can vary greatly, especially for non-antibody products. However, they do share a number of common features and processes, which are highlighted in **Table 1.3**. The manufacturing process usually involves a product synthesis step, where the protein is produced by fermentation. Mammalian cells are the dominant expression system used in recombinant protein production due to their ability to assemble, fold and apply the correct post-translational modifications (Marichal-Gallardo and Álvarez 2012). The fermentation step is followed by a series of processing operations designed to recover and purify the target protein, commonly referred to as downstream processing (DSP). The post-fermentation solution contains large number of impurities, including chemical reagents, host cell components (e.g. proteins, DNA) and various product related impurities (e.g. aggregates, product fragments). The principle aim of the DSP is to remove these impurities, however the diverse nature of these

impurities can lead to complex DSP configurations that dominate the overall manufacturing process.

Table 1.3. Overview of Biopharmaceutical Manufacturing Operations

Product Synthesis
Cell Culture <ul style="list-style-type: none">• Bacteria (e.g. <i>E. coli</i>), yeast or fungi cell culture for non-antibody proteins• Mammalian cell culture for production of antibodies
Product Purification
Isolation / Recovery <ul style="list-style-type: none">• Product in fermentation broth:<ul style="list-style-type: none">– Cell removal and volume reduction• Product inside cells:<ul style="list-style-type: none">– Soluble form: cell disruption, solids removal and volume reduction– Insoluble form (inclusion bodies): homogenization, differential centrifugation, wash and dissolution
Purification / Reaction <ul style="list-style-type: none">• Bulk & Intermediate Purification:<ul style="list-style-type: none">– Primarily for removal of process-related impurities, e.g. reagents, host cell proteins, DNA, endotoxins; some product-related impurities; common methods:<ul style="list-style-type: none">• Precipitation, adsorption, extraction• Chromatography (bind & elution, flowthrough)• Ultrafiltration/Diafiltration (UF/DF):<ul style="list-style-type: none">– Used as needed for product concentration (volume reduction) and buffer exchange (prepared for next step or for storage)• Reaction/product modification:<ul style="list-style-type: none">– Used at an appropriate point in purification train for conversion to bioactive forms (e.g. refold / oxidation, dimer formation, PEGylation)• Polishing:<ul style="list-style-type: none">– Final purification step (invariably using chromatography) to remove close product-related impurities and residual of host cell proteins (HCPs).• Final UF/DF & Sterile Filtration:<ul style="list-style-type: none">– Concentration & buffer exchange for long-term product storage or preparation for drug product formulation

Adapted from Ho et al. 2011.

Section 1.1.1 highlighted the inherent risks associated with biopharmaceutical development. This uncertainty leads to companies having to devise manufacturing schedules and strategies with insufficient information, such as the product dosage, cell line productivity and projected market demands (Farid 2009b). This can lead to companies having unused manufacturing capacity in their facilities or insufficient reservations with a contract manufacturer (CMO) to generate the required clinical material on time. These scenarios can lead to significant financial losses and have placed a growing emphasis on improving the cost-effectiveness of biopharmaceutical manufacturing. Manufacturing costs are often split into two classes with a distinction being made between the invested costs (capital investment) and the operating costs (cost of goods).

1.2.1 Capital Investment

Capital investment is often described as the capital required to construct, validate and licence a manufacturing facility. This includes the base building cost with all the process equipment costs, HVAC systems, process piping, instrumentation and utilities included; plus the indirect costs associated with design, engineering, validation and licensure. Investment costs for cGMP facilities are reported to range from \$25 to \$750 million (Farid 2007) (Pavlotsky 2004) with construction times of 4-5 years to build, validate and licence the resulting facility (Farid 2009b; Kamarck 2006). The most recent construction activity has been for multiproduct manufacturing facilities for the production of antibodies (Pfizer, Grange Castle, Ireland & MedImmune, Frederick, USA). **Table 1.4** highlights the estimated investment cost, facility size and bioreactor capacity for a number of these facilities. The table also allows a number of benchmark costs to be calculated, with investment costs shown relative to facility size of \$660 to \$1780 per square foot and to bioreactor capacity of \$1,765 to \$12,000 per litre (in the range of 20,000 to 200,000L) dependant on the facility design and level of plant automation (Farid 2007).

Table 1.4. Benchmarks for Antibody Manufacturing Facilities

Manufacturing Facility	Date Facility Completed	Capital Investment (\$ million)	Area (sq ft)	Bioreactor Capacity		
				Number	Size (L)	Total (L)
Genentech, Vacaville, CA	2000	250	310000	8	12000	96000
Imclone, Branchburg, BB36, NJ	2001	53	80000	3	10000	30000
Biogen, LSM, RTP, NC	2001	175	245000	6	15000	90000
Boehringer Ingelheim, Bireach, Germany	2003	315	-	6	15000	90000
Lonza Biologics, Portsmouth, NH	2004	207	270000	3	20000	60000
Amgen, BioNext, West Greenwich, RI	2005	500	500000	9	20000	180000
Genentech Expansion, Oceanside, CA	2005	380	470000	6	15000	90000
Imclone Expansion, Branchburg, BB36, NJ	2005	260	250000	9	11000	99000
Biogen Idec, Hillerod, Denmark	2007	350	366000	6	15000	90000
Lonza Biologics, Tuas, Singapore	2009	250	-	4	20000	80000
Genentech, Vacaville, CA	2009	600	380000	8	25000	200000
Bristol-Myers Squibb – Devens, MA	2011	750	-	6	20000	120000
Pfizer Biotech Campus, Grange Castle, Ireland	2011	1800 ¹	-	6	12500	75000
MedImmune, Frederick, MD	2011	600	337000 ²	4	12500	50000

Adapted from Farid, 2007.

¹ Investment cost includes finish and fill and other auxiliary facilities.

² Extra 100,000 sqft of production capability available.

Cost benchmarks are commonly employed to estimate the investment required for future cGMP manufacturing facilities. For example, Pavoltsky (2004) utilises facility size benchmarks to derive the projected investment cost. Werner (2004) relates the investment cost to the required output of facility, deriving his cost estimates from benchmarked bioreactor capacity costs (Werner 2004). Although benchmark investment costs are useful, Farid (2007) highlights a number of limitations of datasets used to derive benchmark investment costs. For example, facility costs and areas are often quoted without clarification of whether they account for warehouses and support facilities or without specification of the exact set-up of the processing equipment in the facility (for example the number of purification trains or level of automation). Better-cost estimates can be derived using factorial estimates but these require more detailed knowledge of factors, such as the type and number of key process equipment. Factorial estimates use a cost factor derived from previous construction projects, relating the capital outlay used in facility construction to the cost of equipment in the facility. The factorial method is often attributed to Lang (1948) and has been used to estimate capital investment in chemical facilities, water treatment plants and biopharmaceutical facilities (Lang 1948). Chemical facilities often use values in the range of 3-5 (Peters et al. 2006; Sinnott et al. 2005), with biopharmaceutical facilities using much larger values, ranging from 3.3-8.1 for stainless steel based facilities and values up to 23.7 for single-use based facilities (Farid 2007; Novais et al. 2001; Pollock et al. 2013b). The high Lang Factors used in biopharmaceutical facilities are due to the requirement to maintain higher cGMP suite contaminant level ratings, which result in increased HPAC/HVAC and SIP costs.

1.2.2 Cost of Goods

Operating costs are often described as any cost associated with the production of the product (goods) and hence referred to as 'Cost of Goods'. The Cost of Goods (COG) typically comprise of direct costs related to production, such as raw materials and utilities, and indirect costs which account for the depreciation and maintenance of the manufacturing facility. Labour costs are often reported as direct (hourly rate related to manufacturing activities) or indirect costs (FTE annual labour cost) depending on the reporting methods preferred. The exact impact of each cost parameter on the overall COG varies with both the scale of operation and cell culture titre. The relationships between each cost factor are succinctly summarised by Farid (Farid 2009b). **Figure 1.2** highlights how the overall COG per gram (COG/g) declines with increased annual production capacity (**Figure 1.2.a**), while the ratio of indirect and direct costs shifts so that the material costs dominate the COG/g and the labour and indirect costs fall and therefore represent a reduced fraction of the COG/g (**Figure 1.2.b**). The relationships presented highlight how at small-scales of production indirect costs tend to dominate and thus any change in material costs will have minimal impact. In contrast, any reduction in material cost at larger scales will significantly impact COG/g, particularly the DSP raw materials (**Figure 1.2.c**). **Figure 1.2.c** presents a phenomenon often reported as the 'downstream bottleneck' (Langer 2012), where the increase in cell culture titre increases the mass of product requiring purification. The increase in material requiring purification in turn increases the DSP costs, due to the principal purification technology, 'chromatography' being linearly scalable. Therefore, larger columns are employed to process the extra product impacting raw material costs (**Figure 1.2.b**), in place of extra column cycles due to time constraints. The trends highlighted in **Figure 1.2** are expected to become even more pronounced if the increase in annual output is accompanied by an increase in titre (Farid 2009b).

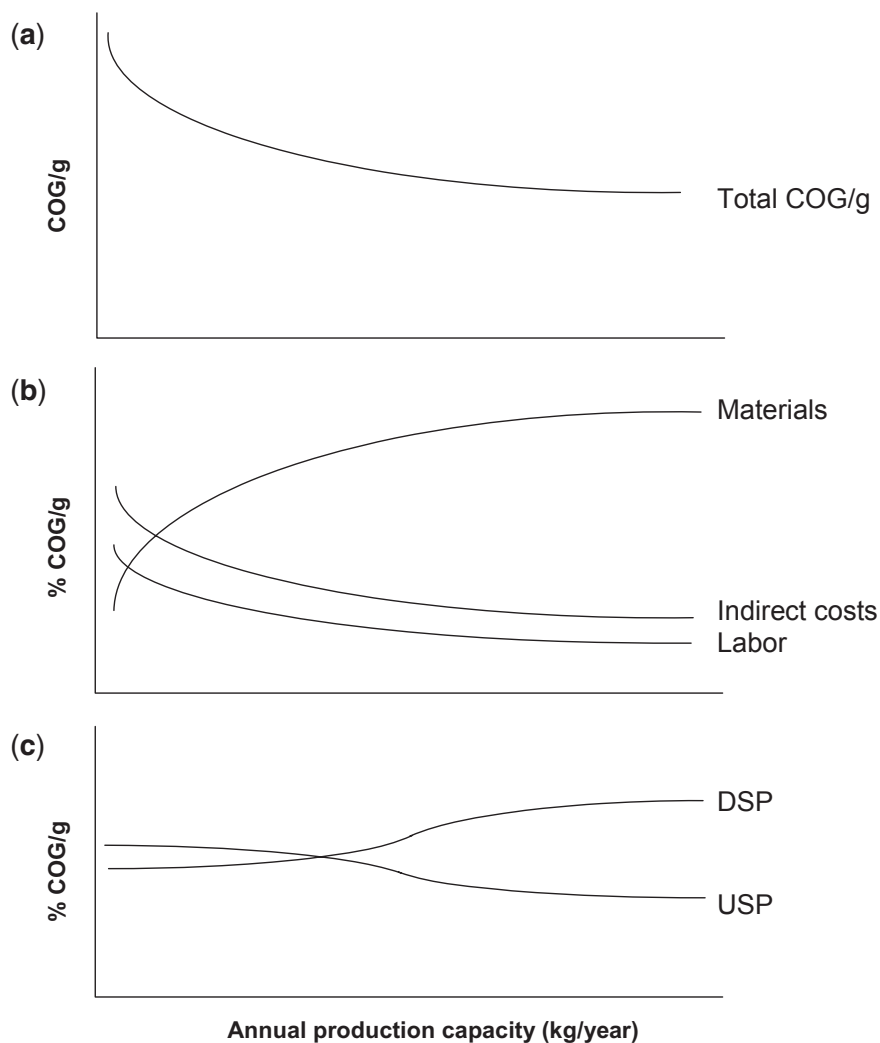


Figure 1.2. Typical cost trends seen as scale increases for a) total cost of goods per gram (COG/g); b) material, labour and indirect costs; c) upstream and downstream operating costs. Adapted from Farid 2009.

Manufacturing COG are reported to represent 15-25% of sales (Farid 2009b), with the recovery of development costs and sales related costs dominating sales price. This trend has made biopharmaceutical companies reluctant to publicise representative COG values. A literature review of COG is further complicated by the fact that annual production rate, titre or fermentation capacities are not always available (Farid 2007; Kelley 2009).

Historic published estimates of COG per gram for antibodies range from \$1000s per gram to \$100s per gram, with more recent estimates from conference proceedings and publications suggesting \$50 - \$100 per gram for current processes with titres ≥ 2 gram per litre (Farid 2007; Kelley 2009).

1.2.3 Environmental Sustainability

Biopharmaceutical manufacturing has a unique environmental footprint compared to other manufacturing sectors, these environmental characteristics are summarised below (Ho et al. 2011).

- The manufacturing processes use very large amounts of water;
- Significantly more water is used in the supporting operations, such as CIP, SIP and facility maintenance;
- The majority of process buffers contain large amounts of common salts such as NaCl which end up as aqueous waste;
- The majority of waste is aqueous and innocuous in nature (very low solvent use);
- Solid wastes in the form of consumables (resins, membranes, filters, single-use bags and tubing/connectors) are on the increase due to rise in single-use technology use.

The major characteristic of biopharmaceutical manufacture is the vast amounts of water used during manufacturing. The fermentation step is responsible for a large amount of this water use. Productive fermentation operations can now achieve protein concentrations of 5-10 g/L, which is only equal to 0.5-1 wt% of the solution (Ho et al. 2011). The fermentation steps therefore consume between 20-25% of the total water used, however, the chromatographic operations are the principle water using steps often surpassing 50% of the total (Ho et al. 2011).

The amount of water and consumables used in the manufacture of a product can be used to establish the environmental burden of a given manufacturing strategy. A widely utilised concept called the E factor was originally developed by Sheldon for the chemical industry to assess the overall environmental impact or greenness of production (Sheldon 1994; Sheldon 1997; Sheldon 2007). The E factor is defined as the total amount of reagents, water and consumables used per kilogram of product produced. The E factor could serve as a very useful environmental index for the production of biopharmaceuticals simply because every manufacturing step uses aqueous solutions and is processed via a range of consumable components (resin, filters, single-use bags and tubing). The E factor can also be used to monitor the water usage for the non-process operations. Typical antibody manufacturing strategies consume water (process and non-process) from 3000 to over 9000 kg water per kilogram of antibody produced and 1 to 16 kg of consumables per kilogram of antibody produced (Ho et al. 2011; Pollock et al. 2013b).

The E factor does have its limitations, namely its inability to highlight the environmental impact of toxic substances. This is not a particular concern for biopharmaceutical manufacture due to the innocuous nature of the aqueous waste streams generated, which are readily discharged as municipal waste (after minor treatment). The solid waste streams from consumable use are typically autoclaved prior to landfill or incineration. In contrast the chemical industry generates more exotic and environmental unsustainable waste streams including large volumes of organic solvents. Irabien et al propose a new index called the Environmental Burden (EB), which addresses pollutant release via air (emissions), water (effluents) and soil (wastes) (Irabien et al. 2009). Each substance monitored is weighted by a “potency factor” that captures the environmental impact of the substance release rather than just the quantity discharged.

1.3 Monoclonal Antibodies

Therapeutic monoclonal antibodies (mAb) are the best-selling biologics accounting for 5 of the top 10 selling drugs in 2012 and 51.8% of total biologic sales (Aggarwal 2011; Merie 2013; Reichart 2013). The top-selling five mAbs account for greater than \$37 billion in annual revenue (Merie 2013). In addition, there are currently approximately 300 antibodies in clinical development (PhRMA 2011). The number of licensed antibodies is growing at a rate of about 11% per annum (Kelley 2009) and the number of clinical antibody candidates has been growing at a rate of 18% since 2004 (PhRMA 2004; PhRMA 2006; PhRMA 2008; PhRMA 2011). Monoclonal antibodies have been the principle drivers of the recent biopharmaceutical sales and are likely to remain so for the foreseeable future with the mAb market expected to increase to \$70 billion in sales by 2015 (Aggarwal 2011; Marichal-Gallardo and Álvarez 2012).

1.3.1 Structure

MAbs are a general class of compounds with a molecular weight around 150 kDa and a defined structure. **Figure 1.3** shows the structure of immunoglobulin G (IgG) a common class of therapeutic mAbs, which also includes IgA, IgD, IgE, and IgM types. Each IgG molecule comprises of a disulphide-bonded pair of heavy chains, each linked to a disulphide-bonded light chain. Each heavy and light chain has two domains, the `constant` domain and `variable` domain. The variable domains are the primary difference between mAbs and contain the complementarity-determining regions (CDR) that are responsible for binding impurities, toxins or antigens with high specificity. The Fc region consists of two heavy chains and may have sugar groups (glycans) attached to the heavy chain by a process called glycosylation, which increases the products heterogeneity and can mediate the appropriate immune response.

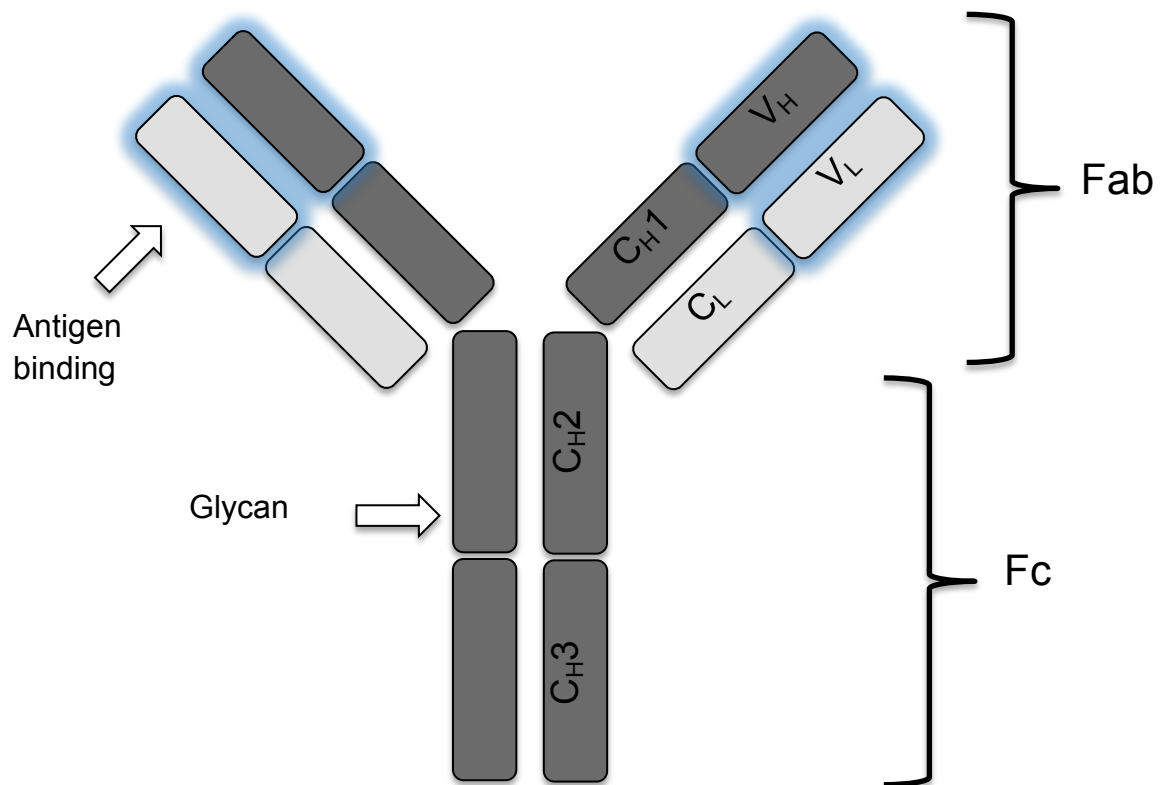


Figure 1.3. General Structure of IgG monoclonal antibody, highlighting the key structural properties including the antigen binding fragment (Fab), crystallisable fragment (Fc), light chain (L), heavy chain (H), constant regions (C) and variable regions (V).

MABs were first produced from mouse genes and referred to a murine mAbs (denoted with the suffix “-momab”), which were not particularly effective in clinical trials (Marichal-Gallardo and Álvarez 2012). Further genetic engineering resulted in chimeric (“-ximab”) and humanised (“-zumab”) mAbs, with Rituxan® (Rituximab) the first chimeric mAb to market in 1997 and Zenapax® (Dacalizumab) the first humanised mAb in 1997. Fully human mAbs (“-umab”) are now the focus due to their ability of generating negligible secondary effects to the patient (Marichal-Gallardo and Álvarez 2012). In 2002, Humira® (Adalimumab) was launched as the first fully human

mAb and is currently the top-selling biopharmaceutical with sales of \$9.534 billion USD in 2012 (Merie 2013). **Table 1.5** provides a detailed breakdown of mAb nomenclature, demonstrating how the generic mAb name is used to describe its structure and target. For example adalimumab is a human mAb (-umab) targeting an immune response (-lim-) and this is reflected in its primary target indications being autoimmune disorders (e.g. rheumatoid arthritis, Crohn’s disease and chronic plaque psoriasis).

Table 1.5. MAb suffix nomenclature based on source and target

Target			
<i>Non-tumour target</i>	Viral	-vir-	
	Bacterial	-bac-	
	Immune	-lim-	
	Infectious lesions	-les-	
	Antifungal	-fung-	
	Cardiovascular	-ci(r)-	
	Neurologic	-ne(r)-	
	Interleukins	-kin-	
	Musculoskeletal	-mul-	
	Bone	-os-	
	Toxin target	-toxa-	
	<i>Tumour target</i>	Colon	-col-
		Melanoma	-mel-
		Mammary	-mar-
Testis		-got-	
Ovary		-gov-	
Prostate		-pr(o)-	
Miscellaneous		-tu(m)-	
Source			
	Human	-umab	
	Murine	-omab	
	Rat	-amab	
	Hamster	-emab	
	Primate	-imab	
	Chimeric	-ximab	
	Humanised	-zumab	
	Rat/murine hybrid	-axomab	
	Chimeric + humanised	-zixumab	

1.3.2 Application of Monoclonal Antibodies

There are currently 35 mAbs approved for EU or US markets, with a third having achieved blockbuster status (over \$1 billion USD in sales). **Table 1.6** lists all the approved therapeutic mAbs to date. Of the 35 approved mAbs 15 (43%) target cancer indications, 11 (31%) inflammatory/autoimmune diseases, 3 (9%) transplant rejection, 2 (6%) infectious diseases and 4 (11%) target other indications. Approximately a third of the marketed mAbs (11) are human derived, 14 (40%) are humanised, 6 (17%) are chimeric and 4 (11%) are murine derived.

Table 1.6. Monoclonal antibodies approved or in review in the EU or US

International non-proprietary name	Trade name	Type	Indication first approved	Approval year EU (US)
Muromonab-CD3	Orthoclone Okt3	Anti-CD3; Murine IgG2a	Reversal of kidney transplant rejection	1986 (1986) ¹
Abciximab	Reopro	Anti-GPIIb/IIIa; Chimeric IgG1 Fab	Prevention of blood clots in angioplasty	1995 (1994)
Rituximab	MabThera, Rituxan	Anti-CD20; Chimeric IgG1	Non-Hodgkin's lymphoma	1998 (1997)
Basiliximab	Simulect	Anti-IL2R; Chimeric IgG1	Prevention of kidney transplant rejection	1998 (1998)
Daclizumab	Zenapax	Anti-IL2R; Humanized IgG1	Prevention of kidney transplant rejection	1999 (1997) ¹
Palivizumab	Synagis	Anti-RSV; Humanized IgG1	Prevention of respiratory syncytial virus infection	1999 (1998)
Infliximab	Remicade	Anti-TNF; Chimeric IgG1	Crohn disease	1999 (1998)
Trastuzumab	Herceptin	Anti-HER2; Humanized IgG1	Breast cancer	2000 (1998)
Gemtuzumab ozogamicin	Mylotarg	Anti-CD33; Humanized IgG4	Acute myeloid leukemia	N/A (2000) ¹

International non-proprietary name	Trade name	Type	Indication first approved	Approval year EU (US)
Alemtuzumab	MabCampath, Campath-1H	Anti-CD52; Humanized IgG1	Chronic myeloid leukemia	2001 (2001)
Adalimumab	Humira	Anti-TNF; Human IgG1	Rheumatoid arthritis	2003 (2002)
Tositumomab-1131	Bexxar	Anti-CD20; Murine IgG2a	Non-Hodgkin lymphoma	NA (2003)
Efalizumab	Raptiva	Anti-CD11a; Humanized IgG1	Psoriasis	2004 (2003) ¹
Cetuximab	Erbitux	Anti-EGFR; Chimeric IgG1	Colorectal cancer	2004 (2004)
Ibritumomab tiuxetan	Zevalin	Anti-CD20; Murine IgG1	Non-Hodgkin's lymphoma	2004 (2002)
Omalizumab	Xolair	Anti-IgE; Humanized IgG1	Asthma	2005 (2003)
Bevacizumab	Avastin	Anti-VEGF; Humanized IgG1	Colorectal cancer	2005 (2004)
Natalizumab	Tysabri	Anti- α 4 integrin; Humanized IgG4	Multiple sclerosis	2006 (2004)
Ranibizumab	Lucentis	Anti-VEGF; Humanized IgG1 Fab	Macular degeneration	2007 (2006)
Panitumumab	Vectibix	Anti-EGFR; Human IgG2	Colorectal cancer	2007 (2006)
Eculizumab	Soliris	Anti-C5; Humanized IgG2/4	Paroxysmal nocturnal hemoglobinuria	2007 (2007)
Certolizumab pegol	Cimzia	Anti-TNF; Humanized Fab, pegylated	Crohn disease	2009 (2008)
Golimumab	Simponi	Anti-TNF; Human IgG1	Rheumatoid and psoriatic arthritis, ankylosing spondylitis	2009 (2009)
Canakinumab	Ilaris	Anti-IL1 β ; Human IgG1	Muckle-Wells syndrome	2009 (2009)
Catumaxomab	Removab	Anti-EPCAM/CD3; Rat/mouse bispecific mAb	Malignant ascites	2009 (NA)
Ustekinumab	Stelara	Anti-IL12/23; Human IgG1	Psoriasis	2009 (2009)

International non-proprietary name	Trade name	Type	Indication first approved	Approval year EU (US)
Tocilizumab	RoActemra, Actemra	Anti-IL6R; Humanized IgG1	Rheumatoid arthritis	2009 (2010)
Ofatumumab	Arzerra	Anti-CD20; Human IgG1	Chronic lymphocytic leukemia	2010 (2009)
Denosumab	Prolia	Anti-RANK-L; Human IgG2	Bone Loss	2010 (2010)
Belimumab	Benlysta	Anti-BLyS; Human IgG1	Systemic lupus erythematosus	2011 (2011)
Ipilimumab	Yervoy	Anti-CTLA-4; Human IgG1	Metastatic melanoma	2011 (2011)
Brentuximab vedotin	Adcetris	Anti-CD30; Chimeric IgG1; immunoconjugate	Hodgkin lymphoma	2012 (2011)
Pertuzumab	Perjeta	Anti-HER2; humanized IgG1	Breast Cancer	2013 (2012)
Raxibacumab	(Pending)	Anti-B. anthraxis PA; Human IgG1	Anthrax infection	NA (2012)
Trastuzumab emtansine	Kadcyla	Anti-HER2; humanized IgG1; immunoconjugate	Breast cancer	In review (2013)
Vedolizumab	(Pending)	Anti-alpha4beta7 integrin; humanized IgG1	Ulcerative colitis, Crohn disease	In review (NA)

Source: The Antibody Society.

¹ Voluntarily withdrawn from the market

Sales per gram of mAb range from \$1000 per gram to \$50,000 per gram depending on dosage (Kelley 2009; Marichal-Gallardo and Álvarez 2012). Anti-TNF and other anti-inflammatory antibodies generated sales of \$45.6 billion USD in 2012, over a third of the biologics market total sales (Merie 2013). Cancer antibodies sales in 2012 were \$23.7 billion USD accounting for approximately 20% of the biologics market (Merie 2013). The only other product class to generate a market share in double digits was insulin and insulin analogs with \$18.9 billion USD (15%) in sales (Merie 2013).

1.4 Manufacture of Monoclonal Antibodies

Early IgG products were sourced from human plasma and purified by multiple fractionation steps based on the Cohn process (Cohn et al. 1946). The Cohn process was initially developed for the production of albumin during World War II to aid the recovery of soldiers suffering from blood loss. The Cohn process is not dissimilar to crude oil fractionation, where crude oil is refined into various products. Human plasma is fractionated by taking advantage of the differential solubility of the plasma proteins and utilises ethanol to precipitate the proteins based on their isoelectric points (Cohn et al. 1946). The Cohn process produces five fractions with the final fraction being enriched in albumin. However the other fractions were found to contain more than 20 valuable proteins including coagulation factors, protease inhibitors and IgGs (Burnouf 2007). **Figure 1.4.a** shows a traditional IgG purification process based on Cohn fractional precipitation; where fractions II and III are collected for further purification via a number of chromatographic steps to yield clinical grade IgG. The first human plasma sourced IgG was launched on the US market in the early 1980s to treat patients with idiopathic thrombocytopenic purpura, an autoimmune disease causing platelet deficiency (Pyne et al. 2002).

1.4.1 Current platform processes

Current recombinant mAb purification processes have borrowed very little from plasma fractionation processes, apart from the virus inactivation steps and ultrafiltration/diafiltration operation. The first cGMP processes for mAb purification were based on 1980s and early 1990s technologies (Kelley et al. 2009). These early processes were highly diverse, employing multiple technologies and a variable number of chromatographic steps. In addition, early chromatographic operations provided low binding capacities and were often operated in the cold (Kelley et al. 2009). The diversity found in early mAb manufacturing processes can be attributed to the lack of substantial process knowledge at the time and the historical progression from murine to fully humanised mAbs. The high degree of equivalence found among

humanised mAbs CDRs and constant domains have made it possible to develop platform-manufacturing processes capable of processing many different mAbs with only minor changes to the operating conditions (Shukla et al. 2007).

Figure 1.4.b presents a typical recombinant mAb platform process. The target mAb is expressed recombinantly in mammalian cells due to their ability to assemble, fold and apply the correct post-translational modifications (Marichal-Gallardo and Álvarez 2012). In the past, cell culture mAb titres reached only mg/L values, but now the norm is 2–3g/L with processes in development with reported titres of 5 g/L and higher (Bisschops et al. 2009b; Kelley 2009). The harvested cell culture bulk is processed by centrifugation, followed by depth filtration to remove the mammalian cells. The resulting harvested cell culture fluid (HCCF) is then clarified by Protein A chromatography, the first DSP step. Protein A chromatography offers direct, high-capacity mAb capture from the HCCF and achieves excellent purity (>95%), recovery, plus several logs of DNA & HCP clearance and a partial reduction in product aggregates (Gagnon 2012). The low-pH elution also acts as a virus inactivation step by denaturing enveloped viruses. Two further chromatographic polishing steps are used to reduce host cell proteins (HCP), DNA, process related impurities (leached Protein A) and product aggregates. Anion-exchange (AEX) chromatography is regularly used as a polishing step due to its ability to offer several logs of clearance for DNA, viruses, endotoxin, leached Protein A, and acidic HCP (Gagnon 2012). The second polishing step often employs cation-exchange (CEX) chromatography to remove any remaining HCP and remove product aggregates. CEX is occasionally replaced with hydrophobic interaction chromatography (HIC) but its use is restricted due to the high salt conditions required to elute the mAb (Gagnon 2012). The product stream is then processed by virus retention filtration (VRF), the second dedicated virus reduction step, which utilises nanofiltration techniques to remove viruses by size exclusion. Ultrafiltration/diafiltration (UF/DF) is the final step in drug substance manufacture and is used to concentrate and formulate the mAb. The efficacy and robustness of the current mAb platform process, shown in **Figure 1.4.b**,

has made process yields of 60-80% routine (Marichal-Gallardo and Álvarez 2012).

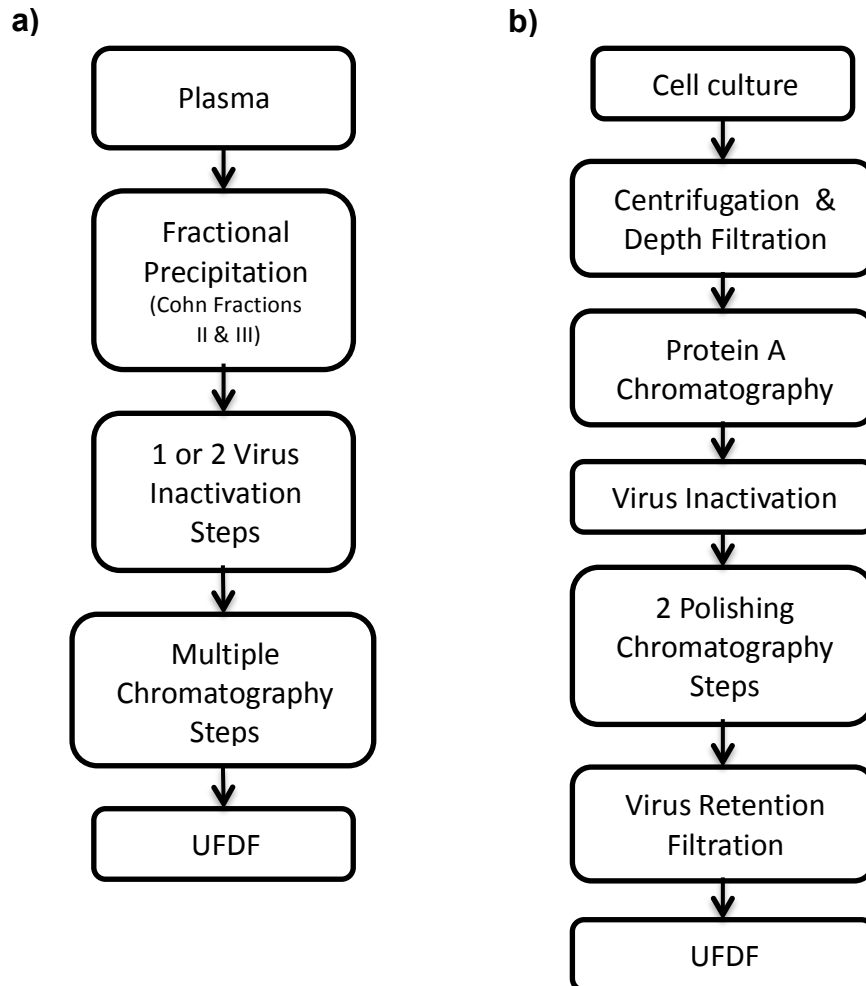


Figure 1.4. Typical manufacturing processes for a) Cohn-based IgG platform and b) typical recombinant mAb platform. UFDF, ultrafiltration/diafiltration.

1.4.2 Future platform processes

The next generation of mAbs are under increasing pressure from both public and private healthcare providers to offer cost effective treatments and contend with the intensified competition from rival manufacturers (novel and biosimilars). The success of these new mAb therapeutics will be highly dependent on their economic performance (Cohen 2009; Mitchell 2005). As a

result production cost, capacity utilisation and the ability to rapidly accommodate fluctuating market conditions are becoming critical success indicators (Farid 2009a; Kamarck 2006; Pellek and Arnum 2008). This is increasing the pressure on companies to produce more economically sustainable therapies and hence, adopt more cost-effective manufacturing strategies. The current platform processes are able to fulfil a number of these aims, however, they can only be reached if the process does not undergo significant changes for a reasonably long period of time (Shukla et al. 2007). However, this does not mean that the purification of mAbs is a mature engineering field and that no further process improvements can be made. In reality, since the emergence of the three-column purification platform in the early 1980s, the platform has been constantly evolving with minor updates. For example, over the years Protein A resins have become more rigid, allowing faster flow rates and shorter residence times, plus higher capacity variants have been available since 2003 (Curling 2009). This is a major benefit to the platform purification, but its cost overshadows its performance and inspires motivation to replace it (Gagnon 2012).

The economic burden associated with Protein A has led to suggestions that the next generation of platform purification processes should look for an alternative capture step. CEX is becoming a popular alternative due to it being an order of magnitude cheaper and its ability to offer dynamic binding capacities higher than 100mg IgG/ml resin (Gagnon 2012; Marichal-Gallardo and Álvarez 2012). Typical HCCF has a pH between 6.5-7.6 and conductivity around 10-20 mS/cm (Li et al. 2009), this latter factor will need to be reduced to achieve the high binding capacities reported (Gagnon 2012). The introduction of a new conditioning step negates some of the proposed savings offered by changing resin, plus the non-Protein A elution pool is unlikely to be purer than the Protein A pool (Curling 2009). A number of non-chromatographic operations have been suggested including precipitation, positively charged ultrafiltration membranes and aqueous two-phase extraction to name a few. Prevailing opinion is that if these technologies were going to mount a serious challenge to Protein A as a capture operation, it

would have happened already (Curling 2009; Gagnon 2012; Marichal-Gallardo and Álvarez 2012).

The majority of second-generation purification platforms are still reliant on Protein A chromatography (Gagnon 2012) and any change in capture technology will follow a path of evolution (increased capacity & reduced cost) rather than revolution (adoption of CEX). The principle developments are likely to occur to the polishing chromatographic steps, with the introduction of new chromatographic resins and modes of operation. The high purity of Protein A pools make the use of a single polishing step possible with the latest technologies. **Figure 1.5** shows two leading contenders for the emerging two-column purification platform. These emerging platforms will have significant benefits for facility fit, operational ease and savings in COGs, development and validation costs (Kelley et al. 2008).

AEX chromatography's high impurity clearance properties make it the logical choice from which to develop a single superior polishing step enabling two-column purification processes (Gagnon 2012; Kelley et al. 2008). New, mixed-mode chromatographic resins represent a diverse range of ligands that harness two or more chemical functions. Mixed-mode resins can be divided into three subsets based on their dominant characteristic; augmented anion-exchangers with hydrogen bonding, augmented metal coordination with electrostatic interactions and augmented hydrophobic interactions with other functions (Gagnon 2012). Anion-exchangers enhanced with hydrogen bonding are likely candidates to replace both AEX and CEX, by offering the contaminant and viral clearance of AEX and the aggregate clearance of the CEX.

An alternative to changing to a new chromatographic matrix is to utilise the current AEX matrix in a new mode of operation, namely weak partitioning. Weak partitioning refers to the binding strength of the product to the resin during isocratic operations and is a combination of bind and elute mode, and flowthrough mode (Kelley et al. 2008). When AEX is operated in flowthrough the product partition coefficient (K_p) is very low ($K_p < 0.1$), in contrast a high $K_p > 100$ would signify a bind and elution mode of operation (Kelley et al.

2008). Weak partitioning is defined under conditions where the product and aggregates starts to bind to the resin (K_p is between 0.1-20), this would lead to significant product loss, but by significantly increasing the loading (x5 mg mAb/mL resin) yields are brought back to acceptable levels. The result is a step that offers the contaminant clearance seen in AEX flowthrough mode augmented with aggregate removal.

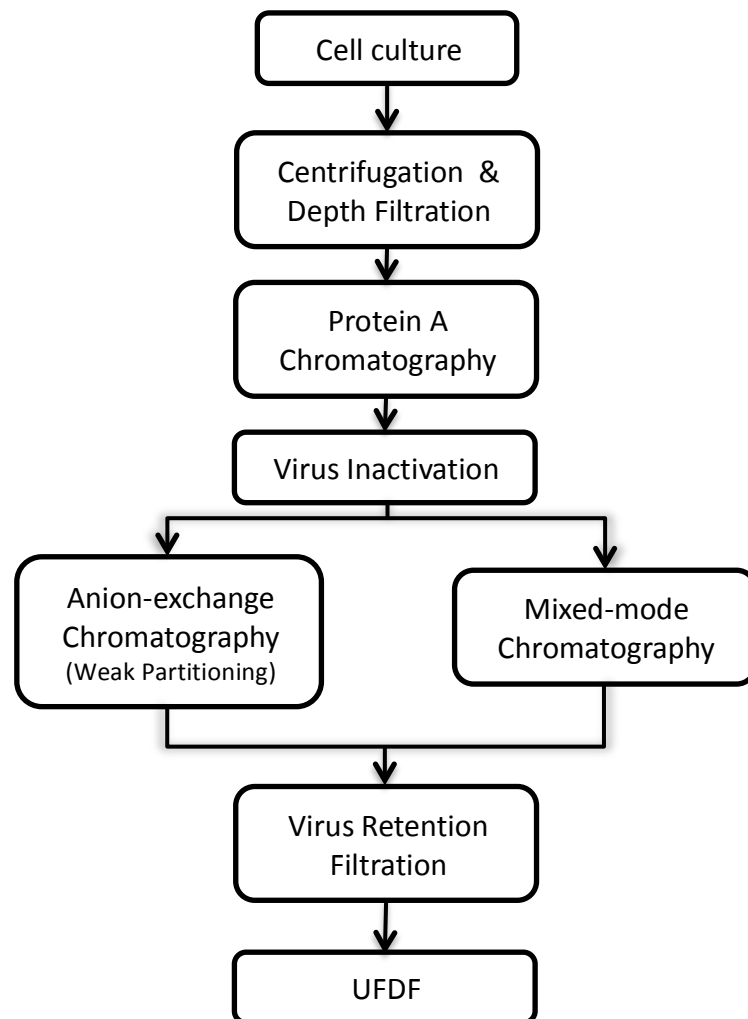


Figure 1.5. Emerging two-column recombinant mAb manufacturing platforms. UFDf, ultrafiltration/diafiltration.

1.4.3 Continuous unit operations

MAb manufacturing and general biopharmaceutical manufacture is synonymous with batch processing in the way that each manufacturing process step is operated independently to the preceding and subsequent process steps (Gagnon 2012; Godawat et al. 2012; Kelley 2007; Marichal-Gallardo and Álvarez 2012; Warikoo et al. 2012). This approach has been the prevailing mode of biopharmaceutical manufacture over the last decades due to the support by the industry and regulatory bodies for the tried and tested approach. By contrast, a number of other industries have undergone continued process intensification through their conversion from batch to continuous manufacturing, such as the petrochemical, chemical, polymer, pharmaceutical, and food industries (Godawat et al. 2012; Mollan and Lodaya 2004; Warikoo et al. 2012). The common advantages offered by continuous manufacturing regardless of industry are always the same. Namely steady state operations, reduced equipment sizes, high volumetric productivity, streamlined process flow, low cycle times and reduced capital and operating costs (Schaber et al. 2011; Warikoo et al. 2012).

Continuous processing is making inroads into the biotech industry, with the resurgence of perfusion cell culture technologies and the emergence of semi-continuous chromatography. Continuous manufacturing technologies have long been perceived to be more complex to implement and validate in the biotech sector. However, more recent continuous systems aim to overcome these obstacles with the promise of higher productivities and lower failure rates. This has led to various companies evaluating the potential continuous processing for the next generation of future high-efficiency platforms for mAb manufacturing (Hou 2012; Warikoo et al. 2012). A number of companies are publically increasing their investment in continuous processing evaluations; with Novartis, for example, investing \$65 million USD in a combined research project with MIT called the Novartis-MIT Centre for Continuous Manufacturing (Palmer 2013). Some companies are even looking to build first of its kind continuous manufacturing facilities, with GlaxoSmithKline reportedly investing over 50million USD in a Singapore facility (Palmer 2013). The remaining big biopharma companies may not be

actively declaring their investments or strategies in the area, but Genzyme, Amgen, Pfizer, Bayer, Genentech and Merck have all been presenting their own work actively on the conference scene in the last year (Brower 2013; Mahajan et al. 2012; Palmer 2013; Pollock et al. 2013a; Vester 2013; Warikoo et al. 2012). These efforts are being actively encouraged and supported by the FDA and ICH who are paving the way for the implementation of continuous manufacture by removing regulatory obstacles and introducing new Quality by Design initiatives necessary to foster continuous processing in a cGMP environment (ICH Q8, Q9 & Q10).

1.4.3.1.1 Perfusion

Perfusion cell-culture-derived biopharmaceuticals offer the potential of greater daily productivities and hence smaller facility footprints than batch and fed-batch culture manufacturing strategies (Bosch et al. 2008; Lim et al. 2006; Lim et al. 2005; Pollock et al. 2013b; Voisard et al. 2003). However, their use has been hampered historically by perceived greater logistical and validation complexity as well as higher likelihoods of technical failures (Lim et al. 2005). More recent perfusion culture systems aim to overcome some of these obstacles with the promise of higher productivities and lower failure rates (Centocor 2006; Crowley et al. 2008). This combined with the introduction of single-use technologies for cell culture operations have triggered renewed interest in the potential of bioprocesses based on perfusion culture systems.

Table 1.7. Current perfusion cell culture manufacturing strategies.

Product	Protein or mAb	Indication	Company	First Approved	Perfusion Mode	Reactor Size	Reactor Number
ReoPro®	mAb- abciximab	PCTA	Janssen Biotech ²	1994	Spin-filter (internal)	500L	5-20 (Leiden)
Cerezyme®	Beta-glucocerebrosidase	Gaucher disease	Genzyme	1994	Gravity settler ¹	2000 L	4 (Allston)
Gonal-f®	r.FSH	Anovulation	Merck-Serono	1997	Spin-filter ¹	ND	ND
Remicade®	mAb - infliximab	RA + other AI diseases	Janssen Biotech ²	1998	Spin-filter (internal) & Spin-filter (external)	500L 1000 L	5-20 (Leiden) 8 (Malvern)
Simulect®	mAb- basiliximab	Transplant rejection	Novartis	1998	Rotational Sieve Filtration	250 L	ND
Rebif®	Interferon beta-1a	Multiple sclerosis	Merck-Serono	1998	Fixed bed	75 L	22 (Corsier-sur-Vevey)
Kogenate- FS®	r.Factor VIII	Haemophilia A	Bayer	2000	Gravity settler	200 L	8 (Berkeley)
Xigris®	r. activated protein C	Sepsis	Eli Lilly	2001	Gravity settler	1500L	2 (CMO)
Fabrazyme®	Agalsidase beta	Fabry disease	Genzyme	2003	Gravity settler ¹	2000 L	2 (Allston) 2 (Framingham)
Myozyme®	Alglucosidase alfa	Pompe disease	Genzyme	2006	Gravity settler ¹	4000 L	3 (Geel)
Simponi®	mAb - golimumab	RA + other AI diseases	Janssen Biotech ²	2009	ATF	1000L 500L	3 (Cork) 5-20 (Leiden)
Stelara®	mAb - ustekinumab	Psoriasis	Janssen Biotech ²	2009	ATF	500L	5-20 (Leiden)

Sources: This data was derived through interviews with industrialists in each company. ND = not disclosed. ¹ Microcarrier based process. ² Formerly Centocor

Table 1.7 highlights 10 commercial therapeutic biologics that utilize perfusion culture systems for their manufacture. These include recombinant blood factors, enzymes, and mAbs. The choice of perfusion culture has sometimes been a necessity in cases with labile products (e.g., Xigris® [Eli Lilly], Kogenate® [Bayer], Cerezyme® [Genzyme]). Historically for mAbs the choice has been due to company experience and low titres. For example, perfusion culture was the basis of Centocor's (now Janssen Biotech) platform process in the 1980–1990s for both low dose products such as Reopro® (30mg) and high dose products such as the blockbuster Remicade® ($\leq 1,050$ mg). However, the increase in fed-batch titres combined with their ease of operation has established fed-batch cell culture as the platform choice for most mAbs in recent years (Gagnon 2012; Godawat et al. 2012; Kelley 2007; Marichal-Gallardo and Álvarez 2012; Warikoo et al. 2012). **Table 1.7** also reveals that the most common perfusion systems adopted in commercial processes are spin-filters (Deo et al. 1996; Yabannavar et al. 1992) and gravity settlers (often bespoke; Voisard et al., 2003), with up to 4,000L bioreactors. However, examination of the post-launch process changes for Remicade® revealed modifications to the perfusion systems used from 500 L internal spin-filter perfusion culture at the Leiden (Netherlands) site to 1,000 L bioreactors with external spin-filters at the Malvern (Pennsylvania) site in an effort to minimize culture failure due to adverse filter fouling (Wojciechowski et al. 2007). In its Ringaskiddy (Cork) site, Janssen Biotech has switched to a newer perfusion technology, alternating tangential flow (ATF) perfusion (Refine Technology, Edison, NJ) for the production of more recent mAbs, such as Simponi® (Centocor 2006). The ATF system achieves media exchange by circulating the broth back and forth between the bioreactor and an external hollow-fibre filter via the action of a diaphragm pump (Crowley et al. 2008; Shevitz 2000). The vendors report that the pulsating motion allows greater media perfusion rates, reduces the dead volume outside the reactor and minimizes the shear stress the cells are exposed to. These multiple effects allow the ATF perfusion system to minimize filter fouling and achieve higher cell densities and therefore reach higher productivities compared to earlier perfusion systems.

There are a few contributions in the literature that compare the process economics of perfusion and fed-batch manufacturing strategies. Cacciuttolo (2007) concluded that fed-batch culture would be cheaper than perfusion culture as the cost of larger media and harvest tanks in perfusion were considered to outweigh the benefits of higher productivity. The analysis focused on the changes to the cell culture stages rather than the whole bioprocess. Bosch et al. (2008) took into account the complete bioprocess from seed train to final bulk drug substance. Comparing a microcarrier-based perfusion strategy to a fed-batch strategy generating a tonne of mAb with an expected titre <1 g/L. Bosch et al. (2008) found that the perfusion manufacturing strategy offered savings in COG/g due to the 10-fold increase in productivity relative to the fed-batch bioreactor. The analysis did not consider the consequences of bioreactor failure and focused on a single scale of production. Lim et al. (2005, 2006) compared a spin-filter perfusion to a fed-batch strategy under uncertainty, for an output of 50 kg/year and a titre of 1 g/L. No significant difference in COG/g was seen at this scale in the deterministic analysis. However, the authors used a stochastic analysis to demonstrate the reduction required in the failure rate of the spin-filter perfusion strategy for it to compete with the fed-batch strategy at this scale.

1.4.3.1.2 Semi-continuous chromatography

Over the last decade mAb manufactures have been looking to increase upstream capacity, productivity and yields (Bisschops et al. 2009b; Holzer et al. 2008). This has led to a rapid increase in cell culture mAb titres from only mg/L values, to the current norm of 2–3g/L and with processes in development with reported titres of 5 g/L and higher this is likely to rise further (Bisschops et al. 2009b; Kelley 2009). The notable successes in upstream development has placed increased burden on downstream operations and improvements are urgently needed to tackle the growing `downstream bottleneck` (Bisschops et al. 2009b; Holzer et al. 2008; Langer 2012). The current and future mAb purification platforms are still dominated by chromatographic methods and Protein A as the preferred primary capture

step (Gagnon 2012; Marichal-Gallardo and Álvarez 2012). Protein A resins are the leading material cost contributor in the current and future platforms (Pollock et al. 2013a; Pollock et al. 2013b). During commercial manufacture Protein A contributes to 10% of the direct costs, however, in early development Protein A can account for 53% of the direct manufacturing costs (Pollock et al. 2013a). During clinical manufacture product specific chromatographic resins are often used for just a few cycles, particularly if the DC is unsuccessful, leading to the resin being discarded before reaching its full potential cycle lifetime. The impact of poor resin utilisation is a particular concern in mAb development and improving utilisation of these expensive resins can have a significant effect on the manufacturing and development costs by reducing the cost burden associated with failed DCs.

Typically, the protein A column is loaded up to 90% of 1% breakthrough capacity, underutilising the resin's capacity. This loading regime results in the entry (top) of the column being saturated and the exit (bottom) unsaturated upon completion of loading, leading to an excess buffer consumption caused by washing, elution and cleaning of the unsaturated column portion. Various methods have been employed to increase the productivity and utilisation of Protein A columns, including the use of dual flowrate loading strategies (Ghose et al. 2004) and flow-through recycling in an effort to fully saturate the whole resin (Mahajan et al. 2012). An alternative approach to increase utilisation is to divide the column into multiple portions and wash and elute the saturated top portion of the column and continue loading the unsaturated portion of the column until saturated. This principle is applied in semi-continuous chromatography, which allows the columns to be loaded to a higher binding capacity, reducing the resin volume required and the overall buffer consumption. Semi-continuous chromatography has been shown by Mahajan et al (2012) to be an effective way to increase resin utilisation. This concept is similar to the simulated moving bed concept commonly used in the chemical and pharmaceutical industries (Juza et al. 2000; Pellek and Arnum 2008; Strohleim et al. 2007), but to date this concept is not widely used in mAb purification. The expertise from these industries is now being applied to biopharmaceutical processes, with companies including Novasep (Pompey,

France) offering BioSC (2-6 columns) and Tarpon (Leiden, Netherlands) with BioSMB (6-12 columns). This has also led companies already supplying the biopharmaceutical industry to develop their own systems based on the SMB concept, such as GE Healthcare (Uppsala, Sweden) with its periodic counter current (PCC) system (3-4 columns). Recent papers have provided a proof-of-concept for semi-continuous chromatography linked to a fed-batch process (Mahajan et al. 2012) and to an alternating tangential flow perfusion process (Godawat et al. 2012; Warikoo et al. 2012) for mAbs. These publications highlight the operational benefits of semi-continuous chromatography systems with resin volume reductions ranging from 40-50% and buffer usage decreases of 40-49% causing total reduction in total process buffer usage of 12-15% (Mahajan et al. 2012; Pollock et al. 2013a; Warikoo et al. 2012).

While the proposition of continuous processing in biopharmaceutical manufacture is likely to face continued scepticism, this does not mean its benefits will not be realised. Continuous processing in other industries faced similar concerns and scepticism before its successful implication (Mollan and Lodaya 2004; Schaber et al. 2011; Warikoo et al. 2012). This is reflected in the disclosed activities and publications by a number of biopharmaceutical manufactures on their use and assessment of semi-continuous chromatography as shown in **Table 1.8**. The majority of large biopharmaceutical manufactures and semi-continuous chromatography system manufactures are included in **Table 1.8**. However based on this analysis there will also be a further number who have not disclosed their intentions. This hypothesis is based on the most notable omission of Novasep's BioSC system, which has been available since 2007 yet no notable disclosures were found. To date no semi-continuous chromatography systems have been used to purify mAbs destined for clinical trials or commercially available product (no public disclosures).

Table 1.8. Current commercial use of semi-continuous chromatography

Company	Systems Evaluated / Employed	Reference
Amgen	GE AKTA PCC	Jocelyn Materie et al, ACS 2010 San Francisco, CA.
Bayer	Undisclosed	Thomas Daszkowski PIMS, London, UK.
Biogen-Idec	Tarpon BioSMB	Bisschops et al, 2009
Centocor	GE AKTA PCC	Karol Lacki et al, Gab 2004, Nice, France.
Genentech	GE AKTA PCC	Mahajan et al, 2012
Genzyme	GE AKTA PCC	Warikoo et al, 2012 Godawat et al 2012
Lonza	Tarpon BioSMB	Allen et al 2010
Merck	Tarpon BioSMB	Bisschops et al, Prep Symposium 2012, Boston, MA
Pfizer (formerly Wyeth)	Tarpon BioSMB GE AKTA PCC	Stephen Lyle, M.S. IBC Antibodies 2010, Carlsbad, CA. Pollock et al, 2013

1.5 Computational Decision Making Tools

This chapter has highlighted how the maturing biopharmaceutical industry is under increasing economic and regulatory pressure when developing and manufacturing mAbs and other biopharmaceuticals. Consequently, biopharmaceutical companies have to make many strategic decisions in multiple business areas such as the design of manufacturing processes and facilities, as well as capacity sourcing and portfolio management (Farid 2012). Many of these strategic decisions involve large capital expenditures that are further complicated by a number of sector specific constraints, namely tight regulatory requirements and increasing cost pressures (Farid 2012; Velayudhan and Menon 2007). **Figure 1.6** presents the complex decisional domain biopharmaceutical companies have to operate within and highlights the most common constraints and uncertainties

seen. To successfully operate in this environment a detailed understanding of how these decisions and their inherent constraints and uncertainties affect the companies' key financial and operational performance are required (Farid 2012). Advanced simulation tools are becoming essential in achieving this goal and are now available in a number of key decisional domains in the biopharmaceutical industry from portfolio management (George and Farid 2008a; George and Farid 2008b; Rajapakse et al. 2005; Rajapakse et al. 2006) to capacity planning (Lakhdar et al. 2007; Simaria et al. 2011; Stonier et al. 2011) and finally process and facility design (Farid et al. 2005; Lim et al. 2006; Lim et al. 2005; Pollock et al. 2013a; Pollock et al. 2013b; Stonier et al. 2012).

Critical Path	Drug Development Cycle (Preclinical, Phase I - III)				Market
Process Development	Process development	→	Scale-up development	→	Process characterisation
Manufacturing	Pilot scale cGMP manufacturing batches → Tech transfer & Facility fit → Large-scale cGMP manufacturing batches				Post-approval changes
Decisions	Portfolio selection?	Process design?	Capacity Sourcing?	Build single / multi-product facility?	
Uncertainties	Clinical (e.g. doses, transition probabilities)		Technical (e.g. titres, equipment failure)		Commercial (e.g. sales forecasts)
Constraints	Time	Capacity	Budget	Regulatory	Skilled labour
Metrics	Speed	Ease of scale-up	Cost of goods	Fit to facility	Robustness

Figure 1.6. Key constraints and uncertainties in biopharmaceutical drug development. Sourced from Farid, 2012.

The purpose of an advanced simulation tool is to enable the user to predict the impact of the desired changes on the real-world system (existing or proposed); this is usually impractical, too expensive or even impossible to conduct with the actual system of interest (Banks 1998; Maria 1997). These advanced tools offer a simulated system that includes multiple models, which are similar but simpler than the real-world system they represent (e.g. manufacturing equipment models in a manufacturing facility system) (Maria

1997). This is because most real-world systems are too complex to allow realistic models to be evaluated analytically and therefore these models are studied by simulation (Kelton and Law 2000). In essence, a simulation tool simulates the real-world system via the operation of a model or models of the real-world system and infers the behaviour of the real-world system and sub-systems (Banks 1998; Kelton and Law 2000; Maria 1997).

Simulation systems can be divided into two classes, discrete and continuous. A discrete system is a system for which the states of the simulated variables remain constant over intervals of time and change instantly at defined points in time, often referred to as `events` (Banks 1998; Kelton and Law 2000). An example of a discrete system would be a queuing event, such as the number of customers in a shop (simulated variable), where the number of customers only changes when a customer is served and departs or a new one joins the queue (time events). In contrast, the states of the simulated variables in a continuous system change continuously over time and are defined by differential or difference equations (Banks 1998; Kelton and Law 2000). An example of a continuous system would be the movement of a projectile, for which position and velocity (simulated variables) are changing continuously over time.

The simulation models used within the two classes of system can be classified along three different dimensions, static vs. dynamic; deterministic vs. stochastic; and continuous vs. discrete (Kelton and Law 2000). Static and dynamic simulation models can be separated based on their use of time (Banks 1998; Kelton and Law 2000). A static simulation model is a `snapshot` of a system at a given point in time or one in which time plays no role (e.g. spreadsheet derived models). In dynamic simulation models time plays a crucial role; they represent a system as it evolves over time. Deterministic and stochastic simulation models can be distinguished by their use of probabilistic variables (Kelton and Law 2000). Deterministic simulation models do not use any probabilistic variables; the output of the model is determined by the input values and relationships in the model and will therefore be constant. Whereas stochastic models utilise probabilistic

variables; the output will be random and is only an estimate of the many possible outputs. Continuous and discrete simulation models are defined in the same way as continuous and discrete systems were defined previously. However, discrete simulation models are not always used to model discrete systems and vice versa (Kelton and Law 2000). For example, in a discrete system the variables can be treated as a flow using differential equations in a continuous model if the characteristics and movement of individual variables are not important (Kelton and Law 2000). Discrete-event simulation models, which are discrete, dynamic and stochastic, are one of the most common types of simulation models used (Banks 1998; Kelton and Law 2000; Maria 1997).

1.5.1 Process Simulations Tools for the Biotech Industry

Simulation tools have been actively utilised for process design and simulation in both the chemical and petrochemical industry since the early 1960s (Petrides et al. 2002; Toumi et al. 2010). Computer-aided process simulation tools are now standard tools used to plan, design, optimise and evaluate chemical and petrochemical process (Farid 2007). Simulation tools used in these industries are designed to capture continuous processes, however, most biopharmaceutical processes are operated in a batch-to-batch manner. Biopharmaceutical processes are therefore represented more realistically with batch process simulators that account for time and event scheduling (Toumi et al. 2010). However, batch based simulation models tend to be more challenging to develop due to their time-dependant behaviour and therefore early biopharmaceutical simulation tools were adaptations of available chemical process simulation tools (Farid 2007; Petrides et al. 2002; Toumi et al. 2010). The first simulation tool capable of simulating biopharmaceutical processes was 'Batches' from Batch Process Technologies (West Lafayette, IN), which entered the market in the mid-1980s (Petrides et al. 2002). The tool employed continuous models that utilised differential equations between defined event times (Petrides et al. 2002).

The first simulation tools utilising batch time-dependant models targeted at biopharmaceutical manufacturing processes did not arrive until the mid-1990s. Aspen Technology, Inc. (Cambridge, MA) introduced Batch Plus®; a recipe-driven modelling technology for batch processes (now called Aspen Batch Process Developer®) built on Aspen's chemical process simulator Aspen Plus®. Early versions of the simulation tool proved to be difficult to adapt to biopharmaceutical processes, due to the lack of specific biopharmaceutical unit operations and the retained chemical process characteristics from Aspen Plus® (Kahn et al. 2001; Shanklin et al. 2001). Recent simulation model add-ons from Aspen Technology, Inc. include Aspen Chromatography®; this has the capability to model individual chromatographic steps and to capture multiple chromatographic operations in a manufacturing process when linked with Aspen Batch Process Developer® (Evans et al. 2010).

Intelligen, Inc. (Scotch Plains, NJ) introduced BioPro Designer® (now called SuperPro Designer®) around the same time as Aspen's Batch Plus®. It was initially developed within the Massachusetts Institute of Technology (Cambridge, MA) in the late 1980s before Intelligen Inc. acquired and further developed the simulation tool prior to launch. SuperPro Designer® is built around a static model which the users access via a graphical interface. The tool has a large library of in-built unit operations to address the needs of the biopharmaceutical industry (Petrides et al. 1996). Early versions of SuperPro demonstrated its capability to perform detailed mass and energy balances, and equipment scaling and costing (Petrides et al. 1996). The release of a number of extension modules (e.g. EnviroPro®, SchedulePro®) improved the capabilities of the tool allowing it to capture the environmental footprint of a process and select production schedules based on process and facility constraints (Gosling 2005; Shanklin et al. 2001; Toumi et al. 2010). Toumi et al (2010) demonstrated how SuperPro Designer® and SchedulePro® were used in the successful technology transfer of a mAb manufacturing process; highlighting process improvements and establishing equipment and utility requirements for the transfer.

The most recent simulation tool designed specifically for biopharmaceutical industry was released by Biopharm Services (Bucks, UK) in the early 2000s. BioSolve® is a static simulation tool created in Microsoft Excel (Microsoft Corporation, Redmond, WA, USA) which captures the time-dependant nature of batch processing with extensive coding in Visual Basic for Applications (VBA). The tool, like other static spread-sheet based models is capable of conducting material balances, equipment sizing and cost analysis (Sinclair 2008; Toumi et al. 2010). Biosolve® has an inbuilt library of biopharmaceutical unit operations and an extensive cost and process database which, in contrast to other cost models is regularly updated (Sinclair 2008).

Alongside the simulation tools targeted specifically at the biopharmaceutical industry there are a number of discrete-event simulators, which are highly utilised in the other industries are now being readily used in biopharmaceutical process modelling. Discrete-event simulations are usually employed when a detailed understanding of time-dependency events is required, often on the minute-by-minute level (Paz and Puich 2004; Toumi et al. 2010). Due to their dynamic nature they are often used to evaluate the impact of variation and random events, such as equipment failures, resource constraints and process delays (Farid 2007; Paz and Puich 2004; Shanklin et al. 2001; Stonier et al. 2012; Toumi et al. 2010). Tools of this type include Arena® from Rockwell Automation, Inc. (Pittsburgh, PA), Simul8® from Simul8 Corporation (Boston, MA), ProModel® from ProModel Corporation (Orem, UT) and ExtendSim® from Imagine That, Inc. (San Jose, CA). These simulation tools all include a common toolbox of predefined code to carryout simple operations within a dynamic environment such as time delays, queuing events and mathematical calculation modules. The common toolbox of pre-described modules allows a diverse range of systems to be represented, making these tools highly versatile. This versatility is reflected in their use, with most industries utilising discrete-event simulation tool for their modelling needs (Banks 1998; Kelton and Law 2000; Maria 1997).

Discrete-event simulation tools do not contain predefined biopharmaceutical unit operations. These have to be constructed within the tools, meaning tool construction can be highly labour intensive in contrast to the industry targeted simulation tools. However, due to their unique abilities, which are not currently available in industry targeted simulation tools, their use is increasing. For example, ProModel® has been successfully deployed to optimise the planning, scheduling and throughput of a final-stage biopharmaceutical manufacturing facility. Haekler et al (2010) highlighted how the use of ProModel® had resulted in cost avoidance of \$3 million USD per year and a revenue increase of over \$25 million USD per month (Haekler et al. 2010). Simul8® was also successfully utilised by Wyeth (now part of Pfizer, Inc., NY) to evaluate utility requirements, which resulted in reallocation of \$1.2 million USD of expected capital expenditure to other key capital projects (simul8.com). ExtendSim® appears to be the most widely utilised simulation tool in the industry, with demonstrated case studies looking at portfolio selection (Rajapakse et al. 2005; Rajapakse et al. 2006); facility capacity optimisation (Paz and Puich 2004); facility fit of legacy facilities (Stonier et al. 2012); process synthesis and facility design for existing technologies (Lim et al. 2006; Lim et al. 2005; Mustafa et al. 2006); and future technologies (Farid et al. 2005; Pollock et al. 2013a; Pollock et al. 2013b). ExtendSim`s® success can be explained by its high versatility which is reflected in the variety of problem domains it has been used to tackle. This high versatility comes from the ability to edit the existing code modules, referred to as `blocks`, and the ability to create new bespoke blocks (Gosling 2005; Pollock et al. 2012; Stonier et al. 2012). The other simulation tools like ProModel® also have this ability, but any custom coding must be carried out in an external package and called upon when required in the simulation tool, adding to the tools complexity (Heflin and Harrell 1998).

Table 1.9. Summary of functionality and capabilities of common biopharmaceutical simulation tools

	Aspen Batch Process Developer	SuperPro Designer	BioSolve	ProModel	ExtendSim
Mass Balance	✓	✓	✓	✓	✓
Batch	✓	✓	✓	✓	✓
Continuous	✓	✓		✓	✓
Dynamic	✓			✓	✓
Customisable				✓	✓

Table 1.9 presents a summary of the most prevalent simulation tools used in the biopharmaceutical industry and highlights their functionality and capabilities (based on reported use and publications). This is not an exhaustive summary, there will be many other simulation tools being used in the industry including other discrete-event simulation tools and bespoke simulation tools offered by a range of simulation consultancy companies, such as Bioproduction Group, Inc. (Bio-G, Berkley, CA).

1.5.2 Risk Modelling

The simulation tools described so far are primarily designed to operate in a deterministic manner, which means all the simulation events will inevitably occur and hence their outputs can be termed as `non-risk`. These non-risk outputs would be identical if the same scenario was investigated multiple times by the simulation tool. However, biopharmaceutical manufacture is not

a non-risk environment. There are a several uncertainties in manufacturing processes, such as fermentation titres, step yields, batch failure, production times and mass throughput to highlight a few (Banks 1998; Bower et al. 2005; Papavasileiou et al. 2007; Papavasileiou et al. 2009). These uncertainties lead to variation in the facility throughput, production costs, capital investment requirements and product demands. Incorporating these uncertainties (risks) into any analysis requires a subjective assessment of the probability distributions of the variables in question. This is achieved by assessing historical data or knowledge from industry subject matter experts (Farid et al. 2007). Two methods often employed to evaluate these risks are `risk adjustment` and `Monte Carlo Simulation`.

Risk adjustment is a concept that was first used in mid 1980s by the Bankers Trust to assess market risk on capital investments. This was achieved by multiplying the capital investments by a risk value (percentage); generating the risk-adjusted return on capital (Borge 2002). This technique can also be employed on other simulation outputs, but is primarily used on economic metrics (Borge 2002).

The Monte Carlo method was developed in the 1940s at Los Alamos National Laboratory while physicists were trying to establish the diffusional properties of neutrons through various materials (how far a neutron on average would travel before hitting an atomic nucleus) (Anderson 1986). Conventional deterministic simulation was unable to solve this problem, but by running the simulation multiple times with random statistical sampling they were able to establish a probability distribution of the solution. This heuristic approach was given the moniker of the Monte Carlo method (Anderson 1986). The growth in computational power seen in the 1950s, brought Monte Carlo simulation into multiple fields of research and its popularity has increased inline with the increase in computational power seen in recent decades (Anderson 1986; Nicholas et al. 1953). In addition, a number of easy-to-use commercial packages capable of running Monte Carlo simulations are now readily available such as the Excel® based add-ons @Risk® from Palisade Corp. (Ithaca, NY) and Crystal Ball® from Oracle

Corp. (Redwood City, CA). These tools have the ability to turn any deterministic simulation tool into a stochastic tool capable of running Monte Carlo simulations. Bower et al (2004), among others, demonstrated how SuperPro Designer® could be linked to the Crystal Ball® add-in to allow the definition of stochastic input variables, the random number generation of the specified variables and the resulting output probability distributions (Bower et al. 2005; Papavasileiou et al. 2007; Papavasileiou et al. 2009). The highly versatile discrete-event simulation tools discussed earlier also have this capability by linking to external add-ons or by utilising their own internal Monte Carlo algorithms. For example, ExtendSim® is capable of defining probability distributions and generating random numbers with the specified distributions for the multiple simulation runs required in a stochastic Monte Carlo analysis without external add-ons (Lim et al. 2006; Lim et al. 2005; Mustafa et al. 2006; Pollock et al. 2013b; Rajapakse et al. 2005; Stonier et al. 2013; Stonier et al. 2012). Lim et al demonstrated how this functionality could be used to assess the annual throughput and resulting cost of goods (Fermentation titre variation and DSP yield) of fed-batch and perfusion cell culture processes (Lim et al. 2006; Lim et al. 2005). Stonier et al also used this functionality to assess current and future process robustness (fermentation titre variation) and the short-term facility fit issues on tech transfer to a new facility (fermentation titre, eluate volumes and step yield variation) (Stonier et al. 2013; Stonier et al. 2012). These publications demonstrate how discrete-event simulation tools specifically ExtendSim® can be utilised to evaluate a large number of different scenarios found throughout the biopharmaceutical industry.

1.5.3 Multiple Criteria Decision Analysis

The simulation tools described so far are capable of generating quantitative outputs (annual throughput, COG etc.). However, when evaluating alternative manufacturing or portfolio strategies qualitative outputs (ease of development, ease of control etc.) are also important to consider. Often both quantitative and qualitative outputs, in alternative strategy

evaluation can be conflicting leading to situations where it is not apparent which strategy is the most preferential. For example in investment strategy comparisons, profit may be in conflict with the inherent risk of each strategy.

Multi-criteria decision-making (MCDM) is a method of decision-making that is capable of reconciling these conflicting attributes (quantitative and/or qualitative) when evaluating strategy alternatives against a set of decision criteria (Triantaphyllou 2000). Triantaphyllou describes how MCDM can be divided into multi-objective decision-making (MODM) and the more common multi-attribute decision-making (MADM) (Triantaphyllou 2000). MODM is used when the decision space is continuous (undefined alternatives), whereas MADM is used in decision problems with discrete decision spaces (predefined alternatives). Regardless of the approach used there are three steps seen in all MCDM approaches (Triantaphyllou 2000):

1. Determining the relevant decisional criteria and alternatives.
2. Assign numerical measures ranking criteria on importance and also to the impact of the alternatives on these criteria.
3. Process the resulting numerical values assigned to each alternative and then establish the preferential ranking of the alternatives.

There are multiple methods available in MCDM that have been widely used in multiple decision spaces in multiple industries (Triantaphyllou 2000). The oldest and most widely used method is the weighted sum method (Deb 2008; Fishburn 1967), followed by the weighted product method (Miller and Starr 1960) and the analytical hierarchy process method (Saaty 1980). These methods are primarily reported in literature in decision-making scenarios concentrating on financial responses, as demonstrated by Steuer and Na (2003). However, more recently these techniques have been employed to assess a number of scenarios specific to the biopharmaceutical industry. Farid et al (2005) demonstrated the use of MCDM methods to combined both quantitative and qualitative attributes in order to assess the use of single-use technologies in clinical manufacturing facilities. Also, George et al (2008) demonstrated how MCDM methods could be used in portfolio management and capacity planning. These bodies of work demonstrate how MCDM has

the ability to support decision-makers in the biopharmaceutical industry when evaluating alternative manufacturing strategies with conflicting quantitative and qualitative attributes.

1.5.4 Modelling of Continuous Processes

The use of continuous processing in other industries such as the petrochemical, chemical, polymer, pharmaceutical, and food industries has been previously highlighted. Simulation tools played a key role during the period of conversion from batch to continuous manufacturing experienced by these industries and is now often the norm in a number of activities including facility design, optimisation and scheduling (Farid 2007; Mollan and Lodaya 2004; Petrides et al. 2002; Toumi et al. 2010). Simulation tools used in these industries are designed to capture continuous processes, however, as previously discussed most biopharmaceutical processes are operated in a batch-to-batch manner. The emergence of continuous processing in the biopharmaceutical industry does not mean existing simulation tools from other industries can be readily employed. This is due to the nature of continuous processing and the continuous unit operations seen in the biopharmaceutical industry.

A key concept of a continuous process is that continuous, steady-state processing extends from the bioreactor to the final purification operation. However, this concept is currently not possible in biopharmaceutical manufacture due to the lack of suitable technology. For example, continuous perfusion bioreactors do generate a continuous stream of harvested cell culture fluid (HCCF), but they can only achieve this in a batch operation. Firstly, the cell culture has to reach the desired steady-state cell density to achieve a constant concentration of HCCF; then it can only produce a continuous stream of HCCF for a defined period, before a new cell culture batch is required. This semi-continuous mode of operation is also found in the search for continuous downstream processing operations, where chromatography systems that are described as continuous are capable of continual loading but only generate discrete elution pools of product.

Therefore, any simulation tool capable of modelling continuous processing in the biopharmaceutical industry must be able to model batch (e.g. bind & eluate mode chromatography, viral inactivation), semi-continuous (e.g. periodic counter current chromatography, perfusion cell culture) and continuous unit operations (e.g. filtration, flowthrough mode chromatography) in the same manufacturing process. Toumi et al highlights that biopharmaceutical processes are represented more realistically with batch process simulators that account for time and event scheduling (Toumi et al. 2010). However, batch based simulation models tend to be more challenging to develop due to their time-dependant behaviour; this will be further complicated with semi-continuous and continuous unit operations. This is reflected in the fact that the majority of the simulation efforts to date have concentrated on a single continuous unit operation, with the majority utilising static-spread sheet based simulation tools to establish economic, productivity and scheduling information (Bosch et al. 2008; Mahajan et al. 2012). Lim et al (2004) demonstrated how discrete-event simulation tools could be adapted to model semi-continuous and batch unit operations within the same simulation environment. However, to date the publication of any dynamic simulation tools capable of capturing multiple continuous/semi-continuous unit operations, or even a continuous biopharmaceutical process has not been seen.

1.6 Aims & Organisation of Thesis

The preceding sections of this chapter have provided a description of the current-state and future direction of biopharmaceutical development and manufacturing, highlighting the impact of monoclonal antibodies as therapeutic agents. In addition, an overview of the current position of computational design-support tools available to the industry has been discussed. However the presented literature review highlighted that at present no design-support tool is capable of capturing the economic, environmental and operational feasibility of continuous mAb manufacturing.

Consequently, the aim of this thesis is the development of a decision-support framework that is capable of simulating and optimising continuous mAb manufacturing processes in the challenging environment biopharmaceutical manufactures currently find themselves. This will facilitate more informed decision-making when evaluating continuous and semi-continuous manufacturing strategies, with respect to their economic, environmental and operational feasibility. In order to realise this aim a set of objectives was established and these form the basis of each of the proceeding chapters.

In **Chapter 2**, a decisional framework is presented to facilitate the evaluation of continuous manufacturing alternatives. Initially a description of the problem domain that is addressed by the decision-support framework is presented. The hierarchal approach adopted throughout the framework is then introduced, followed by a detailed explanation of the modelling approach taken. Highlighting key process models for both batch and continuous unit operations. A multi-attribute decision making technique is also presented to allow the reconciliation of both quantitative and qualitative metrics generated by the framework. **Chapter 2** also describes the materials, equipment and analytical techniques used to evaluate a semi-continuous chromatographic system prior to implementation into the framework.

Chapter 3 presents the use of the decision-support framework in the evaluation of fed-batch and perfusion cell culture manufacturing strategies for commercial mAb production. The chapter use a combination of deterministic and stochastic analysis techniques to verify the historical perception of poor productivities and high cell culture failure rates. Before highlighting the benefits of the latest perfusion cell culture technologies compared to conventional stainless steel fed-batch facilities as well as emerging single-use fed-batch facilities. The information generated from this analysis is then combined with qualitative attributes to determine a ranking of the manufacturing alternatives.

In **Chapter 4** an integrated approach to technology evaluation is described that combines experimental evaluation and simulation assessment

employing the decision-support framework. A systematic design methodology is presented that uses a number of small-scale single-column chromatography experiments to determine the key design and operating parameters for an optimised semi-continuous chromatography operation. The resulting design methodology was validated with semi-continuous constituency runs and incorporated into the simulation framework. The decision-support framework was then used in combination with a dynamic cycling study to evaluate the potential impact of adopting semi-continuous chromatography for commercial manufacture.

Chapter 5 presents a vision for a number of integrated continuous manufacturing strategies, combining the batch and continuous technologies evaluated in **Chapters 3 and 4**. The economic impact and operational robustness of these future-manufacturing strategies was then assessed via the decision-support framework. Addressing a number of unique scenarios throughout the development pipeline for a range of manufacturing scales and company sizes. The resulting analysis provides a wide-ranging overview of the performance of continuous processing relative to the current batch platform for the mAb sector.

Chapter 6 presents an assessment of the issues and challenges faced when validating a continuous manufacturing process. Looking at the guidance provided by regulatory bodies and how these can be interpreted for a continuous process. The chapter also provides insight into how manufacturers would demonstrate process understanding, robustness and reproducibility of a continuous unit operation.

In **Chapter 7** a summary of the main conclusions of this thesis are presented and some future avenues of research to augment this work are presented. Finally, papers by the author, published during the course of this work are shown in the appendices.

2 Materials & Methods

The preceding chapter highlighted the challenging environment in which biopharmaceutical manufactures currently find themselves. To remain complete in such an environment companies are looking to reduce R&D and manufacturing costs by improving their manufacturing platform processes whilst maintaining flexibility and product quality. As a result companies are now exploring whether they should choose conventional batch technologies or invest in novel continuous technologies, which may lead to lower production costs. In this chapter, a decision-support framework is presented that is capable of simulating and optimising continuous mAb manufacturing processes in this challenging environment, and is therefore capable of aiding design-makers when evaluating these alternative manufacturing strategies.

The chapter is organised as follows: **Section 2.1.1** provides a description of problem domain that is addressed by the decision-support framework. The scope and requirement specification of the framework are addressed in **Sections 2.1.2 and 2.1.3**. This is followed by a detail explanation of the modelling approach taken in **Section 2.1.4**. **Section 2.1.5** describes the multi-attribute decision making technique used to reconcile the quantitative and qualitative metrics generated by the framework. A brief description of the data collection methods employed is given in **Section 2.1.6**. **Sections 2.2.1, 2.2.2 and 2.2.3** describe the materials, equipment and analytical techniques used to evaluate a semi-continuous chromatographic system prior to implementation into the framework. The final section then summaries the significant properties of the decision-support framework.

2.1 Decision-Support Framework

2.1.1 Domain Description

The key features of the biopharmaceutical manufacturing problem domain are identified in this section. Biopharmaceuticals such as mAbs are produced for a range of demands for either clinical trials or commercial product sales. Prior to commercial manufacture, the drug candidate (DC) will be manufactured at a number of different manufacturing scales as the DC progresses through the development pipeline. These range from multiple commercial scale batches in the order of 10 – 100s kilograms of product for validation studies and small pre-clinical batches only producing grams of product. Throughout the development pipeline manufacturing must adhere to strict current Good Manufacturing Practices (cGMP) and comply with the unique process validation requirements for biopharmaceutical manufacturing facilities. It is of critical importance that these regulations are followed due to the influence they have on product quality, safety and regulatory approval.

MAbs are primarily produced in batches derived from mammalian cell culture fermentation and purified through a series of orthogonal purification steps. Each batch is produced in a stirred-tank bioreactor, which can be operated in a batch, fed-batch or continuous perfusion mode. The resulting cell culture broth is a complex mixture containing low concentrations of the target product, cells and cells debris. Further purification is required by a number of processing steps to yield the purified target protein. These steps include: primary recovery, product capture and polishing. Primary recovery often includes centrifugation and depth-filtration to remove cells and large debris. The resulting harvest cell culture fluid (HCCF) is typically purified further using a number of chromatographic operations. The initial product capture is typically carried out using affinity based capture in the form of Protein A chromatography. The product is then purified through a further sequence of chromatographic operations and filtration operations. In addition to these processing operations, the manufacturing process must demonstrate viral clearance, with a mandatory inclusion of two dedicated viral clearance

operations (viral inactivation & viral retention filtration). Inactivation is commonly seen after the initial product capture in the form of a low pH hold step. Virus retention filtration is carried out towards the end of the process to minimise filter fouling and is often found immediately before a final concentration and diafiltration step prior to final bulk formulation. Alternative semi-continuous unit operations are increasingly being seen in manufacturing including second-generation perfusion fermenters and semi-continuous chromatographic operations. These semi-continuous manufacturing operations require careful integration into the manufacturing facility due to their unique resource and scheduling requirements.

Alongside the aforementioned manufacturing operations, there are a number of ancillary operations that are not directly involved in the manufacture of a product batch. These include the formulation of intermediary materials including process buffers, fermentation media and cleaning-in-place buffers. Another key ancillary operation is the preparation and management of equipment and vessels (product and buffer), namely column packing, equipment and vessel cleaning-in-place (CIP) and sterilising-in-place (SIP) activities.

The biopharmaceutical facility has a number of complex sizing and scheduling options that need to be optimised to generate the required throughput of material and meet the target product demand. The scaling and scheduling of the upstream processes (USP) (fermentation and primary recovery) balance the frequency of harvest volumes which is determined by reactor number and cell culture duration against the USP equipment sizes and running costs. The resulting harvest volumes and frequency dictate the size of the vessels and equipment required in the downstream processing (DSP) operations. The principle aim of the biopharmaceutical manufacturer is to select a size of USP and DSP equipment that meets the DSP slot length (time between harvest volumes) at a minimum cost while ensuring that the neither the USP nor DSP becomes a bottleneck in the production schedule.

Establishing the optimal sizing and scheduling options for a biopharmaceutical manufacturing facility is a complex trade-off between

processing time and costs. However the complexity of the problem domain increases further when the inherent uncertainties found in manufacturing are considered. There are a number of uncertainties around key variables that lead to significant variation between batches, including cell culture titres and chromatography binding capacities. These variations can lead to delays, yield losses and even to some batches surpassing regulatory limits of product quality and resulting in the complete batch loss. Alongside the inherent variability in key manufacturing parameters there is also a high risk of equipment and sanitation failure that can also result in product losses or complete batch loss. Fermentation is a key example of both variability and risk, with variation being seen in cell culture titres and the risk in equipment failure or cell culture contamination leading to either product loss or batch failure. Accounting for these variations and risk events can assist in the design and operation of more robust manufacturing processes and facilities.

2.1.2 Scope of Framework

Defining the scope of the framework was a crucial task in the initial development of the framework to ensure the analysis did not become too complex to handle and remained focused on the complex problem domain described. As mentioned earlier the aim of the simulation tool was to capture the key costs and operating concerns in biopharmaceutical manufacture and use these findings to assess the operational, environmental and business/financial implications of multiple manufacturing strategies. More explicitly, the scope was defined as follows:

- To model multi-suite facilities with different process configurations, demands and performances for mAb manufacture on a campaign basis.
- To evaluate the performance of alternative manufacturing technologies across a range of cell culture titres and scales in terms of cost, throughput, environmental impact and risk metrics.'

The model was also required to capture the unique challenges found with the incorporation of continuous manufacturing technologies into the current batch process sequences discussed earlier. These included:

- The ability to capture the resource requirements for both batch and continuous manufacturing technologies in a dynamic discrete-event environment.
- The ability to track and record the creation, division and merging of product batches into sub-batches, which is an inherent consequence of continuous processes.
- The ability to screen sizing and scheduling strategies for both batch and continuous manufacturing strategies to establish the optimal equipment and scheduling strategy with respect to cost and time.

The simulation tool should also be able to make a number of key decisions in the evaluation of a number of manufacturing alternatives, including:

- Facility decisions – e.g. the use of stainless steel product and process vessel versus disposable bag technologies.
- Process decisions – e.g. the use of continuous perfusion cell culture versus fed-batch cell culture and semi-continuous chromatography with conventional batch chromatography.
- Strategy decisions – e.g. the best pooling strategies of sub-batches in hybrid batch and continuous manufacturing strategies.

The following sections of this chapter demonstrate the approach taken to create a framework capable of fulfilling the aforementioned scope by modelling the economic, operational and environmental aspects of biopharmaceutical manufacturing.

2.1.3 Requirement Specification & Software Selection

The definition of the scope of the framework and the analysis of the problem domain meant it was possible to establish a requirements specification that describes what the software platform should be able to accomplish. The requirements specification of this framework was styled on previous work conducted at UCL (Farid et al. 2007; Stonier et al. 2012; Stonier et al. 2009). The requirements specification presented in this chapter builds on the need to rapidly reconfigure multiple process alternatives in multi-suite facilities and manipulate and share the resulting data sets. The key addition was to meet all these requirements for both batch and continuous unit operations, whilst maintaining the ability to capture uncertainty and present the resulting data in an easy to interpret visual format. A summary of the requirements specification is shown in **Table 2.1**, with the feature specifically required to capture continuous manufacturing technologies are shown in bold.

The suitability of commercially available bioprocess simulation packages to meet the requirements specification was investigated. These packages comprise of mainly spread-sheet based static models that can generate cost estimates but that are unable to capture the impact of resource constraints and the resulting delays in manufacturing (Farid 2007; Paz and Puich 2004; Pollock et al. 2013b; Shanklin et al. 2001; Stonier et al. 2012; Stonier et al. 2009), a critical feature required for this analysis. Furthermore, they did not enable the specific scheduling features of semi-continuous unit operations to be modelled, meaning it was not possible to capture the scheduling interactions between continuous and batch product streams. On the other hand, discrete-event simulation languages were found to offer the flexibility to build dynamic models that had all these required capabilities. Hence, a stochastic dynamic decision-support tool was built to capture the specific scheduling challenges seen in batch and semi-continuous process sequences, as well as the impact of resource constraints, process variability and failure events.

Table 2.1. Requirements specification for the simulation tool

Requirement Type	Specification
Representation of declarative and procedural knowledge	Tasks and their characteristics Resources and their characteristics Material flow and its characteristics Batches, sub-batches and their properties Sequence of sequential and parallel tasks Resource requirements for each task Calculation procedures for mass balances and costing Variables for the calculation procedures Time Hierarchical views of tasks Risk/uncertainty: stochastic variables defined using probability distributions Facility definition Processing Suites Scheduling logic and its consequences
Dynamic simulation	Dynamic simulation of sequential and parallel task sequences Dynamic allocation of resources to sequential and parallel tasks Dynamic invocation of calculation procedure to compute compositions and costs Dynamic invocation of procedures to compute resource utilisation statistics Monte Carlo simulation Single-threaded, multi-threaded and parallel processing
Flexible development environment	Modular Extensible Ability to store large amounts of data Database driven

Note: Features specifically required to capture continuous manufacturing technologies are shown in bold, Adapted from Farid et al, 2007.

ExtendSim (ExtendSim v8, Imagine That! Inc., San Jose, CA) was selected as the discrete event simulation tool due to its multi-domain environment that can dynamically model continuous, discrete-event, discrete-rate, linear, non-linear and mixed-mode systems. ExtendSim models are comprised of a large number of interconnected blocks between which items representing the product stream are passed. These blocks contain functions that generate simulation events on interaction with items. ExtendSim had a number of pre-fabricated blocks representing key discrete-event functions (time delays, queues, resource pools, etc.). Due to the common programming language ModL (based on C++) found in all the blocks, the existing pre-fabricated blocks can be customised or specialist custom blocks can be coded. This resulting flexibility was a key driver in the selection of ExtendSim as the discrete-event simulation due to its ability to meet the key specified requirements with the existing block infrastructure and was able to meet all the other requirements due to the software's inherent customisation ability.

A key requirement in the specification for the simulation tool was the ability to specify a wide range of process sequences whilst maintaining the ability to manage and access the large datasets created. A distinction between input and output tables was seen as vital to the interpretation of the scenarios investigated. The internal database present in the ExtendSim software is embedded in the ModL programming language that has no distinction between input and output tables making management and access challenging. As a result linking ExtendSim to an external database platform was seen as an efficient way of meeting the requirement specification. The external database selected for incorporation into this framework was the MySQL distribution (MySQL AB, Uppsala, Sweden) of structured query language (SQL). SQL is an open source specialised programming language for managing large data volumes in relational databases by using a logical structure for relating data and maintaining organisation.

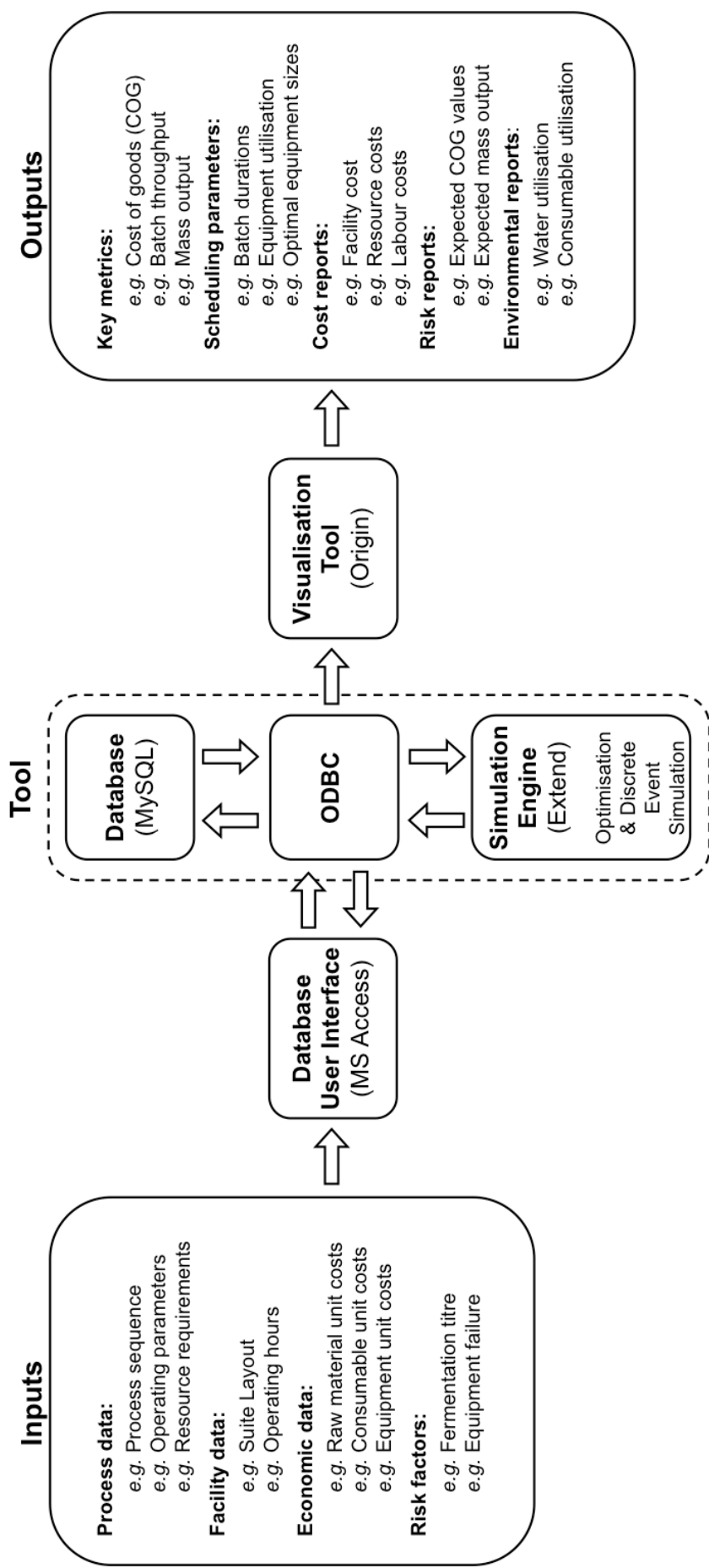


Figure 2.1. Overview of simulation tool structure highlighting key communication directionality and content with respect to key inputs and outputs. ODBC; open data base connectivity.

The SQL data access functionality in ExtendSim is possible but is a slow and inefficient way to access the input and output data tables. A more efficient method was used which involved linking the MySQL database to the internal ExtendSim database and importing all the input data tables on initialisation of the simulation and upon completion export the output tables back to the MySQL database. This approach allowed the ExtendSim blocks to rapidly access the internal database when running discrete-event functions significantly improving simulation times. The data communication required between ExtendSim and MySQL was achieved through Microsoft Open Data Base Connectivity (ODBC). **Figure 2.1** demonstrates how the use of a middleware such as Microsoft's ODBC (Microsoft Corporation, Redmond, WA, USA) allowed the simulation framework to connect to third party applications including database user interfaces such as Microsoft Access (Microsoft Corporation, Redmond, WA, USA) and visualisation packages such as Origin (OriginLab, Northampton, MA, USA).

2.1.4 Tool Implementation

2.1.4.1 Modelling Approach

The framework utilised a hierarchical approach throughout the framework, assigning key activities to a series of levels. This hierarchal approach has been used extensively by researchers at UCL to represent the phases of drug development (George and Farid 2008a; George and Farid 2008b; Rajapakse et al. 2005; Rajapakse et al. 2006) and the key manufacturing operations found in biopharmaceutical production (Farid et al. 2007; Stonier et al. 2012; Stonier et al. 2009). The hierarchal structure presented in this chapter focuses on the manufacturing operations, where different levels of the process and facility are defined.

Previous hierarchical structures adopted at UCL have focused on five principal hierarchical levels (Campaign, Batch Recipe, Unit Operation, Task, Sub-Task) (Stonier et al. 2012). These levels are all linked in a whole-part relationship where a parent level can have one or many children, while one

child can only have one parent. For example a campaign has one or many batches and a batch is part of a single campaign. This modular structure is highly extensible by allowing further levels of detail to be added when required. High-level activities seen in the campaign level allow a summary of the key financial, environmental and operational to be created. With each new child level an increasingly accurate value of key operating parameters can be found. For example the sub-task level is able to capture exact values for buffer usage, improving the overall financial, environmental and operational summary. This structure of levels allowed the resulting framework to cost, track and record the progress of a batch in a campaign, as it progresses through the specified number of unit operations, completing the required tasks for each unit operation.

In combined continuous and batch manufacturing processes batches are often divided into smaller volumes in continuous unit operations that are then processed subsequently by batch unit operations, before being recombined into larger volumes again. The existing five level approach described is not capable of capturing the realities of these continuous unit operations, since they lack the ability to track the merging and splitting of batches. The introduction of a new level was required that linked the batches (in a campaign) to not just the unit operation level but also to a new level accounting for possible divisions of that batch (sub-batches). Sub-batches are the child group of a batch and come into existence when a parent batch is split or when multiple existing sub-batches are merged. This means a batch can consist of multiple sub-batches at any one time, which can be processed by different unit operations in the same process sequence, thus conducting different manufacturing tasks in parallel. The new hierarchal structure adopted is shown in **Figure 2.2** in the form of a Unified Modelling Language (UML) class diagram, which represents the main classes implemented into the framework.

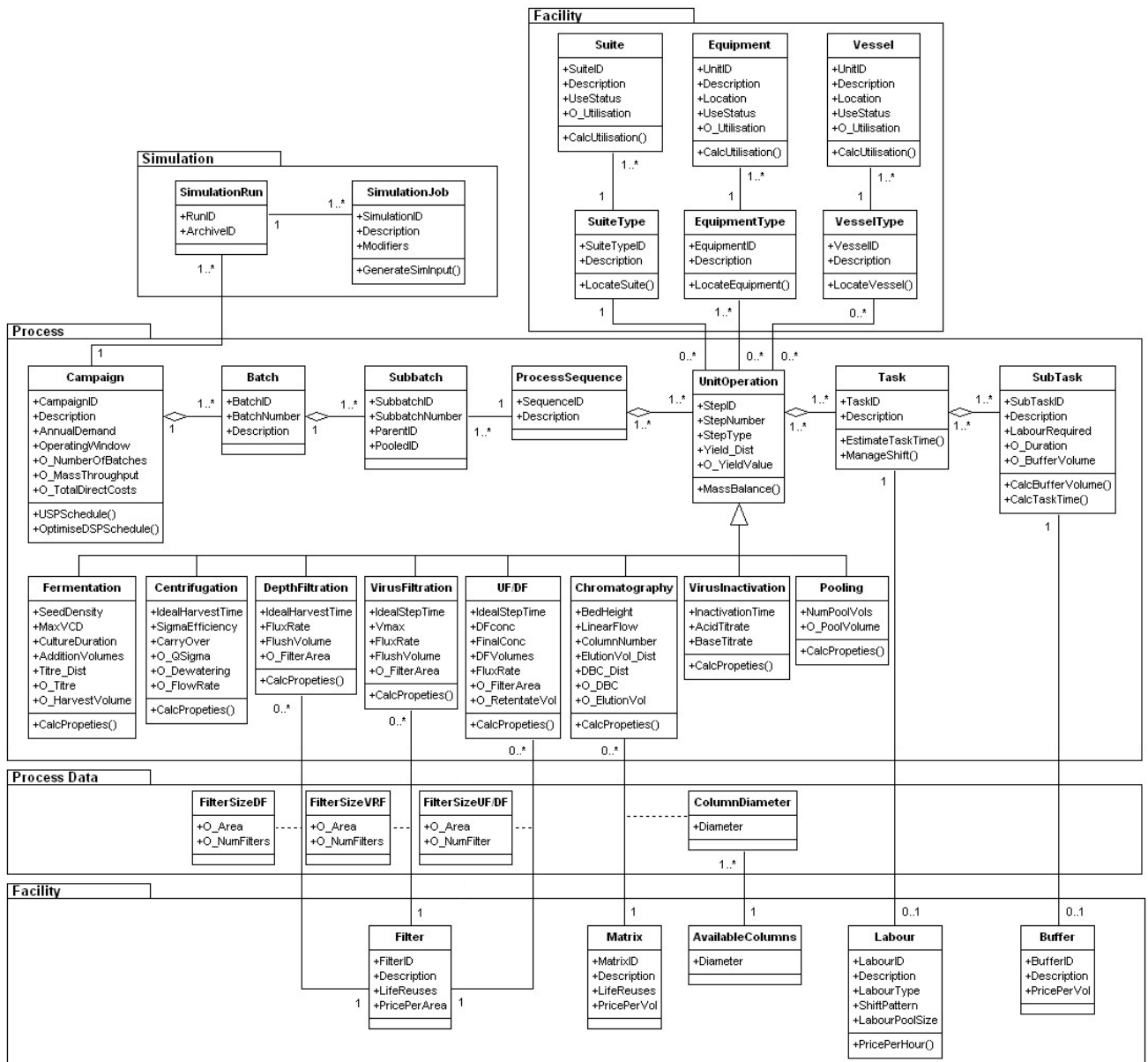


Figure 2.2. UML class diagram representing the main classes and associations in the framework. Each block represents a class (e.g. Suite), with attributes (e.g. SuiteID, Description etc.) and procedures (e.g. CalcUtilisation). Lines symbolise the associations and number the multiplicity between the classes. An unfilled triangle and a solid line represent a generalised relationship (e.g. Chromatography is a type of Unit Operation), with an unfilled diamond and a solid line as a aggregated relationship (e.g. one Process Sequence is made of Unit Operations) and a dashed line as an associated class (e.g. FilterSizeDF exists for a particular Unit Operation and Filter).

The Unified Modelling Language (UML) (Bennett et al. 2010) is a standardised modelling language used to describe object-orientated systems and UML class diagrams are a common method to specify the structure of databases in an object-orientated manner. **Figure 2.2** shows the different objects (classes) and how their affiliations interact between packages (grouped objects). Each block represents a class, which has a list of attributes and operations. The attributes of each class are either input values (attributes with no prefix) or output values calculated within the classes (attributes with a `O_` prefix). Most of the attributes have a single value (attributes with no suffix), however a number of the attributes can have either a single value or a distribution of values (attributes with a `_Dist` suffix). Lines symbolise the associations (relationships) between classes, where the multiplicity of an association is shown as a number on the line (e.g. one *Vessel* has exactly one *VesselType*, while one *VesselType* can have one or more *Vessels* associated with it). A generalisation association (unfilled triangle and a solid line) shows the abstraction of a common feature among the classes, for example the class *UnitOperation* and the classes representing the different process steps. This relationship type can be expressed as *Fermentation* `IS A` *UnitOperation*. There are also a number of aggregation relationships (unfilled diamond and a solid line) showing whole-part associations between classes, where one represents a whole and the others parts of that whole. These whole-part associations determine the hierarchical nature of the framework, where *Campaigns* are the highest level and *Sub-Tasks* the lowest. **Figure 2.2** highlights the seven hierarchal levels used in the framework, where the additional levels (versus five levels) occur from the incorporation of sub-batch recognition into the framework. In this framework the level *Batch Recipe* is replaced by three new levels (Batch, Sub-Batch, Process Sequence) where a *Batch* is made of one or many *Sub-Batches* of which all use only one *Process Sequence*.

2.1.4.2 Database Structure

The SQL database structure used in this framework is derived from the UML class diagram shown in **Figure 2.2**. The UML object-oriented class diagram was converted by a set of guidelines described by Bennett et al, to a relational structured database. The guidelines show how to map the classes and multiplicities from the class diagram to data tables in a relational database. The classes all have a simple data structure and therefore can be directly converted into data tables, where the attributes become fields. The class associations are enforced by the use of primary and foreign keys. For example the *Batch* class is transformed into the *BatchTable*, which has primary key of *BatchID* and a foreign key of *CampaignID*. The common foreign key (*CampaignID*) forms the aggregated relationship between the *Batch* and *Campaign* classes and the primary key (*BatchID*) forms the aggregated relationship between the *Batch* and *Subbatch* classes shown in **Figure 2.2**. This equates to a single record in the *CampaignTable* linked to multiple records in the *BatchTable*.

The data tables can also be grouped along the lines of the packages of classes shown in **Figure 2.2**. The tables in the *Process* package contain all the information directly relative to the manufacture of a batch. The package contains the seven hierarchal layers previously specified. The data in this package ranges from the number and properties of the batches at the highest level to the buffer and labour requirements of an individual sub-task at the lowest level. The variables in the sub-task level are scale-independent, which allows multiple simulation jobs with different batch sizes to be run without requiring extensive data entry. For example buffer requirement is specified as column volumes or filter areas with respect to chromatography or a filtration unit operation. The actual buffer volume is calculated during simulation runs based on the equipment size used.

Information on the infrastructure of the facility is found in the *Facility* package, which contains data on equipment sizes, suite availability, shift patterns and consumable resources (filter membranes, chromatography resins etc.). The tables in this package can be edited separately to the

process package, allowing the impact of different facilities configurations to be investigated with minimal data entry. For example the same process can be run in an 8-hour shift facility or a 24-hour shift facility.

The *Simulation* package contains all the data required to initiate the simulation runs, detailing which variable modifiers to apply on each simulation job. These modifiers can be applied to each of the previous packages, by changing key variable values or distributions. This is a very useful mechanism that allows multiple simulation jobs to be queued in the *SimulationJob* table and trigger the key variables to alter during initialisation of the simulation run without requiring manual data entry between simulation runs. The resulting simulation jobs are distinguished by a unique identifier stored in the *SimulationRun* table, which allows multiple simulation jobs to be easily compared upon completion. This is an important feature that allows multiple simulation results to be compared a key requirement in any analysis of alternative manufacturing strategies.

2.1.4.3 Discrete-Event Simulation Tool

The discrete-event simulation tool in the framework was built in ExtendSim (ExtendSim v8, Imagine That! Inc., San Jose, CA), using a selection of prefabricated, customised and bespoke blocks using the ModL programming language. These simulation blocks contain functions that either carryout simulation events or perform numerical calculations. Appendix **Table A2.1** highlights the principle types of blocks and their functions in the simulation tool.

2.1.4.3.1 Model Structure

Figure 2.3 shows the core structure of the simulation engine, which is formed of three modules: initialisation, router and unit operations. The remaining modules that are not part of the core structure are responsible for the ancillary operations (e.g. buffer preparing, vessel cleaning etc.) are discussed in **Section 2.1.4.3.3**.

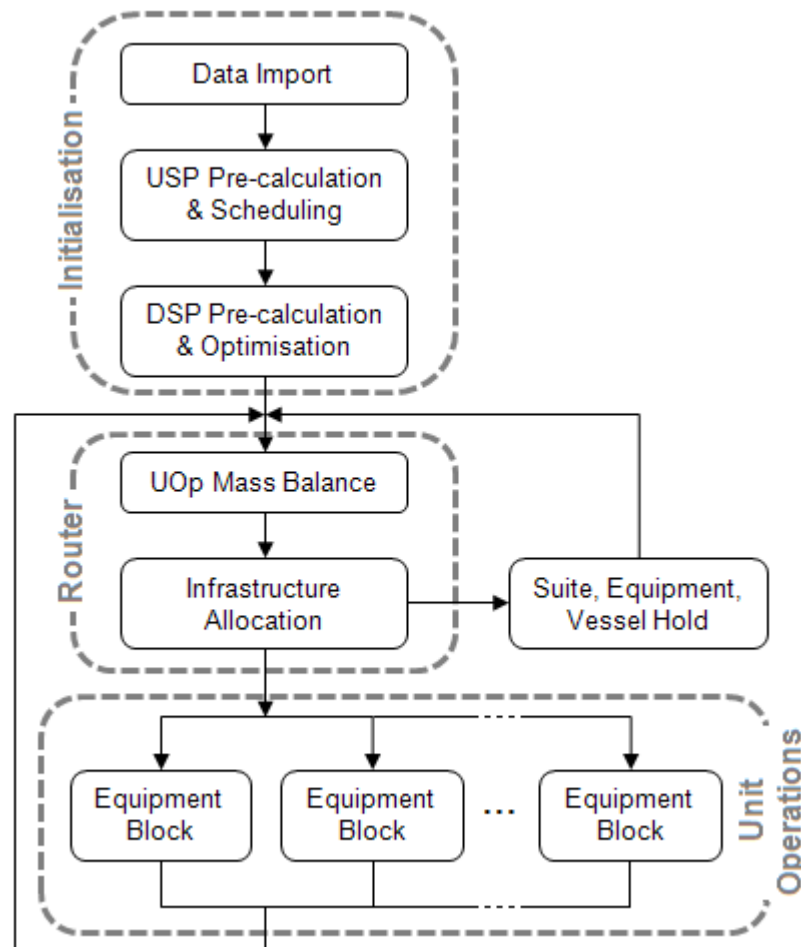


Figure 2.3. Core structure of the simulation engine. USP, upstream processing; DSP, downstream processing; UOp, unit operation.

The simulation begins by running the initialisation module, with the first action being the data import of the relational SQL database via the ODBC into the simulation tools internal database. The data import function corresponds to the SimulationJob class function GenerateSimInput() shown in **Figure 2.2** (Simulation package). This function imports a copy of the

database and then amends field values using the attributes specified in the SimulationJob class. The next step in the module is the USP pre-calculation and scheduling block, this block runs the USPSchedule() procedure seen in the campaign class (process package). The procedure calculates the number of batches that will be required to fulfil the annual demand (kg/year) and also select the size and number of the fermentation reactors based upon cell culture mode and reactor size limitations to achieve this throughput. The procedure then produces a schedule upon which items will enter the seed train to generate a product batch. The items representing product streams are assigned with a number of unique identifiers (item attributes). These include the BatchID, SubbatchID, StepID and stream properties (volume & product concentration). The BatchID will remain constant throughout the life of the item, constantly linking the item to the batch class. The SubbatchID will be altered during the simulation as product streams are split or merged and the consequences will be tracked in the sub-batch table derived from the sub-batch class. The StepID will alter after every unit operation is completed and be updated to the next unit operations StepID based upon the process specified in the process sequence table. The last block in the initialisation module is the DSP Pre-calculation and Optimisation block, which runs the OptimiseDSPschedule() procedure from the campaign class. The procedure optimises the DSP by finding the most cost effective DSP sizing that meets the slot time constraint (time between harvests). The procedure then predicts the buffer demands for all the unit operations and populates a buffer order table to make sure buffer is prepared in time for each task.

After all the procedures in the initialisation module have been completed the item enters the Router module. The Router module contains a series of blocks that calculate the mass balance of the given unit operation and then assign the item to a particular suite before allocating the required equipment and vessels. The UOp Mass Balance block represents the UnitOperation class and runs the MassBalance() procedure calculating the resulting changes to the product stream (volume & concentration). The block also runs the CalcProperties() procedure for all the possible unit operations, calculating the key operating parameters for each unit operation. These parameters are

either stored on the item as attributes or written to the unit operations corresponding data table (e.g. Fermentation table). The next block (Infrastructure Allocation) allocates the facility infrastructure for a particular unit operation. The location and status of suites, equipment and vessels are stored in the database and are called by the Locate() and CalcUtilisation() procedures found in the Facility package. If a suite, piece of equipment or vessel is unavailable (i.e. assigned to a different location, already in use or awaiting CIP) the item is routed to holding, where it waits until the suite, equipment or vessel required is available for use. If all the required infrastructure is available the item is routed to an Equipment block. Each Equipment block corresponds to a record in the Equipment table (Equipment class), allowing the equipment type and properties to be readily modified. This is possible because each Equipment block is identical and is capable of performing all the possible unit operation tasks. This modelling approach follows the key software principal of abstraction, which is the process of selecting all the common features of multiple procedures and combining them into a single procedure. This technique was used to reduce the models complexity and simplify development by placing all the unit operation mass balances and parameter calculations into a single block in the Router (UOp Mass Balance block) and by also combining all the task and sub-task procedures into a single block that can be cloned multiple times (Equipment block).

2.1.4.3.2 Unit Operation Model Structure

The Equipment blocks contain all the necessary functions to simulate all the types of unit operations investigated by the simulation. The Equipment blocks are hierarchal blocks that include a series of further blocks that allocate resources, calculate processing times, manage vessels usage and schedule sub-tasks. **Figure 2.4** shows the detailed structure of the Equipment block, demonstrating the paths taken by the item and the lines of communication between key blocks and resource manager blocks. The Equipment block contains a new type of block (denoted with `D`) that can

delay an item to represent the duration of a task (e.g. filling of a vessel) or the delay an item until the next labour shift. These blocks are actually formed of two simulation blocks a bespoke passing block, which calculates the delay, and an activity block that causes the item delay (see **Table A2.1**).

When the Equipment block first receives an item from the Router, it checks if the unit operation uses a process vessel (e.g. UFDF), if it does the item is delay representing the filling of this vessel. The next block (Pooling Operation) is used in the pooling of sub-batches. The block delays the item until sufficient number of sub-batches has been collected, before releasing the updated item as a new sub-batch and records its creation in the sub-batch table. After these initialisation steps the Equipment block starts to cycle through the sub-tasks required to complete the unit operation. The Sub-task Calculator block runs a number of Sub-task class procedures, including CalcBufferVolume() and CalcTaskTime().

The buffer volumes and durations for the particular sub-task are recorded in the sub-task data table as scale-dependant variables, for example chromatography buffer requirements are specified in column volumes (CVs). The resulting buffer volumes and durations values calculated in the procedures are written in the sub-task data table and as attributes on the item. The item then moves to the Shift Manager where the procedures EstimateTaskTime() and ManageShift() from the Task class are run. These functions calculate the duration of a unit operation task (a group of sub-tasks that must be completed together) and manage the labour shift, which results in one of the three outcomes specified below:

1. There is sufficient time in the shift for the task to continue processing.
2. There is insufficient time in the shift to process the task, the item is delayed until the start of the next shift.
3. There is insufficient time in the shift to process the task, however the task can be completed in over-time and processing can be continued.

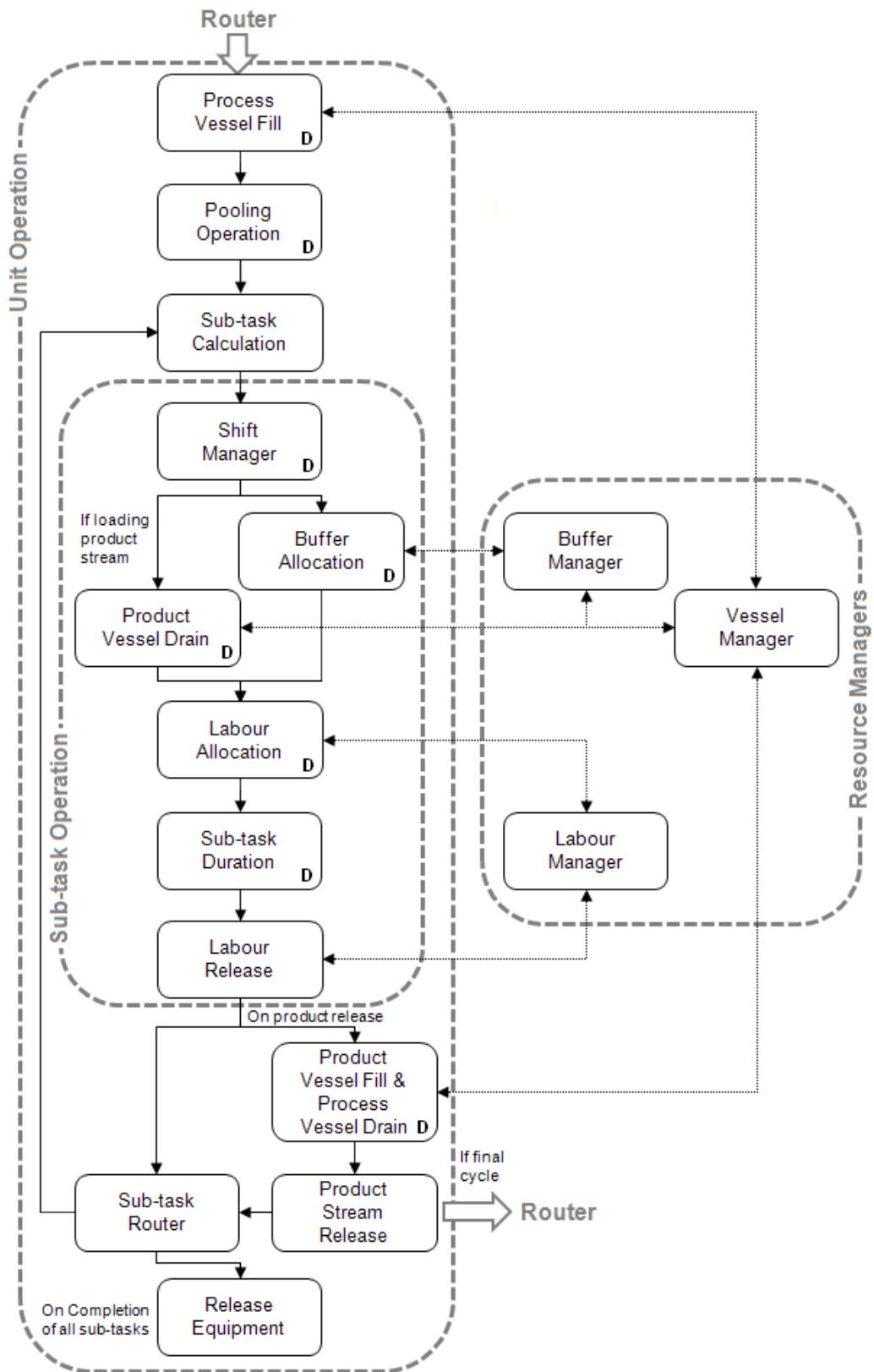


Figure 2.4. The structure of an Equipment block, where the solid line show the items path and the dotted line the lines of communication between blocks and resource managers. Blocks that can delay the items are marked with 'D'.

The item then either requests a volume of buffer based on the stored attribute, or triggers the draining of the previous steps product vessel if loading the product stream. The item then requests the required labour to complete the sub-task and triggers a delay for the task duration (stored as an item attribute) before releasing the labour used. After releasing the labour the item is directed to either the Sub-task Router block or the Product Vessel Fill block. If the sub-task is a product release sub-task the item moves to the Product Vessel Fill block where it records the filling of the current product vessel. The item is then released from the Equipment block and returned to the router to trigger the next unit operation at this point unless it is not the final cycle of a chromatographic operation. The rest of sub-tasks just trigger the item to proceed to the Sub-task Router. The Sub-task Router moves the item onto the next sub-task and either directs the item back to the Sub-task Calculation block or if it is the final sub-task triggers the release of the equipment.

2.1.4.3.2.1 Sub-task Routing

The majority of the unit operations follow the prescribed iterative sub-task progression in a linear fashion, starting at the first sub-task and progressing through all the sub-task until they have all been completed. Chromatography and some continuous unit operations behave slightly differently, due to the use of different types of sub-task routing. **Figure 2.5** demonstrates 'Task Cycling' and shows all the sub-tasks required to complete three cycles in a bind and elute chromatography unit operation. The chromatography sub-tasks are grouped into three tasks; Initialisation, Cycle and Storage. The item completes the initialisation task 'Set-up' before progressing through all the sub-tasks in the 'Cycle' task group. The two highlighted sub-tasks show interactions with the vessel manager block, with the 'Load' sub-task triggering a partial draw of material from the previous steps product vessel and the 'Bag' sub-task triggering a partial fill of the current steps product vessel. When the 'Cycle End' sub-task is reached instead of progressing to the final 'Storage' task, the sub-task count is reset and the item starts the complete

'Cycle' task again. This continues until the final cycle, with the total number of cycles being calculated in the Router block during the MassBalance() and CalcProperties() procedures. The final 'Load' sub-task triggers the complete draining of the previous steps product vessel and the 'Bag' step triggers the product vessel filling and release of the item. The final task 'Storage' is now completed and the Equipment block is released afterwards ready for reassignment.

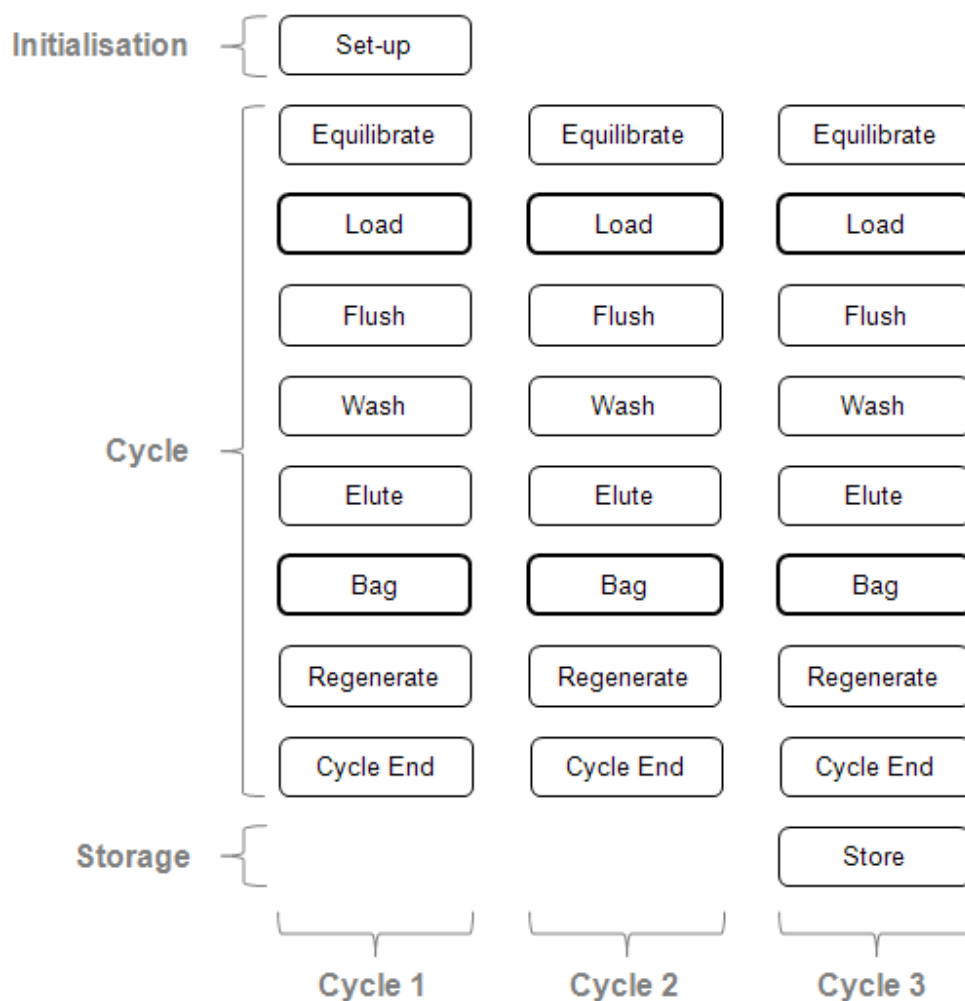


Figure 2.5. Overview of the sub-tasks used in a bind and elute chromatographic unit operation demonstrating the Task Cycling routing methodology. Highlighted sub-tasks show vessel manager interactions.

Continuous unit operations behave differently to the previous two sub-task routing methodologies (linear progression and task cycling). **Figure 2.6** demonstrates the sub-task cycling methodology used in continuous perfusion fermentation unit operations. A fermentation unit operation groups all the sub-tasks into three task groups: Initialisation, Fermentation and Cleaning. The conventional batch fermentation mode progresses through the sub-tasks using the linear progression methodology. The 'Inoculate' sub-task triggers the draining of the previous product vessel (e.g. seed train fermenter) and the 'Bag' sub-task the harvesting of the fermenter and filling of the current product (harvest) vessel. In a continuous perfusion fermentation unit operation media is exchanged daily resulting in daily material harvests. The simulation tool captures this by cycling around a distinct sub-task in a task group, unlike chromatography that cycles the whole task group. During a continuous perfusion fermentation the initialisation task is completed, alongside the 'Inoculate' and 'Ferment' sub-tasks. After this point the item is re-set to run the 'Ferment' and 'Bag' subtasks every day for the duration of the fermentation operation to represent the daily media exchanges and harvests. On the last day of the fermentation operation the material is harvested and then the item is routed to the 'CIP' sub-task allowing the equipment block to be released ready for reassignment. These three types of sub-task routing, linear progression, task cycling and sub-task cycling allow the simulation tool to capture a number of different types of unit operations using the same simulation architecture.

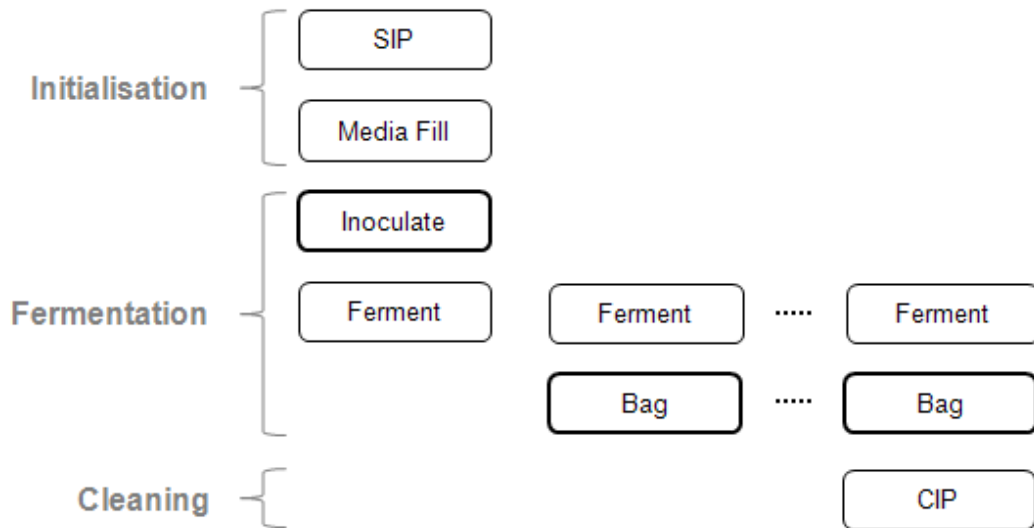


Figure 2.6. Overview of the sub-tasks used in a continuous perfusion unit operation demonstrating the Sub-task Cycling routing methodology. Highlighted sub-tasks show vessel manager interactions, where *Inoculate* triggers the draining of the N-1 reactor and *Bag* triggers the filling of the harvest vessel.

2.1.4.3.2.2 Resource Allocation

The allocation of resources in the Equipment block is controlled by the resource manager blocks. The resource managers receive resource requests from the sub-task blocks and attempt to meet this demand without causing a process delay due to unavailable resources. The Buffer Manager for example communicates with the requested buffer pool represented as a record in the Buffer table and checks if there is enough buffer available for the sub-task. If there is not enough buffer it triggers an additional buffer preparation request, this will be discussed further in **Section 2.5.4.3.3**.

The Labour Manager receives requests and release notifications, which signal when labour has completed a task and is available for reassignment. If labour is not currently available (e.g. being employed already), the Labour

Manager will signal a process delay and only trigger the release of the item when sufficient labour is available.

The Vessel Manager controls the status and properties of the vessels for the unit operations. There are two types of vessels in the model; Process vessels and Product vessels. Process vessels are used in conjunction with a particular piece of equipment (i.e. permeate vessel used in UFDF operations). Product vessels hold the product stream between unit operations (i.e. a chromatography elution pool). When a sub-task block signals the filling of a vessel, the vessels status in the Vessel data table is updated to full and the volume recorded. Upon emptying of a vessel the subtask block again signals the vessel manager, which marks the vessel as empty and awaiting CIP in the vessel data table. The vessel is then queued ready for vessel CIP; this is discussed further in the next section.

2.1.4.3.3 Ancillary Model Operations

There are two key ancillary operations; buffer preparation and vessel CIP. Both these operations use the same principles of abstraction to reduce the complexity of the simulation tool by using a router and equipment block structure. The ancillary operations both use the same architecture, with a single 'Manger' block replacing the Router, which still performs the required parameter calculations and assigns infrastructure if required. The Manager block then directs the item to an Ancillary Equipment block, which behaves exactly the same as the core models Equipment Block, but represents a buffer prep or CIP skid instead.

Buffer preparation orders are specified in the buffer order table during the OptimiseDSPSchedule() procedure run in the DSP Pre-calculation & Optimisation block. The buffer order table interacts with a bespoke remote generation block type and the executive block (see appendix **Table A2.1**) to generate items at the requested buffer order times. Upon the creation of the item (represents a buffer order not a product stream) the Manager block pulls the requested BufferID and order volume from the Buffer Order table and

assigns the resulting values as item attributes. The item is then assigned a buffer preparation (process vessel) and buffer holding vessel (process vessel) before being directed to an available Ancillary Equipment Block, which represents a buffer prep rig. The item then completes all the buffer prep sub-tasks using the linear progression routing methodology. On completion of the last sub-task a signal is sent to the Manager block, which updates the required buffer resource pool and record in the buffer table showing buffer availability. If the Buffer Manager from the core models Equipment Block has a buffer shortage it signals the Manager block, which generates a new item to fulfil the requested shortfall.

Vessel CIP has its own manager block (CIP Manager) which receives signals from the Vessel Manager in the core models Equipment Block, when a vessel empty and marked for CIP. An item is then generated to represent the vessel, it then proceeds to an available Ancillary Equipment Block, which represents a CIP rig. Upon completion of all the CIP sub-tasks the CIP Manager updates the status of the vessel in the vessel data table to available and ready for use.

2.1.4.3.4 Process Models

Up to this point only an overview of the procedures used in the simulation tool has been given. Attention is now turned towards the process models within the procedures used to describe the manufacturing processes. The process models used to describe each unit operations are found in the MassBalance() and CalcPropeties() procedures called in the UOp Mass Balance block. The process models specified in this section are used to calculate the product stream properties and as well as key unit operation parameters, using a number of design and mass balance equations. The key outputs of each process model are summarised in **Table 2.2**, where the common output variables of Output Volume, Output Concentration and Processing Time are not shown.

Table 2.2. Key outputs from the unit operation process models.

Unit Operation	Key Outputs
Fermentation	Total Cell Integral Total Cell Mass Feed Volume Flush Volume Daily Cell Integral Daily Perfusate Volume
Centrifugation	Cell Mass Carry Over Dewatering Level Settling Velocity
Depth Filtration	Filter Area Flush Buffer Volume
Chromatography	Cycle Capacity Number of Cycles Buffer Volumes Number of System & Column Cycles
Viral Inactivation	Base Volume Acid Volume
Virus Removal Filtration	Filter Area Flush Buffer Volume
Concentration & Diafiltration	Filter Area Diafiltration Buffer Volume

Note: Outputs specifically required for the process models of continuous manufacturing technologies are shown in bold.

2.1.4.3.4.1 Fermentation

2.1.4.3.4.1.1 Fed-batch Cell Culture

In a fed-batch fermentation process, a low density of cells is added to a bioreactor containing a nutrient rich environment, which is controlled with further additions to promote sufficient cell proliferation. The increasing cell densities lead to an increase in product protein concentrations and are therefore maximised where possible. Detailed mass-stoichiometry models can be used to establish the key relationships between substrates and product. However this level of detail was deemed to be unnecessary due to the extra level of complexity it would add to the fermentation process models. The key outputs from **Table 2.2** show how the volumes of the media and feed buffer are required but not the chemical composition of these buffers. Therefore a cell integral model was used to calculate the final product concentration and hence derive the bioreactor volumes required for a particular batch throughput (Cacciuttolo 2007). **Figure 2.7.a** shows the relationship between viable cell density (x) and resultant titre (+) for four fed-batch fermentations.

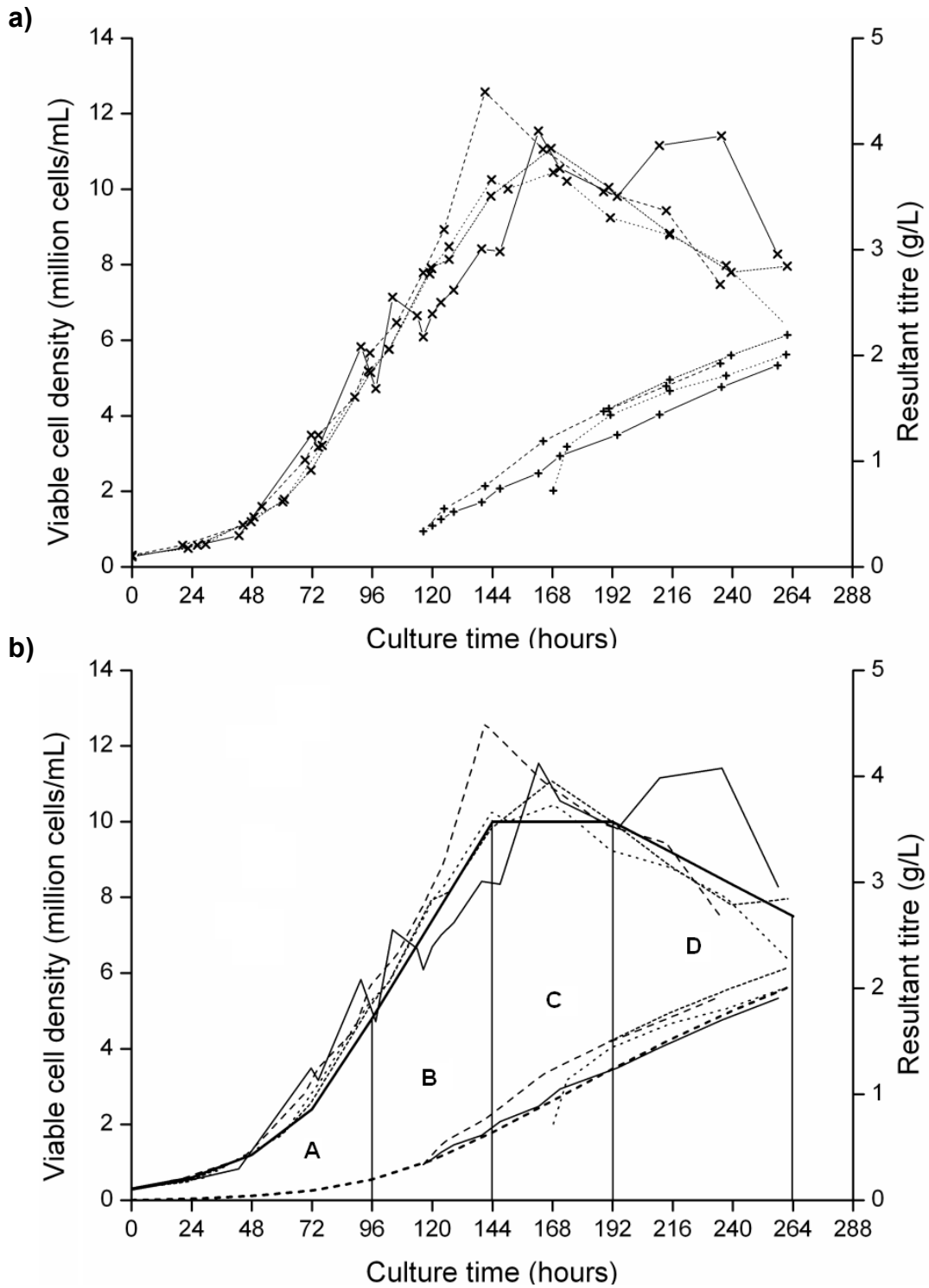


Figure 2.7. Fed-batch fermentation cell culture growth profiles of four fermentation runs a) tracking the viable cell density (x) and resultant product titre (+), and b) with fitted viable cell density (bold black line) and estimated product titres (bold dashed line), with key growth regions highlighted.

Figure 2.7.b highlights how a fed-batch cell culture growth profile can be readily divided into four different growth regions. The titre can be found by calculating the viable cell integral in each of these regions and then based on the cells specific productivity a product concentration can be estimated. Region A represents the exponential growth phase and the Integrated Viable Cell Density (IVCD) (cell hr ml⁻¹) can be calculated using **Equation 2.1**.

$$IVCD_{Exponential} = \frac{X_0}{\mu} ((e^{\mu t_0}) - (e^{\mu t_1})) \quad (2.1)$$

Where

- X_0 = Seeding density (cells ml⁻¹)
- μ = Specific growth rate (hours⁻¹)
- t_0 = 0 hours
- t_1 = 96 hours

Region B shows the deceleration phase; at this point a cold temperature shock is applied to prevent runaway cell proliferation. The viable cell growth is no longer exponential due to the cold shock and cell death. Instead a linear approximation can be made until the maximum Viable Cell Density (VCD) is achieved.

$$IVCD_{Deceleration} = \frac{1}{2} (t_2 - t_1) * ((X_0 e^{\mu t_1}) + X_{Max}) \quad (2.2)$$

Where

- X_{Max} = Maximum VCD (cells ml⁻¹)
- t_2 = 144 hours

The fermentation then maintains the maximum VCD for 48-hour period (Region C – **Equation 2.3**) before the level of cell death increases and the

overall viable cell count declines (Region D – **Equation 2.4**). At this point it becomes a balance between increasing product titre versus high cell death and therefore cell-related impurities. This relationship defines the harvest cell viability, which is normally expressed as the drop in cell density from the maximum VCD.

$$IVCD_{Stationary} = X_{Max} * (t_3 - t_2) \quad (2.3)$$

$$IVCD_{Decline} = \frac{1}{2}(t_4 - t_3) * (X_{Max} + (X_{Max} * Harvest)) \quad (2.4)$$

Where Harvest = % of maximum VCD that triggers harvest

$$t_3 = 192 \text{ hours}$$

$$t_4 = 264 \text{ hours}$$

The resulting cell integrals can be summed and used to establish the expected titre ($Conc_{Ferm}$), using the cells productivity (q_p , $pg \text{ cell}^{-1} \text{ day}^{-1}$).

$$Conc_{Ferm} = IVCD_{Total} * q_p \quad (2.5)$$

Figure 2.7.b demonstrates how **Equations 2.2 – 2.5** can be employed to generate the expected VCD curve (bold black line) and resultant titre (bold dashed line) and how these predictions compare to the actual fermentation data from **Figure 2.7.a**. Now that the cell culture properties have been established the principal output variables can be calculated. The expected titre (**Equation 2.5**) can be used in conjunction with the cell culture harvest volume ($Vol_{Harvest}$) to establish the mass of product synthesised ($Mass_{out}$) and the resulting volumetric productivity ($Productivity_{Vol}$) of the bioreactor

(**Equations 2.6 – 2.9**). However, the volume at harvest is not the same as the initial volume at the start of fermentation (inoculum and media). The final volume incorporates a number of additional feeds. These feeds consist of a number of different buffers added from the fourth day onwards (start of region B) to promote cell proliferation and later product synthesis.

$$Vol_{Feed} = Vol_{Initial} * Feed \quad (2.6)$$

$$Vol_{Harvest} = Vol_{Initial} + Vol_{Feed} \quad (2.7)$$

$$Mass_{Out} = Conc_{Ferm} * Vol_{Harvest} \quad (2.8)$$

$$Productivity_{Vol} = \frac{Conc_{Ferm}}{t_4} \quad (2.9)$$

Where Vol_{Feed} = Total volume of feeds added to bioreactor

$Vol_{initial}$ = Volume of fermenter at t_0 (inoculum and media)

Feed = % increase in volume produced by feed additions

$Vol_{Harvest}$ = Volume of fermenter at t_4 (inoculum, media and feeds)

With all the cell culture parameters now established the principal output variables for volume (Vol_{Out}), concentration ($Conc_{Out}$) and mass of cells (M_{Cell}) can be calculated (**Equations 2.10 – 2.13**). The volume out of the fermentation step is not the same as the harvest volume, due to use of a further flush buffer addition step. The flush buffer addition (Vol_{Flush}) has two aims firstly to rinse the fermentation vessel to maximise product recovery and secondly the addition of collating agents (e.g. EDTA) to prevent excessive product degradation, as the harvest is further processed.

$$Vol_{Flush} = Vol_{Harvest} * Flush_{FB} \quad (2.10)$$

$$Vol_{Out} = (Vol_{Harvest} * (1 - Ev)) + Vol_{Flush} \quad (2.11)$$

$$Conc_{Out} = \frac{Mass_{Out}}{Vol_{Out}} \quad (2.12)$$

$$M_{Cell} = \frac{X_{Harvest}}{VCD_{Harvest}} * Cell_{mass} * Vol_{Harvest} \quad (2.13)$$

Where $Flush_{FB}$ = % of harvest volume required to flush fermenter

Ev = % of volume lost to evaporation

$X_{Harvest}$ = Viable cell density at harvest

$VCD_{Harvest}$ = Cell viability at harvest

$Cell_{Mass}$ = Mass of a single mammalian cell

2.1.4.3.4.1.2 Perfusion Cell Culture

In a perfusion cell culture process, a low density of cells is added to a bioreactor containing a nutrient rich environment, which is controlled with continuous media exchanges to promote sufficient cell proliferation. The increasing cell densities lead to an increase in product protein concentrations, which is maintained to maximise product expression. The continuous media exchanges result in a daily volume of harvested material enriched in the product protein, which is then purified.

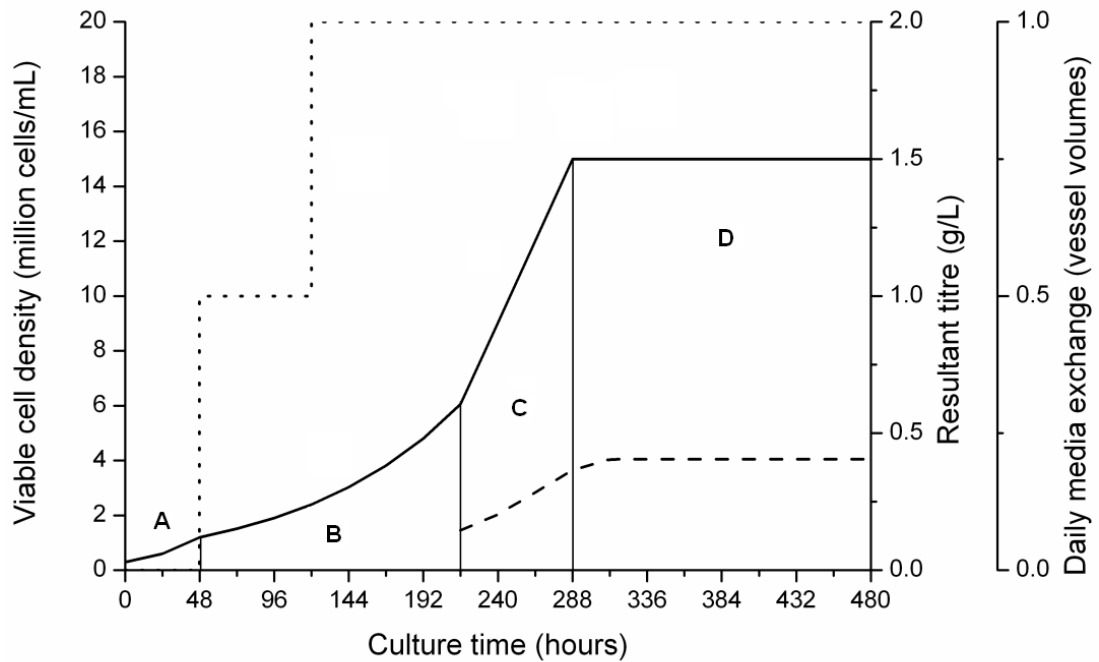


Figure 2.8. Continuous perfusion fermentation cell culture growth profile for viable cell density (black line), estimated product titre (dashed line) and perfusion rate (dotted line), with key growth regions highlighted. The growth profiles shown were derived from discussions with Morten Munk, Christoffer Bro and Jacob Jensen (CMC biologics, Copenhagen, Denmark) and based on valid fermentation data.

The cell integral methodology described for fed-batch cell culture can also be utilised for continuous perfusion cell cultures but with some subtle differences. Instead of establishing the total cell integral for the total duration of the cell culture, a daily cell integral is used to calculate the product titre for that day of production. Region A shown in **Figure 2.8** represents the batch growth phase where the cells grow exponential using the existing nutrients in the media. Perfusion is started after 2 days and the media nutrients are refreshed by the addition of new media and removal of spent media. At this point a cold shock is applied to the cell culture to prevent uncontrolled cell proliferation due to the increase in nutrients, this results in the reduced rate of growth seen in region B. The perfusion rate starts at 0.5 vessel volumes per

day (vv/day) and increases to 1 vv/day after the initial cell doubling to maintain the progression of cell proliferation. Region C highlights the deceleration phase where the viable cell growth is no longer exponential due to the limitation of nutrients and increase in cell death. At this point (day 9) the cells density is sufficient to generate daily harvests with sufficient product concentrations to make it worthwhile to purify. The fermentation then maintains the maximum cell density in the steady phase represented by region D, which will last to the end of the cell culture duration selected.

The daily perfusate volumes from the continuous perfusion cell culture are only collected after day 8 (first on day 9) during the deceleration phase when the product concentration values are required. Therefore the daily cell intergral is only required from day 9, this is achieved by establishing the viable cell density at the end of the batch (X_{Batch}) and perfusion ($X_{Perfusion}$) growth phases (region A and B) using **Equations 2.14 and 2.15**.

$$X_{Batch} = \frac{X_0}{\mu_{Batch}} (e^{\mu_{Batch}t_0}) \quad (2.14)$$

$$X_{Perfusion} = \frac{X_0}{\mu_{Perfusion}} (e^{\mu_{Perfusion}t_1}) \quad (2.15)$$

Where	X_0	= Seeding density (cells/ml)
	μ_{Batch}	= Batch phase specific growth rate (hours ⁻¹)
	$\mu_{Perfusion}$	= Perfusion phase specific growth rate (hours ⁻¹)
	t_0	= 48 hours
	t_1	= 216 hours

For daily cell integrals required during deceleration phase (region C) and steady state (region D) **Equations 2.16 - 2.18** are employed.

$$X_i = X_{i-1} + \left(\frac{X_{Max}}{n}\right) \quad (2.16)$$

$$IVCD_{PreSteadyState} = \frac{1}{2}(X_{i-1} + X_i) \quad (2.17)$$

$$IVCD_{SteadyState} = X_{Max} \quad (2.18)$$

Where X_{Max} = Maximum viable cell density (cells/ml)
 X_i = Viable cell density on day i (cells/ml)
n = Number of days culture is deceleration phase

For the first media exchange on day 9 X_{i-1} equals $X_{Perfusion}$. The resulting daily cell integrals can be used to establish the daily harvest output volume (Vol_{Out}) and target protein product concentration ($Conc_{Out}$) of the bioreactor. The volumetric productivity ($Productivity_{Vol}$) of the perfusion bioreactor is calculated with **Equation 2.9**, where $Conc_{Ferm}$ is the average concentration of product harvested from day 9 to the final day of the culture.

$$Conc_{Perfusion} = IVCD_i * q_p \quad (2.19)$$

$$Mass_{Out} = Conc_{Perfusion} * Vol_{Initial} \quad (2.20)$$

$$Vol_{Out} = Vol_{initial} * PR \quad (2.21)$$

$$Conc_{Out} = \frac{Mass_{Out}}{Vol_{Out}} \quad (2.22)$$

Where $Conc_{Perfusion}$ = Expected daily titre
 q_p = Cells productivity ($pg \text{ cell}^{-1} \text{ day}^{-1}$).
 $Vol_{initial}$ = Volume of fermenter at t_0 (inoculum and media)
PR = Perfusion rate (vessel volumes)

2.1.4.3.4.2 Centrifugation

Centrifugation is used to separate suspended solids from a heterogeneous mixture based on their differences in size and density. Centrifugal forces are used to increase the settling velocities of heavy particulates (cells and cell fragments) to produce a solid based sediment and a supernatant depleted in solids. **Table 2.2** shows the key output parameters generated by the centrifugation process model. Where the settling velocity (u_g) is used to establish the key operating parameters (sigma efficiency) and the dewatering level is used to assess step performance. The remaining mass balance equations are shown in the appendix.

$$u_g = \frac{(\rho_{Solid} - \rho_{Liquid}) * CutOff^2 * g}{18\eta} \quad (2.23)$$

$$M_{sediment} = M_{Cell} - (M_{Cell} * CarryOver) \quad (2.24)$$

$$Dewatering = \frac{(M_{Sediment} / \rho_{Solid})}{(Vol_{Sediment} + (M_{Sediment} / \rho_{Solid}))} \quad (2.25)$$

- Where ρ = Density of the solid or liquid phase
- CutOff = Mass Cut Off achieved by the centrifuge
- η = Viscosity
- M = Mass of key component

2.1.4.3.4.3 Chromatography

2.1.4.3.4.3.1 Batch Chromatography

Chromatography is a high-resolution technique, which separates complex mixtures based on differences in binding specificity, ionic charge and hydrophobicity. The simulation tool captures two modes of chromatography; bind and elute (B&E) where the product is bound on to the resin and eluted by a change in buffer conditions, and flow through (FT) where the product passes through the column and contaminants are bound instead.

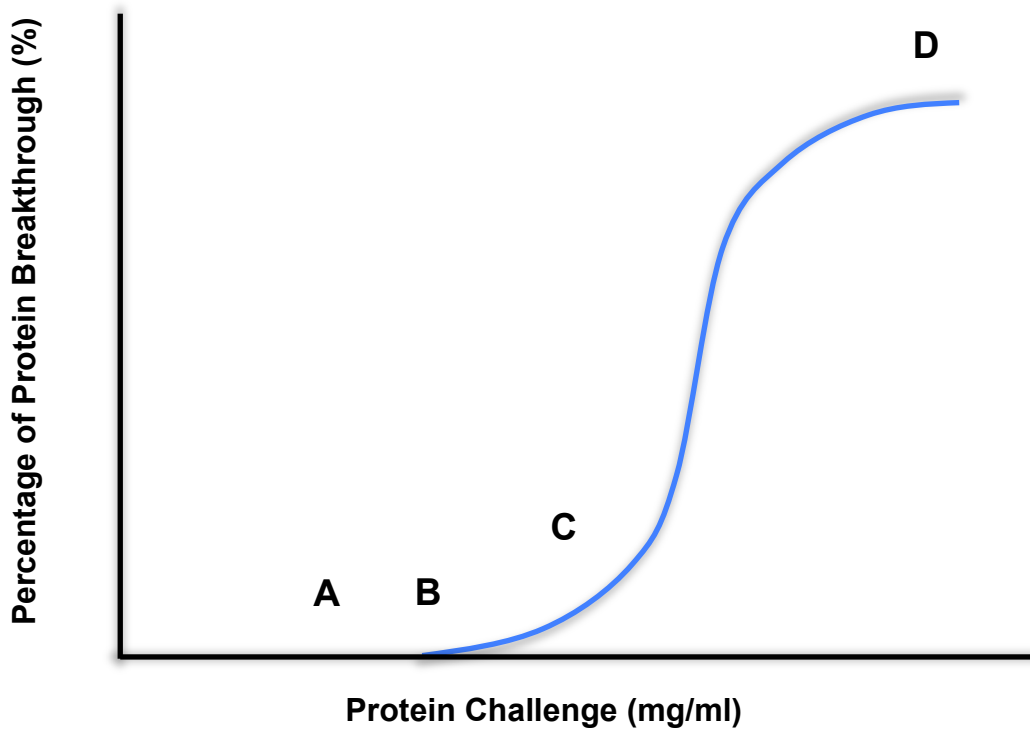


Figure 2.9. Protein breakthrough curve for a column operated in bind & elute mode, highlighting A) the dynamic binding capacity used in manufacturing (90% of 1% breakthrough), B) the point of breakthrough (1% breakthrough), C) 10% breakthrough and D) resin saturation.

A typical chromatography column operated in bind and elute mode is loaded up to 90% of 1% breakthrough capacity, underutilising the resin's capacity (**Figure 2.9**). This strategy is used to offer a safety margin to reduce product losses in the flow-through during loading caused by product concentration variation and variation in dynamic binding capacity (ligand loss, fouling, lot-to-lot variation etc...). **Figure 2.9** also highlights the actual DBC of the resin at the point of breakthrough (B), the point of 10% breakthrough (C) and the loading required to fully saturate the resin (D). After point B some of the protein starts to breakthrough in the flowthrough, as the resin no longer captures it. By point D the breakthrough curve levels off as no more protein is retained due to saturation of the resin. This makes calculating DBC more complex than just recording the value shown on the x-axis (which is possible for point A & B). The DBC can be found at points C and D by calculating the integral of the breakthrough curve, where the area beneath the curve is the unbound protein and the area above the curve the bound protein. The integral of the total bound protein can be used to establish the DBC. A column operated in flowthrough mode is still assigned a protein based DBC, even though it is not binding the target protein but contaminants instead. To simplify the scale-up and operation of flow-through columns a protein based DBC is defined using the same technique shown in **Figure 2.9**. The figure would display the breakthrough of contaminants rather than target protein and the protein DBC selected is for a point prior to the breakthrough of the contaminants.

Equations 2.26 - 2.28 demonstrate how the cycle capacity (Cap_{Cycle}), column volume (Col_{Volume}) and Dynamic Binding Capacity (DBC) can be used to determine the number of cycles (N_{Cycles}) a column is used during a batch.

$$Cap_{Cycle} = Col_{Volume} * DBC \quad (2.26)$$

$$N_{Cycles} = \frac{M_{In}}{Cap_{Cycle}} \quad (2.27)$$

$$N_{Cycles} = Ceiling(N_{Cycles}, 1) \quad (2.28)$$

The number of column cycles calculated using **Equation 2.27** may not be a whole number; but to reflect reality (not possible to process a fraction of a cycle) a ceiling function is applied to generate a whole integer value for the number of cycles (**Equation 2.28**). The buffer requirements for each chromatography sub-task (i) are specified in column volumes (CV); a scale dependant variable. These values are then transformed into buffer volumes using **Equation 2.29**.

$$Vol_i = Col_{Volume} * CV_i * N_{Cycles} \quad (2.29)$$

$$Vol_{Cycle} = Vol_{In} + Vol_{Flush} \quad (2.30)$$

The final volume out of the chromatography step depends on the mode of operation. The final volume for the B&E operated chromatography steps is calculated using **Equation 2.29**, where CV_i equals the elution peak volume. The defined volume of elution buffer causes the dissociation of the product from the resin, which in reality is either a specified volume for collection or a volume collected based on UV stop gate (when protein UV signal decreases below threshold the elution flowthrough is no longer collected). **Equation 2.30** shows the calculation required for a column operated in FT mode, where the flush volume (Vol_{Flush}) is found using **Equation 2.29**. The remaining scheduling and mass balance equations are shown in the appendix.

2.1.4.3.4.3.2 Continuous Chromatography

The previous section highlighted how a typical chromatography column operated in B&E mode is only loaded up to 90% of 1% breakthrough capacity, underutilising the resin's capacity. This loading regime results in the entry (top) of the column being saturated and the exit (bottom) unsaturated upon completion of loading, leading to an excess buffer consumption caused by washing, elution and cleaning of the unsaturated column portion. An approach to increase utilisation would be to divide the column into multiple portions and wash and elute the saturated top portion of the column and continue loading the unsaturated portion of the column until saturated. This principle is applied in semi-continuous chromatography, which allows the columns to be loaded to a higher binding capacity, reducing the resin volume required and the overall buffer consumption

This section describes the updates made to the batch chromatography process model to account for the operation of a semi-continuous chromatography system. The same mass balance equations are utilised for both the batch and PCC chromatography systems. However, there are some additional equations due to the extra columns. For example **Equation 2.28** calculates the number of cycles required to process the total product mass per batch. For a semi-continuous chromatography step this value equates to the total number of cycles completed by all the columns ($N_{Columns}$), so the number of cycles calculated in **Equation 2.28** is equal to the number of system cycles ($N_{System\ Cycles}$). The number of cycles an individual column (N_{Cycles}) is utilised for can be found using **Equation 2.31**.

$$N_{Cycles} = \frac{N_{System\ Cycles}}{N_{Columns}} \quad (2.31)$$

The remainder of the batch chromatography equations can be utilised in the same manner for the semi-continuous chromatography system. However a number of input parameters will be different, most notably the DBC. The

higher DBC is realised by loading the column to full saturation represented by point D in **Figure 2.9**. To prevent loss of the protein that breakthroughs from the primary column, the load effluent is passed over a secondary column to capture any protein. Upon full saturation of the primary column, the secondary column becomes the new primary column with respect to loading and the previous primary column is washed and eluted. This column switching mechanism is explored further in **Chapter 4**.

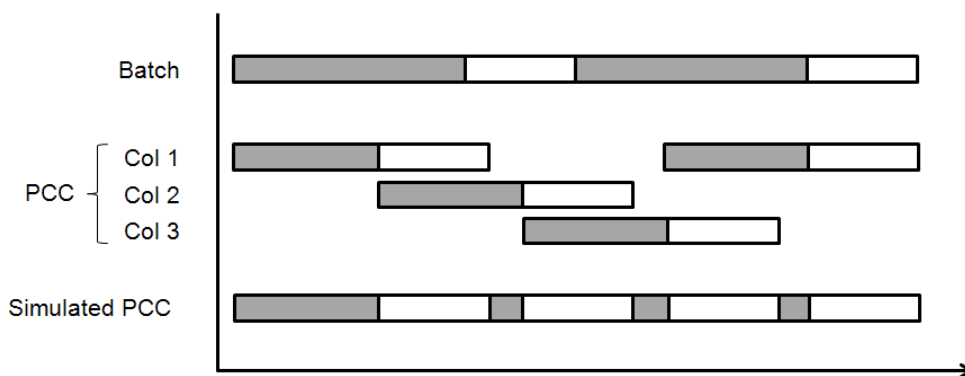


Figure 2.10. Schedule of the loading (grey) and non-loading (white) processes for the batch, 3-column periodic counter current chromatography system and the simulations interpretation of the periodic counter current chromatography system.

Figure 2.10 demonstrates how a semi-continuous system processes a number of operations at the same time in different columns, where a grey block represents the loading of a column and a white block the non-loading operations. The semi-continuous chromatography system represented in **Figure 2.10** is the GE Healthcare (Uppsala, Sweden) 3-column periodic counter current (PCC) system. To avoid major changes to the structure of the equipment blocks and follow the software principal of abstraction adopted throughout the development of the simulation framework. The semi-continuous chromatography's systems resource requirements (buffers & labour) were converted into a single column system, which the current

equipment block and sub-task routing rules previously highlighted can be applied without alteration. This was achieved by reducing the apparent duration of the loading operations, to the loading time remaining after the non-loading operations have been completed. **Figure 2.10** shows the reduced loading time for the simulated semi-continuous chromatography system and can be best visualised by overlaying all the columns of the system. This methodology made it possible to convert multiple parallel operations into a single operations schedule, but still request the right amount resources at the correct time. The design and optimisation of a semi-continuous chromatographic system with respect to switch times, possible DBCs and column sizing is explored in **Chapter 4**.

2.1.4.3.4.4 Viral Inactivation

The remaining viral clearance step (Viral Inactivation) often occurs after Protein A chromatography, because the elution pool will already be at a low pH due the elution buffers composition. The step therefore requires less acid to achieve the required inactivation pH. After the inactivation time the product streams pH is adjusted ready for the next processing step. The following equations demonstrate how the volumes of acid and base required are calculated, using the molar ratios ($Titrate_{Acid}$ and $Titrate_{Base}$) to establish the amount of titrant to add.

$$Vol_{Acid} = Vol_{In} * Titrate_{Acid} \quad (2.32)$$

$$Vol_{Base} = Vol_{In} * Titrate_{Base} \quad (2.33)$$

2.1.4.3.4.5 Membrane Filtration

Filtration exploits differences in particle sizes to separate target particles from complex mixtures. The simulation tool captures two modes of filtration; cross-flow used in concentration and diafiltration operations and dead-end filtration used in depth and virus retention filtration.

2.1.4.3.4.5.1 Depth Filtration

Depth Filtration (DF) is often used in primary recovery to remove the fine cell particles and reduce key containments still present in the feed stream after centrifugation. When a depth filter is run in series with a centrifuge the average flow rate across the filter unit should match the centrifuge flow rate to remove the requirement for a holding vessel. At the same time the resulting filter area are must of sufficient size to prevent contaminant breakthrough. **Equations 2.34 and 2.35** both calculate a filter area ($Area_{DF}$). The largest value for the resulting areas is then selected. The resulting area is then rounded to the nearest available unit size for a depth filter using the ceiling() function (**Equation 2.36**). The remaining mass and scheduling equation are shown in the appendix.

$$Area_{DF} = Q_{In} / J_{DF} \quad (2.34)$$

$$Area_{DF} = Vol_{In} / V_{max} \quad (2.35)$$

$$Area_{DF} = Ceiling(Area_{DF}, UnitSize) \quad (2.36)$$

Where Q_{In} = Flowrate into the unit

J_{DF} = Average flux rate

V_{max} = Max volumetric challenge before breakthrough

2.1.4.3.4.5.2 Viral Retention Filtration

Viral Retention Filtration (VRF) is one of the two dedicated viral clearance steps required in biopharmaceutical manufacturing. The principle aim is to retain all the possible viral bodies in the feed stream and therefore generate a permeate stream that contains no viral bodies or viral fragments. VRF is also operated in the dead-end filtration mode but the required filter area is calculated using **Equation 2.37**, which actively over-scales the filter area ($Area_{VRF}$) by a pre-defined safety margin to make sure the filter is never over-challenged.

$$Area_{VRF} = \left(\frac{Vol_{In}}{t_{VRFTarget}} \right) * \left(\frac{t_{VRFTarget}}{V_{Max}} + \frac{1}{J_{VRF}} \right) * (1 + Safety) \quad (2.37)$$

Where $t_{VRFTarget}$ = Target processing time for the step

Safety = % Over-scale applied to filter area

The resulting filter area is then rounded to the nearest available unit size using the ceiling function shown in **Equation 2.36** and the remaining mass balance equation are shown in the appendix.

2.1.4.3.4.5.3 Concentration and Diafiltration

Concentration and Diafiltration (UFDF) operates in tangential flow mode, where the product stream passes through semi-permeable membrane whilst under tangential flow across the membrane. The UFDF operation is divided into three distinct phases of operation; Concentration, Diafiltration and Final Concentration. The first phase (Concentration) concentrates the feed stream to the required product concentration ($Conc_{DF}$) used during the diafiltration phase. The resulting volume ($Vol_{DFRetentate}$) then undergoes diafiltration,

where the volume of diafiltration buffer ($Vol_{DFBuffer}$) can be found using **Equation 2.38** and the number of buffer volumes you intend to exchange (DFVolumes).

$$Vol_{DFRetentate} = \frac{Vol_{In} * Conc_{In}}{Conc_{DF}} \quad (2.38)$$

$$Vol_{DFBuffer} = DfVolumes * Vol_{DFRetentate} \quad (2.39)$$

If the final product concentration ($Conc_{Final}$) is higher, a further concentration step is employed to establish the final product stream volume ($Vol_{Retentate}$).

$$Vol_{Retentate} = \frac{Vol_{DFRetentate} * Conc_{DF}}{Conc_{Final}} \quad (2.40)$$

The final process time can be found by summing all the processing times calculated in **Equations 2.41 - 2.43**, with the remaining mass balance equations shown in the appendix.

$$t_{Concentration} = \frac{Vol_{In} - Vol_{DFRetentate}}{J_{Concentration} * Area_{UFDF}} \quad (2.41)$$

$$t_{DF} = \frac{DfVolumes * Vol_{DFRetentate}}{J_{DF} * Area_{UFDF}} \quad (2.42)$$

$$t_{Final} = \frac{Vol_{DFRetentate} - Vol_{Retentate}}{J_{Final} * Area_{UFDF}} \quad (2.43)$$

2.1.4.3.5 Optimisation Protocols

The simulation was operated in two facility sizing modes; Rating mode, where the facility size (equipment and vessels) was fixed and Design mode, where the simulation tool decided the facility size. During initialisation of the simulation tool the item passes through two blocks, the USP Pre-calculation and Scheduling block and DSP Pre-calculation and Scheduling block. These two blocks contain the facility scaling procedures for the USP and DSP unit operations. When the simulation tool was operated in design mode it called these procedures to scale the USP and DSP, however these procedures were bypassed in rating mode.

The USP unit operations were sized during design mode when the Campaign class procedure `USPSchedule()` was called. The procedure runs an iteration sequence constructed of the principle USP scaling equations. The first equation (**Equation 2.44**) calculated the batch time (t_{Batch}), the time the fermenter is in use, with respect to cell culture time ($t_{\text{CellCulture}}$) and CIP downtime (t_{Downtime}). The resulting batch time was then called via **Equation 2.45** to establish the number of batches (N_{Batches}) that can be achieved in the prescribed operating window (N_{Days}). The final equation (**Equation 2.46**) in the iteration established the required bioreactor volume (Vol_{Ferm}) based upon the mass demand (M_{Demand}), process yield ($\text{Yield}_{\text{Process}}$) and expected bioreactor productivity ($\text{Conc}_{\text{Ferm}}$) from **Equation 2.12 or 2.22**. Once all these equations were run the iteration was subject to a conditional statement with a Boolean condition that dictated if a further iteration was required. **Equation 2.47** highlights this condition, which establishes if the calculated bioreactor volume is larger than the maximum constraint set ($\text{Vol}_{\text{FermMax}}$). If the calculated volume was greater than the maximum constraint then the number of fermenters was increased by one and the iteration was reinitiated at **Equation 2.44**.

$$t_{Batch} = \frac{t_{CellCulture} + t_{Downtime}}{N_{ferms}} \quad (2.44)$$

$$N_{Batches} = FLOOR\left(\frac{N_{Days}}{t_{Batch}}, 1\right) \quad (2.45)$$

$$Vol_{Ferm} = \frac{(M_{Demand}/N_{Batches})/Yield_{Process}}{Conc_{Ferm}} \quad (2.46)$$

$$if(Vol_{Ferm} > Vol_{FermMax}) \text{ then } N_{Ferm} + 1 \quad (2.47)$$

The use of the prescribed iteration sequence allowed the simulation tool to establish the required number and scale of bioreactors to meet defined mass throughputs under a number of constraints (Max bioreactor volume, operating window, bioreactor productivity etc.). The procedure also calculated the scale of the seed train bioreactor and predicted when to inoculate the first seed bioreactor to make sure a new batch was ready for DSP purification every batch interval (t_{Batch}). The USPSchedule() procedure adds great versatility to the simulation tool by allowing a number of different demand scenarios to be simulated without constantly needing to manually redefine the facility scale between simulations.

The DSP unit operations were sized during design mode when the Campaign class procedure OptimiseDSPSchedule() was called. The aim of the procedure was to establish the optimal process configuration by selecting the scales of DSP equipment that resulted in the minimum batch cost but still met the DSP slot length (time between harvest volumes). The procedure behaves like the router in the simulation engine, but instead of routing items, the procedure called the Unit Operation, Task and Sub-task class procedures to estimate mass balances, buffer costs and task durations. These functions were called within the procedure and not by simulation events and therefore only generate parameter values for an unconstrained facility. This mimics the approach seen in static spreadsheet based simulation tools and only results in an estimation for time and cost, where resources are not constrained. This approach was still able to track shift changes but is unable to capture the

delay of a key resource, however this was sufficient for comparing multiple process configurations in an optimisation procedure.

The procedure starts by generating a decision space for all the equipment size configurations that can be implemented in the facility. The principle equipment size variable investigated was the size of the chromatography columns with respect to the columns diameter. The remaining DSP unit operations are filtration based and are scaled based on upon the ideal filter time constraint (i.e. the filter step must be completed in a defined time period). The number of possible configurations options ($N_{Options}$) was therefore dependent on the number of chromatography steps (N_{Steps}) and the number column diameter sizes ($N_{ColDias}$) and can be calculated using **Equation 2.48**.

$$N_{options} = N_{ColDias}^{N_{Steps}} \quad (2.48)$$

Equation 2.48 highlights the potentially high number of process configurations that needed to be investigated. For example a process sequence with three chromatographic steps and a facility with ten possible column sizes resulted in one thousand process configurations. If the procedure was used to estimate the time and cost for every process configuration for the whole manufacturing campaign (multiple batches), then the computational burden would be very high. To address these computational time and power concerns, the procedure only tracked a single 'Master Sub-batch'. This methodology reduced the computational burden of the procedure by running a single sub-batch instead of the potentially high number of batch and sub-batches that are present in a complete manufacturing campaign. The procedure uses the time and costs from a single sub-batch ('Master Sub-batch') to extrapolate the complete batch cost. For example if a chromatography step is required to process multiple sub-batches the batch cost was increased by the number of sub-batches that would be processed.

The cost and time data generated for all the process configurations is then stored in an array along with a number of key process parameters shown below.

- DSP equipment scales
- Number of chromatography cycles
- Duration of chromatography processes
- Overall process time
- Batch cost

The process configuration parameters were then used to select the optimal process configuration. The primary aim of the procedure was to establish the most cost effective process configuration, however it also had to meet a number of processing rules. For example the Protein A chromatography steps processing time must not surpass the maximum harvest cell culture fluid holding time. Once all the selection criteria set by the user were applied, a pool of viable process configurations would remain. From these viable process configurations the most cost effective option was selected and labelled as the optimal process configuration. The procedure then used the optimal process configuration to predict the order times and volumes for all the buffer requests made during the manufacturing campaign. These values were then used to populate the buffer order table, which in conjunction with the buffer resource manager block, made sure buffers are made in time for each task.

2.1.4.3.6 Cost Models

The key financial performance metrics, used to compare alternative manufacturing strategies, were the Fixed Capital Investment (FCI) and the Cost Of Goods (COG). The simulation tool employed two cost models to establish the FCI and COG. This section summarises the two cost models used.

2.1.4.3.6.1 Fixed Capital Investment

The fixed capital investment was approximated using a factorial method, which is often attributed to Lang (1948). The Lang factor method for cost estimation uses a cost factor (LangFactor) derived from previous construction projects, relating the capital outlay used in facility construction to the cost of equipment in the facility (Lang 1948). Therefore the fixed capital investment (FCI) can be given as a function of total equipment purchase cost ($Cost_{Equipment}$) shown in **Equation 2.49**. Lang Factor values depend on the type of facility. For chemical facilities used for liquid or solids processing, values in the range of 3-5 are often used (Peters et al. 2006; Sinnott et al. 2005). For biopharmaceutical facilities much larger values are seen, ranging from 3.3-8.1 (Farid 2007; Novais et al. 2001). The high Lang Factors used in biopharmaceutical facilities are due to the requirement to maintain higher GMP suite contaminant level ratings, which result in increased HPAC/HVAC costs.

$$FCI = LangFactor * \sum Cost_{Equipment} \quad (2.49)$$

To make more accurate facility cost estimates, the cost factors that are normally combined to create a Lang Factor value were considered individually. **Table 2.3** shows a breakdown of these capital investment costs incurred in the construction of a conventional (stainless steel dominated) and disposables-based facility. The cost factors were then combined into a more accurate single Lang factor for a biopharmaceutical facility.

Table 2.3. Biopharmaceutical facilities capital investment factors and corresponding “Lang” factors

	Factor Description	Conventional / (Conventional TEPC)*	Disposable / (Conventional TEPC)*	Disposable / (Disposable TEPC)
1	Equipment (incl. utilities) (Total Equipment Purchase Cost)	1	0.2	1
2	Pipework and installation	0.9	0.3	1.49
3	Process control	0.37	0.37	1.85
4	Instrumentation	0.6	0.4	1.98
5	Electrical power	0.24	0.24	1.2
6	Building works	1.66	1.33	6.64
7	Detail engineering	0.77	0.39	1.93
8	Construction and site management	0.4	0.30	1.5
9	Commissioning	0.07	0.07	0.35
10	Validation	1.06	0.53	2.65
	Contingency factor	1.15	1.15	1.15
	“Lang” Factor	8.13	4.73	23.67

*Adapted from Novais et al 2001

To use the described factorial costing methodology the total equipment purchase cost must be known. The purchase cost of a piece of equipment was estimated using the R factor method (six-tenths rule); which relates the cost and size of the equipment (Williams 1947). **Equation 2.50** highlights this exponential scaling relationship, where the unknown equipment cost ($Cost_1$) is related to a known cost ($Cost_2$) and the ratio of their sizes ($Size_1/Size_2$) to the power of a coefficient (C).

$$Cost_1 = Cost_2 * \left(\frac{Size_1}{Size_2}\right)^C \quad (2.50)$$

Historically an exponential scaling coefficient value of 0.6 was commonly used. However, Remer et al (1991) warns against the use of a single scaling coefficient for multiple types of equipment, by demonstrating how the scaling coefficients for biopharmaceutical equipment range between 0.37 and 1.16 (Remer and Idrovo 1991). **Table A2.2** highlights the equipment dependant exponential scaling coefficients, sizes and costs used throughout this work. Most equipment types are linearly scalable, however their purchase cost is not always. For example, small-scale bioreactors costs are dominated by the ancillary components not the vessel, whereas for larger scale bioreactors the vessel cost dominates the overall purchase cost. This phenomenon was accounted for in the tool, and as such is reflected in Table A2.2, where some pieces of equipment have multiple costing models. The required costing model was selected based on the equipment size and low and higher selection thresholds corresponding to the different costing models.

2.1.4.3.6.2 Cost Of Goods

Manufacturing costs or Cost of Goods (COG) typically comprise of indirect costs and direct production costs. The indirect costs are a fixed overhead which is related to the equipment purchase cost ($Cost_{Equipment}$), fixed capital investment (FCI) and project life span ($t_{Project}$) as shown in **Equations 2.51 – 2.54**. These values were then summed to calculate the fixed annual overhead representing the indirect costs.

$$Depreciation = \frac{FCI}{t_{Project}} \quad (2.51)$$

$$Maintenance = 0.1 * \sum Cost_{Equipment} \quad (2.52)$$

$$Project Insurance = 0.01 * FCI \quad (2.53)$$

$$Project\ Tax = 0.02 * FCI \quad (2.54)$$

The direct costs are variable costs that are dependent on the amount of material manufactured such as raw materials, consumables and labour. Labour can be calculated as a fixed overhead or a direct cost related to the operational activities in the facility. However, labour in the simulation tool was considered to be a direct cost and charged at a rate of \$58/hour. A number of the consumables in biopharmaceutical manufacture can be re-used multiple times for the manufacture of the same molecule. This reduces the overall cost of the consumable per batch, because a consumable may be used in multiple batches and hence the cost will be split over these multiple batches. **Equation 2.55** takes into account the number of times a consumable (Num_{Uses}) has been used and offsets the resulting cost ($Cost_{Consumable}$) against the total number of re-uses allowed ($Num_{TotalUses}$).

$$Cost_{Consumable} = \left(\frac{Cost_{UnitSize} * (EquipScale / UnitSize) * Num_{Uses}}{Num_{TotalUses}} \right) \quad (2.55)$$

All the consumable costs (membrane filter, chromatographic resins, bags etc.) and raw materials (buffers etc.) used in this work are shown in the appendix.

2.1.4.3.7 Environmental models

The simulation tool's process models generate water and consumable usage allowing the environmental burden of a given manufacturing strategy to be assessed. A widely utilised concept called the E factor was adopted. The E factor was originally developed by Sheldon for the chemical industry to assess the overall environmental impact or greenness of production (Sheldon 1994; Sheldon 1997; Sheldon 2007). The E factor is defined as the total

amount of reagents, water and consumables ($Mass_{Used}$) used per kilogram of product ($Mass_{Product}$) produced, shown in **Equation 2.56**.

$$E \text{ factor} = \frac{Mass_{Used}}{Mass_{Product}} \quad (2.56)$$

The environmental impact of a manufacturing strategy was assessed by the simulation framework using the E factor method to assign a score of greenness. This was achieved by recording the water and consumable usage for each manufacturing strategy and then using **Table A2.5** to calculate the mass of all the water/consumables used.

2.1.4.3.8 Risk Modelling

So far the simulation tool assumes that all the simulation events and their outputs will inevitably occur and hence can be termed as `non-risk` outputs. These non-risk outputs would be identical if the same scenario was investigated multiple times by the simulation tool. However, biopharmaceutical manufacture is not a non-risk environment. There are a number of uncertainties around manufacturing processes, such as fermentation titres, step yields, batch failure, production times and mass throughput (Banks 1998). The simulation tool captured these uncertainties by performing a stochastic analysis using the Monte Carlo simulation technique (Nicholas et al. 1953). The technique uses the uncertainties in the input variables to determine the resulting probability distribution of the outputs; the resulting method tends to follow the pattern shown.

1. Define the domain of the input values.
2. Generate inputs randomly from a probability distribution or probability event.
3. Perform the multiple deterministic simulation iterations on the random inputs generated.
4. Aggregate all the simulation outputs to generate the output probability distributions.

The uncertainties in the input values were found by either applying a probability distribution to the values or a probability event related consequence. Input values that were deemed to be variable, were generated during each simulation iteration using a triangular distribution. The triangular distribution was expressed as three values instead on the single deterministic value representing the upper limit, lower limit and mode. The function GetTrigValue() called within the simulation engine, generates a random number and then converts this into a value within the triangular distribution every time a value is required. The other uncertainties are generated by probability events and the input values set on the consequence of these events. This method was used to capture cell culture contamination and equipment failure events, in the manufacturing scenarios.

The simulation tool captured two types of probability events, non-weighted and weighted. A non-weighted probability event would generate a random number within a defined range and use the resulting value as a score to establish which consequence to enact. For example if an event has a one in thousand chance of occurring, a random number between 1-1000 was generated and if the value is equal to one the event is deemed to have occurred. The event could represent a failure event or yield loss and would therefore lead to an input value being altered to represent the occurrence of that event. This technique was used to describe media contamination and filtration failures. Every filter use or addition to the cell culture reactor would trigger the generation of a random number and a potential failure consequence. The second type of probability event used the same methodology as described but on the occurrence of the event, it would trigger

the generation of a further random number. The second random number was used to select an input value from a weighted distribution. This technique was used to capture the fouling of perfusion cell culture separating devices, where the event is likely to occur after enough time has passed for the cells to adhere and propagate to block the filter.

2.1.5 Multi-Attribute Decision Making

The previous sections demonstrate how the simulation framework is capable of generating output values for the economic, environmental and operational feasibility of a manufacturing strategy. Using these single performance values to compare multiple strategies is insufficient as these values are likely to involve conflicting objectives. Furthermore the qualitative differences between manufacturing strategies, such as the ease of control/operation of the different strategies, are important to consider when ranking strategies. Multi-Attribute Decision-Making (MADM) techniques provide a framework for comparing qualitative and quantitative performance values and generating an overall strategy ranking score. The overall strategy score allows the end-user to evaluate the alternative strategies for a range of different scenarios, where different performance values may be deemed to be more important than others.

The simulation framework employed the weighted sum method to reconcile the qualitative and quantitative outputs so as to identify the most preferred alternative. This allowed the impact of relative importance of the outputs to be assessed by assigning different weightings for a number of scenarios. The quantitative performance values for the economic and environmental feasibility were derived from the simulation tool. The qualitative performance values representing the operational feasibility were obtained through a survey questionnaire sent to industrial experts with experience operating the alternative manufacturing strategies or a risk score generated to capture the robustness of the strategy. All attribute values (x_{ij}) were standardized (Deb 2008; Triantaphyllou 2000) to convert them to a

rating value (r_{ij}) with a common dimensionless scale between 0 – 100 using **Equation 2.57**.

$$r_{ij} = \left(\frac{\chi_{ij} - \chi_{i \text{ Worst}}}{\chi_{i \text{ Best}} - \chi_{i \text{ Worst}}} \right) * 100 \quad (2.57)$$

Where , $\chi_{i \text{ Worst}}$ = the worst value for attribute i for the strategies.

$\chi_{i \text{ Best}}$ = the best value for attribute i for the strategies.

The relative importance of the total weighted economic, environmental, operational scores in the decision making process was captured using a set of combination ratios (dimensionless weight values) whose sum equals one (Deb 2008). The overall aggregate strategy score (S_j) is generated by the weighted sum method, using the **Equation 2.58**.

$$S_j = \left(\frac{\sum_{i=1}^n r_{ij \text{ Economic}}}{n} * R_1 \right) + \left(\frac{\sum_{i=1}^n r_{ij \text{ Environmental}}}{n} * R_2 \right) + \left(\frac{\sum_{i=1}^n r_{ij \text{ Operational}}}{n} * R_3 \right) \quad (2.58)$$

Where R_1 , R_2 and R_3 represent the economic, environmental and operational combination ratios respectively.

2.1.6 Data Collection

The data used throughout this body of work was collected from a number of sources: industrial experts, historical data, literature and vendors. The principle source of data was from the projects industrial sponsor (Sa V Ho, Pfizer R&D Global Biologics, MA, USA). Data collection with regards to perfusion cell culture technologies involved a series of discussions with a number of representatives from Centocor, Genzyme, Merck-Serono, Novartis, Bayer and Eli Lilly. More-in depth discussions occurred with Richard Francis (Francis Biopharma Consulting), Morten Munk, Christoffer Bro and Jacob Jensen (CMC). A further series of discussions concerning continuous chromatography were held with Karol Lacki and Roger Nordberg (GE Healthcare, Uppsala, Sweden).

2.2 Chromatography Experimental Protocols

2.2.1 Materials

2.2.1.1 Chemicals

All Chemicals were purchased from Sigma-Aldrich (St Louis, MO, USA & Dorset, UK) unless stated.

2.2.1.2 Harvested Cell Culture Material

The IgG1 mAb used was expressed in Chinese Hamster Ovary (CHO) cells and produced at Pfizer Inc., Andover, Massachusetts. Multiple batches of material were generated via a 14-day fed-batch fermentation with an average harvest viability of 85% and viable cell density of 13 million cells/mL. Each batch was harvested by centrifugation followed by depth filtration and sterile filtration. The material was then frozen and then thawed prior to use.

2.2.2 Chromatography

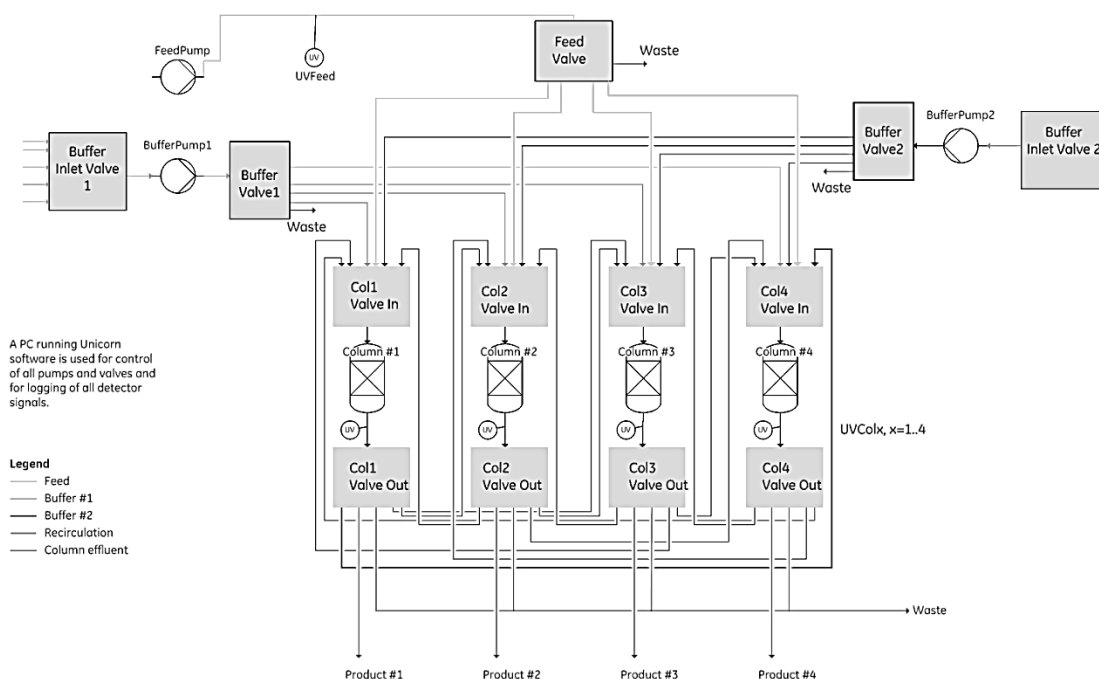
Protein A chromatography was used to capture the IgG1 mAb using MabSelect (GE Healthcare, Uppsala, Sweden), which is an agarose-based Protein A affinity matrix. The Protein A chromatography steps were scaled down from the manufacturing operations by maintaining the protein/buffer residence time used at process scale, while altering the column heights and radii. The buffers used were also the same as those used in the manufacturing operations. The columns were equilibrated with five column volumes (CV) of 150mM NaCl, 50mM Tris (pH7.5). After loading the harvested cell culture fluid (HCCF), the columns were flushed with 2CV of equilibration buffer. The subsequent wash step used a 5CV high molarity salt wash (1.8M CaCl₂, 50mM Tris, pH 7.5) to remove product-related impurities, followed by a 5CV low salt wash (10mM NaCl, 10mM Tris, pH7.5) to reduce the high salt conditions in the column prior to elution. The columns were then eluted using 10mM NaCl, 50mM glycine (pH3), where the peak was collected for 2.5CV followed by a 5CV strip using the same buffer, before the column was cleaned using 0.5M sodium sulphate, 50mM NaOH. All columns were packed and stored in 16% ethanol, 150mM NaCl, 50mM Tris (pH7.5) when required.

2.2.2.1 ÄKTA FPLC System

Conventional chromatographic runs were performed on a ÄKTA FPLC system (GE Healthcare, Uppsala, Sweden) at room temperature. The system used a single UV monitor (UV-900) and a fraction collector (Frac-950) to monitor and collect flow-through fractions.

2.2.2.2 Periodic Counter Current Chromatography System

All semi-continuous chromatographic runs were performed using the periodic counter current (PCC) chromatography system, which is a custom modified ÄKTA Explorer system from GE Healthcare (Uppsala, Sweden), designed to operate with up to four columns (Figure 2.11). The system was equipped with five UV monitors (UV-900), three pumps (P-900), multiple eight-port valves (PV-908) and an analog/digital converter (AD900) to allow the linking of the multiple components. Three or four Tricorn columns (GE Healthcare, 1mL, bed-height 50mm, 0.5mm I.D) manually packed with MabSelect were used. The system was controlled using UNICORN software with a customised



© GE Healthcare Bio-Sciences AB 2008

strategy capable of running both the 3-column and 4-column PCC system.

Figure 2.11. Schematic of 4-column PCC system (copyright GE Healthcare).

2.2.3 Analytical Techniques

2.2.3.1 NanoDrop Concentration Measurements

The mAb concentration for purified samples (Protein A elution peaks & bulk drug substance (BDS)) was measured using a NanoDrop 2000 (Thermo Scientific, Wilmington, DE, USA). Sample volumes of 2µl were measured at 280nm in triplicate and converted to mAb concentration using an extinction coefficient for IgG1 of 1.38. A calibration curve is shown in **Figure 2.12** for the serial dilution of BDS (53.9 mg/ml, Pfizer Inc., Andover, MA, USA). The NanoDrop 2000 was found to be able to measure sample concentrations for concentrations between 0.25 – 25 mg/ml, any samples of higher concentrations were diluted to lie within the calibration range.

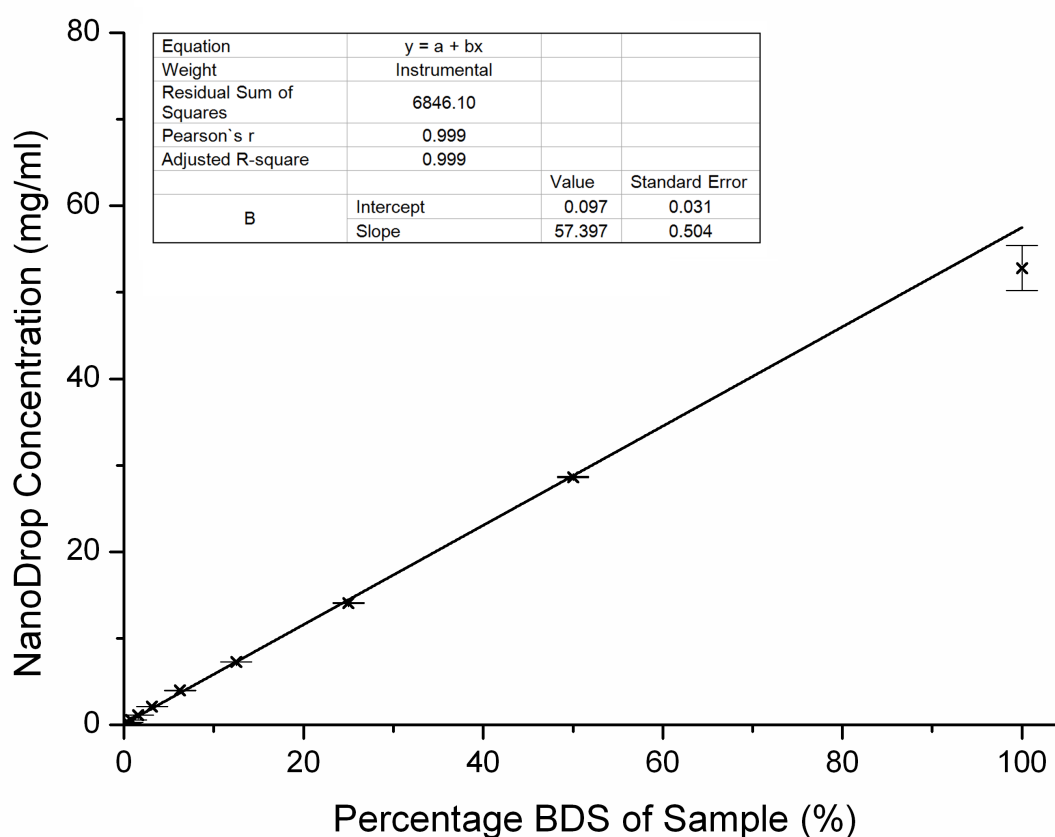


Figure 2.12. Calibration curve for the NanoDrop 2000 for the serial dilution of bulk drug substance.

2.2.3.2 Protein A HPLC

Quantification of mAb from purified and non-purified samples (HCCF & column flowthrough) was measured using a POROS A20 Protein A analytical HPLC column (Applied Biosystems, Forest City, CA, USA). Buffer A (50mM Sodium Phosphate, 150mM NaCl, pH7) and Buffer B (0.5% Phosphoric Acid, 100mM Sodium Phosphate, 400mM NaCl) were operated in a step elution for a total run time of 10 minutes per sample. The calibration curve shown in **Figure 2.13** was performed by using dilutions of BDS (53.9 mg/ml, Pfizer Inc., Andover, MA, USA). Protein A HPLC was used for sample concentrations between 1- 20 mg/ml, any samples of higher concentrations were diluted with Buffer A to lie within the calibration range.

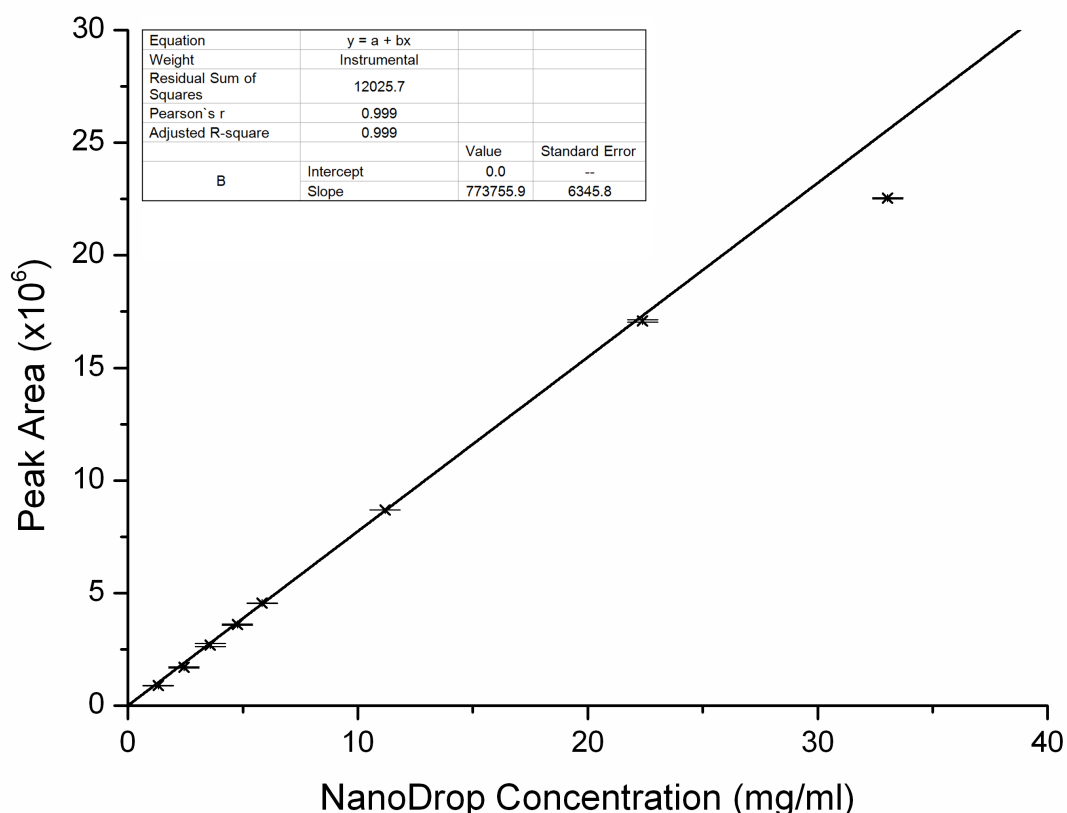


Figure 2.13. Calibration curve comparing Protein A HPLC peak area to known concentrations of BDS.

2.2.3.3 CEX HPLC

CEX-HPLC using a Dionex ProPac WCX-10 (Dionex Corporation, Sunnyvale, CA, USA) weak cation exchange column was used to analyse the product species profile of the elution pool. Buffer A (25mM Sodium Phosphate, pH7.6) and Buffer B (25mM Sodium Phosphate, 500mM NaCl, pH7.6) were run at 1 ml/min operated in a gradient elution for a total run time of 70 minutes per sample. **Figure 2.14** shows an example chromatographic profile, where species that elute prior to the designated species were considered to be in the acidic region and those that elute after the designated species, the basic region.

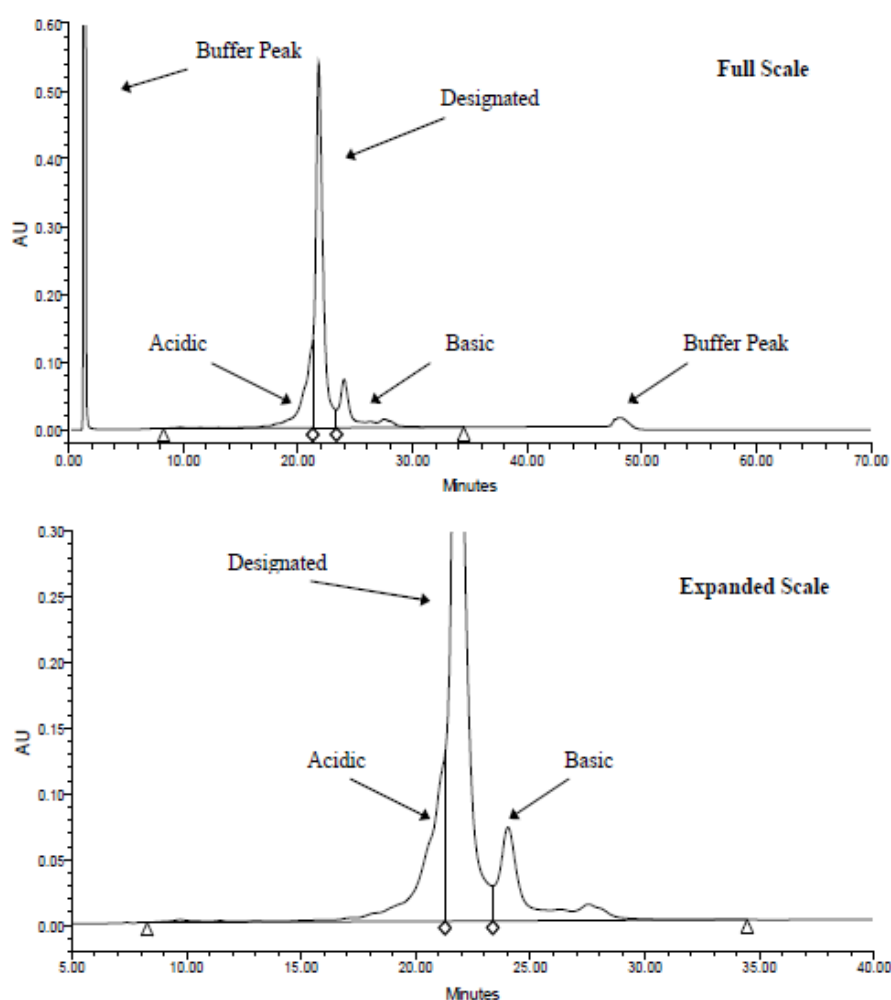


Figure 2.14. Example chromatographic profile of a cation exchange HPLC run for a purified IgG1 sample, denoting the acidic, designated and basic species of the sample.

2.2.3.4 SEC HPLC

The aggregate profile of the elution pool was captured using analytical SEC HPLC with a TosoHass TSK-GEL (Tosoh Biosciences, King of Prussia, PA, USA) HPLC column. Buffer A (10mM Sodium Phosphate, 500mM NaCl, pH7.3) was run at 0.2 ml/min for a total run time of 70 minutes per sample. **Figure 2.15** shows an example chromatographic profile, where species that elute prior to the monomeric species were considered to be high molecular weight (HMW) species (dimer, trimer etc..) and those that elute after the monomeric species to be low molecular weight (LMW) species.

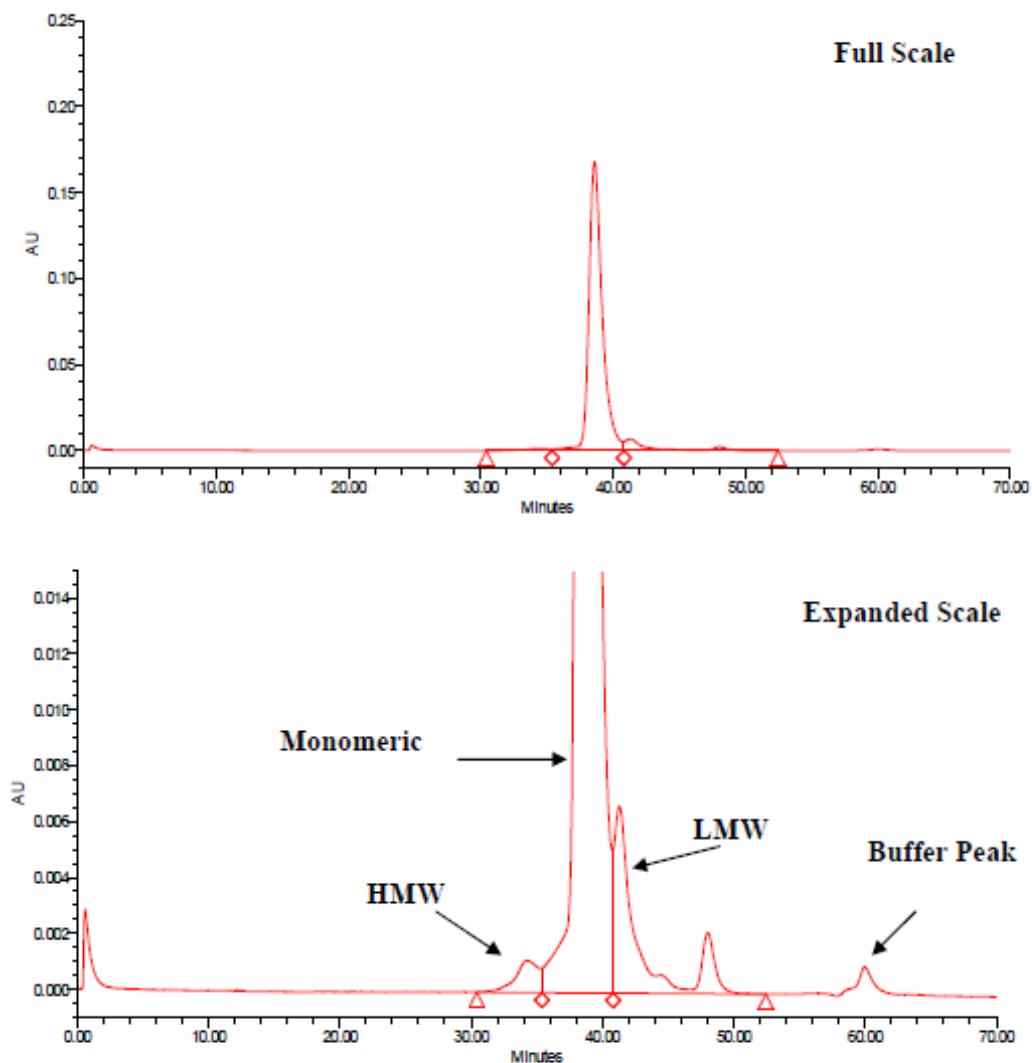


Figure 2.15. Example chromatographic profile of SEC HPLC run for a purified IgG1 sample, denoting the HMW, Monomeric and basic LMW of the sample.

2.2.3.5 Batch Uptake

A set amount of MabSelect resin was collected from the packed columns, then resuspended and washed with equilibration buffer (150mM NaCl, 50mM Tris, pH7.5) to remove the storage ethanol solution. The resin was allowed to settle by gravity, before being measured and resuspended to make a 50% (v/v) resin slurry. 80 μ l of slurry was then aliquoted into a 2 ml Eppendorf tube. Adsorption was started by adding 2ml of model IgG1 antibody at concentration of 2.5 mg/ml (provided by Pfizer Inc., Andover, Massachusetts) to the resin sample. The Eppendorf was kept under constant agitation, except at fixed times when it was rapidly centrifuged for 10 seconds at 1200 g, before a 50 μ l sample was taken and the sedimented resin particles were resuspended and agitation continued. The sample was taken from the supernatant and collected for subsequent analysis using the NanoDrop 2000 to establish mAb concentration at the given time point.

2.2.3.6 Isotherms

The MabSelect resin samples were each prepared as previously shown in section 2.2.3.5. 50 μ l of slurry was aliquoted by Tecan (Tecan Freedom EVO 150, Tecan Group Ltd. Mannedorf Switzerland) for accuracy into each well in a 96-well 0.45 μ m filter plate, (Whatman, GE Healthcare, Uppsala, Sweden). Ten different dilutions of model IgG1 antibody feed solution (provided by Pfizer Inc., Andover, Massachusetts) were prepared. Adsorption was started with the addition of 150 μ l of the corresponding feed solution into each well and agitated on a Tecan plate shaker at 1200 rpm for 3 hours until equilibrium was reached (as calculated by experiments in **Section 2.2.3.5**). At equilibrium the plates were centrifuged for 4 minutes at 1200 g and supernatant collected in a receiver plate. A 150 μ l wash of equilibrium buffer (150mM NaCl, 50mM Tris, pH7.5) was added to remove any remaining unbound mAb followed by two 150 μ l elution buffer washes (10mM NaCl, 50mM glycine, pH3) to elute all the bound protein. The filter plates were centrifuged for 4 minutes at 1200 g and the supernatant collected in a receiver plate after every wash addition. The receiver plate samples were

then analysed using the NanoDrop 2000 to establish mAb concentration for each wash in every well.

The resulting adsorption equilibriums were described by the Langmuir adsorption isotherm shown in **Equation 2.59** (Langmuir 1916). With q being the concentration of mAb in the stationary phase when at equilibrium, q_{\max} the maximum equilibrium binding capacity, K_d the equilibrium dissociation constant and C the concentration of mAb in the mobile phase. To establish the K_d and q_{\max} of each resin the data collected from the isotherm experiments was linearised using Langmuir regression (Langmuir 1918), where the reciprocal of slope is equal to the maximum equilibrium binding capacity (q_{\max}) and the y-intercept equal to the reciprocal of $K_d \cdot q_{\max}$ (**Equation 2.60**).

$$q = \frac{q_{\max} \cdot C}{K_d + C} \quad (2.59)$$

$$\frac{C}{q} = \frac{C}{q_{\max}} + \frac{1}{K_d \cdot q_{\max}} \quad (2.60)$$

2.2.3.7 Scanning Electron Microscope

Resin sample preparation for scanning electron microscope (SEM) imaging consisted of sample drying followed by the application of a gold-palladium coating to avoid the charge effect. A thin layer of resin sample was pipetted onto a pre-coated glass slide and excess liquid was carefully adsorbed using filter paper without contacting the resin sample, before being left for 30 minutes for the remaining liquid to evaporate. The dried resin sample was then mounted in a copper block and transferred to a high-resolution ion beam coater (Gatan model 681, Oxford, UK). The Argon ion beam coater was operated at 6 mA at an acceleration voltage of 10 keV and was used to ion sputter the resin sample with a 2-3 nm gold-palladium

surface coating at an angle of 45°. The coated resin surfaces were subsequently imaged with a JEOL JSM-7410F field emission scanning electron microscope (JEOL Ltd., Tokyo, Japan) at 1 keV accelerating voltage.

2.3 Conclusions

This chapter has presented the development of a decision support framework to assist decision-making in the evaluation of alternative manufacturing strategies employing semi-continuous unit operations. The framework was built to tackle the complex problem domain found in biopharmaceutical manufacturing. This was achieved through the utilisation of deterministic discrete-event simulation, MADM and Monte Carlo simulation techniques. Hence, the framework is capable of describing a large number of scenarios within the industry, highlighting the key economic, environmental and operational metrics of the facilities, processes and technologies investigated under uncertainty.

This was made possible by the hierarchal nature of the framework, which simulated the manufacturing scenarios on a number of levels of detail ranging from high-level process performance metrics to low-level ancillary task estimates. This approach made the resource-demand profiles for tasks more realistic, allowing the constraining nature of facility resources to be modelled more accurately in both deterministic and stochastic simulations. The hierarchal approach adopted also aided the development of semi-continuous unit operation process models with the addition of a sixth hierarchal layer (sub-batches) making it possible to track the merging and splitting of batches. The framework is therefore capable of capturing a number of individual semi-continuous unit operations (**Chapter 3; Perfusion cell culture, Chapter 4; Semi-continuous chromatography**) and also a manufacturing strategy linking multiple semi-continuous unit operations (**Chapter 5; Integrated continuous processing**).

Prior to the integration of the semi-continuous unit operations into the simulation framework a detailed understanding of the technologies

performance and resource requirements were required. This was achieved by consulting industrial experts, vendors, historical data, literature, and by hands on technological evaluations. The chromatography experimental protocols presented in this chapter were employed in the evaluation of a semi-continuous chromatographic system, which will become evident in **Chapter 4**.

3 Fed-batch & Perfusion Culture

3.1 Introduction

Perfusion culture manufacturing strategies for cell-culture-derived biopharmaceuticals offer the potential of greater daily productivities and hence smaller facility footprints than batch and fed-batch culture manufacturing strategies. However, their use has been hampered historically by perceived greater logistical and validation complexity as well as higher likelihoods of technical failures. More recent perfusion culture systems aim to overcome some of these obstacles and this has seen their use increase, with the promise of more cost-effective processing, higher productivities, lower failure rates and improved environmental performance. For example, Janssen Biotech has implemented a newer perfusion technology, alternating tangential flow (ATF) perfusion (Refine Technology, Edison, NJ) for the production of its more recent mAbs, such as Simponi® (Centocor 2006). This combined with the introduction of single-use technologies for cell culture operations have triggered renewed interest in the potential of bioprocesses based on perfusion culture systems. It is also important to consider less tangible operational factors such as the ease of development and flexibility as well as the environmental burden of these strategies. Previous work evaluating batch and continuous cell culture technologies has either focused on the impact on the cell culture stages rather than the whole process, or on a particular scenario in terms of titre and scale of operation, or not accounted for failure and uncertainties.

Hence this chapter describes how the simulation framework was used to evaluate fed-batch strategies and both a first generation perfusion system (spin-filter) and second generation perfusion system (ATF) whilst considering the impact of single-use bioreactors. Whilst assessing the impact on downstream processing, equipment sizing and process economics across a range of scales and titres under uncertainty. The chapter is organised as follows: **Section 3.2** describes the case study and assumptions used in this assessment. This followed by the deterministic analysis in **Section 3.3.1**, which address the impact of scale and titre on the economic performance of

the cell culture technologies. **Section 3.3.2**, build on the deterministic analysis using the stochastic Monte Carlo technique to understand the impact of failure and its consequences on the robustness of the alternative manufacturing strategies. The chapter then takes into account the qualitative concerns associated with the adoption of perfusion technologies and combines these findings with the calculated economic and environmental performance metrics in **Section 3.3.3**. The final section then summarises the principle conclusions of the preceding sections of the chapter.

3.2 Methods

3.2.1 Fermentation

The deterministic and stochastic analysis shown in this chapter were achieved using the simulation framework defined in **Chapter 2**. The fermentation process models shown in **Section 2.1.4.3.4.1** detail the growth profiles and mass balance equations for both fed-batch (FB) and perfusion based cell cultures. The same cell integral modelling approach was utilised for both the spin-filter perfusion (SPIN) and alternating tangential flow (ATF) perfusion systems. **Figure 3.1** shows the projected growth profiles of the SPIN and ATF system and the four different growth regions expected. The growth profiles shown were derived from discussions with Morten Munk, Christoffer Bro and Jacob Jensen (CMC biologics, Copenhagen, Denmark) and based on valid fermentation data.

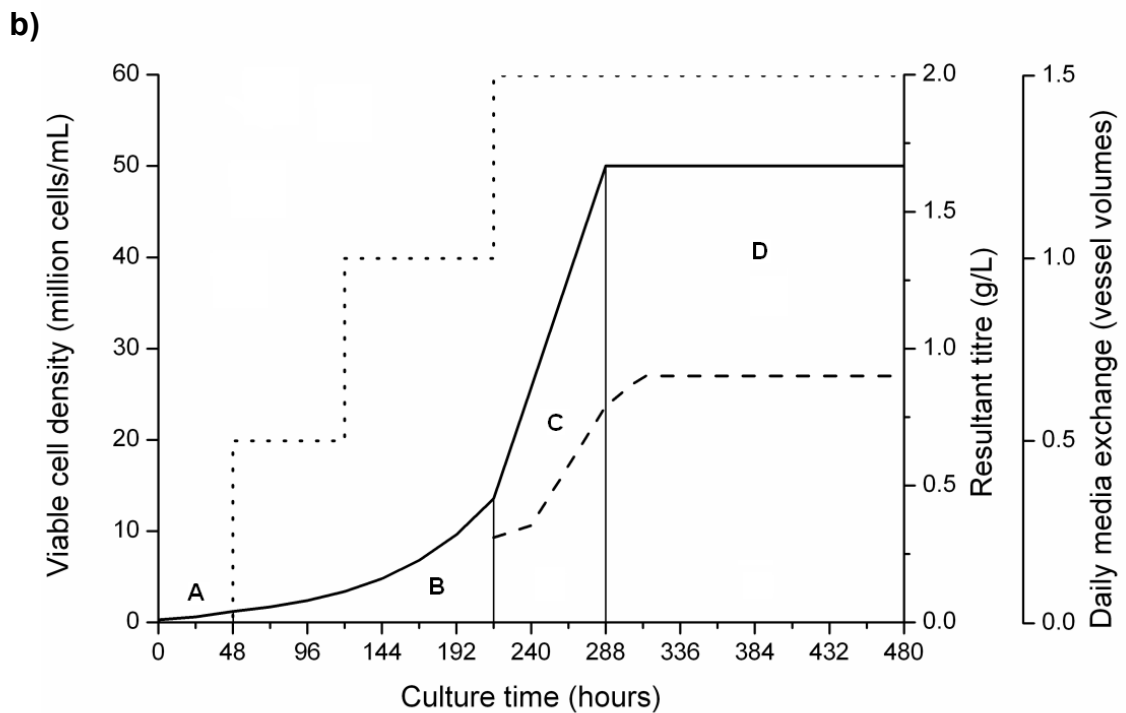
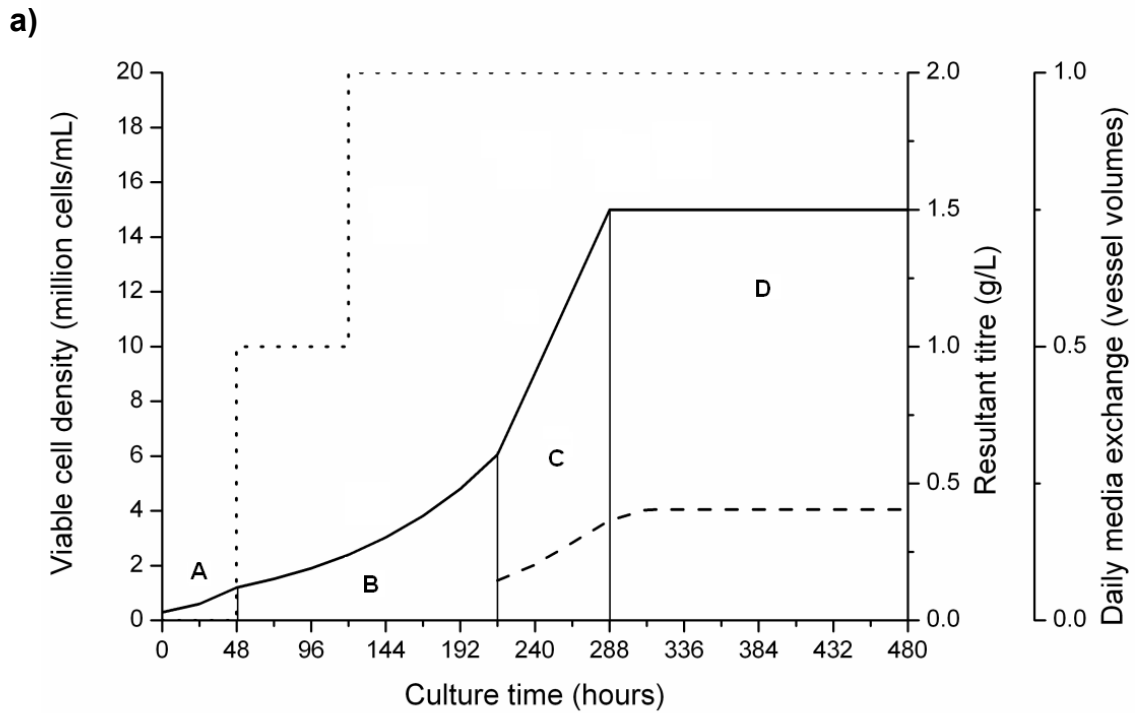


Figure 3.1. Perfusion fermentation cell culture growth profiles for a) spin-filter perfusion cell culture and b) alternating tangential flow perfusion cell culture, where viable cell density (black line), estimated product titre (dashed line) and perfusion rate (dotted line) are highlighted alongside the key growth regions.

Region A shown in **Figure 3.1** represents the batch growth phase where the cells grow exponential using the existing nutrients in the media. Perfusion is started after 2 days and the media nutrients are refreshed by the addition of new media and removal of spent media. At this point a cold shock is applied to the fermenter to prevent uncontrolled cell proliferation due to the increase in nutrients, this results in the reduced rate of growth seen in region B. The perfusion rate starts at 0.5 vessel volumes per day (vv/day) and increases to 1 vv/day after the initial cell doubling to maintain the progression of cell proliferation. The ATF system is able to achieve higher cell densities than the SPIN, and therefore requires a further increase in perfusion rate from 1 vv/day to 1.5 vv.day, to support the nutritional demands of the additional cells. Region C highlights the deceleration phase where the viable cell growth is no longer exponential due to the limitation of nutrients and increase in cell death. At this point (day 9) the cells density is sufficient to generate daily harvests with sufficient product concentrations to make it worthwhile to purify. The fermentation then maintains the maximum cell density in the steady phase represented by region D, which will last to the end of the cell culture duration selected. **Table 3.1** demonstrates how the cell integral model was applied highlighting cell integrals and the corresponding production concentrations (taking into account the dilution caused by the higher perfusion rate in the ATF system). The key operational parameters for the three-cell culture technologies (FB, SPIN and ATF) explored in this chapter are further summarised in **Table 3.2**.

Table 3.1. Cell integral and product concentration calculations for the fed-batch, spin-filter and ATF processes

STEP-SPECIFIC DATA			
Variable	FB	SPIN	ATF
Culture duration	12	60	60
Perfusion rate	-	1	1.5
Max VCD (million cells/ml)	10	15	50
Integrated VCD (million cells/ml/day)	Region A = 6.5	Day 9 = 5.4	Day 9 = 11.5
	Region B = 20	Day 10 = 7.5	Day 10 = 19.6
	Region C = 22	Day 11 = 10.5	Day 11 = 31.8
	Region D = 26	Day 12 = 13.5	Day 12 = 43.9
	Total = 75	Day 13+ = 15	Day 13+ = 50
Cell line productivity (pg/cell/day)	27	27	27
Product concentration (g/L)		Day 9 = 0.14	Day 9 = 0.21
		Day 10 = 0.20	Day 10 = 0.35
		Day 11 = 0.28	Day 11 = 0.57
		Day 12 = 0.36	Day 12 = 0.79
	Day 12 = 2.02	Day 13+ = 0.41	Day 13+ = 0.90

Note: Assumptions for key inputs in this table are discussed in **Sections 3.2.3 & 3.2.4.**

3.2.2 Multi-attribute Decision-Making

The weighted sum method shown in **Chapter 2** was used to reconcile economic, environmental and operational outputs so as to identify the most preferred alternative for scenarios with different weightings assigned to each of these categories. **Table 3.2** lists all the attributes considered in the MADM analysis. The values of the attributes under economic and environmental feasibility were derived from the simulation tool. The attributes were ranked in order of importance, where a higher ranking indicates an attribute of greater significance. For example, the COG/g was deemed to be slightly more important than initial capital investment required to construct a new facility. The attributes representing the environmental feasibility were ranked equally because the environmental impact of water and consumable usage was deemed to be equally disadvantageous to the environment. The operational feasibility scores and weightings were obtained through a survey questionnaire (shown in appendix) sent to industrial experts with experience operating both fed-batch and perfusion culture. The participants were asked to rank the cell culture technologies against each of these qualitative attributes: ease of control/operation, ease of validation (time/effort), ease of development (time/effort), operational flexibility and batch-to-batch variability.

Table 3.2. Attribute grouping and ranking

Attribute Field	Attribute Name	Rank	FB	SPIN	ATF
Economic feasibility	Cost of goods per gram	2	39	45	31
	Initial capital expenditure	1	88	68	48
Environmental feasibility	Water E-factor rating	1	6300	9900	6500
	Consumable E-factor rating	1	0.2	23.9	19.1
Operational feasibility	Batch-to-batch variability	5	5	9	6
	Ease of control/operation	4	3	9	6
	Operational flexibility	3	3	9	8
	Ease of development	2	3	9	7
	Ease of validation	1	3	9	8

Economic and environmental scores (low = best, high = worst), operational scores (3 = best, 9 = worst)

3.2.3 Case Study

The simulation framework was used to compare commercial mAb facilities using three cell culture systems: fed-batch (FB) culture, spin-filter perfusion (SPIN) and alternating tangential flow (ATF) perfusion. The case study explored the trade-offs between the higher productivities, and hence smaller upstream and downstream capacities, versus the higher cell culture failure rates caused by filter fouling and contaminations with perfusion systems relative to FB systems. Commercial manufacture of highly successful mAbs can require annual demands of 1000 kg/year (Kelley 2007; Rodrigues et al. 2010). An analysis of drug substance demand for 15 mAb and Fc-fusion products by Kelley (2009) demonstrated that annual kg output ranged from 1200 kg/yr to less than 100 kg/yr, with a median annual kg output of 200 kg/yr. This case study therefore compared each of the cell culture technologies over a range of scales of production from 100 – 1000 kg/yr so as to explore the rankings over the entire design space. Cell culture titre will also have a large effect on the results of any process comparison (Farid 2009a). In the past mAb titres reached only mg/L values, but now the norm is 2-3 g/L, with processes in development with reported titres of 5 g/L and higher (Kelley 2009). Titres of 10 g/L or higher could become the norm in the next 5-10 years. To capture the industry's current and future titre capabilities the case study investigated the following titre values: 2, 5 and 10 g/L. The key metrics used to evaluate the merits and limitations of the three strategies were: COG/g, capital investment, E factor and operational feasibility.

3.2.4 Assumptions

Figure 3.2 illustrates the process flowsheets for the production of mAbs using the three cell culture technologies, FB, SPIN and ATF. Each cell culture operation fed into a single purification train regardless of the number of cell culture reactors. When multiple reactors were required to achieve the desired annual demand, two different scheduling approaches were used. The FB process staggered any additional reactors, and altered the scale of the purification train according to the revised times between harvests. In contrast the SPIN and ATF operations operated the additional reactors in parallel, where the resultant daily perfusate harvests were pooled into a single daily harvest prior to Protein A capture. This combining of different reactor harvests was made possible by inoculating each reactor from the same seed reactor. **Figure 3.2** also highlights the differences between the primary recovery operations in each flowsheet where the FB process requires the most steps for cell removal and liquor concentration in contrast to the ATF process that does not require any given its external hollow fibre filter. The purification train was based on a generic mAb purification platform using three orthogonal chromatographic steps with intermediate filtration and viral clearance steps (Farid 2006; Kelley 2007; Liu et al. 2010). The perfusion culture purification train also includes a pooling operation, where the daily Protein A chromatography eluates were pooled into a larger volume, before being released for further purification. Although it is possible to locate the pooling operation pre-Protein A and post cation-exchange chromatography, the current commercial manufacturing norm is post-Protein A pooling due to the benefits of operating a smaller highly utilised Protein A column (Wojciechowski et al. 2007).

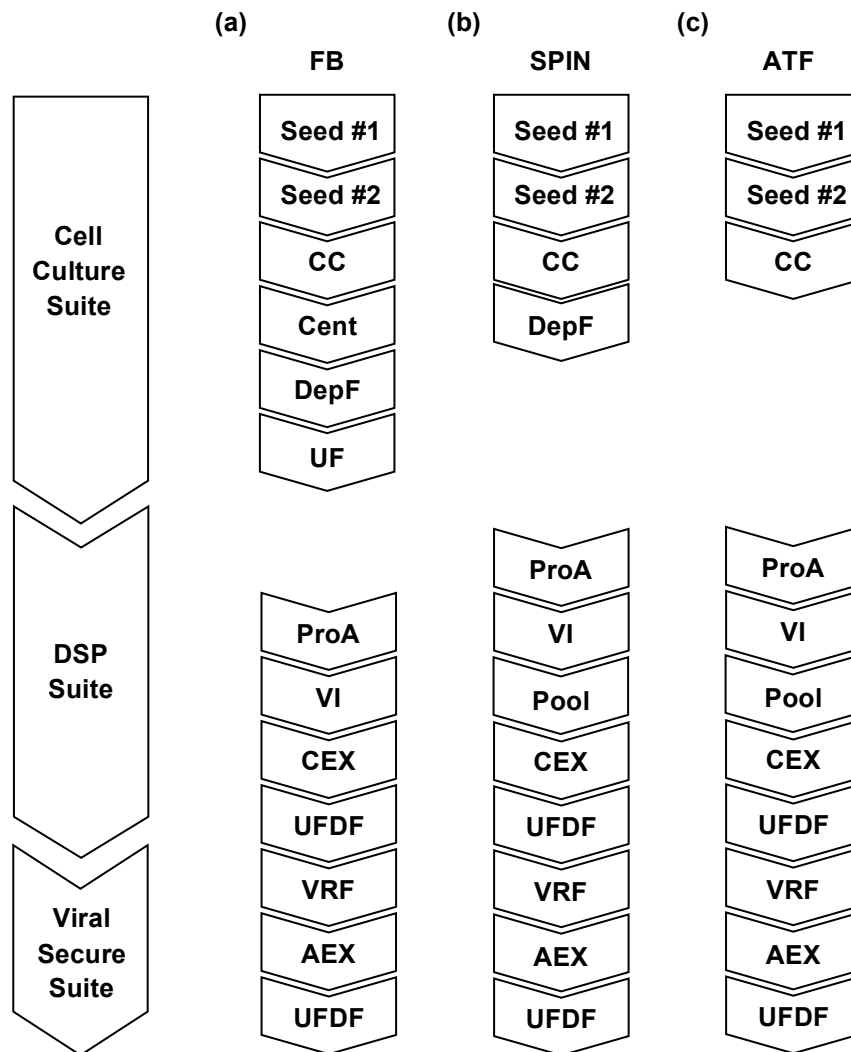


Figure 3.2. Case study process sequences and suite configuration for (a) the fed-batch (FB), (b) the spin-filter (SPIN) and (c) the alternating tangential flow (ATF) process. CC = cell culture, Cent = centrifugation, DepF = depth filtration, UF = ultrafiltration, ProA = Protein A chromatography, VI = virus inactivation, Pool = daily perfusate volume pooling, CEX = cation exchange chromatography, UFDF = ultrafiltration/diafiltration, AEX = anion exchange chromatography, VRF = virus retention filtration.

Table 3.3 lists a number of key assumptions that differ between the processes, including the overall process yield, which is lowest for the FB process due to the extra centrifugation and depth filtration operations. The FB culture step ran for 12 days in contrast to the SPIN and ATF cultures, which ran for 60 days. A typical maximum cell density for FB cultures of 10 million cells/mL, was assumed. The SPIN culture can generate cell densities of 20 million cells/mL but to maintain the longer culture duration in this case study, a cell density of 15 million cells/mL was selected to prevent premature cell culture termination due to filter fouling. The ATF system is able to reach cell densities of 100+ million cells/mL (Carstens et al. 2009) according to the vendor (Refine Technology, Edison, NJ), however to maintain a stable product quality and feasible perfusion rate a more conservative cell density of 50 million cells/mL was used (personal communication with Christoffer Bro and Jacob Jensen of CMC Biologics, Copenhagen, DK). The differences in maximum cell densities result in very different volumetric productivities, with the SPIN and ATF processes offering 2 and 6.6 fold increases in productivity respectively. The cell culture technologies also differ in terms of scalability; FB reactors can reach 20,000 L, whereas SPIN systems peak at 2000L and the ATF system at 1500L due to the limitations in the maximum perfusion rates currently achieved. The smaller reactor volumes employed by the perfusion systems potentially allow the use of single use bioreactor (SUB) technology. Due to the use of an internal cell separation device in the spin-filter perfusion system, it is not able to use SUBs. In contrast, the ATF system can successfully employ SUBs in all scenarios due to its use of an external cell separation device. The fed-batch system is capable of employing SUBs for reactor volumes below 2000L. For the standard fed-batch base case, the use of SUBs was restricted to the seed train where appropriate and stainless steel bioreactors were used for the final production stage as is common industry practice at present for commercial production. In addition, the impact of using SUBs for production bioreactors operated in fed-batch mode was also explored by using new concept facility designs involving multiple smaller SUBs operated in a staggered fashion.

Table 3.3. Key assumptions for the fed-batch, spin-filter and ATF processes

STEP-SPECIFIC DATA			
Variable	FB	SPIN	ATF
Input			
Cell culture time (days)	12	60	60
Max VCD (million cells/ml)	10	15	50
Max bioreactor volume (L)	20,000	2000	1500
Max perfusion rate (vv/day)	–	1	1.5
Calculated			
Process yield	65%	68%	69%
Annual # batches	22	5	5
Max product concentration (g/L)	2 – 10	20% FB	45% FB
Volumetric productivity (mg/L/day)	169 - 847	2.15 x FB	7.16 x FB
Annual bioreactor capacity required	1 x FB	1/9 x FB	1/29 x FB
Installed bioreactor capacity	1 x FB	1/2 x FB	1/6 x FB
Grams of product per litre of media	1.2 – 6.3	19% FB	44% FB
GENERAL COST DATA			
Equipment	Investment Cost (\$)	Consumable Cost (\$)	
Single use bioreactor¹			
200 L	88,000	4200	
500 L	98,000	5460	
1000 L	110,000	8260	
2000 L	175,000	9800	
Perfusion Device²			
Spinfilter	35,000	N/A	
ATF 4 System	30,000	714	
ATF 6 System	90,000	3,570	
ATF 8 System	130,000	7,140	
ATF 10 System	180,000	16,300	
Key Material Costs			
Protein A resin cost (\$/L)		8000	
Cell culture media ³ (\$/L)		3.15	
Fed-batch feed additions (\$/L)		13.1	
Labour Cost (\$/hour)		58	

1 - Investment cost includes: disposable bioreactor support vessel, agitator motor, gas & fluid pumps, Consumable cost includes: bioreactor bag.

2 - Investment cost includes: filter unit, controller & auxiliary media pump, Consumable cost includes: filter.

3 - Cell culture media used for initial media fill in fed-batch cell culture and daily perfusion media exchanges.

3.2.4.1 Monte Carlo Assumptions

Table 3.3 summarises the probability distributions assigned to the key uncertainties along with the consequences of each failure event used when performing the stochastic cost analysis with Monte Carlo simulations. The probability of cell culture contamination was calculated for each strategy assuming that each addition to the reactor had a 1 in 1000 chance of causing contamination. The FB strategy had a total of ten reactor additions (initial media fill and nine feeds) and therefore had a 1% probability of batch contamination. In contrast the perfusion strategies had approximately sixty additions due to the daily media exchanges and therefore had ~6% probability of contamination. The risk of equipment failure due to filter fouling in the perfusion strategies was also considered. The SPIN strategy had a higher probability of filter failure compared to the ATF strategy due to the use of an internal filter that actually relies on a degree of surface cell growth to prevent excessive cell carryover into the perfusate. The probability of filter fouling increases with duration of the perfusion cell culture (Deo et al. 1996; Vallez-Chetreau et al. 2007). The probability of filter failure is shown as a percentage in **Table 3.3** but when the tool selects a filter failure scenario, the occurrence of the failure is weighted to occur at the latter stages of the cell culture duration. Batch-to-batch titre fluctuations in cell culture were also captured as they can have a significant impact on the mass of antibody generated impacting the purification operations and hence annual kg output and COG/g. Typical titre fluctuations at commercial scale are $\pm 20\%$. This was implemented by applying a triangular distribution to the cell line productivity for each batch with the minimum and maximum values being $\pm 20\%$ of the most likely base value. A further common uncertainty is failure of in-process filtration (IPF) operations associated with every product tank/bag fill or draining protocol. The majority of IPF failures occur due to the blocking of the sterile filters, hence the probability of IPF failure is significantly higher after viral inactivation due to the increased probability of aggregate formation due to the low pH holding conditions.

Table 3.4. Monte Carlo assumptions

Process event	p(Failure)	Consequence
Fed-batch culture contamination	1 %	Batch loss
Spin-filter culture contamination	6 %	Batch loss & discard two pooled perfusate volumes
Spin-filter filter failure	4 %	Batch loss & no pooled volumes are discarded
ATF culture contamination	6 %	Batch loss & discard two pooled perfusate volumes
ATF filter failure	2 %	Replace filter & discard next 24 hours of perfusate
In process filtration failure; General	5 %	4 hour delay & 2% yield loss
In process filtration failure; Post viral inactivation	20 %	4 hour delay & 2% yield loss

Table 3.4 also highlights the consequences of a failure event, which vary depending on the cell culture strategy. For the FB scenario a contamination resulted in the loss of the whole batch. However for the perfusion strategies material harvested prior to the contamination event could be processed apart from the two latest pooled perfusate volumes that were discarded. The perfusion strategies are also prone to filter failure which would also halt the cell culture upon a failure event. The use of an external filter by the ATF strategy meant the filter could be replaced and the cell culture resumed, after discarding the subsequent day's perfusate volume due to high levels of HCP. The SPIN strategy employs an internal filter which cannot be replaced mid-culture resulting in the halting of the cell culture, but allows all prior harvested material to be processed. When a failure event occurred, the discrete-event simulator triggered the start of the subsequent planned batch so as to prevent idle time and poor facility utilisation, with a time lag of approximately 2 weeks for the production reactor inoculum to be generated. This had little effect on the fed-batch scenario since the batch interval was also approximately 2 weeks, meaning the next planned batch would be available

prior to any replacement batch. In contrast for the perfusion systems with long culture durations, the rescheduling could potentially allow a replacement batch to be processed depending on the timing of the failure event. In the event of an IPF failure event, the process was delayed by four hours and 2% of the product material was lost. Advice from industrial experts was solicited to sanity check the validity of these risks and the resulting consequences on production.

3.3 Results and Discussion

The tool was used to assess how the cost-effectiveness of the fed-batch and perfusion strategies changes across a range of titres and scales of production. This was initially carried out deterministically and then expanded to account for the impact of equipment failures and uncertainties in performance. The economic outputs were then considered alongside operational and environmental metrics using a multi-attribute decision-making technique.

3.3.1 Deterministic Cost Comparison

3.3.1.1 COG/g Comparison Across Scales

Figure 3.3 shows the COG/g for the FB, SPIN and ATF strategies for the 5g/L scenario across a range of scales of production (100kg/yr, 500kg/yr, 1000kg/yr). The analysis suggests that although the SPIN strategy offers similar COG/g values to the FB strategy at the smallest production scale of 100kg/yr, it becomes less economically attractive at the higher production scales. In contrast the ATF strategy is seen to offer cost advantages across all production scales of ~20% in the 5g/L scenario.

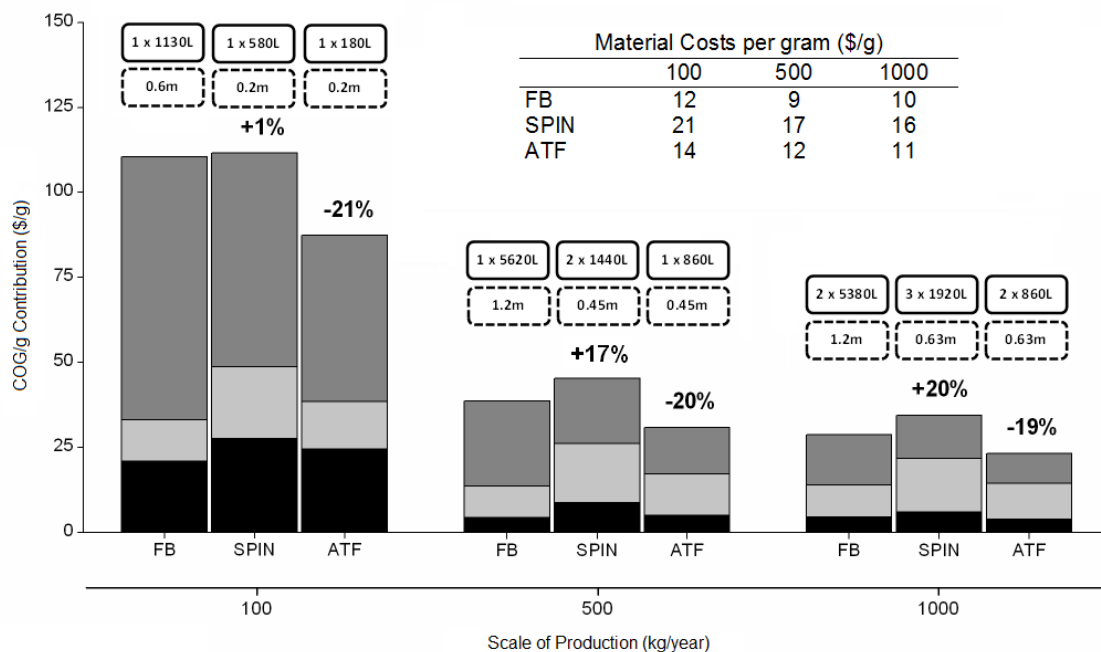


Figure 3.3. A comparison of the cost of goods per gram on a category basis for labour costs (black), direct material costs (light grey), and indirect costs (dark grey) between the fed-batch process (FB), the spin-filter process (SPIN) and the alternating tangential flow process (ATF) over a range of scales of production for an equivalent fed-batch titre of 5 g/L, where the percentage difference is relative to the fed-batch process. The embedded table highlights the materials cost per gram for the production strategies. The optimal sizing strategy for each process is indicated in the boxes above each bar highlighting the number and scale of bioreactor(s) (solid box) and the column diameter for the Protein A chromatography step (dashed box) across a range of scales of production.

A closer examination of the COG/g breakdowns highlighted in **Figure 3.3** reveals how changes in the relative importance of different cost categories influence the cost-benefit rankings. The trade-off between the lower indirect costs and higher material costs with the SPIN strategy relative to the FB strategy is dependent on the production scale. At the smallest production scale, changes in material costs can be seen to have much less influence due to the dominance of the investment-driven indirect costs, as has been echoed in other reports (Farid 2009b; Farid et al. 2007). Across all production

scales, the material costs per gram decrease at a slower rate than the other leading cost contributors as illustrated in the embedded table in **Figure 3.3** and the SPIN strategy exhibits a ~1.8-fold increase in material costs (16 – 21 \$/g) relative to the FB strategy. This difference in material costs becomes increasingly more significant at the higher production scales as material costs represent a much higher proportion of the COG/g, contributing to the reduced competitiveness of the SPIN strategy. In contrast, the ATF strategy is able to compete across all scales since its superior cell density and hence volumetric productivity coupled with a smaller highly utilised purification train results in significantly larger savings in indirect costs (~40%) combined with only a ~1.2-fold increase in material costs. This translates into overall savings irrespective of the dominance of either indirect or material costs at either extremes of the production scales.

The tool was also used to identify the material cost drivers for each strategy. **Figure 3.4** presents a detailed percentage breakdown of the COG/g, for all three strategies in the scenario at 5g/L and a 500kg/y production scale, on a category basis with particular emphasis on the key material costs. The higher material cost contributions in the perfusion systems can be attributed primarily to the higher usage of culture media, product-holding bags, and SUB liners (for ATF systems). It is interesting to note that although the dominant material cost shifts from chromatography resins (36% material costs) in the FB strategy to culture media (31% material costs) in the SPIN strategy, this shift in dominance is not seen in the ATF strategy. This is in spite of the fact that increases do occur in other cost categories. This can be attributed to the more productive ATF systems utilising comparably less media than the SPIN strategy; hence the increase in media cost is not substantial enough to outweigh the high costs associated with the chromatographic resins.

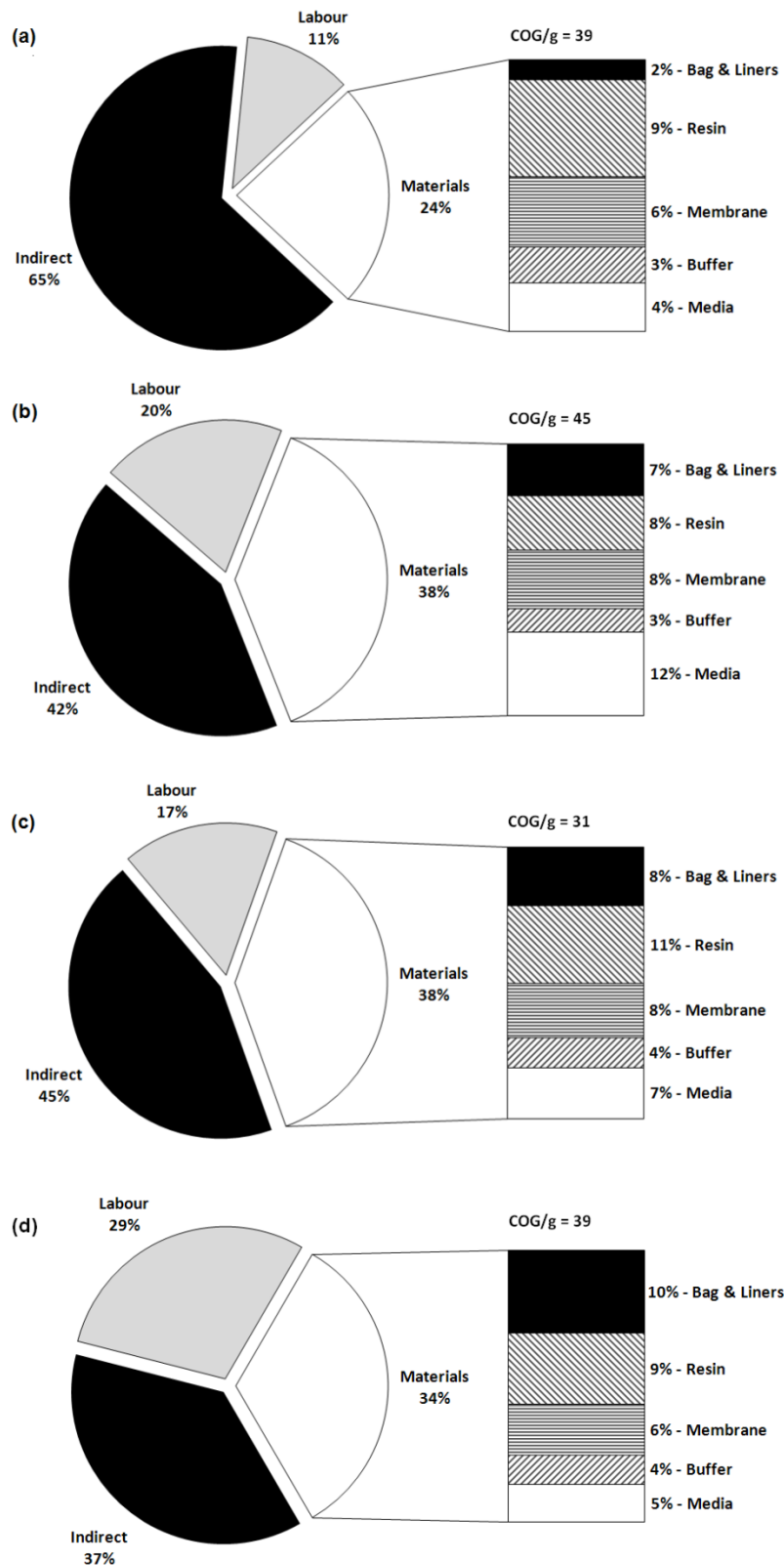


Figure 3.4. A comparison of cost of goods per gram with a detailed breakdown of material costs on a category basis for (a) the fed-batch process, (b) the spin-filter process, (c) the alternating tangential flow process and (d) the concept fed-batch SUB process, for a 500 kg/yr scale of production and an equivalent fed-batch titre of 5 g/L. The COG/g values for each process are also indicated in \$/g.

The impact of new concept facility designs based on multiple staggered single-use bioreactors operated in FB mode was also investigated. A new concept SUB facility (FB-SUB) with a 500 kg/yr scale of production and a 5g/L titre would require four 1500L staggered SUBs with a harvest frequency of 3 days, compared to a single 5600L stainless steel bioreactor with a harvest frequency of 12 days. Capital investment estimates (Total Equipment Purchase Cost (TEPC) x Lang factor) required the derivation of a suitable Lang Factor (23.67) for the SUB-based cell culture suites so as not underestimate their infrastructure costs (see **Table 2.3**). Despite a shift in the COG breakdowns to a more evenly spread distribution across indirect, material and labour costs (**Figure 3.4d**), no significant difference was seen in the magnitude of COG values between the FB and FB-SUB strategies. Consequently, FB strategies with multiple SUBs are still unable to compete with the ATF COG savings.

3.3.1.2 Key Economic Metrics Across Scales and Titres

The impact of both scale of production (100kg/yr, 500kg/yr, 1000kg/yr) and titre (2g/L, 5g/L, 10g/L) on the competitiveness of the three strategies was investigated. The contour plot in **Figure 3.5a** shows the results for the SPIN strategy relative to the FB strategy when expressed as percentage change. The corresponding number and scale of the reactors employed is shown in **Table A3.5**. The figure highlights that the SPIN strategy is only able to compete with the FB strategy at either the low production scales (100kg/yr), irrespective of titre or at the high titres of 10g/L across all the scales (with a $\pm 10\%$ difference). Both these sets of conditions place low demands on bioreactor capacity where the savings on investment-related indirect costs dominate. Hence the benefits of installing a single bioreactor train that is typically half the size of the FB strategy is balanced against the higher material costs. In contrast, as the scale of production (kg/yr) increases, coupled with decreases in titres, the SPIN strategy becomes increasingly unattractive. This effect is particularly pronounced at the lowest titre (2g/L) and the highest scale of production (1000kg/yr), where the SPIN strategy's

COG/g reaches double that of the FB strategy. This can be attributed to the need for a high number (8) of SPIN reactors to cope with the large-scale of production, given their scale limitations combined with the larger bioreactor capacities required at lower titres. This negates any potential advantages offered by having lower total installed bioreactor capacities with the SPIN strategy relative to the FB strategy. Instead the results generated by the tool indicate that the difference in capital investment and the related indirect costs (x1.4) as well as labour costs (x3) between the SPIN and FB strategies become exaggerated. These increases coupled with the higher material costs in perfusion strategies illustrate how the SPIN strategy loses its competitive advantage under high bioreactor capacity demands that result in scale-out to multiple bioreactors.

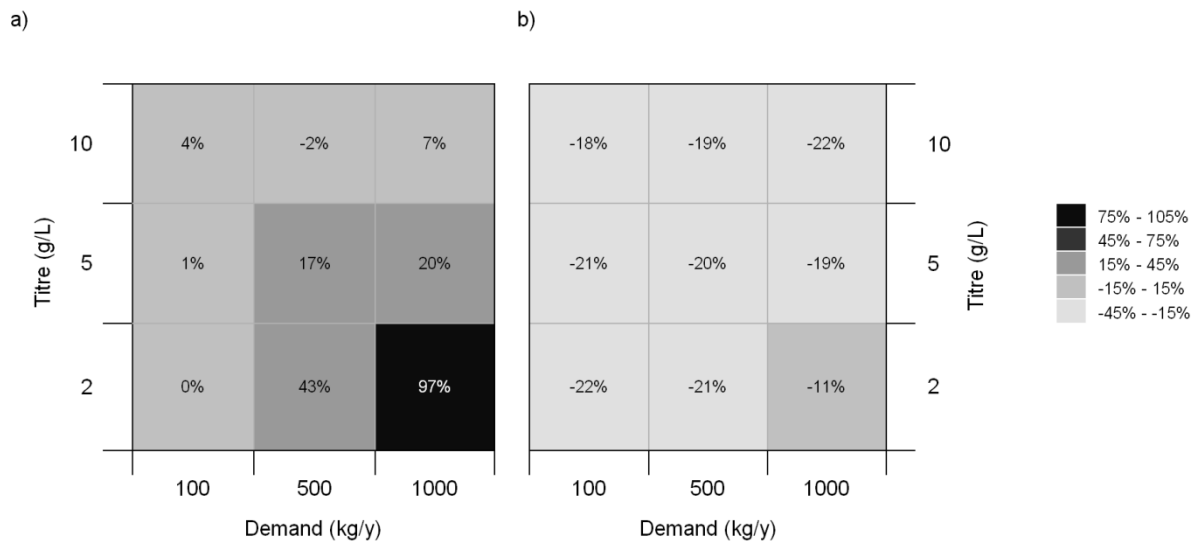


Figure 3.5. Contour plot showing the impact of scale of production and titre on the percentage difference in COG/g relative to the fed-batch process for (a) the spin-filter perfusion process and (b) the alternating tangential flow (ATF) perfusion process. The processes are resized for each combination of scales of production and titres.

In contrast the impact of increasing titre across the different scales of production does not significantly affect the cost-effectiveness of the ATF strategy (**Figure 3.5b**) in the same manner as the SPIN strategy. The superior cell density of the ATF strategy relative to the FB strategy (5 fold higher), leads to significantly smaller bioreactor volumes compared to the SPIN strategy and prevents the rapid increase in bioreactor number and COG/g values seen. This translates into an installed reactor capacity that is approximately 6 times smaller than the FB strategy in comparison to the SPIN strategy's ability to only offer half the installed reactor capacity of the FB strategy. The installed bioreactor capacities are derived from the annual bioreactor capacities divided by the number of batches. Given that the perfusion strategies only operated five batches annually compared to twenty-two for the FB strategy, the ATF strategy offers a 29-fold decrease in annual reactor capacity compared to only a 9-fold decrease with the SPIN strategy. The superior productivity of the ATF strategy coupled with a small highly utilised purification train, allows the ATF strategy to offer capital investment savings of ~40% and COG/g savings of ~20% across all titres and scales of production compared to the FB strategy. These results assumed a 5-fold difference in maximum viable cell density between the ATF and FB systems. The tool was also used to investigate the relationship between the ATF systems maximum cell density and both the scale of production and titre (**Figure 3.6**). The tool predicted that even if the ATF cell density dropped such that only a 3 fold difference in cell densities was achieved (**Figure 3.6b**), it would still offer COG/g savings compared to the FB strategy across the different combinations of production scales and titre, except for the worst case combination of low titres (2g/L) and high production scale (1000kg/yr). When the ATF system only has a 2 fold difference in cell density it is only able to offer a saving for low production scales (100kg/yr) and high titre (10g/L) scenarios (**Figure 3.6a**), due to the reduced reactor productivity resulting in a higher number of reactors (7) being required, mirroring the trend exhibited by the spin-filter system in low titre (2g/L) scenarios.

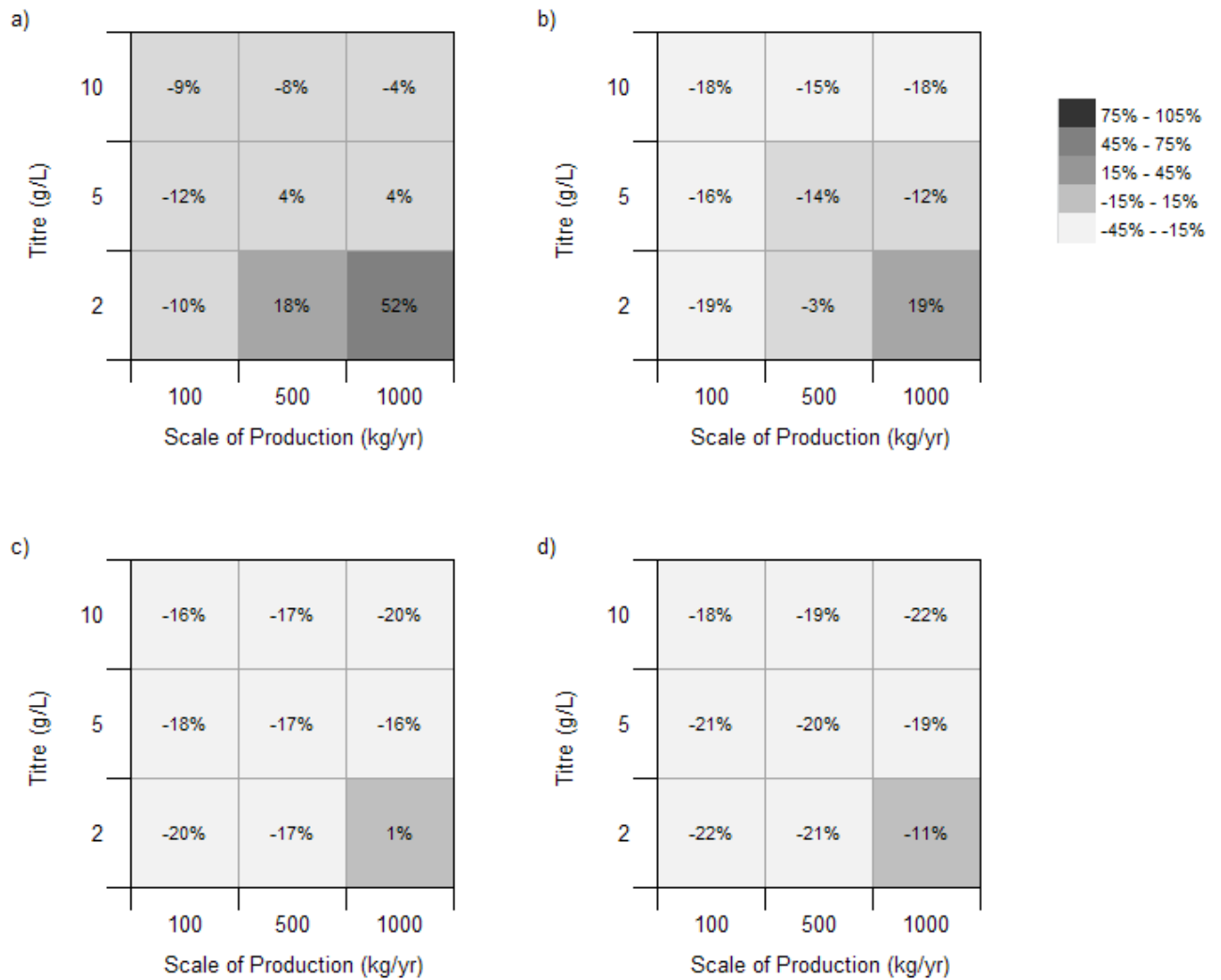


Figure 3.6. Contour plot showing the impact of the ATF system's viable cell density at different scales of production and titres on the percentage difference in COG/g relative to the fed-batch process for (a) 20 million cells/mL, (b) 30 million cells/mL, (c) 40 million cells/mL, and (d) 50 million cells/mL. The fed-batch system was assumed to achieve a maximum viable cell density of 10 million cells/mL. The processes are resized for each combination of scale of production and titre.

3.3.2 Stochastic Cost Comparison

The initial deterministic cost comparison highlighted the overall economic advantages offered by operating the ATF strategy. The study was extended to include the perceived risks associated with perfusion based strategies, namely cell culture failure attributed to either contamination or equipment failure due to filter fouling over the long culture durations. The Monte Carlo simulation technique was used to characterise the variability in the kg output and COG/g values caused by fluctuations in failure rates and titre. The following discussion highlights the key findings from this analysis and assesses the robustness of the FB and perfusion strategies.

3.3.2.1 Expected Scenario Outputs

Figure 3.7 shows the expected kg output and COG/g values for the FB, SPIN and ATF strategies under uncertainty at a 500 kg/yr scale of production and a titre of 5g/L. **Figure 3.7a** depicts the expected annual output achieved by each cell culture strategy, showing every kg output value recorded (thin lines), the frequency that the values occur (and the expected annual output) (horizontal dashes), alongside the frequency that the values occur (histogram). The FB strategy is the most robust strategy as indicated by the narrower spread of the frequency values (410 – 490 kg/yr). The frequency of annual output values for the FB scenario has a distinct shape which was found to relate directly to the number of batch failures in any given year of production. This is highlighted in **Figure 3.7c** where the biggest bar represents no batch failures and the subsequently smaller bars represent the occurrence of one and more batch failures per year. The robustness of the FB strategy can be attributed to the low probability of cell culture failure (1%) and the high number of batches (22 batches/yr) lessening the effect of titre variation on annual kg output. In contrast the perfusion strategies are not as robust as the FB strategy due to their higher probability of failure and fewer number of batches per annum (5 batches/yr) amplifying the effect of titre variation on the annual kg output achieved. The shape of the frequency plots depicting annual kg output is not as defined as the FB strategy either, due to

the variability in the timing of a failure event dictating how much material has been processed from the failed batch. The perfusion strategies both have occurrences of kg outputs over 500kg/yr due to scenarios when all the titres achieved that year are above average and there were no cell culture failures. The ATF strategy achieves high kg outputs more readily due to only 6 in 100 cell cultures runs failing compared to 1 in 10 failures for the SPIN strategy. This results in the ATF strategy having a higher expected annual kg output of 488kg/yr compared to the SPIN strategy value of 470kg/yr and the FB strategy value of 472 kg/yr, even though the SPIN strategy often fails to achieve kg output values above 400kg/yr. The t-Statistic value for the ATF strategy versus the FB strategy indicates that there is a statistically significance difference.

Figure 3.7b shows the expected values for the COG/g, where the COG/g frequency plots are a reflection of the annual kg output frequency plots, given that a higher output results in better facility utilisation and hence a reduced COG/g value. The only exception to this rule occurs when the ATF strategy achieves an annual output over 500kg/yr, which is a higher output than the facility design, resulting in a higher COG/g than expected due to the extra costs required to process the extra material, resulting in a frequency plot more aligned with the FB strategy. The ATF strategy further demonstrates its economic superiority by maintaining a ~20% reduction in COG/g with an expected value of 32 \$/g compared to the FB strategy's expected COG/g value of 41 \$/g. The ATF strategy is also able to maintain this COG/g advantage over the FB strategy even in its worst-case scenario involving multiple failure events. Overall the expected stochastic COG/g values are ~5% higher than the deterministic values and maintain the economic ranking shown in the deterministic cost comparison. However the stochastic analysis gives a clear indication of the robustness of the manufacturing strategy employed unavailable through deterministic analysis.

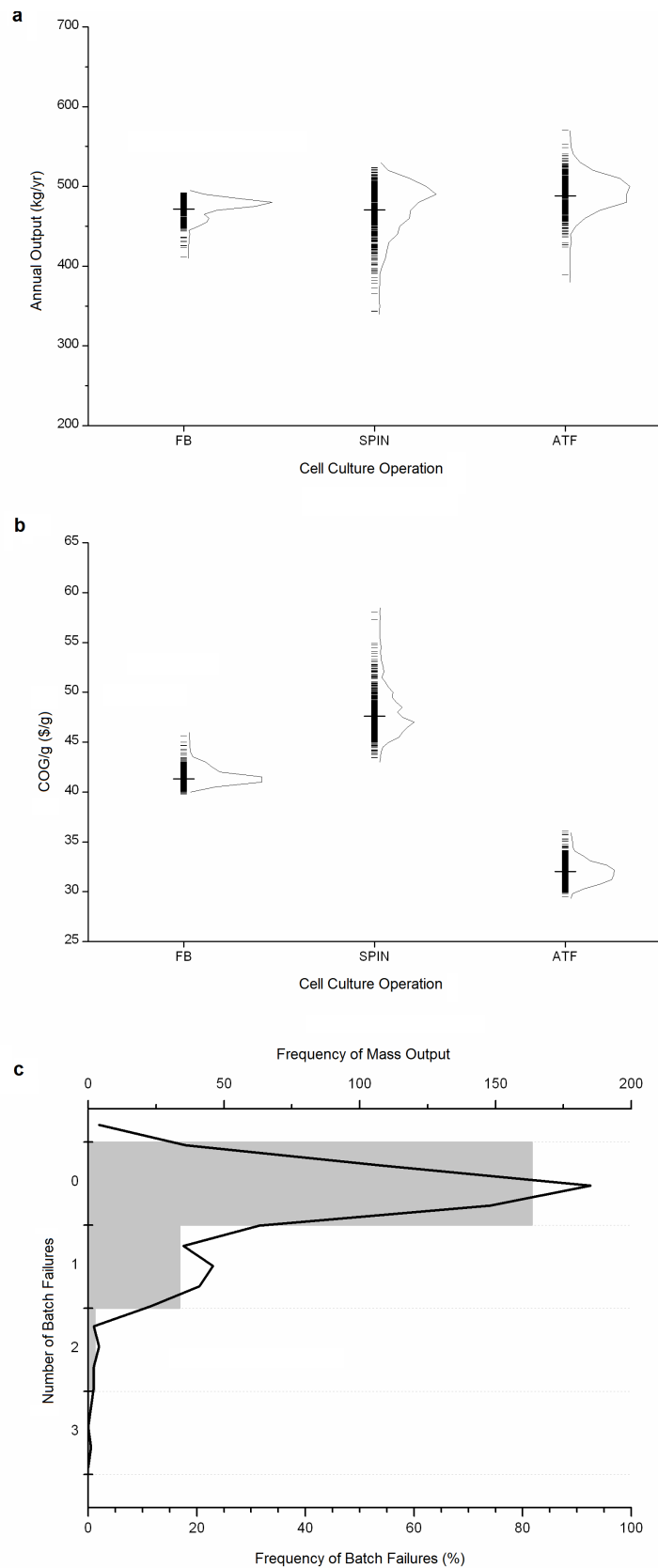


Figure 3.7. Frequency distribution plots depicting the expected process outputs under manufacturing uncertainty for (a) the expected annual kilogram output, (b) the expected cost of goods per gram, and (c) the number of fed-batch culture failures, for a 500 kg/year scale of production and equivalent fed-batch titre of 5 g/L.

3.3.3 Multi-attribute Decision Making

This section extends the analysis beyond economic metrics to include the environmental and operational benefits of each strategy.

3.3.3.1 Environmental Impact Analysis

The tool was also used to capture the water and consumable usage of the strategies to assess the environmental impact of the FB and perfusion strategies across a range of titres and scales of production. E factor values were derived for the usage of process water (cell culture media & process buffers), non-process water (CIP buffers & rinse water) and consumables (bags, membranes & resins). Typical FB manufacturing strategies consume water (process and non-process) from 3000 to over 7000 kg water per kg product. The cell culture steps consume between 20-25% of the total, with the chromatographic operations often surpassing 50% of the total (Ho et al. 2011).

As expected the perfusion strategies have a much higher process water E factor value in comparison to the FB strategy, where the higher process water E factors can be directly related to the volumetric productivity of the perfusion strategies and their resulting media usage. The perfusion strategies' extra burden on CIP caused by the highly utilised primary clarification operations and purification train for the high number of pooled perfusate volumes, results in the SPIN strategy consuming double the non-process water relative to the FB strategy. In contrast the ATF strategy has a ~30% lower non-process water E factor value relative to the FB strategy, due to the ability of the strategy to utilise single-use bioreactor (S.U.B) technology and the removal of a dedicated primary clarification operation. The consumable E factor values are highly dependent on the amount of single use technologies employed by the strategies. This effect is particularly pronounced at the smallest scale of production (100kg/yr), where all the manufacturing strategies can successfully employ single-use technologies, resulting in higher consumable E factor scores and lower non-process water

E factor scores. The smaller purification train in the perfusion strategies is ideally suited to such technologies across all the scales of production, leading to the high consumable E factor scores seen in **Table 3.5**.

Table 3.5. E-Factor scores for water and consumable consumption

	E-Factor scores (kg/kg product)		
	FB	SPIN	ATF
Process water	4300 – 5050	4950 – 9800	4700 – 5300
Non-process water	1150 – 4950	2600 – 12,500*	1400 – 6300
Consumables	0.2 – 16.1	7 – 48.8	4.6 – 37.4

*High spin-filter perfusion strategy water E-Factor scores are a consequence of a high number of reactors employed

3.3.3.2 Qualitative Operational Benefits

Qualitative attributes related to the operational feasibility of the strategies were derived from survey responses from industrial experts with both FB and perfusion experience (shown in appendix). In terms of attribute weights, the responses highlighted that the batch-to-batch variability and ease of control/operation were considered more important than the other attributes. In terms of rating each strategy against these attributes, **Table 3.2** indicates that the FB and ATF strategies scored evenly with regard to batch-to-batch variability due to the ability to successfully control the cell culture conditions for the strategies. The FB strategy was the clear favourite with regard to ease of control/operation due to the added complexity associated with the perfusion strategies' cell retention devices and daily feeding operations.

3.3.3.3 Overall Aggregate Strategy Scores

The results of reconciling the trade-offs between economic, environmental and operational outputs using a single multi-attribute score are reviewed in this section. The key output was the overall aggregate strategy score over a range of combination ratios to reflect the impact of the relative importance of the economic, environmental and operational scores on the ranking of the manufacturing strategies. **Figure 3.8** depicts the sensitivity of the overall aggregate strategy scores to the economic attribute combination ratios for the FB, spin-filter and ATF strategies at a 500 kg/yr scale of production and a titre of 5g/L. For the scenario shown in **Figure 3.8a** the operational attribute combination ratio was fixed at 0.1 and the environmental attribute combination ratio varied with the economic attribute combination ratio such that the sum of all the combination ratios always remained equal to one. **Figure 3.8a** illustrates that when the environmental and economic scores are equally weighted ($R_1 = R_2 = 0.45$), the ATF strategy has the highest aggregate score and therefore would be the preferred manufacturing strategy. If the environmental benefits are considered to be approximately 1.5 times as important as the financial benefits ($R_1 = 0.35$, $R_2 = 0.55$) the FB and ATF strategies are equally attractive and outperform the SPIN strategy. The FB strategy only comes out as the superior strategy over the ATF and SPIN strategies when the environmental benefits are considered over twice as important as the financial savings. Interestingly, **Figure 3.8b** shows that when the environmental attribute combination ratio is fixed at 0.1 and the operational and economic scores are equally weighted ($R_1 = R_3 = 0.45$), the FB and ATF are equally ranked. **Figure 3.8b** illustrates that when the economic benefits are considered more important the ATF strategy is the preferred manufacturing strategy, however if the operational benefits are more important the fed-batch strategy becomes the favoured manufacturing strategy. Appendix **Figures A3.1 and A3.2** demonstrate how these relationships were maintained across all the annual kg outputs investigated.

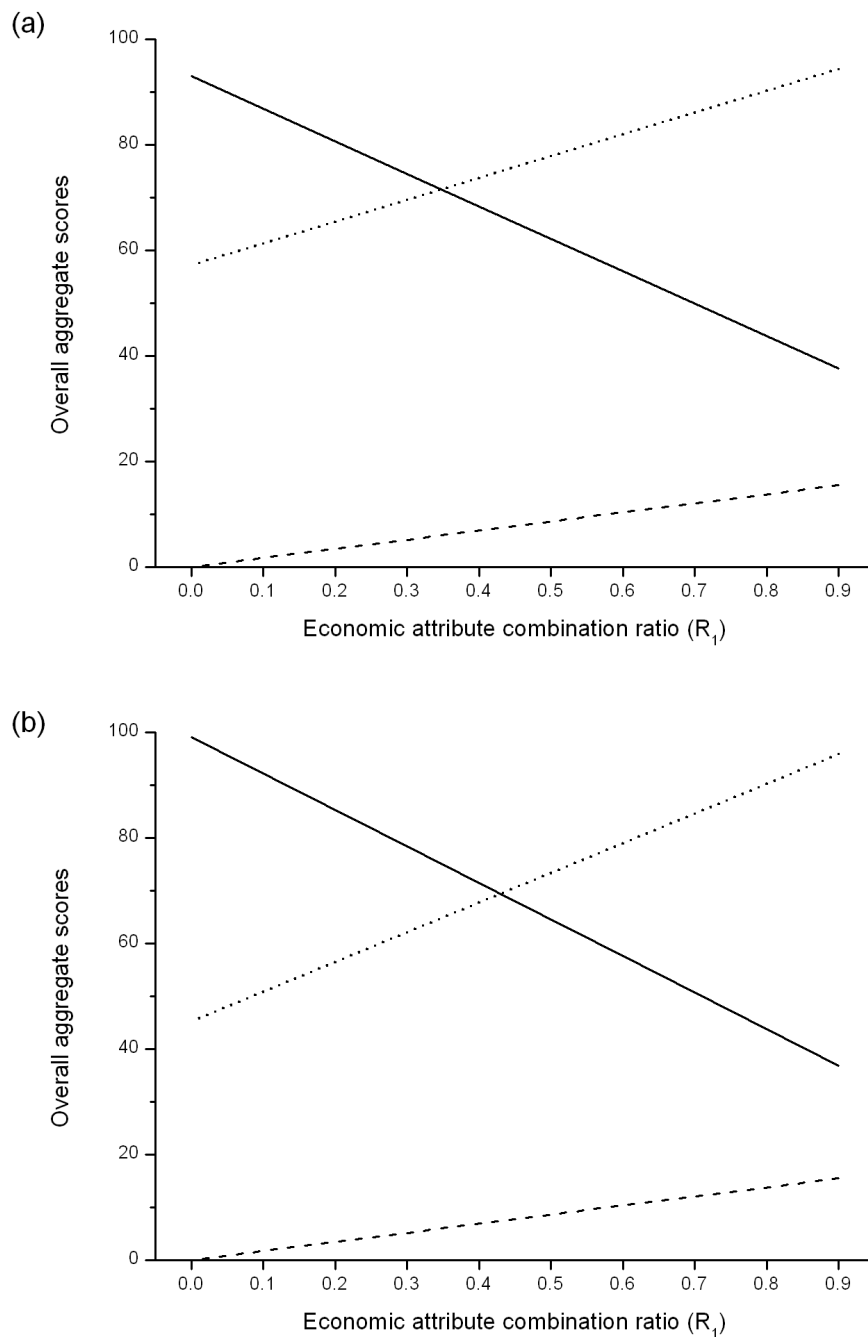


Figure 3.8. Sensitivity plots showing the effect of the economic attribute combination ratio (R_1) on the overall aggregate scores when (a) the operational attribute combination ratio is constant and (b) the environmental attribute combination ratio is constant. For the fed-batch (solid line), spin-filter (dashed line), and ATF (dotted line) processes, for 500 kg/year scale of production and equivalent titre of 5 g/L.

3.4 Conclusions

This chapter presents the utilisation of the simulation framework to assist in cost-effective bioprocess design in the presence of uncertainty and multiple conflicting outputs relating to economic, environmental and operational feasibility. The tool was configured to cope with the continuous nature of perfusion cultures, the consequences of failures as well as the use of single-use bioreactors and bags when the scale was appropriate. The tool was used to provide an in-depth analysis of the potential of mAb facilities based on fed-batch processes compared to 1st (spin-filter) and 2nd (ATF) generation perfusion systems across a range of titres and scales of operation so as to represent different possible scenarios of relevance to industry. The analysis highlighted the underlying cost drivers for each process and identified the robustness of each process along with the root causes for the differences. The derivation of environmental indices not only provided useful benchmarks of E factors for fed-batch and perfusion processes but also enabled the economic, environmental and operational outputs to be assessed simultaneously. This was achieved using a multi-attribute decision-making technique that provided a more holistic approach to managing conflicting outputs. The tool's predictions that the spin-filter perfusion strategy struggles to compete on economic, environmental, operational and robustness fronts at most titres and scales provides insight into its limited use in industrial processes. In contrast, the ATF perfusion strategy is predicted to offer economic benefits that outweigh its lower robustness, even when it achieves cell densities that are only 3 fold higher than fed-batch strategies for typical titre and demand levels. However, the analysis highlighted that if environmental or operational feasibility (e.g. ease of operation and validation) are considered more important than process economics savings then the fed-batch strategy is found to be preferred. The simulation framework therefore acts as a valuable test bed for assessing the potential of novel strategies to cope with future titres and scales of operation.

4 Batch & Semi-Continuous Chromatography

4.1 Introduction

The manufacture of mAbs is typically achieved using a series of product specific chromatographic resins. During clinical development manufacture these resins are often used for just a few cycles, particularly if the drug candidate (DC) is unsuccessful, the resin will then be discarded before reaching its full potential cycle lifetime. The impact of poor resin utilisation is a particular concern in mAb development due to the use of costly protein A capture resins. Improving utilisation of these expensive resins can have a significant effect on the manufacturing costs by reducing the cost burden associated with failed DCs. Semi-continuous chromatography has been shown by Mahajan et al (2012) to be an effective way to increase resin utilisation. This concept is similar to the simulated moving bed concept commonly used in the chemical and pharmaceutical industries, but to date this concept is not widely used in mAb purification.

This chapter explores the potential of semi-continuous chromatography to reduce clinical and commercial mAb manufacturing costs. An integrated approach to the technology evaluation is described that encompasses experimental evaluation and simulation assessment employing the decisional-support framework. The chapter is organised as follows: **Section 4.2** provides a description of the semi-continuous technology evaluated in this chapter, alongside a systematic design methodology to determine the key design and operating parameters for an optimised semi-continuous chromatography operation. In **Section 4.3** the resulting design methodology was validated with semi-continuous constituency runs (**Section 4.3.1**) and incorporated into the decision-support framework to assess the performance and economic feasibility of the technology (**Section 4.3.3**). The framework was then used in combination with a dynamic cycling study (**Section 4.3.4**) to evaluate the potential impact of adopting semi-continuous chromatography for commercial manufacture. The final section then summarises the principle conclusions of the preceding sections of the chapter.

4.2 Methods

The materials and protocols used for the chromatography experiments are outlined in **Chapter 2**.

4.2.1 Three and Four Column Periodic Counter Current Chromatography

The periodic counter current chromatography system was operated in both the 3-column and 4-column mode using either three or four 1ml columns, respectively. **Figure 4.1** details the process description for the PCC system when operated in the 4-column mode. In an effort to utilise the full resin capacity, the harvested cell culture fluid (HCCF) was loaded onto column 1 until the column reached 100% breakthrough (BT) capacity, with the flow-through (FT) HCCF passing to column 2 (**Figure 4.1a**). When 100% BT was achieved in column 1 the HCCF loading was switched to column 2; meanwhile the flush from column 1 was passed to column 3 to retain any unbound protein (**Figure 4.1b**). Upon completion of the column 1 flush step, column 1 underwent two dedicated wash steps before elution of the target protein, whilst the FT of column 2 was directed to column 3 (**Figure 4.1c**). The system's next switch point occurred when 100% BT was reached in column 2, resulting in column 3 entering the HCCF loading position, column 2 undergoing a flush operation with column 4 in the FT position and column 1 conducting a strip step (**Figure 4.1d**). In the 3-column mode the switch only occurred after column 1 had been equilibrated and was ready to switch to the FT position to capture the flushed protein from column 2. In the 4-column system column 2 then entered the wash and elution position whilst column 1 was regenerated and equilibrated for further HCCF loading. Meanwhile column 4 switched to the FT position from column 3 (**Figure 4.1d**). The system continued to switch and load as described until all HCCF was loaded at which point the system ramped down with the columns in the final load and FT position being eluted and cleaned in tandem. The PCC system was therefore operated such that loading of the HCCF stream was continuous, while the collection of the purified product was discrete and periodic.

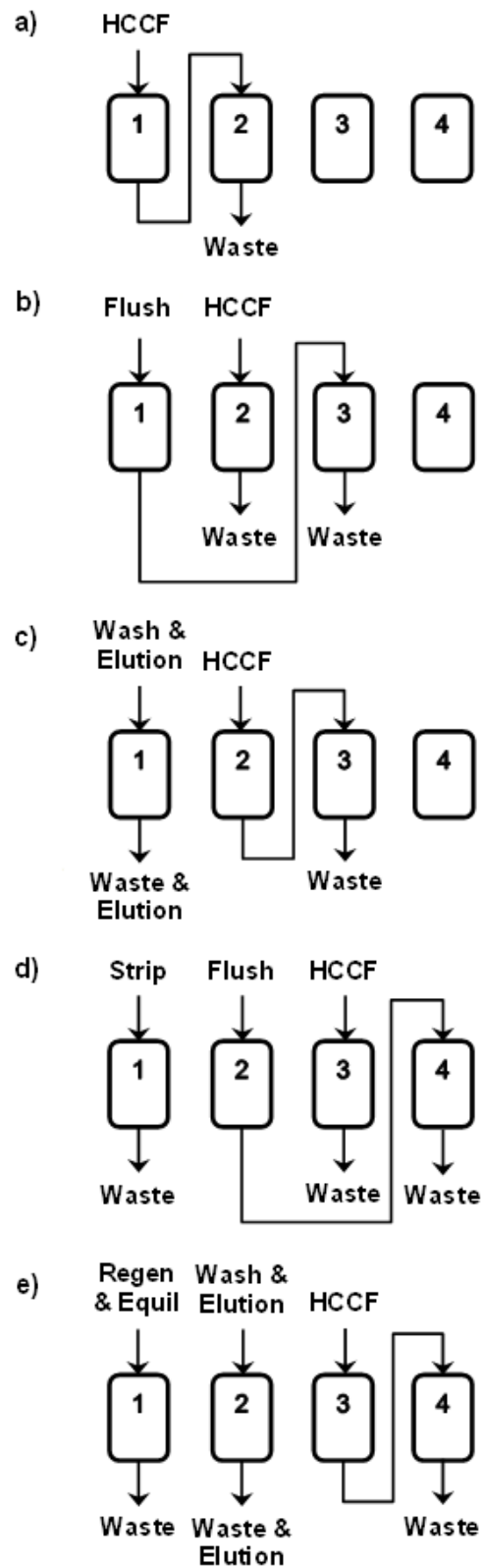


Figure 4.1. 4C-PCC process description (a) column 1 HCCF loading, (b) column 1 flush and column 2 loading, (c) column 2 loading and column 1 wash & elution, (d) column 2 flush, column 3 loading and column 1 strip, (e) column 3 loading, column 2 wash & elution and column 1 regeneration & equilibration.

4.2.2 Switch Time and Optimisation Calculation

The system switch time is the time taken to achieve 100% BT during HCCF loading in the load column and switch HCCF loading to the next column. When operating the PCC system the switch time must be the limiting time versus the non-loading steps to allow continuous loading of HCCF. The ideal PCC system would therefore have a switch time which is equal or marginally longer than the non-loading steps, allowing the maximum utilisation and productivity for the given purification process to be reached. When determining the switch time, the total time required for all the non-loading steps must be known (flush, wash 1 & 2, elution, strip, regeneration and equilibration). The 3-column system has only one column in the non-loading position at any one time and therefore the switch time will have to be greater than all the non-loading steps. In contrast, the 4-column system has two columns in the non-loading position allowing it split the non-loading steps between the columns, effectively halving the minimum possible switching time.

The switch time is dictated by two properties, the HCCF protein concentration and the loading flowrate. To set the switch time to the desired time interval based upon the duration of the non-loading steps either of these two properties can be altered. Concentrating or diluting the HCCF prior to the PCC loading was considered undesirable and could have required the addition of an extra processing step and potentially affect product or feed stream quality. The system was therefore optimised by adjusting the loading flowrate and as a result the protein's residence time in the column, thus causing the BT profile to change. Small-scale single-column (1mL) experiments were performed to generate the BT curves at different flowrates.

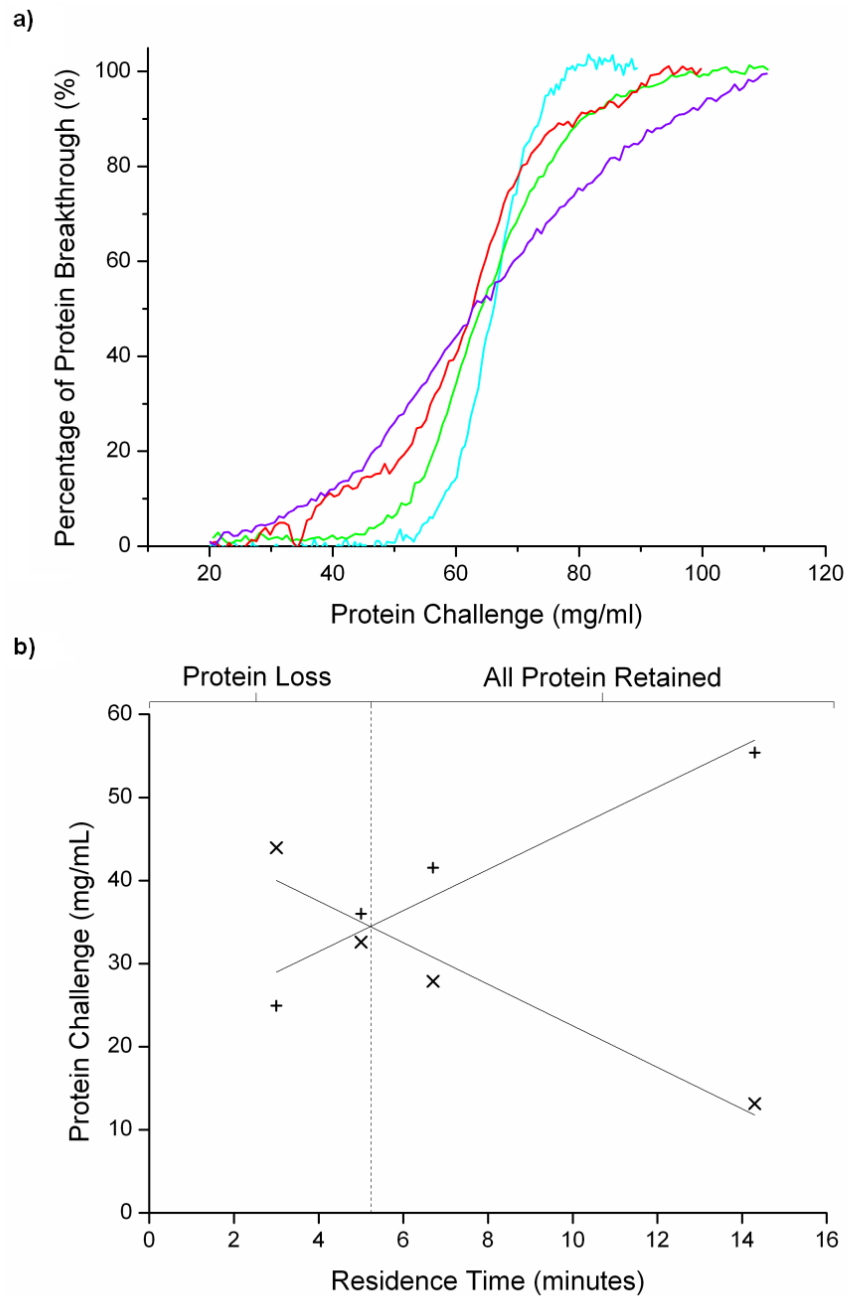


Figure 4.2. The effect of residence time on (a) the protein breakthrough (BT) profile from a 2.77 mg/ml load concentration with a residence time of 14.3 minutes (21 cm/hr) (Blue), 6.5 minutes (45 cm/hr) (Green), 5 minutes (60 cm/hr) (Red), 3 minutes (100 cm/hr) (Purple) and (b) the relationship between the amount of unbound protein in the flowthrough (FT) of the column being loaded to 100% BT (x) and the maximum protein challenge the FT column can capture (protein challenge at 1% BT) (+), resulting in either protein loss or retention.

These curves were used to determine the maximum residence time and hence flowrate allowed so as to avoid product loss. Changes in residence times mean different protein loads would be required to achieve 100% BT in the loading column (**Figure 4.2a**) and as a result the unbound protein passing onto the second column in the FT position would vary (**Figure 4.2b**). **Figure 4.2a** highlights these changes in the BT profile indicating that as the residence time decreases (linear velocity increases), a higher load challenge is required to reach 100% BT (Hahn et al. 2005). These BT-derived plots allowed two key characteristics to be established: a) the maximum allowed protein challenge (mg protein applied / ml resin) that could be applied to the column before material was present in the FT, represented by the protein challenge at 1% BT, b) the actual amount of unbound protein in the FT at 100% BT (the actual FT protein challenge) determined by integrating the area under the BT curves (mg unbound protein/ml resin). **Figure 4.2b** highlights how these two values (the maximum allowed protein challenge and the actual FT protein challenge) interacted with respect to residence time resulting in two intersecting lines. This relationship highlighted the critical residence time (6 minutes) below which the amount of unbound material in the FT of the column being loaded to 100% BT would be too high for the column in FT position to capture (surpassing the maximum allowed protein challenge) and would therefore result in material losses. Therefore in an effort to find the optimal switch time by altering the loading flowrate, careful consideration was paid to potential losses of unbound material.

Figure 4.3 details the systematic design approach developed to establish the optimal system parameters and switch time intervals that avoid product loss. The flowchart logic and underlying equations derived from **Figure 4.2b** were entered into the UNICORN method when running experiments and used in the simulation model to predict the performance of the PCC system in either 3-column or 4-column mode.

It may be possible to use real time absorbance measurement of antibody breakthrough as real time indicator of switch time. However the absorbance of small amounts of antibody breakthrough through the resin was small

compared to the absorbance of impurities flowing through the column, making this approach less robust in this case. It is possible that with more sensitive analytics and/or a higher ratio of product to impurities this approach would be successful.

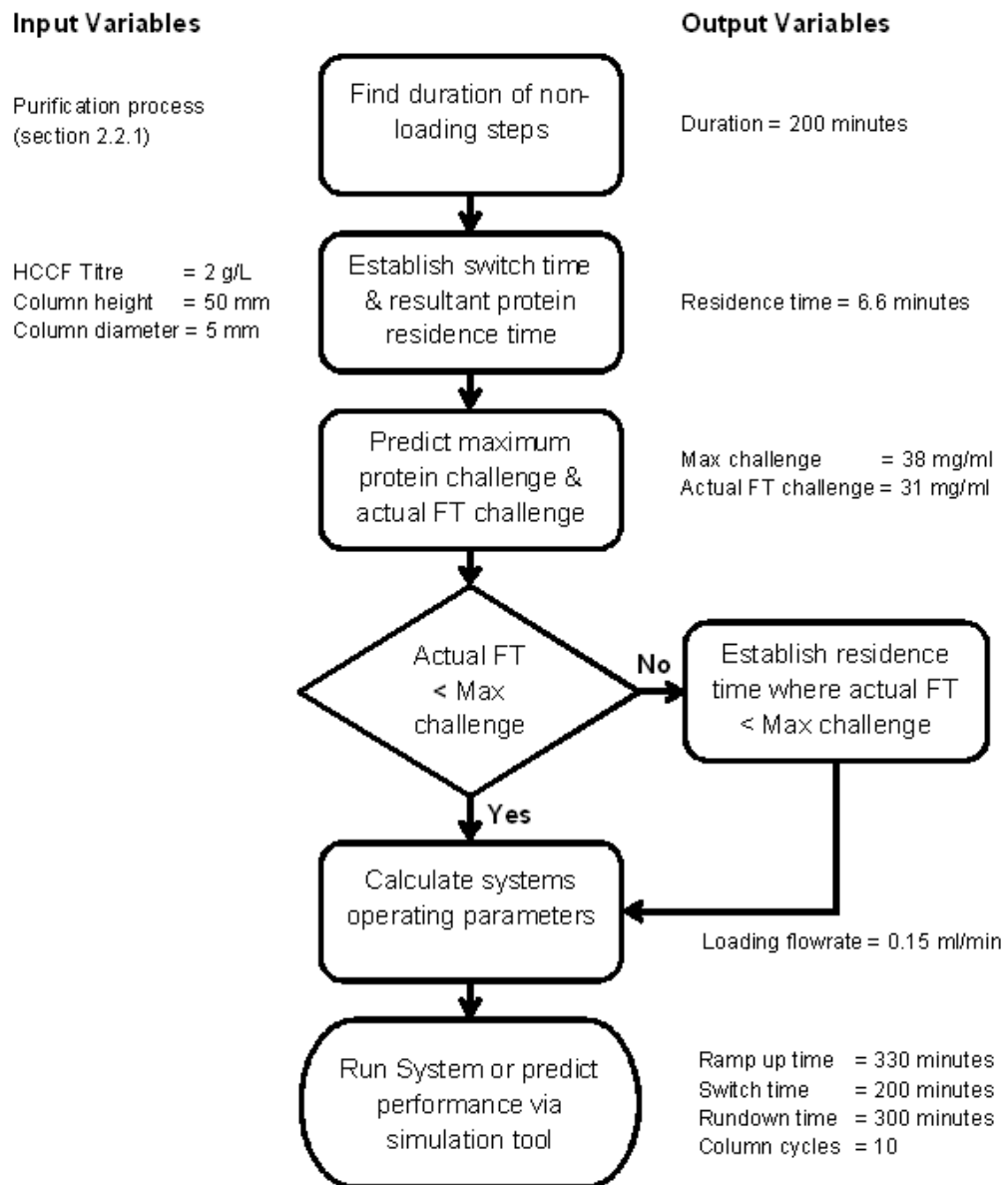


Figure 4.3. Flow-sheet detailing a systematic design approach to optimise the performance of a 3-column or 4-column periodic counter-current chromatographic process, with example input and output variables for a completed verification run.

4.2.3 Wash Step Optimisation

The wash step optimisation study was performed on an ÄKTA FPLC using a 1mL column (0.5mm I.D., 5cm height) and the purification buffers specified in **Chapter 2**. The high salt wash buffer's molarity was reduced over a number of cycles to reduce wash step yield losses where the column was loaded with HCCF to 100% BT. The product quality of the resulting elution pools was analysed using the methods outlined in **Chapter 2**.

4.2.4 Resin Reuse Study

Resin reuse studies are typically performed using small-scale columns (ml column volumes) which is resource expensive, laborious and restricts the variables studied (Łączki 2012). This is in contrast to high throughput miniaturised methods regularly employed for screening of chromatography conditions. Hence, careful consideration was applied to the resin cycling studies shown in this paper to determine the useful lifetime of the protein A affinity resin under two different loading conditions, balancing resource constraints with experimental output. Both cycling studies were operated on the ÄKTA FPLC and used the process buffers specified in **Chapter 2**. The first study was conducted by the Purification Process Development group at Pfizer Inc., Andover, Massachusetts and was designed to replicate the standard batch process with a 40mg/ml protein load challenge per cycle, loaded at 230cm/hr giving a residence time of 6.5 minutes, for 200 cycles. The dynamic binding capacity at 10% BT was established every 50 cycles. The study employed a 24ml column with a 1.1cm I.D. and a column height of 25cm. The second study was designed to capture the conditions found when operating the PCC system, with the resin challenged to 100% BT resulting in a final protein load challenge per cycle of ~110mg/ml. The dynamic binding capacity was recorded every 5 cycles at both 10% and 100% BT. A 3ml column was used with a 0.5cm I.D. and 15cm bed height, and was loaded at 46cm/hr with a residence time of 6.5 minutes, for 100 cycles.

4.2.5 Decisional Tool

The economic analysis shown in this chapter was achieved using the simulation framework defined in **Chapter 2**. The chromatography process models shown in **Section 2.1.4.3.4.3** detail the scheduling and mass balance equations for batch chromatography and semi-continuous chromatography (PCC). The same mass balance equations are utilised for both the batch and PCC chromatography systems. However **Figure 4.1** demonstrates how the PCC system processes a number of operations at the same time in different columns. The scheduling of these different operations is shown in **Figure 4.4**, where the loading of a column is represented by a grey block and the non-loading operations by a white block. To avoid major changes to the structure of the tool and follow the software principal of abstraction adopted throughout the development of the simulation framework. The semi-continuous chromatography's systems resource requirements (buffers & labour) were converted into a single column system. The tool was then able to predict the resource requirements of the semi-continuous system without significant adaption. This was achieved by reducing the apparent duration of the loading operations, to the loading time remaining after the non-loading operations have been completed. This can be best visualised by overlaying all the columns of the PCC system (**Figure 4.4**). The methodology made it possible to convert multiple parallel operations into a single operations schedule, but still request the right amount resources at the correct time. This methodology was also successfully applied to the 4-column PCC system.

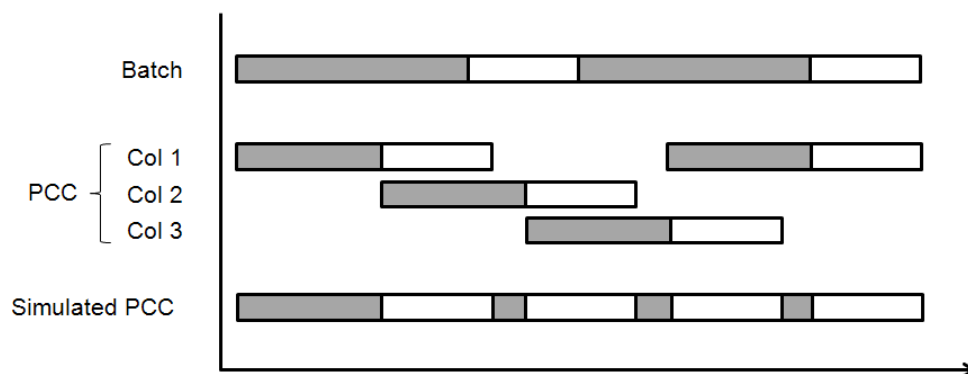


Figure 4.4. Schedule of the loading (grey) and non-loading (white) processes for the batch, 3-column periodic counter current chromatography system and the simulations interpretation of the periodic counter current chromatography system.

4.2.6 Case Study & Assumptions

The simulation tool was used to compare the cost-effectiveness of the 3-column and 4-column PCC system to the standard batch process throughout the development pipeline, exploring the trade-offs between reduced column and buffer volumes versus the higher number of column cycles.

Table 4.1 illustrates the clinical trials estimates used throughout this case study to calculate the amount of mAb required for each phase of the clinical trials throughout the development pipeline. The case study uses the quick win, fail fast development paradigm (Paul et al. 2010), where the material required for Phase I & II is generated in a single batch for the Proof-of-Concept (PoC) development phase. Assuming the average body weight of a US male to be 86kg (Ogden et al. 2004), a single 4kg batch of mAb was required for PoC development also accounting for non-clinical uses. This amount increases to 40kg of mAb for the phase III clinical trials and is produced by four 10kg batches at the Commercial batch scale allowing parallel process validation studies. The 10kg Commercial batch size is based on the median market demand of the top 15 mAb (200kg) (Kelley 2009) and the ability to process 20 batches per year. The cell culture titre also increases

with clinical phase, where due to continued process development the titre was assumed to increase 2-fold from the PoC batch to the Phase III & Commercial batches. The case study looks at two titre scenarios capturing the current and future mAb titres in the development pipeline. The scenario produced a 2.5g/L titre for the minimally developed PoC batch before increasing to a final titre of 5g/L.

Table 4.1. Case Study Assumptions

Clinical Trial Estimates	
Variable	Value
Dosage (mg/kg body weight)	7
Number of doses per patient per year	26
Individuals in Phase I clinical trials (single dose)	40
Individuals in Phase II clinical trials (6 month dose)	200
Individuals in Phase III clinical trials (year dose)	2000
Process Parameters	
Maximum Binding Capacity (g/L)	65
Bed Height (m) – Standard Batch Process	0.25
– PCC process	0.1
Shift Duration (hours) – Standard Batch Process	12
– PCC process	24
Maximum Media Hold Time (hours)	72
Cost Parameters	
Protein A Resin Cost (\$/L)	8000
AEX Resin Cost (\$/L)	1500
Virus Removal Filtration Membrane (\$/m ²)	3250
Labour Cost (\$/hour)	58
Chromatography Process Skid (15-600L/hr) (\$)	226,000
PCC Process Skid (15-600L/hr) (\$)	1,080,000
Chromatography Column (Dia = 0.2m) (\$)	132,000
Chromatography Column (Dia = 2m) (\$)	218,000

The manufacturing process used in the case study was based on a generic two-column mAb process (Kelley 2007; Kelley et al. 2008). The key differences between the PCC based process and standard batch process lie

in the operation of the capture chromatography step (protein A) and are highlighted in **Table 4.1**. The standard batch process employs a single column utilising multiple cycles which are loaded with HCCF up to 90% of 1% BT (safety factor accounting for capacity losses with resin reuse), resulting in a maximum protein challenge of 40g/L. The resulting protein A cycles occur over three 12 hour shifts due to a constraint on the maximum HCCF holding time of 72 hours. The PCC systems employ multiple columns (3 or 4) for multiple cycles which are loaded to 100% BT resulting in a dynamic binding capacity of 65g/L. The continuous nature of the PCC system means that it has to be operated in a 24-hour shift to truly harness the benefits of the system, but it is still constrained by the maximum HCCF hold time of 72 hours. The case study assumes that both systems are able to offer comparable product quality and yield, as this was proven through experimental validation (see **Table 4.2**). However, any change in product pool concentration and volume was accounted for by altering the scaling of the downstream purification operations where necessary.

4.3 Results and Discussion

4.3.1 Verification of Optimisation Strategy for Semi-Continuous Chromatography

The verification study comprised a number of runs for a range of loading residence times (3 - 14.3 minutes) and HCCF titres (0.9 - 5.3 g/L) for both the 3-column and 4-column PCC system. The performance of the system was measured in terms of UV profile, product quality and step yield. The system design approach from **Figure 4.3** was utilised to predict the switch time, as well as ramp-up and ramp-down times. The sample input and output variable values indicated in **Figure 4.3** provided the basis for the 3-column PCC verification runs shown in **Figure 4.5a**.

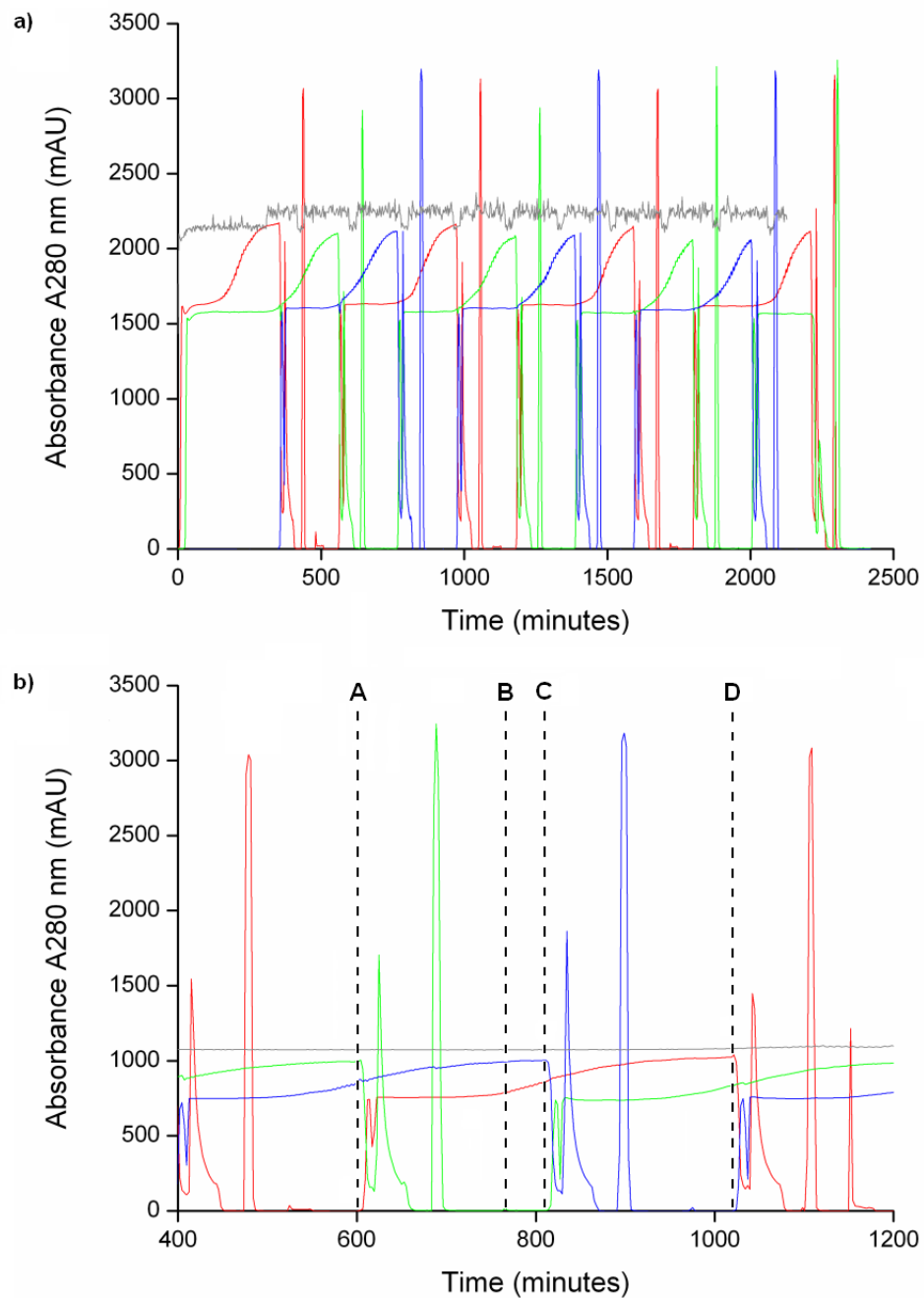


Figure 4.5. UV profiles for the 3-column PCC verification runs (column 1; red, column 2; green & column 3; blue). (a) A 3-column PCC run loaded with 2g/L HCCF at 0.15 ml/min with a residence time of 6.5 minutes, including system ramp-down. (b) A detailed plot of a 3-column PCC run loaded with 0.9 mg/ml HCCF at 0.33 ml/min with a residence time of 3 minutes, detailing column 1 (red) in the FT position with column 3 in the loading position (blue), before switching to the loading position. Point A highlights when column 1 enters the FT position, capturing any unbound protein from column 3. The increase in UV signal at point B highlights the loss of unbound protein, before column 1 switches to the load position at point C. Column 1 loading ends at point D and the non-loading steps start.

The system was loaded with HCCF at 2g/L and a residence time of 6.5 minutes, resulting in 3 system cycles (10 column cycles including system ramp-down) to process ~650mg of mAb. The UV profiles in **Figure 4.5a** and the other verification runs demonstrated no secondary BT of unbound protein from the column in the FT position, due to successful implementation of the design approach. To evaluate the accuracy of the small-scale single-column data (**Figure 4.2**) and design approach (**Figure 4.3**), an example run was conducted where the residence time was set to be below 5.5 minutes. Based on **Figure 4.2b** a loss of material was projected, this was seen as BT in the FT column and resulted in a 10% lower yield than projected. **Figure 4.5b** demonstrates the results of this validation run where the residence time was set to 3 minutes and loaded with HCCF titre of 0.95g/L. **Figure 4.5b** shows an expanded scale chromatogram highlighting column 1 (red UV profile) throughout a single cycle. Point A highlights when column 1 enters the FT position and records an increase in UV signal as material starts to pass through column 1 from the loading of column 3 (blue UV profile). The UV signal for column 1 then plateaus signifying the maximum signal for impurity-related BT. After point B the signal should remain linear (as seen in **Figure 4.5a**), however the UV signal increases highlighting that the target protein is passing through column 1 unbound in the FT and being lost. Column 1 is then switched into the loading position at point C and achieves column saturation at point D where it has completed loading and moves to the wash position.

At high column loadings the potential exists for strongly binding antibody variants to displace weaker binding antibody variants. This would result in different product quality in the eluate pools from the continuous system compared to the batch system. Product quality of the eluate pool volumes was assessed by CEX-HPLC and SEC-HPLC evaluating acidic/basic species and high molecular weight species content (HMW), respectively. **Table 4.2** shows that the product-related impurity profile in the eluent pools from the verification runs was consistent regardless of the loading residence time and was found to be comparable to the eluate pool data generated from the same batch of HCCF but processed in the conventional batch conditions (40mg/ml

protein challenge). Recent publications (Mahajan et al. 2012; Warikoo et al. 2012) corroborate these findings for product quality.

Table 4.2. Protein Pool Product Quality

% Species of Protein Pool			
<i>CEX-HPLC</i>	Acidic	Designated	Basic
Standard	18.4 ± 2.5	74.8 ± 2.7	6.9 ± 0.3
3C-PCC	18.3 ± 0.6	75.8 ± 1.5	5.9 ± 1.0
Wash	18.0 ± 0.6	76.2 ± 0.9	5.7 ± 0.3
Cycle	19.3 ± 0.8	75.0 ± 1.2	5.7 ± 0.9
<i>SEC-HPLC</i>	HMW	Designated	LMW
Standard	1.0 ± 0.1	96.9 ± 0.1	2.1 ± 0.0
3C-PCC	0.4 ± 0.1	98.0 ± 0.1	1.6 ± 0.2
Wash	0.6 ± 0.1	98.1 ± 0.2	1.3 ± 0.1
Cycle	0.7 ± 0.2	97.6 ± 0.3	1.7 ± 0.2

The step yield for the PCC verification runs was approximately 10% lower than expected when compared to the standard batch process (80 – 90%). The difference in step yield was investigated by conducting a full system mass balance for each verification run. This illustrated that the reduction in step yield was not caused by losses in unbound protein in the FT, verifying the findings from the UV profiles (**Figure 4.5a**). The reduced step yield was attributed to the higher losses in the dedicated salt wash step, where higher levels of bound protein were found to be washed off the column with the product-related impurities in the PCC system compared to the standard batch process. As a result, the impact of the wash step conditions performance was investigated further.

4.3.2 Wash Step Evaluation

The increasing loss of bound protein in the high salt wash step has been seen in historical runs of the standard batch process with increasing resin cycle count. The impact of reducing the wash step molarity on the losses in bound protein was investigated due to its prior success for the standard batch process and its ease of implementation with no requirement to alter the UNICORN method. The standard batch process only uses approximately 2/3 of the available protein A ligand due to the reduced challenge load (40 mg/ml) to prevent FT losses. As the resin cycle count increases protein A ligand is lost, eventually leading to a point where the batch process is using 100% of the available protein A ligand to capture all the protein challenge, mirroring the state seen in the PCC system. At this time higher losses of bound protein are seen in the high salt wash step. To counter this loss of bound protein the molarity of the salt wash is reduced in line with cycle number, reducing bound protein loss and maintaining product related impurity clearance. An alternative method would be to pass the high salt wash FT over a column in FT position similar to the flush step, potentially retaining any lost protein. This approach has a number possible concerns with respect to product quality (recapturing target protein and product-related impurities) and the potential impact of the high salt wash on subsequent HCCF loading (precipitation and non-binding) without a new equilibration step on the FT column, which would increase the total buffer volume and wash time. If the wash step had no impact on subsequent HCCF loading the recapturing of material in the FT of the wash step would be more favourable.

The results of reducing the wash step molarity in a column loaded to 100% BT to mimic PCC operation is shown in **Figure 4.6** and **Table 4.2**. The evaluation found that the salt molarity had to be reduced by ~ 70% to reach a similar step yield seen in the standard batch process. **Table 4.2** highlights how the reduction in wash step molarity had no adverse effect on product quality, offering the same product-related impurity clearance as the standard batch process. The lower salt wash was not believed to impact the removal of DNA, viruses, and host cell proteins but was not measured in this case. The experimental studies therefore demonstrated that the PCC system could

achieve similar yields and product quality to the standard batch process. These findings were then used in the process economic study to assess the economic feasibility of using the PCC system to generate clinical and Commercial material.

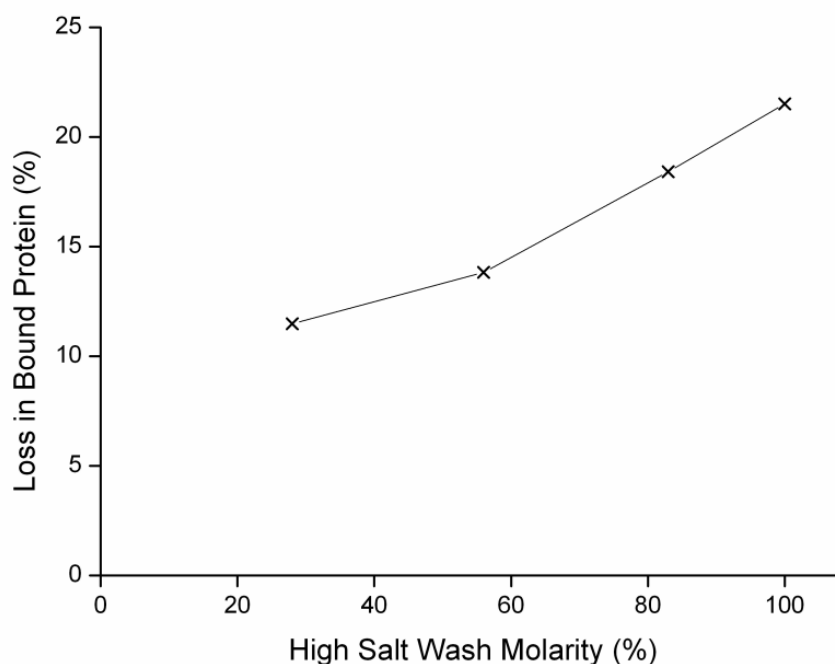


Figure 4.6. The impact of salt molarity of the high salt wash step on percentage loss of bound protein for a 100% breakthrough challenged column, for a minimally (3 cycles) cycled protein A resin.

4.3.3 Economic Impact of Semi-Continuous Chromatography

The simulation tool was used to assess the cost-effectiveness of the 3-column and 4-column PCC system versus the standard batch process for a range of titre and manufacturing scenarios. The system's cost-effectiveness was assessed by calculating the direct costs (labour, buffers, chromatographic resin, filter membranes etc.) at the given scale of production. **Figure 4.7** shows the direct cost per gram for the 3-column, 4-

column and standard batch process for a range of production scales in the clinical development pipeline (4kg, 40kg, 200kg). The analysis suggests that although the PCC system offers reduced manufacturing costs for the generation of early phase Proof-of-Concept (PoC) material, the advantage becomes less significant later in the development pipeline (Phase III and Validation batches) eventually offering similar manufacturing costs during Commercial manufacture.

A detailed examination of the direct manufacturing costs highlighted in **Figure 4.7** reveals how the decreased competitiveness of the PCC system with production scale can be attributed to the decreasing contribution of the protein A resin cost to the total cost, as illustrated in the embedded table. **Table A4.1** shows the ensuing equipment number and sizes for the scenarios shown in **Figure 4.7**. This is demonstrated in the standard batch process which employs a single 31.4L column (five cycles) to process the singular 4kg PoC batch at a resin cost of \$250k (USD 2011) per batch which accounts for 58% of the total direct costs for the batch. The PCC system is able to reduce the total direct costs per gram by reducing the volume of resin required by utilising the whole resin capacity. The model predicted that the 3-column PCC system would require three 4.9L columns for 17 column cycles (5.7 system cycles). This resulted in a ~50% reduction in total resin cost to \$118k, resulting in a 31% reduction in batch manufacturing direct costs. The level of cost savings was less than anticipated due to an 8% increase in the labour cost caused by the switch from shift-based manufacturing to the 24-hour manufacturing regime required to operate the PCC system continuously. The 4-column configuration is able to offer a slightly higher level of saving by employing yet smaller columns (4 x 3.1L) and using them more frequently (6.5 system cycles, 26 column cycles) leading to a 34% reduction in batch manufacturing direct costs.

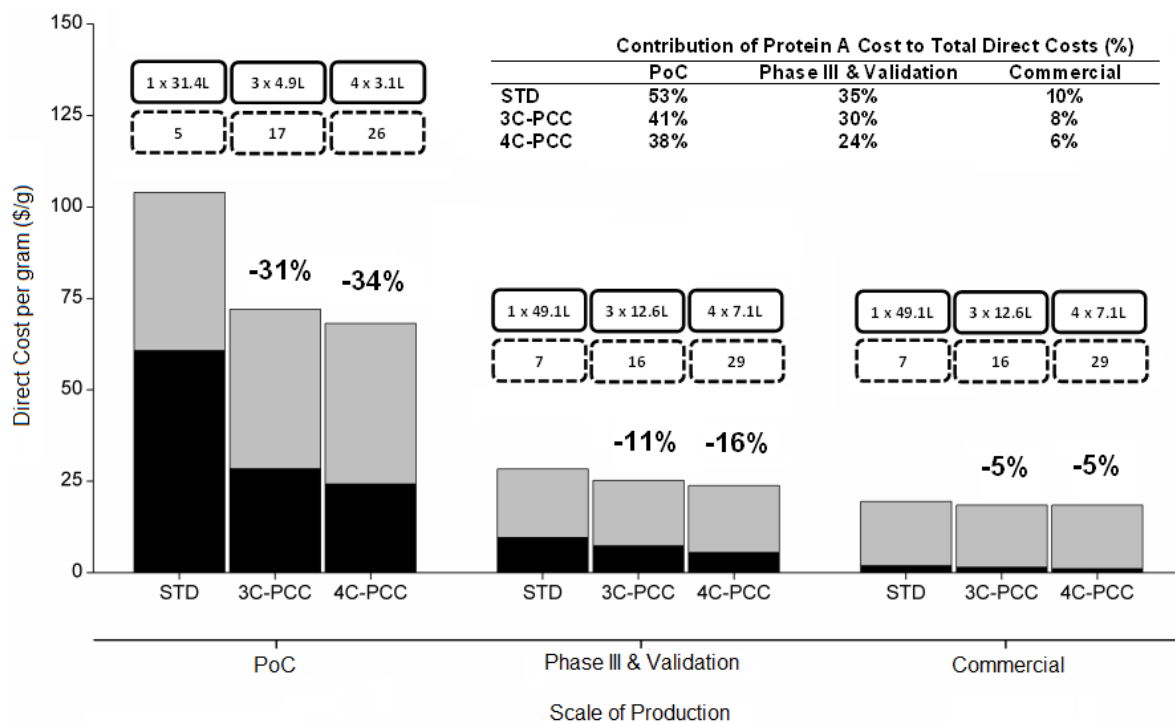


Figure 4.7. A comparison of direct cost per gram highlighting the protein A cost (black) to the other direct costs (grey) between the standard batch process (STD) and the 3-column (3C-PCC) and 4-column periodic counter-current chromatographic (4C-PCC) process over a range of scales of production for the low titre scenario, where the percentage difference is relative to the standard batch process. The embedded table highlights the percentage contribution of the protein A resin towards the total direct costs. The optimal sizing strategy for each process is indicated in the boxes above each bar highlighting the number and scale of columns (solid box) and the number of system cycles (dashed box) across a range of scales of production.

The savings offered by the PCC system are reduced significantly as the scale of production increases from the generation of PoC material (1 x 4kg batch) to the generation of Phase III clinical material (4 x 10kg batches) and Commercial material (20 x 10kg batches per annum). This effect is due to the fact that the protein A resin is only used for a few cycles in the PoC batch and Phase III batches. Due to the requirement to keep the resins product-

specific, it cannot be reused for another drug candidate, resulting in a higher cost burden because the resin may be discarded before reaching its full potential cycle lifetime. For example the protein A cost (\$250k) accounts for over half the direct costs at the PoC scale for the standard batch process. However for a 10 kg batch the resin costs \$390k (49.1L column, 7 cycles) and this cost is split between the multiple batches and therefore reduces the overall cost contribution to 34% and 10% for the Phase III (4 batches) and Commercial (20 batches) material respectively. The PCC systems maintain the same level of column volume reduction with the increase in scale, but as shown by the embedded table in **Figure 4.7** they fail to offer the same level of savings as the protein A cost becomes less significant as other process costs dominate the manufacturing cost. For cases where it is possible to use the same lot of protein A for both PoC and Phase III batches; the protein A cost contributions for late-phase batches would be even lower.

The ability of the PCC system to reduce the column volume, also impacts the volume of chromatographic buffer required. The standard batch process uses 5,500 litres of buffer for the protein A step per PoC batch, which is approximately a quarter of the buffer volume used for the generation of the batch. The 3-column and 4-column system reduce the protein A buffer volume by ~39% and ~49% respectively resulting in an overall process buffer reduction of ~12% and ~15%. These savings have minimal impact at PoC scale of manufacturing resulting in direct cost savings <1%. This relationship was also found during the generation of the 10kg batches for Phase III and Commercial material, where again direct cost savings were insignificant.

4.3.4 Impact of Resin Reuse

Figure 4.7 highlighted the high number of cycles employed by the 3-column and 4-column PCC system allowing them to reduce the overall column volume. The high cycle count combined with the higher protein challenges could potentially affect product quality and will lead to a reduction in binding capacity. The loss of binding capacity will require the PCC system to run more column cycles to purify all the HCCF. This will conceivably increase the protein pool volume outside process design volumes and also the step processing time over the validated media hold-time (72 hours).

4.3.4.1 Resin Reuse Study

The impact of cycle count on binding capacity and product quality was investigated via two cycling studies with MabSelect resin, replicating the conditions found inside the standard batch process and the PCC system. **Figure 4.8a** shows the effect of cycle count on dynamic binding capacity at 10% BT for the standard batch process and 100% BT for the PCC system which utilises the whole resin capacity every cycle. A binding capacity loss of ~20% and ~40% was observed over 100 cycles in the standard and 100% BT studies. The process buffers used throughout both studies were kept constant and therefore the increased rate of capacity loss seen in the 100% BT study was attributed to the increased volumes of HCCF (x2.2) that the resin was exposed to per cycle. The loss in capacity affects each process differently due to their mode of operation. The standard batch process only uses 2/3 of the resin's capacity and therefore any loss in capacity has no effect on the maximum allowed protein challenge until the resin use reaches 100 cycles. **Figure 4.8b** demonstrates that as the cycle count passes 100 cycles a small percentage of the material loaded was found in the flow-through. In contrast the PCC system is designed to utilise the whole resin capacity making it highly susceptible to any change in binding capacity. Due to the high impact of resin capacity loss on the PCC system, the mechanism for this increased rate of loss was investigated further.

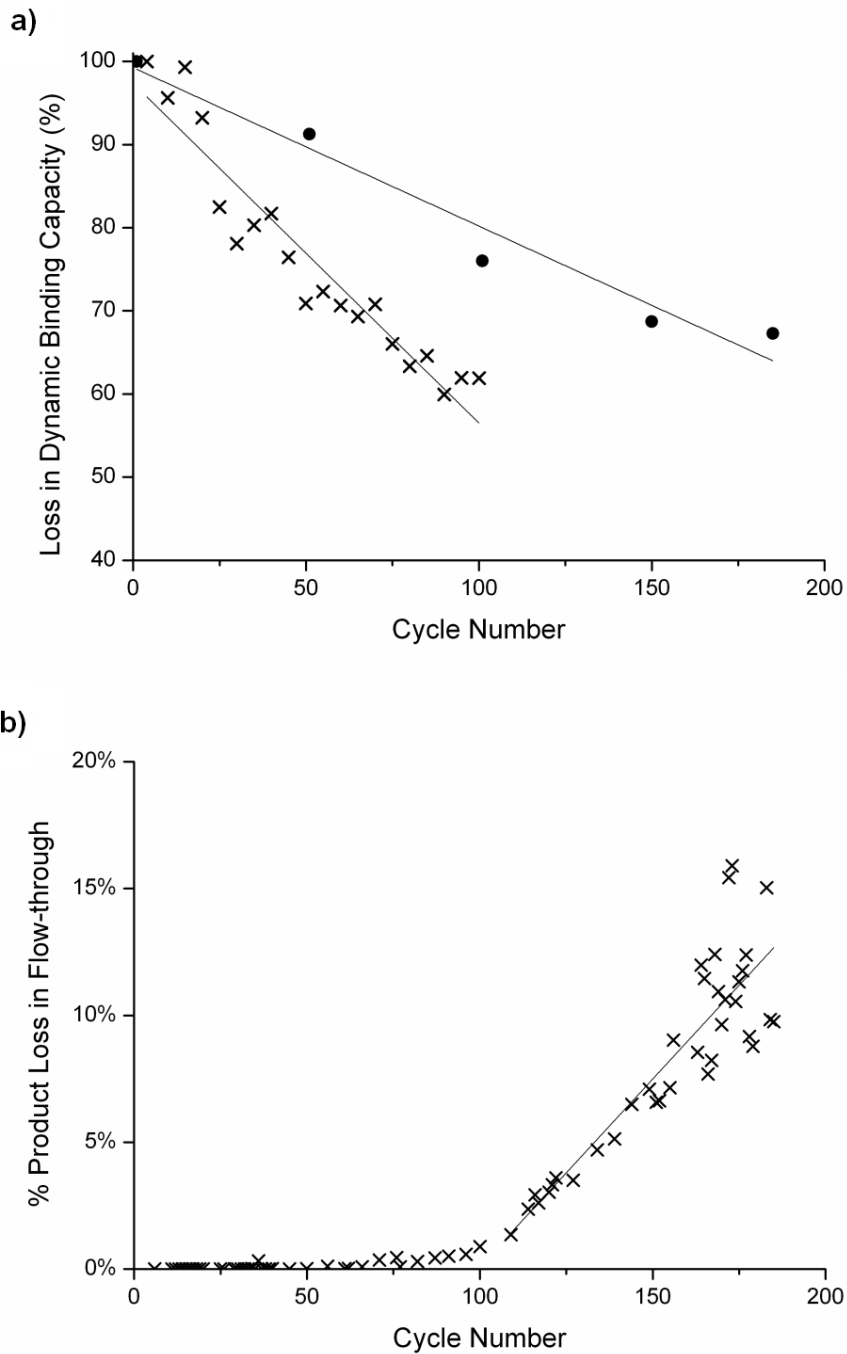


Figure 4.8. The effect of cycle number on (a) binding capacity for standard batch process (40 mg/ml of protein load challenge per cycle)(black circles) and 100% break-through study (~110 mg/ml of protein load challenge per cycle)(crosses), (b) the percentage of the challenge load in the flow-through for the standard batch process.

Table 4.2 shows that throughout the 100% BT study the product quality was found to be constant with respect to specification of the product. However it was noted that the pH of the elution pool decreased (from 4.2 to 3.6) with increasing cycle number (**Figure 4.9**). This was caused by an increase in the volume of elution buffer applied to the column prior to peak collection (pre-peak volume). The increase in pre-peak volume from 1 CV to 1.2 CV resulted in a larger volume of pH 3 elution buffer passing through the column prior to peak collection, thus a smaller proportion of the pH 7.5 wash buffer carried through to the elution pool. This phenomenon strongly suggests that the mass transfer properties of the column were changing with increasing cycle number and that this affect was due to the loss of surface binding sites caused by fouling and/or ligand loss. I.e. due to unavailability of surface biding sites it took the mAb longer to diffuse from inside resin bed to the mobile phase and hence lead to increased pre-peak volumes.

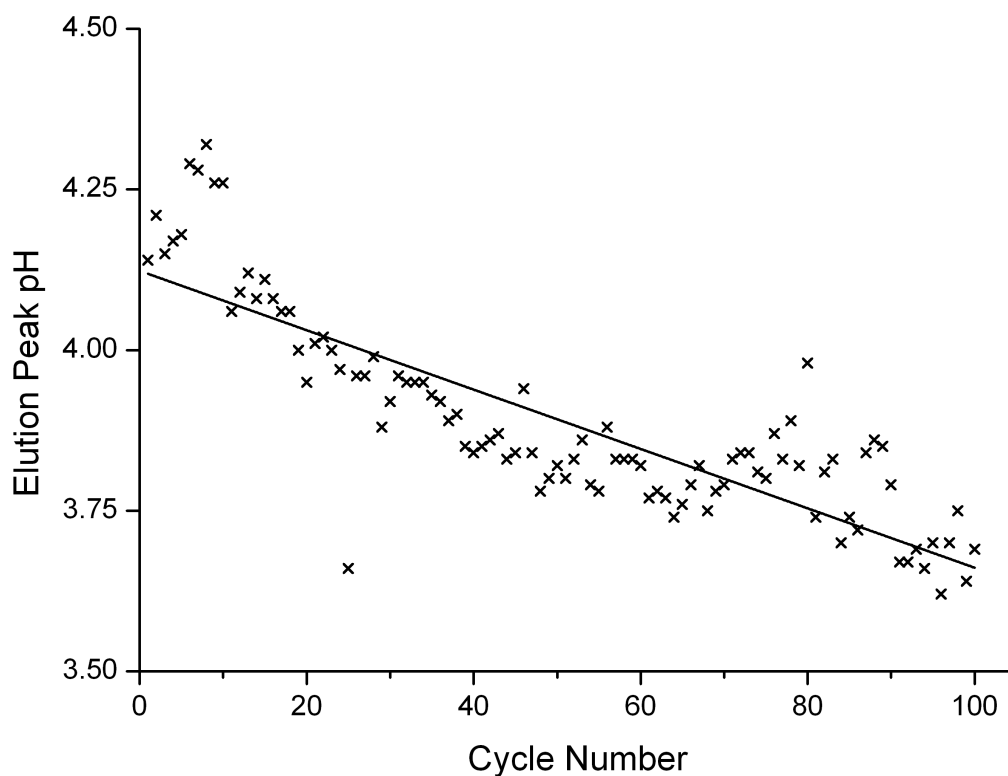


Figure 4.9. Elution peak pH for 100% breakthrough cycle study versus cycle number.

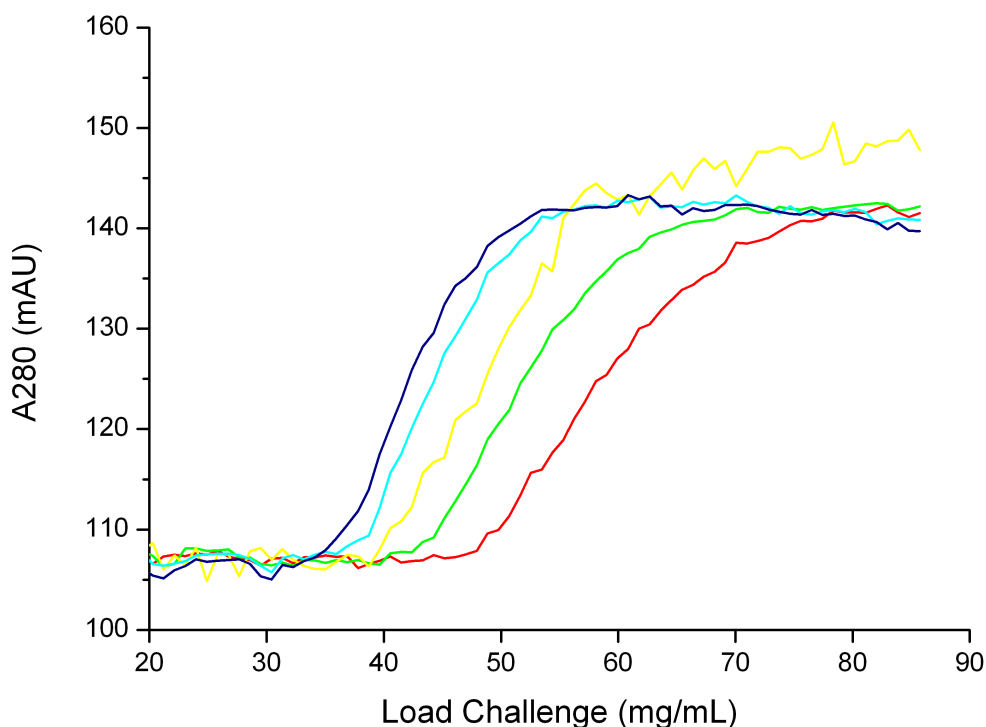


Figure 4.10. Breakthrough profiles on MabSelect resin in the 100% BT cycle study for resin used for 20 cycles (red), 40 cycles (green), 60 cycles (yellow), 80 cycles (light blue) and 100 cycles (purple). The increase in A280 for the breakthrough at cycle 60 (yellow) was caused by an air bubble in the UV monitor.

The breakthrough profile of mAb (**Figure 4.10**) was monitored during the loading phase of the cycle study, and was found to occur earlier with increasing cycle number due to the loss of binding sites corresponding to the decrease in capacity seen in **Figure 4.8**. It was also noted that the columns mass transfer properties changed with increasing cycle number as shown in **Figure 4.9** by the increasing sharpness of the breakthrough profiles.

The leading edge of a breakthrough curve is dominated by the mass transfer of the mAb in the fluid film, whereas the tailing edge is dominated by diffusion of the mAb into the matrix pores (Helfferich and Carr 1993; Siu et al. 2006). Therefore if excessive surface fouling is present the breakthrough curve is likely to exhibit tailing, where the tailing edge of the breakthrough becomes very shallow and takes longer to reach full resin saturation. **Figure**

4.10 shows that the breakthrough profiles exhibit no signs of tailing and therefore strongly suggest that fouling is not having a significant impact on the mass transfer properties of the resin. However fouling may still be present in the form of pore occlusion, where smaller resin pores are blocked preventing access to binding sites. The increasing sharpness of the breakthrough curves demonstrates an improved mass transfer rate into the bead. It can be assumed that for a large molecule such as a mAb, pore diffusion will be the most relevant mass transfer resistance and since pore diffusivity depends on the square of the adsorbents diameter (Hahn et al. 2003). An improvement in mass transfer properties can be attributed to either a reduction in steric hindrance (loss of ligand and widening of pores) or a reduction in particle diameter (loss of resin structural integrity).

4.3.4.1.1 Resin Characterisation

The analysis of the loading breakthrough profiles and increasing elution pool pH during the cycle study suggest that the loss in capacity and changes in mass transfer properties could be due to loss of binding sites, particularly surface ligands. There are a number of mechanisms for the loss of binding sites seen, including pore inclusion, protease digestion and proteolysis of the ligand. To establish which of the described mechanism is principally responsible for the observed effects, the column was unpacked and the resin was further analysed using the techniques described in **Chapter 2**. The cycled resin sample was compared to new resin (conditioned with 3 cycles of HCCF and elution) and NaOH cycled resin (100 cycles of CIP buffer only).

Figure 4.11 shows the batch uptake profiles for the three resins, where the cycled resin sample (dotted line) binds the least mAb and the new resin sample (solid line) the most. Upon saturation the cycled resin binds ~40% less mAb and the NaOH cycled resin ~10% less mAb compared to the new resin sample (See **Tables A4.2, A4.3, and A4.4**). The batch uptake study also demonstrates that the changes in mass transfer properties seen are negated in the highly agitated environment used in the batch experiment.

Where all the resin samples reach ~50% saturation in 12 minutes, ~90% saturation within an hour and equilibrium after 2 hours.

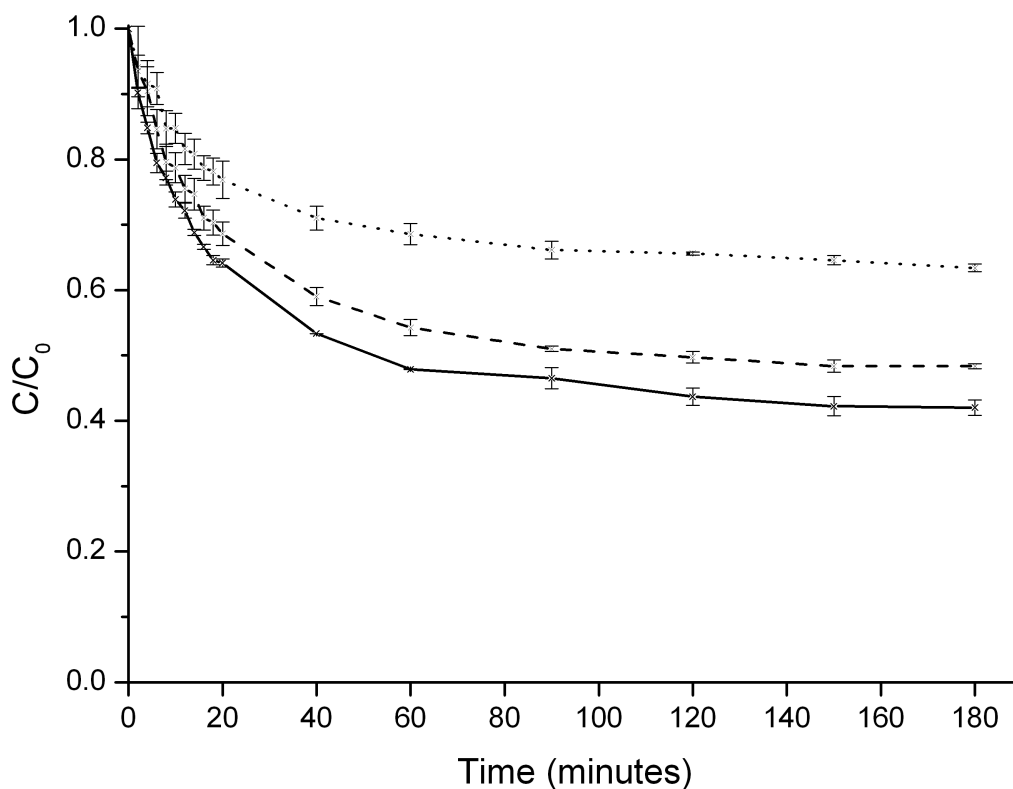


Figure 4.11. Batch uptake curves of 2.6 mg/ml mAb by new (Solid line), cycled (dotted line) and NaOH cycled (dashed line) MabSelect resin samples during batch experiments. (Feed to resin volume ratio 45:1).

Isotherm experiments were then run for all the resin samples to determine the maximum capacity and the dissociation constant. The resulting adsorption equilibrium were described by the Langmuir adsorption isotherm shown in **Chapter 2 (Equation 2.59)** (Langmuir 1916). To establish the equilibrium dissociation constant (K_d) and the maximum equilibrium binding capacity (q_{max}) for each resin the data collected from the isotherm experiments was linearised using Langmuir regression (Langmuir 1918). The reciprocal of slope is equal to q_{Max} and the y-intercept equal to the reciprocal of $K_d \cdot q_{Max}$ (**Chapter 2 - Equation 2.60**). **Figure 4.12** shows the adsorption

isotherms for the resin samples, where the experimental data is fitted using the Langmuir isotherm. The linearised plots and experimental data points used for each resin sample are shown in the appendix.

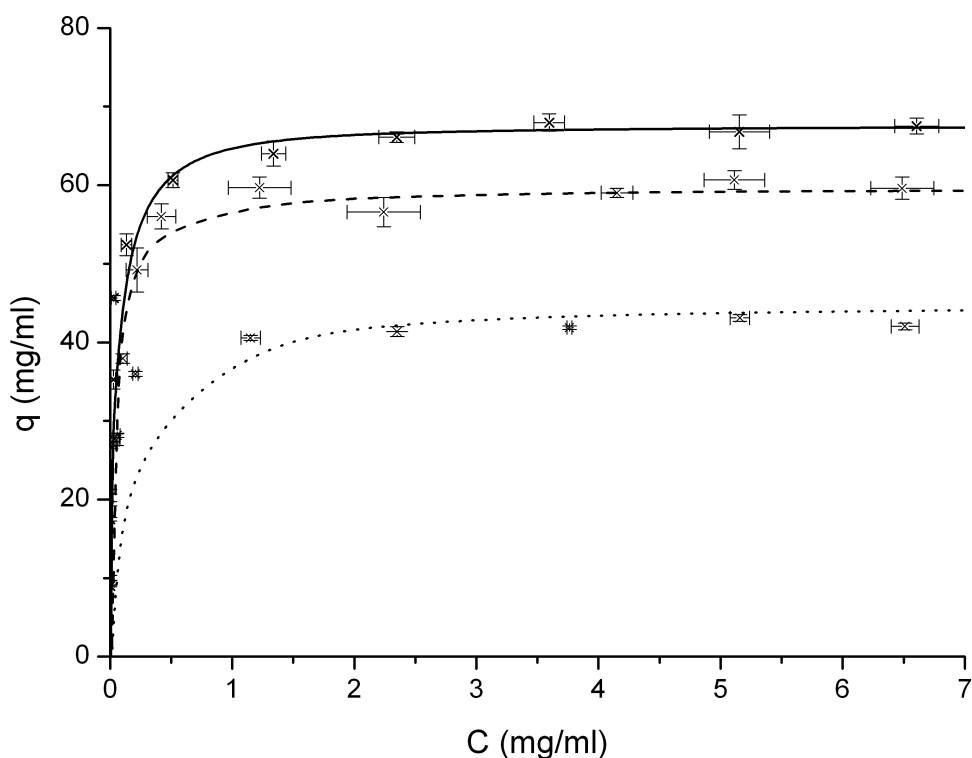


Figure 4.12. Adsorption isotherms for the new (solid line), cycled (dotted line) and NaOH cycled (dashed line) resin samples. The experimental data points were fitted with the Langmuir isotherm.

Table 4.3 highlights the calculated maximum equilibrium binding capacity and equilibrium dissociation constant for the resin samples. The equilibrium dissociation constant increases over 4-fold, these changes can be attributed to the reduction in ligand binding sites and therefore a reduction in ligand protein complexes causing the increase in the dissociation constant seen.

Table 4.3. Equilibrium Constants for the Resin Samples

Resin Sample	q_{Max} (mg/ml)	K_d (mg/ml)
New	67.7 ± 0.9	0.036 ± 0.002
NaOH Cycled	59.7 ± 0.4	0.042 ± 0.012
Cycled	45.0 ± 0.7	0.140 ± 0.014

The capacity losses seen in both the batch uptake and isotherm experiments are comparable to the column experiments and therefore demonstrate that the loss in binding capacity is likely to be caused by irreversible binding site loss (based on the current CIP regime). The previous experiments (batch and isotherm) did not give a clear answer to the cause of the changes seen in mass transfer properties. Therefore scanning electron microscopy (SEM) was used as described in **Chapter 2** to assess the differences in resin structure between samples. **Figure 4.13** shows the SEM images for the resin samples at x250 magnification allowing individual resin particles to be assessed and at x40,000 magnification, to evaluate any changes in resin particle surface pore structure.

The new resin sample has flawless spherical resin particles (A1) and a clear distinction between large and small surface pore structures (B1). The NaOH cycled resin sample shows disfigurement of the spherical resin particles (A2). This disfigurement was attributed to etching of the resin particles agarose linked scaffold by the caustic CIP solution (0.5M sodium sulphate, 50mM NaOH). The etching process appears to have only damaged the outer layers of the resin particle but not the pore structure, with larger and small pores still visible (B2). The cycled resin (C1) shows the same signs of surface etching shown by the NaOH cycled resin (B1) along with a higher degree of resin particle fragmentation. The cycled resin also shows a distinct change in the surface pore structure (C2), where the smaller pores appear to have broadened and a number of these larger pores are blocked with unknown foulant particles.

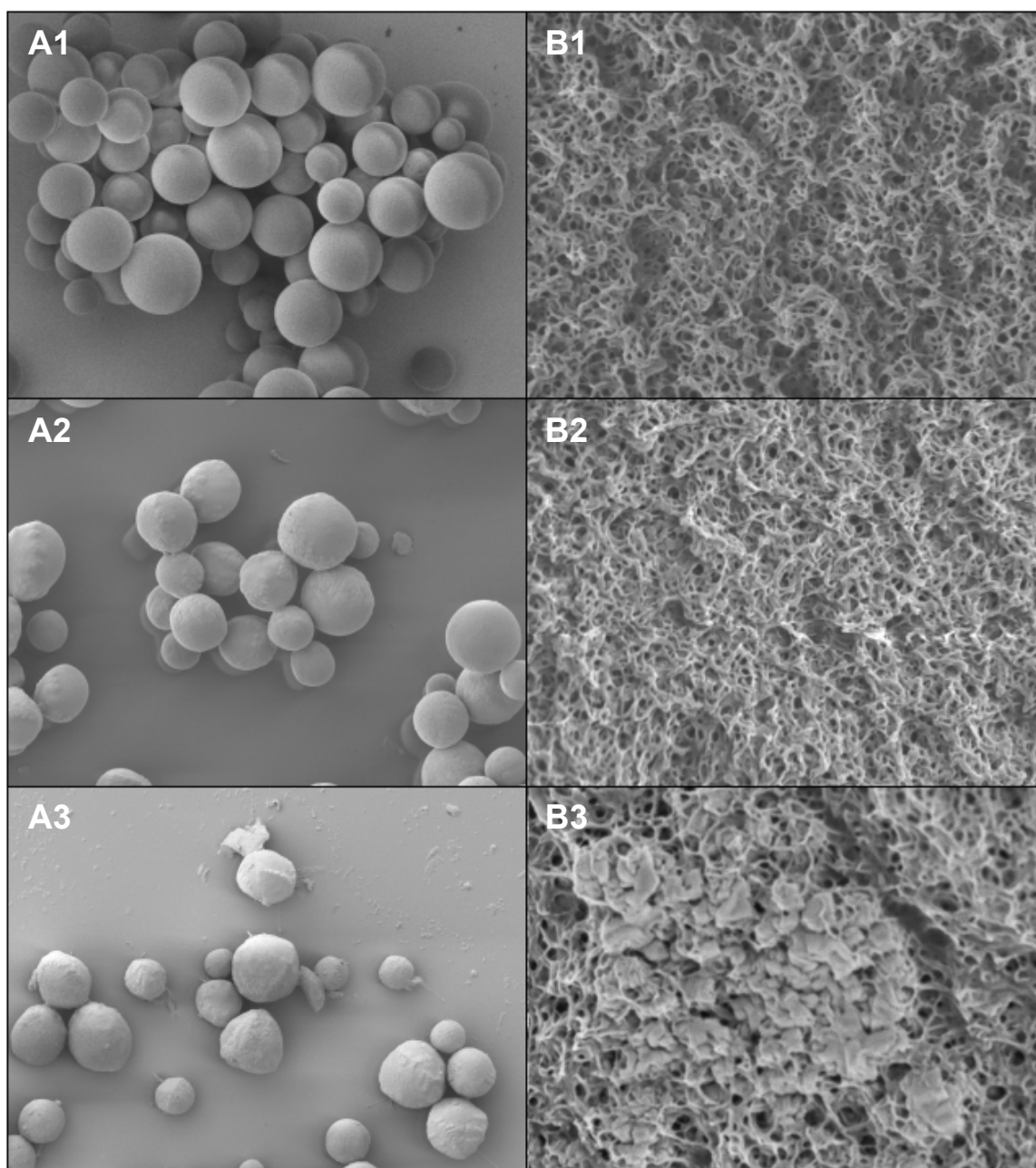


Figure 4.13. Scanning electron microscopy images of the new (1), NaOH cycled (2) and cycled (3) resin samples at (A) x250 and (B) x40,000.

The column and resin characterisation experiments demonstrate that the loss in binding capacity and resulting changes in the column mass transfer properties are caused by multiple mechanisms. The binding capacity loss is principally driven by protease digestion of the ligand and potentially a degree of surface pore occlusion, blocking viable binding sites. However a quarter of the capacity loss seen in the 100% BT cycle study can be attributed to the

NaOH cleaning, which leads to proteolysis and denaturation of the ligand as well. The mass transfer affects seen are likely to be caused by the etching of the resin particles and the loss of ligands due to the ensuing reduction in particle diameter and predicted reduction in steric hindrance caused by fewer ligands and widened surface pores (etching).

Recent publications (Mahajan et al. 2012; Warikoo et al. 2012) have demonstrated lower levels of binding capacity loss over multiple cycles when using another protein A resin from the MabSelect family, MabSelect SuRe (GE Healthcare, Uppsala, Sweden), which is alkali-stabilised and thus offers greater sodium hydroxide and protease resistance. They also did not fully utilise the whole resin capacity by only loading to 70% BT and therefore the resin was less susceptible to binding capacity loss from increased HCCF volumes.

4.3.4.2 Variable Binding Capacity Study

Figure 4.14 demonstrates the influence of the loss in binding capacity on the 3-column PPC system for the generation of Commercial material (10kg batches). The decrease in binding capacity causes the system to operate an increasing number of cycles per batch to process all the HCCF. The increase in system cycles leads to a rise in the step processing time, which exceeds the maximum media hold time on the 11th batch (**Figure 4.14a**) resulting in an inability to process the complete batch within the desired timeframe. The increase in cycles results in a concomitant rise in the protein pool volume due to a higher number of eluate pools. **Figure 4.14b** demonstrates that if the product vessel for the step is fixed on the predicted pool volume not accounting for increasing cycle number, material will be discarded after 6 batches due to insufficient tank volume. This effect is even more pronounced for the 4-column PCC system due to its higher cycle count per batch, which results in it violating the maximum media hold time in the 9th batch and the tank volume in the 6th batch. The standard batch process also exceeds the maximum media hold time, but not until the 18th batch when an extra cycle is

required to counter the loss of material in the flow-through due to decreasing binding capacity post 100 cycles.

The 3-column and 4-column PCC system have demonstrated the ability to offer manufacturing cost savings in early clinical phase material generation. The high number of molecules entering early clinical phase trials for every successful product launch implies that the PCC technology is likely to make a significant impact on clinical manufacturing costs. However **Figure 4.14** demonstrates the limitations of using the PCC system for lengthy Commercial manufacturing campaigns. In addition, the lack of familiarity with the PCC technology could make the technology unfavourable for technology transfer to new facilities or contract manufacturing organisations. A possible scenario for adoption of the PCC technology is to use the system throughout clinical development and on the successful launch of a product, switch to the standard batch process for ease of operation and tech transfer. This type of post-launch process change is likely to be classed as a major change by the regulatory bodies and will therefore require detailed validation and equivalence studies which can take between 12-18 months to complete (Hassan 2009; Wojciechowski et al. 2007).

To address these findings and to investigate the feasibility of such a scenario the simulation tool was reconfigured to design and optimise a manufacturing process that for the given time period (18 months) would remain in specification (HCCF hold time & process scale limits) allowing the process change and the resulting validation efforts to be completed.

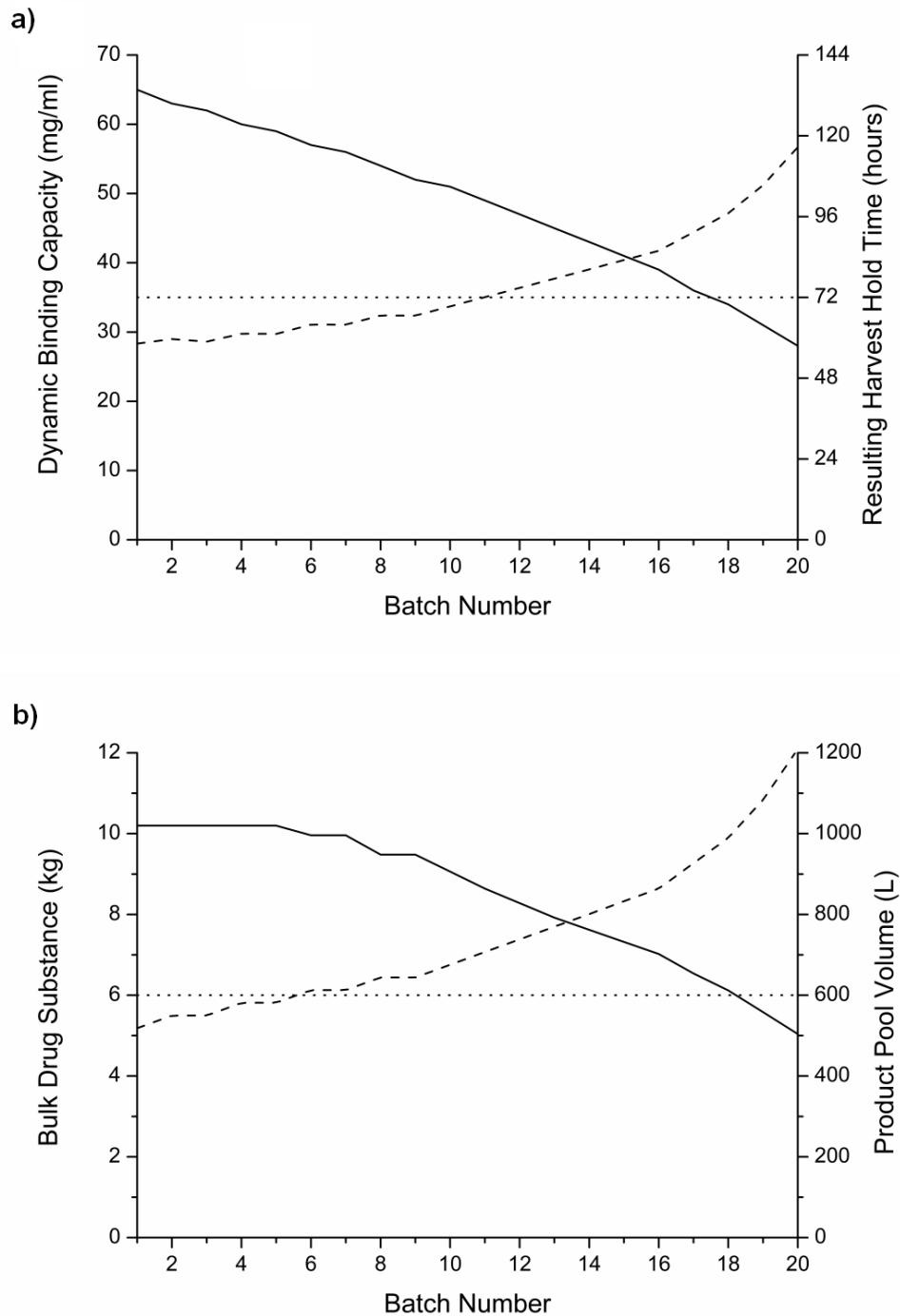


Figure 4.14. The effect of batch number for the Commercial scale of manufacture utilising the 3C-PCC system for (a) dynamic binding capacity (solid line) and resulting harvest hold time (dashed line) with respect to the maximum allowable harvest hold time (dotted line). (b) The product pool volume (dashed line) and resulting bulk drug substance yield (solid line) when constrained by the maximum vessel volume (dotted line).

The approach was initially applied to the standard batch process to address the impact of the redesign and establish a base case design. The redesigned standard process required a 1.4-fold increase in column volume (1 x 70.7L) operated for fewer cycles (5). This would allow the process to cope with the addition of the extra cycle (6) needed post 100 cycles to prevent product loss in the flow-through. In contrast the PCC systems required a 2-fold increase in total column volume to create a robust enough process capable of remaining within the specified design limits for the duration of production. The PCC systems were found to still offer comparable Commercial manufacturing costs, due to the diminished impact of resin costs at this scale of production.

4.3.5 Retrofitting Costs

The PCC system has demonstrated its ability to offer savings in direct costs throughout the clinical development pipeline to Commercial manufacture. To realise these savings a PCC system and columns must be purchased and installed in the facility. This retrofitting process is unlikely to have any adverse effects on the existing facility, where the PCC system's ability to reduce buffer volumes by operating smaller column volumes, will actually reduce the utilities burden in the facility. The potential increase in footprint caused by the PCC skid is unlikely to be sufficient to cause operating issues.

The current PoC scale of production is achieved using a standard batch chromatography skid (15-600L/hr) capable of supporting a 31.4L column, with the skid and column costing ~\$280k. The corresponding PCC system and column cost approximately four times that of the standard batch process, costing ~\$1,150k regardless if it is operated in the 3-column or 4-column mode. The investment cost required for the PCC system designed for the PoC scale of production, could be balanced with the savings realised in the direct costs (~\$150k per batch) after eight PoC batches (8 drug candidates). With the increase in production scale to the PIII & Commercial manufacture (10kg batch) the standard batch process employs a larger skid scale (45-

1800L/hr) to support the larger column volume requirements, resulting in an increase in equipment cost (\$380k). The equivalent PCC system can still utilise the same specification skid as in the PoC scale of production with larger columns, meaning it is only three times more expensive for the 10kg batch scale of production. The reduced savings in direct costs highlighted at the larger scale of production shown in **Figure 4.7**, mean the investment cost would take longer to be recouped, requiring thirty-nine PIII batches (~10 drug candidates). However in producing 10 Phase III drug candidates, a higher number of candidates must have entered the PoC scale of production due attrition rates in clinical trials. Taking this lifecycle perspective highlighted that the direct cost savings obtained by 9 PoC batches (9 DC's) would be sufficient to pay back the cost of the larger scale PCC system for late-stage manufacture.

4.4 Conclusions

This chapter evaluates the feasibility of whole bioprocesses that utilise semi-continuous chromatography (3C-PCC or 4C-PCC) for product capture across a product's lifecycle from PoC to Commercial manufacture. The approach adopted linked small-scale single-column experimental studies with a process economics simulation. The experimental work was key to determining the critical design parameters for the PCC system through the derivation of mass balance, scale-up and scheduling equations. The integrated techno-economic evaluation predicts that semi-continuous chromatography has the ability to offer manufacturing cost savings in early clinical phase material generation which can be significant due to the high attrition rates. The analysis also demonstrated the obstacles to using such a technology at Commercial scale and the importance in the selection of the protein A resin employed. The framework was then employed to determine the semi-continuous system specification required to operate with similar costs to the standard batch process while a process change application is pursued.

In addition to the techno-economic evaluation presented in this chapter, a further dimension concerns the development and validation effort required when implementing alternative technologies such as the PCC system. Development time may not be greatly increased with the PCC system since early purification development can often include experiments to determine aspects such as the wash step conditions and loading flowrate; the latter can be easily adapted for PCC switch time determination. Resin cycling studies for either the standard batch or PCC system would typically occur during late phase process characterisation studies. However it is recognized that the potential benefits of a new or alternative technology need to be balanced against factors such as technology readiness for large-scale manufacture and regulatory concerns. The regulatory impact of new continuous technologies will be discussed further in **Chapter 6**.

5 Integrated Continuous Processing

5.1 Introduction

The next generation of mAbs are under increasing pressure from both public and private healthcare providers to offer cost effective treatments and contend with the intensified competition from rival manufacturers. The success of these new mAb therapeutics will be highly dependent on their economic performance (Mitchell 2005). As a result production cost, capacity utilisation and the ability to rapidly accommodate fluctuating market conditions are becoming critical success indicators (Farid 2009a; Kamarck 2006; Pellek and Arnum 2008). This is increasing the pressure on biotech companies to produce more economically sustainable therapies and hence adopt more cost-effective manufacturing strategies such as continuous processing.

This chapter presents a vision for a number of integrated continuous manufacturing processes and utilises the decision-support framework to assess performance of these future manufacturing strategies, incorporating the findings from **Chapter 3 & 4**. The chapter is organised as follows: **Section 5.2** provides an overview of the continuous mAb manufacturing strategy. **Section 5.3.1** highlights the impact of development phase on manufacturing costs, followed the impact of company size on facility utilisation and resulting costs in **Section 5.3.2**. In **Section 5.3.3** a detailed cost of goods comparison between the batch and continuous manufacturing strategies for all scenarios is investigated. **Section 5.3.4** builds on this analysis to include a number of further continuous manufacturing strategies to establish the optimal combination of batch and continuous unit operations. The chapter then takes into account the operational concerns associated with the adoption of continuous technologies and combines these findings with the calculated economic and environmental performance metrics in **Section 5.3.5**. The final section then summarises the principle conclusions of the wide-ranging overview from preceding sections of the chapter, summarising the performance of continuous processing in the mAb sector.

5.2 Methods

5.2.1 Visualising an Integrated Continuous Process

A key concept of an integrated continuous process is that continuous, steady-state processing extends from the bioreactor to the final purification operation. However this concept is currently not possible in biopharmaceutical manufacture due to the lack of suitable technology and strict regulatory requirements. Continuous perfusion bioreactors for example do generate a continuous stream of harvested cell culture fluid (HCCF), but they can only achieve this in a batch operation. Firstly the cell culture has to reach the desired steady-state cell density to achieve a constant concentration of HCCF and then can only produce a continuous stream of HCCF for a defined period, before a new cell culture batch is required. This semi-continuous mode of operation is also found in the search for continuous downstream processing operations where chromatography systems that are described as continuous are capable of continual loading but only generate discrete elution pools of product. The challenge is further complicated by the stringent quality and regulatory requirements that dominate biopharmaceutical manufacture. The ability of the manufacturing process to demonstrate viral clearance is critical, with a mandatory inclusion of two dedicated viral clearance operations (viral inactivation & viral retention filtration). Both of these operations are currently achieved in a batch operation, for example in a viral inactivation step the product stream is held at a low pH for a defined period of time, before processing continues. A further regulatory complication is batch traceability, a key area of debate surrounding continuous processing, with the principal concern being “how do you define a batch?”.

These factors highlight how continuous processing is not currently possible in biopharmaceutical manufacture. However the use of semi-continuous unit operations can lead to a semi-continuous manufacturing process, potentially capturing some of the economic advantages seen in continuous processing. The upstream can be operated in a semi-continuous manner by using perfusion culture, which is fed and bled at a constant rate to

generate a constant stream of HCCF when steady-state cell density is achieved. The downstream is more complicated due to the number of orthogonal purification operations. The initial capture of the product from HCCF can be achieved in a continuous manner, using semi-continuous chromatography. The resulting process stream is now being created in discrete elution volumes, which can either be pooled into larger volumes or processed individually before moving to the subsequent purification steps. These sub-batches can be processed in the conventional batch manner for the remaining purification steps or can be processed in a continuous manner.

Figure 5.1a shows the downstream scheduling for a typical process sequence operated in batch mode, where each step is completed before the product stream is passed to the next. **Figure 5.1b** shows an adapted process sequence where HCCF is continually loaded onto a semi-continuous chromatography step and the resulting elution volumes are pooled into larger volumes before proceeding in a batch manner similar to **Figure 5.1a** for the remaining purification steps. **Figure 5.1c** demonstrates a flow-sheet where the individual discrete elution volumes from the semi-continuous chromatography step are individually passed onto the subsequent anion-exchange (AEX) chromatography step and the flowthrough is continually passed through the virus retention filtration (VRF) step. Therefore the product stream flows through the AEX chromatography column and straight into the VRF step in a continuous manner. The VRF unit would be sized by calculating the filter area capable of matching the volumetric flowrate from the AEX chromatography step whilst maintaining the same transmembrane flux (20 LMH) seen in the batch orientated processes (**Figure 5.1a & b**). Both process flowsheets operating the semi-continuous chromatography capture step collect all the viral secure sub-batches (post VRF) into one final batch prior to the final ultrafiltration/diafiltration (UFDF) step. This pooling approach solved the regulatory requirement for batch traceability, by defining the batch as all the material created in a single fermentation run. This approach also reduces the quality burden by reducing the number of batch releases for a given manufacturing strategy.

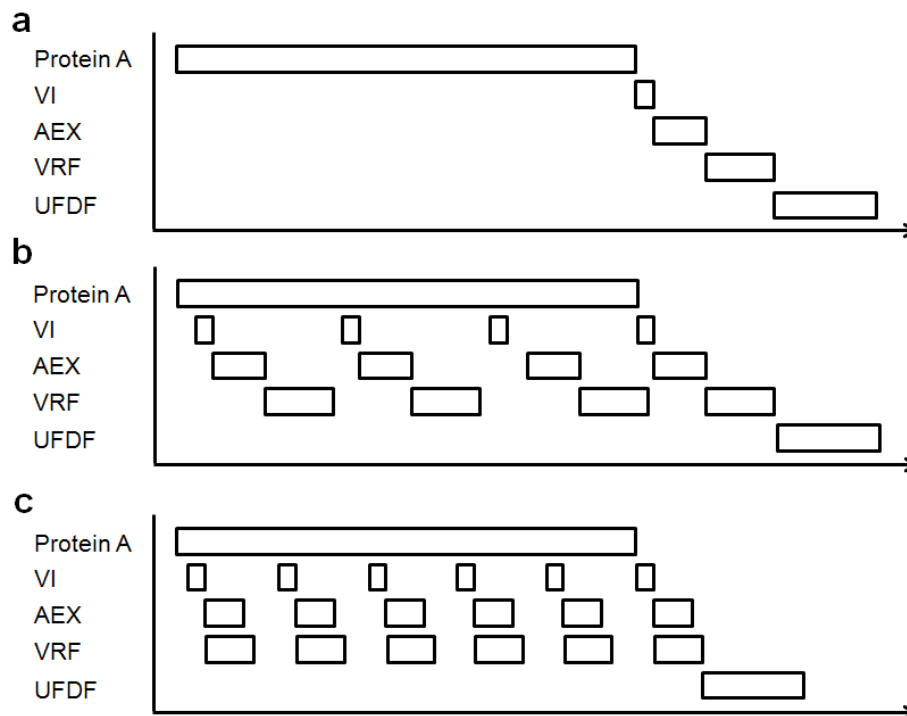


Figure 5.1. Downstream process scheduling for a) the base case process sequence, b) the continuous to batch process sequence and c) the continuous process sequence. Protein A chromatography; VI, viral inactivation; AEX, anion exchange chromatography; VRF, viral retention filtration; UFDF, ultrafiltration/diafiltration.

Table 5.1 demonstrates how this concept results in five different manufacturing strategies, where the capture step is defined as the mode of Protein A chromatography used and the polishing steps (AEX & VRF) are defined by how the resulting purification steps are operated. The base case strategy employs a fed-batch reactor generating a single discrete batch, which is purified in a batch manner (**Figure 5.1a**). Similarly the fed-batch, continuous capture and batch polishing (FB-CB) strategy also employs a fed-batch reactor, but the ensuing batch is purified using semi-continuous chromatography in a 72 hour window with the polishing steps operated in the batch manner (**Figure 5.1b**). In contrast the ATF perfusion, continuous

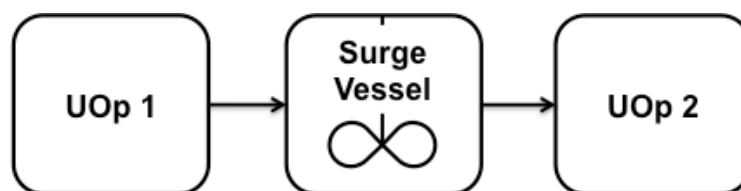
capture and batch polishing (ATF-CB) strategy employs an alternating tangential flow (ATF) perfusion reactor to generate a constant stream of HCCF which is captured directly onto the semi-continuous chromatography step for the duration of the perfusion run, prior to batch operated polishing steps. The remaining strategies (FB-CC; Fed-batch, continuous capture, continuous polishing, and ATF-CC; ATF perfusion, continuous capture, continuous polishing) both employ a continuous capture step which generates discrete sub-batches which are then processed in a continuous manner in the polishing purification steps as shown in **Figure 5.1c**.

Table 5.1. Mode of operation for key stages of the alternate strategies

Manufacturing Strategies	USP	Capture	Polishing
Base case	Fed-batch	Batch	Batch
FB-CB	Fed-batch	Continuous	Batch
ATF-CB	ATF perfusion	Continuous	Batch
FB-CC	Fed-batch	Continuous	Continuous
ATF-CC	ATF perfusion	Continuous	Continuous

5.2.2 Decisional Tool

The deterministic analysis shown in this chapter was achieved using the decision-support framework defined in **Chapter 2**. The version of the framework used throughout this chapter includes the process model updates for perfusion cell culture demonstrated in **Chapter 3** and semi-continuous chromatography from **Chapter 4**. The continuous unit operations exhibited in the previous chapters allowed the framework to capture a single continuous unit operation within a batch dominated manufacturing process. This section details the unique adaptations made to the decision-support framework to account for the passing of continuous product streams between unit operations.



Mode of Flow	Event Time	In Flow	Surge Volume	Out Flow
Continuous	-	200 L/h	-	200 L/h
Discretised	1	200 L	200 L	
	2		150 L	50 L
	3		100 L	50 L
	4		50 L	50 L
	5	200 L	200 L	50 L

Figure 5.2. Continuous flow between two unit operations in a discrete event environment. UOp, Unit Operation.

The decision-support framework employs a discrete event simulation tool, which by its nature captures events in discrete time intervals and is therefore not capable of representing a product stream as a rate (volume/mass per time). This was not an issue previously (**Chapters 3 & 4**) as the use of a single continuous unit operation meant the product stream was passed between unit operations in a batch manner. For example each perfusion volume was discretised into the volume collected per day before being passed to a batch chromatographic process. To avoid major changes to the structure of the simulation tool and follow the software principle of abstraction adopted throughout the development of the decision-support framework a similar approach was utilised for continuous product streams. **Figure 5.2** demonstrates how this was achieved within the framework's existing architecture. Any continuous unit operations product stream was discretised into distinct batch volumes, which were placed into a surge vessel (the unit operations product vessel). The next unit operation (continuous or batch) would then take the required product stream volume from the vessel

when available. If this next step were another continuous unit operation it would also request material in a discretised fashion. This approach allows the discrete event simulation tool to represent a continuous product stream and therefore capture resource requests at the correct time. For example the FB-CC and ATF-CC strategies utilise this feature when representing continuous polishing, with the AEX chromatography and VRF being operated in a continuous manner.

5.2.3 Multi-Attribute Decision-Making

The weighted sum method shown in **Chapter 2** was used to reconcile economic, environmental, and operational outputs so as to identify the most preferred alternative manufacturing strategy for a range of company scales with different weightings assigned to each of these categories. **Table 5.2** lists all the attributes considered in the MADM analysis. The values of the attributes under economic and environmental feasibility were derived from the simulation tool. The attributes were ranked in order of importance, where a ranking of one indicates an attribute of greater significance. For example in the large-sized company the cost per launch is more important than the commercial COG/g and the initial capital investment required in facility construction. In contrast the small-sized company ranks the initial capital expenditure the highest, highlighting the differing financial philosophies found with company size. A large-sized company's main aim is to reduce the cash outlay for a new drug and produce this material as cost effectively as possible. In contrast, the small-sized company will have fewer resources to invest (facilities & drug development) and will therefore want to minimise these costs before looking to alternative funding sources upon product launch (licencing, partnerships, mergers and acquisitions). The attributes representing the environmental feasibility were ranked equally because the environmental impact of water and consumable usage was deemed to be equally disadvantageous to the environment. The operational feasibility was represented by a risk score, which assesses the manufacturing strategies perceived robustness (likeness of batch failure).

Table 5.2. Attribute grouping and ranking for each company scale

Attribute field	Attribute name	Large	Medium	Small
Economic feasibility	Cost per Launch	1	1	2
	Commercial COG/g	2	2	3
	Capital expenditure	3	2	1
Environmental feasibility	Water E factor	1	1	1
	Consumable E factor	1	1	1
Operational feasibility	Batch risk	1	1	1

Note: Rank of 1 refers to most important attribute and 3 to the lowest.

5.2.4 Case Study Assumptions

The decision-support framework was used to compare the cost-effectiveness of the five alternative manufacturing strategies throughout the development pipeline for a range of company sizes, exploring the trade-offs between reduced equipment scales versus increased manufacturing risk. **Table 5.3** illustrates the clinical trials estimates used throughout this case study to calculate the amount of mAb required for each phase of the development pipeline. The earliest development phase captured in this case study is the Pre-Clinical phase where material is required for non-primate animal model studies. Assuming the average non-primate (Macca Mulatta) body weight is ~8kg (Leigh 1996) and the study includes 110 non-primates (25% control group) (Chapman et al. 2009), a single 0.5kg batch of mAb is required for the Pre-Clinical development studies. The case study then uses the quick win, fail fast clinical development paradigm (Paul et al. 2010), where the material required for Phase I & II is generated in a single batch for the Proof-of-Concept (PoC) development phase. The average body weight of a US male was presumed to be 86kg (Ogden et al. 2004) and therefore a single 4kg batch of mAb would be required for PoC development also accounting for non-clinical uses. This amount increases to 40kg of mAb for the phase III clinical trials and is produced by four 10kg batches at the Commercial batch scale allowing parallel process validation studies. The 10kg Commercial batch size is based on the median market demand of the

top 15 mAb (200kg) (Kelley 2009) and the ability to process 20 batches per year. The cell culture titre also increases with clinical phase, where due to continued process development the titre was assumed to increase 2-fold from the PoC batch to the Phase III & Commercial batches. The scenario produced a 2.5g/L titre for the minimally developed Pre-Clinical and PoC batch before increasing to a final titre of 5g/L.

The base case manufacturing strategy used in the case study was based on a generic two-column mAb process (Kelley 2007; Kelley et al. 2008). The principal differences between the batch and semi-continuous unit operations are highlighted in **Table 5.3**. The key difference between the cell culture technologies is the length of culture, where a fed-batch fermentation lasts 12 days allowing 20 batches to be processed a year from a single reactor. In contrast perfusion cell cultures can be run for much longer, however in this case study a culture duration of 28 days was selected, making an annual throughput of 10 batches possible. Longer cell culture durations would limit the reactor throughput and result in a need for more reactors leading to high facility costs to achieve the same batch throughput as a fed-batch reactor. The semi-continuous PCC system utilises three smaller columns compared to the batch system, these are loaded to 100% saturation increasing the binding capacity from 40 to 65 grams of mAb per litre of resin. To achieve the higher productivity the PCC system must be operated continuously requiring a 24-hour manufacturing shift.

Table 5.3. Key assumptions for alternate manufacturing strategies

Clinical Trial Estimates		
Variable	Values	
Non-human primate dosage (mg/kg body weight)	700	
Non-human primate in Pre-Clinical trial	100	
Patient dosage (mg/kg body weight)	7	
Number of doses per patient per year	26	
Individuals in Phase I clinical trials (single dose)	40	
Individuals in Phase II clinical trials (6 month dose)	200	
Individuals in Phase III clinical trials (year dose)	2000	
USP Process Parameters		
	Fed-batch	ATF
Cell culture time (days)	12	28
Harvest volumes	1	20
Max VCD (million cells/mL)	10	50
Max bioreactor volume (L)	20,000	1,500
Annual number of batches	20	10
DSP Process Parameters		
	Batch	PCC
Binding capacity (g/L)	40	65
Bed height (m)	0.25	0.1
Number of columns	1	3
Shift duration (hours)	12	24
Cost Parameters		
QCQA batch release costs (\$/batch)	35,000	
Media cost (\$/L)	3.1	
Protein A resin cost (\$/L)	8000	
AEX resin cost (\$/L)	1500	
Virus retention filtration membrane (\$/m ²)	3250	
Labour cost (\$/hour)	58	
Chromatography process skid (15-600L/hr) (\$)	226,000	
PCC process skid (15-600L/hr) (\$)	1,080,000	
Chromatography column (Dia = 0.2m) (\$)	132,000	
Chromatography column (Dia = 2m) (\$)	218,000	

Table 5.4. Number of drug candidates per company scale scenario

Company Size	Pre-Clinical	PoC	Phase III	Commercial
Large	20	14	4	2
Medium	10	7	2	1
Small	5	3	1	1*

*One successful launch every two years.

Table 5.4 highlights the major differences between different sized companies with respect to the number of drug candidates (DC) at any given stage of the drug development pipeline. A large company has been defined as a company that aims to launch two new products per year. To achieve this level of success 20 new DC`s must enter Pre-Clinical trials, due to the high attrition rates seen in clinical development. The medium-sized company aims to launch one product a year and therefore requires 10 DC`s entering Pre-Clinical trials per year. A small-sized company that aims to launch a new product every 2 years requires only 5 DC`s in Pre-Clinical trials per year.

5.3 Results and Discussion

The decision-support framework was used to assess the cost-effectiveness of five manufacturing strategies with different combinations of batch and continuous operations for cell culture, capture and polishing steps throughout the drug development pipeline. This was initially carried out by determining the direct (labour, media, buffers, chromatographic resin, filter membranes, QCQA batch release costs etc.) and indirect (depreciation and facility-dependent overheads) costs. These were used to establish the cost of goods per gram across combinations of different development phases (Pre-Clinical through to Commercial production) and company sizes (small, medium and large). Each development phase required different manufacturing scales, batch numbers and material re-use strategies, and each company size resulted in different numbers of drug candidates at each

development phase. The economic outputs were then considered alongside operational and environmental metrics using a multi-attribute decision-making technique for all the company sizes investigated.

5.3.1 Impact of Development Phase on Cost Drivers

Figure 5.3 shows the individual cost components per product per phase as well as per gram for the base case batch scenario for each manufacturing scales in the development pipeline (0.5kg, 4kg, 40kg, and 200kg) for a medium-sized company. **Figure 5.3a** highlights that as expected the costs of chemicals (media, buffer) and single-use components (e.g. filters, bags) increase per product across the development phases in proportion to the kg and batch output. Hence the cost per gram for chemicals and single-use components remain relatively constant in **Figure 5.3b** as is typical for variable costs. The resin costs also increase as the manufacturing scale increases across the development phases but in contrast to the other cost categories, the resin cost decreases at the Commercial scale of production. The requirement to keep the resins product-specific, results in a high cost burden per batch in early development phases, because the resin is often discarded before reaching its full potential cycle lifetime. The early manufacturing scales (Pre-Clinical and PoC) only use the resin to purify a single batch of material and therefore the resin purchase cost accounts for over 80% of the material costs per batch. The later manufacturing scales (Phase III and Commercial) use the resin to purify multiple batches of material and therefore reduce the cost impact of the expensive resin as reflected in **Figure 5.3b**. The resin accounts for approximately 67% of the Phase III material costs and 29% of the Commercial material costs. Both manufacturing scales utilises the same sized columns but only the Commercial scale uses the resin until its full lifetime and therefore the resin cost is spread over multiple batches and reduces the related resin costs shown.

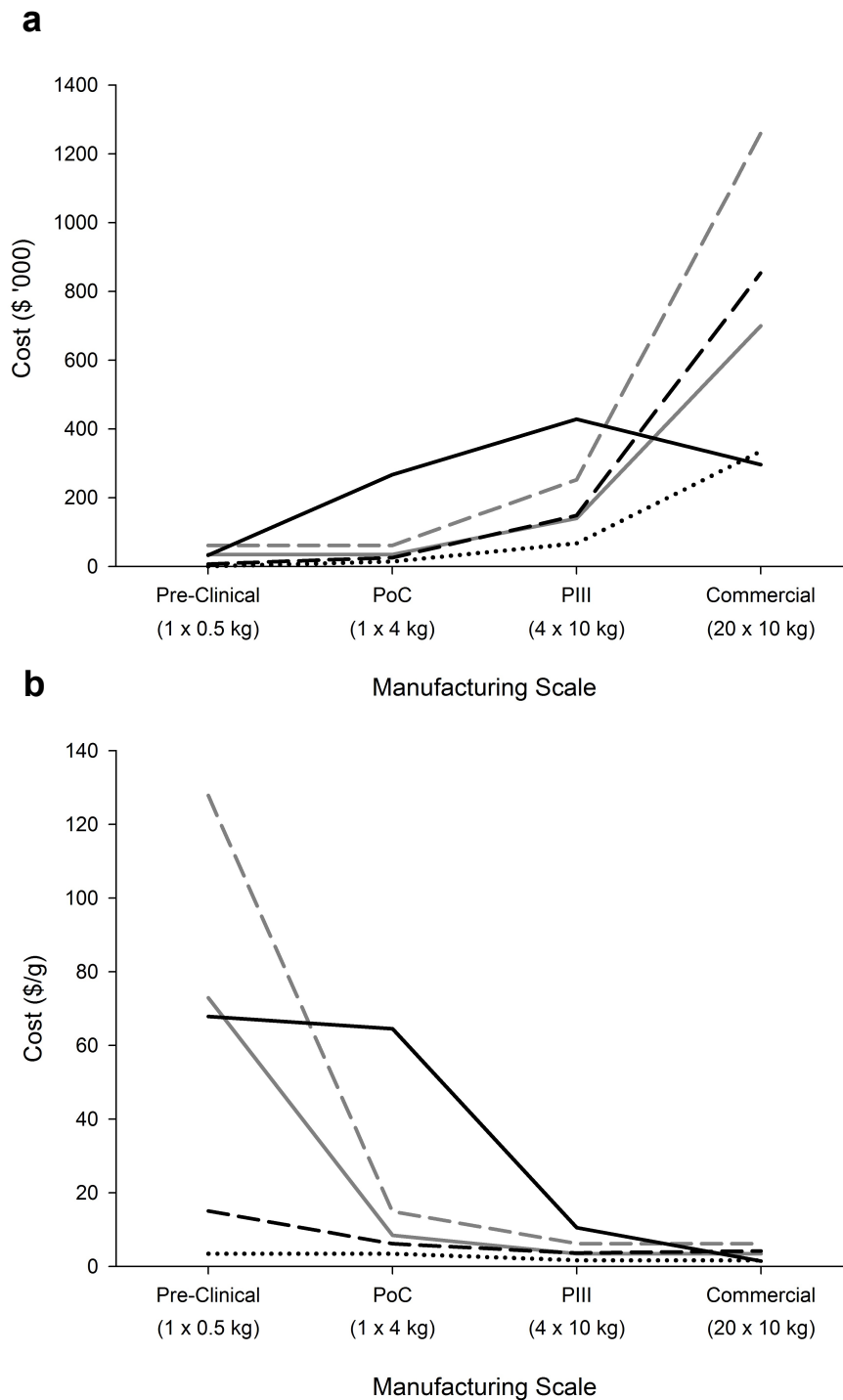


Figure 5.3. Direct cost of goods category breakdown across the different manufacturing scales required for each development phase for the base case scenario a) direct cost per product per phase and b) direct cost per gram. Categories: labour costs (grey dashed line), QCQA batch release costs (grey solid line), chromatographic resin costs (black solid line), fermentation media (black dotted line) and single use components and buffers (black dashed line).

The labour and QCQA costs are scale-independent and rise in proportion to the increase in number of batches required per product across the development phases rather than the kg output (**Figure 5.3a**). As a result, their cost per gram values decrease with kg output (**Figure 5.3b**). Finally the indirect costs increase across the development phases in proportion to the increase in batch size and hence facility size. **Figure 5.4** demonstrates as expected that the indirect cost per gram becomes less significant in the late clinical and Commercial phases since the costs are spread over more batches.

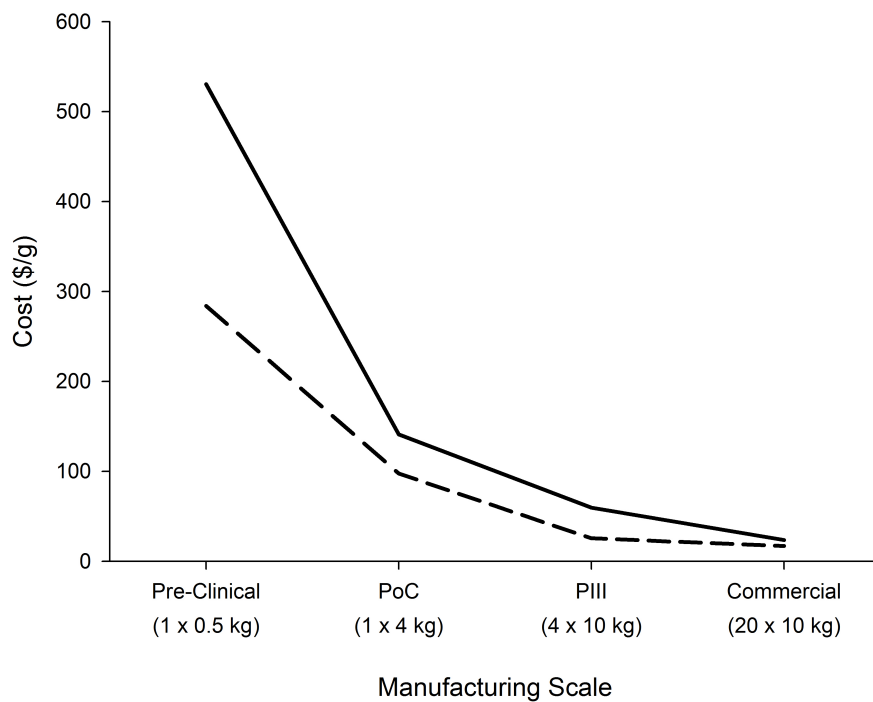


Figure 5.4. Direct (black dashed line) and indirect (black line) cost of goods per gram across the different manufacturing scales required for each development phase for the base case scenario.

5.3.2 Impact of Company Size on Indirect Costs

Table 5.3 highlighted the difference in drug candidate throughput for each company size throughout the development pipeline. The difference in drug candidate throughput will affect the utilisation of the manufacturing suites and in turn impact the resulting manufacturing costs. **Table 5.5** highlights the effect of company size on key indirect costs for the base case scenario at the PoC scale of manufacture. The capital expenditure required to construct the facility to generate a 4kg PoC batch is the same for all the company sizes, however the resulting batch suite cost and indirect cost per gram is dependent on the batch throughput. The large-sized company has the highest batch throughput with 14 drug candidates being processed a year resulting in an utilisation rate of 70% and a batch suite cost of \$292k. In contrast the small-sized company has a batch throughput of 3 drug candidates resulting in a batch suite cost (\$1,364k) that is 4.5-fold higher relative to the large-sized company.

Table 5.5. Effect of company size on indirect cost per gram for the base case scenario at the PoC (4kg) manufacturing scale

Company Size	Capital Expenditure (million \$)	Batch Suite Cost (\$/batch)	Indirect/g (\$/g)
Large	37.6	292,300	71
Medium	37.6	584,600	141
Small	37.6	1,364,000	330

5.3.3 Batch versus Continuous COG/g Comparison

Figure 5.5 shows the COG/g breakdowns for the base case batch strategy and fully continuous strategy (ATF-CC) for the medium-sized company. The analysis highlights that the Pre-Clinical batch costs are dominated by indirect costs for the base case and direct costs for the

continuous strategy. The larger equipment sizes seen in batch processing lead to a higher batch suite cost of \$255K per batch vs. \$120K per batch for the smaller highly utilised continuous equipment. However the continuous operation requires significant labour resources to support the continuous manufacturing operations and therefore this increases the overall direct costs.

The base case is still dominated by indirect costs in the later manufacturing scales in the development pipeline (PoC, Phase III and Commercial). For example, the Phase III COG/g is dominated (70% of COG/g) by the batch suite cost (indirect costs), due to the costs only being spread over four batches in a commercial GMP facility. The continuous strategy sees a shift from the direct to indirect costs dominating COG/g for the later manufacturing scales. However the labour costs still account for a third of the COG/g. Traditionally the direct costs are expected to dominate with an increase in kg output, however due to the relatively low kg output in this scenario (200kg) the indirect costs continue to dominate COG/g. The indirect COG/g does decrease in significance with increasing company size with direct costs starting to dominate as kg putout increases (large company – 2x200kg products).

The smaller batch sizes seen earlier in the development pipeline have higher direct manufacturing costs per gram because some of the costs are scale independent. For example the QCQA batch release costs (\$35,000) are constant between a Pre-Clinical and Commercial batch, but due to the difference in kg output (0.5kg to 200kg) the batch strategies Pre-Clinical QCQA cost per gram is \$73/g compared to \$3.4/g for the Commercial manufacturing scale. The same trend is seen in the batch strategy's labour costs which accounts for nearly half the Pre-Clinical direct manufacturing costs at \$128/g compared to the Commercial manufacturing scale with labour costs of \$6/g. The overall percentage of direct costs increases for the Commercial manufacturing of the batch strategy, even with the real decrease in direct costs per gram. This is due to the significant drop seen in batch suite

costs, from the Phase III (\$600K per batch) to Commercial (\$240K per batch) manufacturing scale.

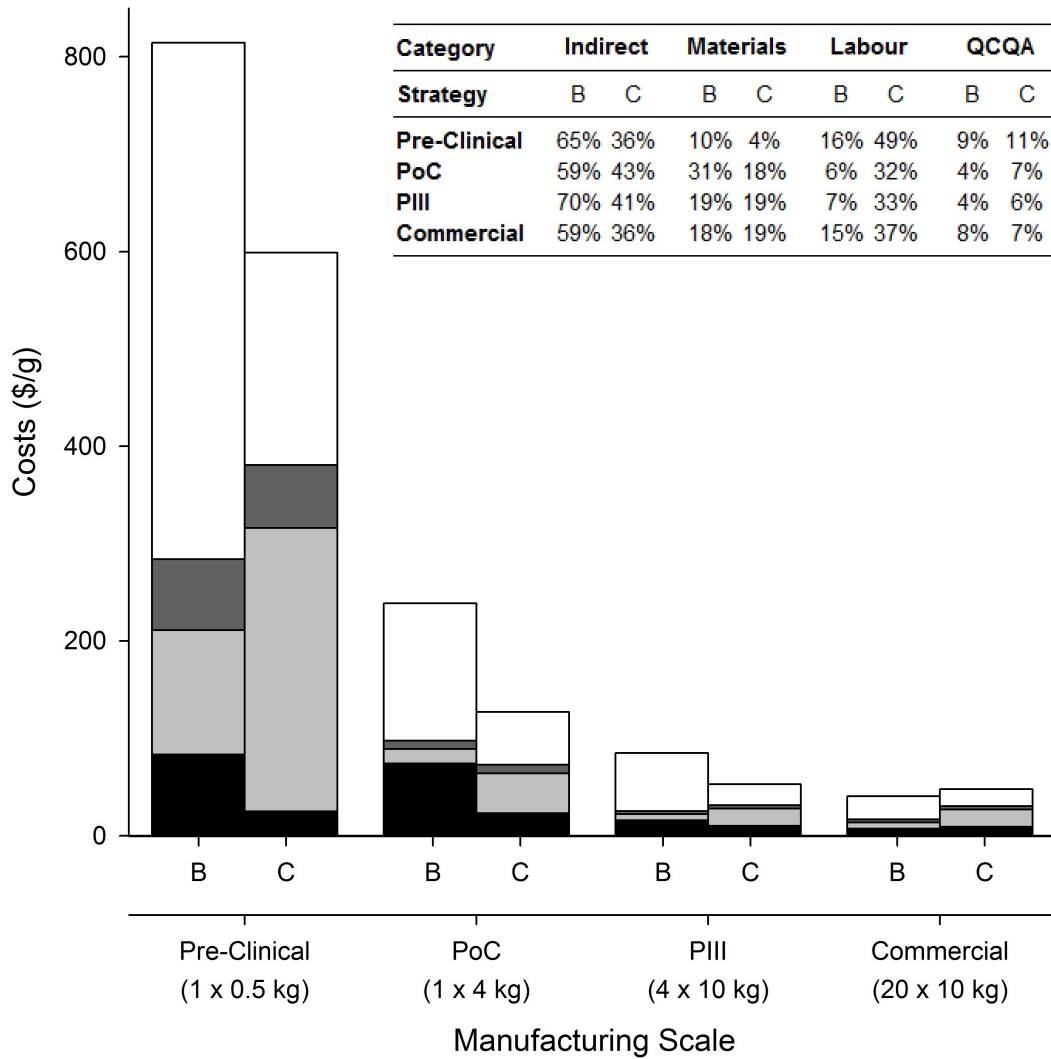


Figure 5.5. A comparison of the direct costs per gram for the base case (B) and continuous (C) strategy on a category basis for material costs (black), labour costs (light grey), QCQA batch release costs (dark grey) and indirect costs (white), between the different manufacturing scales for the base case scenario. The embedded table highlights the percentage cost contribution for the key direct cost categories.

For the medium-sized company, the tool outputs predict that the integrated continuous ATF-CC strategy offers cost savings for Pre-Clinical and Clinical production, but becomes less economically attractive at the Commercial scale. This is due to the requirement for a second manufacturing production line, resulting in the duplication of equipment (USP and DSP). The higher utilisation rate of the GMP facility at this manufacturing scale is expected to lead to a significant reduction in indirect costs (as shown by the batch strategy). However, the extra equipment required for the additional production line means the reduction is not fully realised and with the significant labour requirements seen in the continuous strategy, the strategy is no longer able to offer an economically attractive COG/g as the batch scenario.

5.3.4 Key Economic Metrics Across Company Size and Manufacturing Scale

The impact of both manufacturing scale (Pre-Clinical, PoC, Phase III, Commercial) and company size (small, medium, large) on the competitiveness of the five alternative manufacturing strategies was investigated. The contour plots in **Figure 5.6** (a, b, c) show the percentage difference in cost of goods per gram relative to the base case strategy and **Table A5.1** details the equipment number and scales employed.

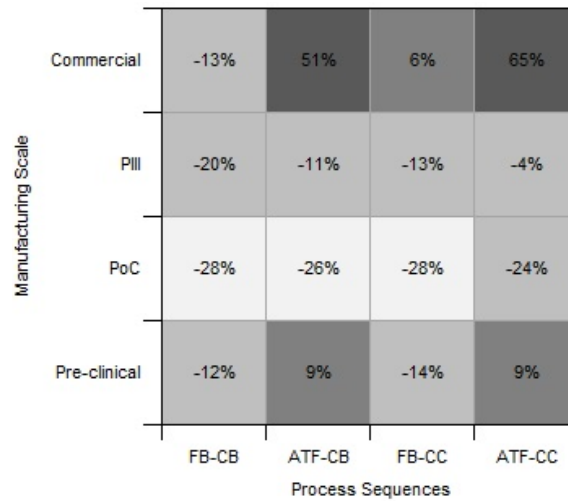
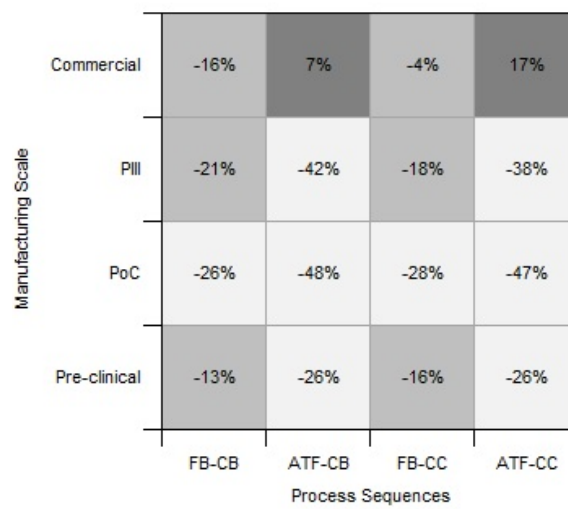
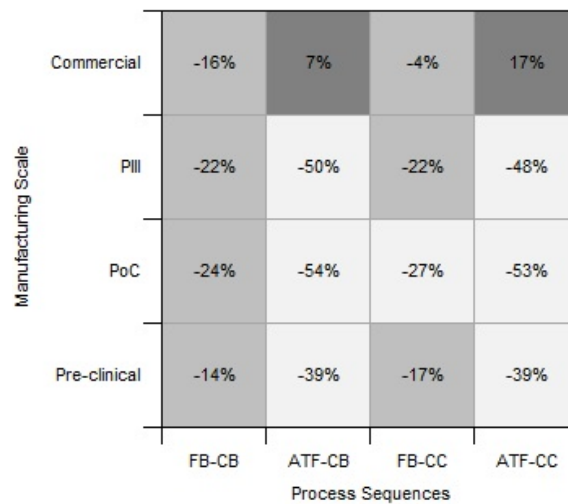
a**b****c**

Figure 5.6. Contour plots showing the impact of manufacturing scale and manufacturing strategies on the percentage difference in cost of goods per gram relative to the base case scenario for a) the large-sized company, b) the medium-sized company and c) the small-sized company. (Pre-Clinical, 1 x 0.5kg; PoC, 1 x 4kg; Phase III, 4 x 10kg; Commercial, 20 x 10kg).

Figure 5.6 highlights that the ATF perfusion-based manufacturing strategies are not able to compete with the fed-batch strategies at the Commercial scale of manufacture regardless of company size. The difference is most pronounced for the large-sized company, where the high drug candidate throughput in the development pipeline, results in the need to manufacture two commercialised products in a year. The ATF perfusion strategies are only able to generate 10 batches per year per production line and therefore require 4 parallel perfusion reactors with dedicated purification trains to meet the 40 batch annual demand. The resulting facilities are approximately twice as expensive as the corresponding fed-batch based facilities, which employ two staggered reactors utilising a single larger purification train. This effect is also seen for the medium and small-sized companies where two production lines are required to manufacture 20 batches of a single successfully commercialised product. The resulting Commercial facilities are comparable in cost to the fed-batch based facilities and offer the same level of capital expenditure saving (~25%) versus the base case due the use of a smaller purification train offered by the continuous capture step. **Figure 5.7a** highlights that the inability of the ATF perfusion strategies to utilise a single production line for Commercial manufacture, results in the fed-batch based strategy FB-CB being the most economically attractive Commercial manufacturing strategy for all company sizes.

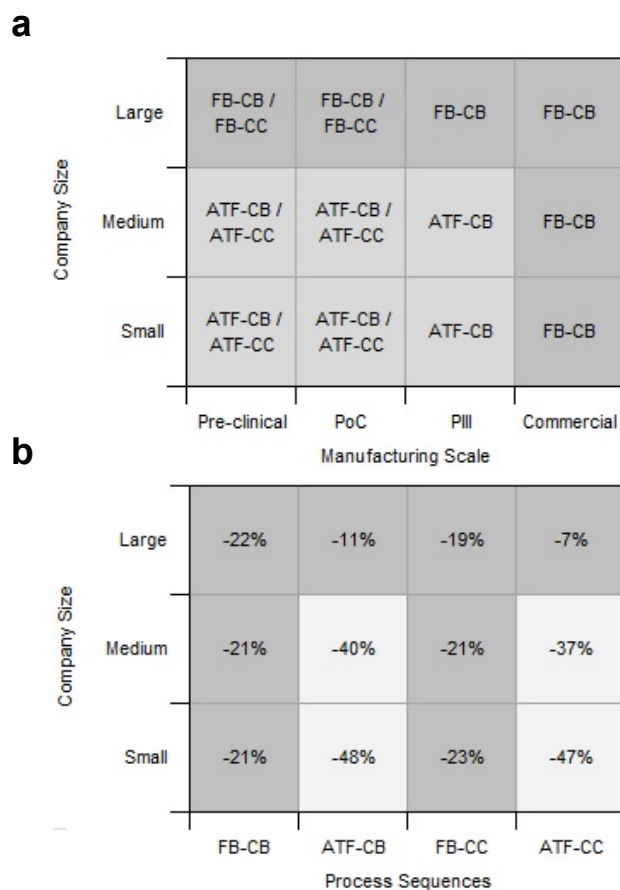


Figure 5.7. Contour plots showing the impact of manufacturing scale and manufacturing strategies on a) the most economically attractive manufacturing strategies for each scenario and b) the resulting cost per launch for all company sizes relative to the base case manufacturing strategy. (Pre-Clinical, 1 x 0.5kg; PoC, 1 x 4kg; Phase III, 4 x 10kg; Commercial, 20 x 10kg).

Figure 5.8 presents a detailed breakdown of the COG/g for all the alternative manufacturing strategies in a medium-sized company at the Phase III manufacturing scale. The figure highlights how the base case and alternative fed-batch based manufacturing strategies COG/g are dominated by indirect costs, due to the larger fermentation and purification capabilities required compared to the smaller highly utilised ATF perfusion-based strategies. The higher utilisation of the smaller process sequences seen in the ATF perfusion-based strategies is off-set by the ~2.5-fold increase in

labour demand required to operate the continuous capture step for the duration of the perfusion cell culture. The high labour demand and multiple production lines seen in the ATF perfusion-based strategies explains the inability of the strategies to offer a competitive alternative to the base case for Pre-Clinical manufacture in a large-sized company.

Figure 5.7a highlights that the FB-CB manufacturing strategy is the most consistent strategy, offering COG/g saving at all manufacturing and company scales relative to the base case. This is possible due to the continuous capture step which reduces the volume of expensive Protein A resin required and generates a more concentrated elution pool allowing a smaller purification train to be employed, reducing both direct and indirect batch costs. However the FB-CB does not offer the highest level of savings. This feat is achieved by the ATF-CB manufacturing strategy, which offers superior COG/g savings during clinical manufacture because it is able to reduce the size of the purification train even further by the continuous generation of small volumes of HCCF. This has a significant impact on the dominant material costs by replacing the resin cost with media cost, due to the 10-fold reduction in column volume and the 4-fold increase in fermentation media use. The FB-CC and ATF-CC also reduce the scale of the purification train they employ, however the continuous polishing steps result in the sub-optimal scaling of the virus retention filtration operation. The batch-operated polishing strategies operate the virus retention filtration step for a complete 10-hour shift to process the larger pooled batch (multiple eluate pools). The continuous-operated polishing strategies process each sub-batch (eluate pool) individually. However, the smaller process volumes do not translate into significantly lower virus filter areas in this case since the step duration is also shortened (to 2-3 hours) due to the coupling of the AEX and VRF steps. This combined with the multiple sub-batches processed per batch leads to a 3-fold increase in VRF filter costs per year. As a result, the optimal polishing strategy switches from continuous to batch at larger scales since the cost of the single-use virus filters required for each sub-batch in the continuous process becomes more expensive than a single larger virus filter in the batch process.

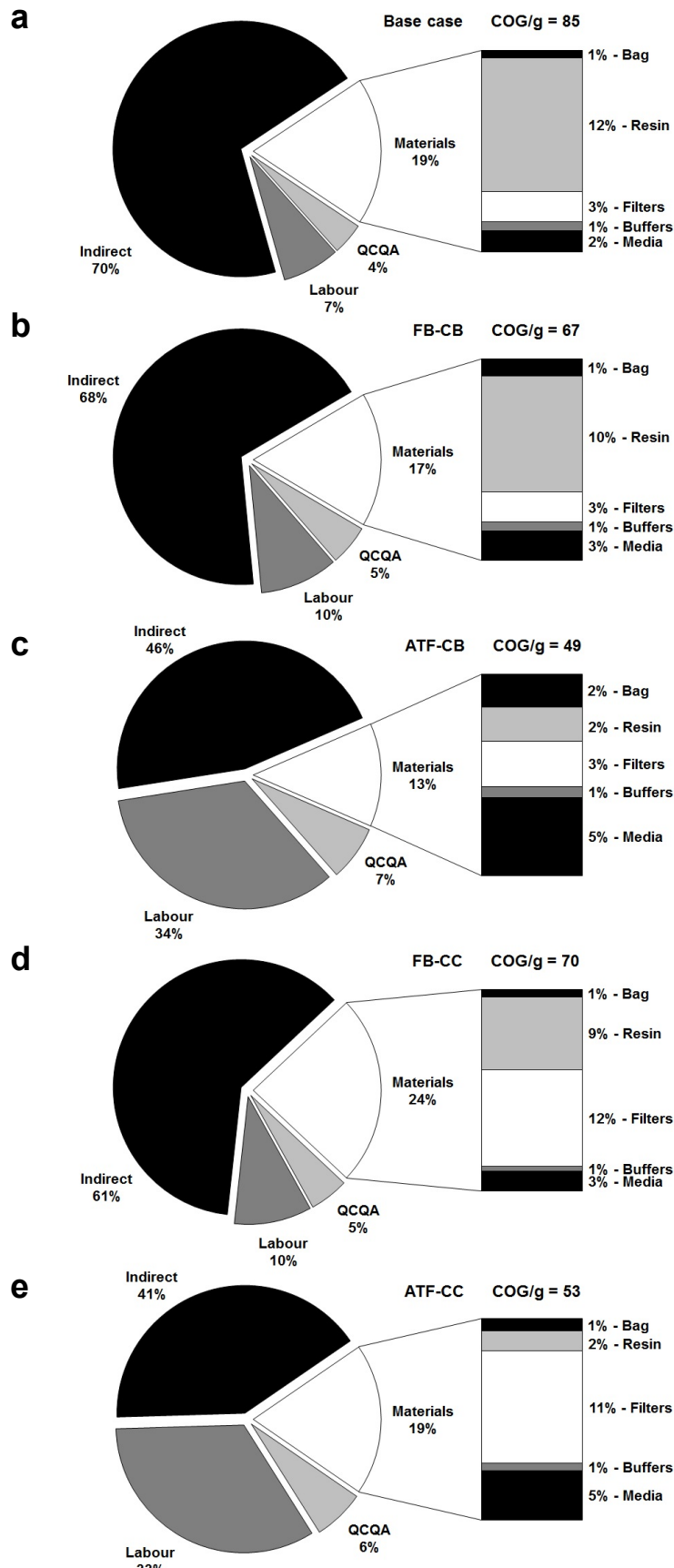


Figure 5.8. A comparison of cost of goods per gram with a detailed breakdown of material costs on a category basis for a) the base case, b) FB-CB, c) ATF-CB, d) FB-CC, e) ATF-CC scenario for a Phase III clinical batch in a medium-sized company.

The cost per launch of a successful drug candidate (DC) was a key economic metric used to compare the alternative manufacturing strategies encompassing the total risk-adjusted clinical development manufacturing cost. The cost per launch captures the costs of all the unsuccessful DCs incurred alongside the development of a successfully commercialised DC (10x Pre-Clinical DCs, 7x PoC DCs and 2x Phase III DCs). **Figure 5.7b** shows the percentage difference in the cost per launch of a successful drug candidate for all the alternative manufacturing strategies for all the company scales. The figure highlights how the FB-CB strategy offers the biggest cost saving (-22%) for a large-sized company. In contrast the ATF-CB strategy offers an even bigger cost saving for the small (-40%) and medium-sized (-48%) companies, because only a single manufacturing line is required throughout. This allows a much smaller facility to be used compared to the FB-CB strategy and as the company size decreases the cost contribution for the indirect costs increase, allowing the ATF-CB strategy to half the cost for launch (small-sized company).

5.3.5 Multi-Attribute Decision-Making

This section extends the analysis beyond economic metrics to include the environmental and operational benefits of each strategy.

5.3.5.1 Environmental Impact Analysis

The tool was also used to capture the water and consumable usage of the alternative manufacturing strategies to assess the environmental impact of the strategies across a range of manufacturing and company scales. E factor values were derived for the usage of water (cell culture media, process buffers, CIP buffers and rinse water) and consumables (bags, membranes and resins) within the manufacturing process. Typical mAb manufacturing strategies (base case) consume water from 3,000 to over 7,000 kg water per kilogram product. The cell culture steps consume between 20% and 25% of

the total, with the chromatographic operations often surpassing 50% of the total (Ho et al. 2011).

Table 5.6. E factor scores for alternate manufacturing strategies

Manufacturing Strategies	Water (kg/kg product)	Consumable (kg/kg product)
Base case	3900–7250	6–73
FB-CB	3000–6400	8–61
ATF-CB	2150–5500	6–35
FB-CC	2750–7450	13–48
ATF-CC	2300–5550	8–25

As expected all the alternative manufacturing strategies have a lower water E-Factor value in comparison to the base case strategy, where the difference in water usage can be directly related to the use of the continuous capture step and the resulting lower buffer requirement. **Table 5.6** demonstrates how the ATF perfusion-based manufacturing strategies have an even lower water E factor value than the fed-batch based strategies. A typical ATF-perfusion process without a continuous capture step has been shown to have higher process water usage compared to a Fed-batch process due to the high media usage. The removal of the dedicated primary clarification step and the use of the single use bioreactors (SUB) by the ATF perfusion process reduces the non-process water usage by ~30% (Pollock et al. 2013b). These trends when combined with a continuous capture step allow the ATF perfusion-based strategies to reduce their total water usage by 25-45%. In contrast the manufacturing strategies utilising continuous capture and polishing (FB-CC, ATF-CC) have higher water E-Factor values compared to the continuous capture and batch polishing manufacturing strategies (FB-CB, ATF-CB). The increase in E-Factor value is due to the higher number of sub-batches processed every batch, causing an increase in CIP buffers and rinse water used in cleaning between sub-batches.

The consumable E-Factor values are highly dependent on the amount of single use technologies and resin volume employed by the strategies. **Table 5.6** highlights how all the manufacturing strategies have a lower consumable E-Factor than the base case due to the use of the continuous capture step reducing the resin volumes used. The ATF perfusion-based strategies have a lower E-factor value than the fed-batch based strategies even though they employ SUBs because this increase in consumable waste is countered by the 10-fold reduction in resin volume seen.

5.3.5.2 Operational Risk Analysis

A risk score was assigned to each manufacturing strategy to assess the operational feasibility with respect to strategy robustness (likeliness of batch failure). The risk score is a ranking value used to compare the alternate strategies and does not capture a true value for batch failure risk. **Table 5.7** shows the risk score for both the upstream and downstream sections of the manufacturing strategies. The upstream risk score was calculated by assuming that each addition to the bioreactor had a 1 in 1,000 chance of causing contamination (Pollock et al. 2013b). The Fed-batch based strategies have a total of ten reactor additions (initial media fill and nine feeds) and therefore have a 1% risk score. In contrast the perfusion strategies had approximately twenty eight additions due to the daily media exchanges and therefore have a risk score of 2.8%. A similar approach was also used for the downstream risk score, where for every virus retention filtration (VRF) operation there was a 1 in a 1,000 chance of a filter or quality control failure. The same logic was applied to chromatographic operations where every cycle there was a 1 in 1,000 chance of a failure event of which 10% of these would lead to a batch failure. **Table 5.7** demonstrates how the ATF perfusion-based strategies have a higher risk score for both the upstream and downstream due to the high number of media exchanges and cycles in the continuous chromatography capture step. The continuous capture and polishing based strategies also have high risk scores due to the numerous VRF operations, resulting in the ATF-CC strategy having the

highest risk score of all the strategies due to high number of processing operations per batch.

Table 5.7. Batch risk for alternate manufacturing strategies

Manufacturing Strategies	USP	DSP	Risk Score
Base case	1%	0.2%	1.2%
FB-CB	1%	0.3%	1.3%
ATF-CB	2.8%	2.3%	5.1%
FB-CC	1%	1%	2%
ATF-CC	2.8%	4.6%	7.4%

5.3.5.3 Overall Aggregate Strategy Scores

The results of reconciling the trade-offs between economic, environmental and operational outputs using a single multi-attribute score are reviewed in this section. The key output was the overall aggregate strategy score over a range of combination ratios to reflect the impact of the relative importance of the economic, environmental and operational scores on the ranking of the manufacturing strategies. **Figure 5.9** depicts the sensitivity of the overall aggregate strategy scores to the economic attribute combination ratios for the alternative manufacturing strategies for a range of company scales (large, medium and small). For the scenario shown in **Figure 5.9**, the environmental attribute combination ratio was fixed at 0.1 and the operational attribute combination ratio varied with the economic attribute combination ratio such that the sum of all the combination ratios always remained equal to one. **Figure 5.9a** illustrates that for a large-sized company the FB-CB is always the preferred manufacturing strategy regardless how important the economic or operational feasibility is ranked. The ATF perfusion-based manufacturing strategies fail to achieve a high aggregate score due to their high risk scores and inability to offer significant economic advantage compared to the preferred FB-CB manufacturing strategy. In a medium-sized company (**Figure 5.9b**) when the economic benefits are 2x as important as

the operational benefits ($R1 = 0.6$, $R3 = 0.3$) the ATF-CB and FB-CB strategies are equally attractive. The ability of the ATF-CB strategy to offer a superior ranking as the importance of the economic benefits increases is due to superior savings offered in the cost to launch and capital expenditure at this company scale. **Figure 5.9c** illustrates how the high importance placed on capital expenditure and cost to launch by the small-sized company, results in the ATF-CB becoming the preferred manufacturing choice with increasing economic importance. However if the operational benefits are more important the FB-CB strategy is still the favoured manufacturing strategy. When the operational attribute combination ratio was fixed at 0.1 and the environmental attribute combination ratio varied with the economic attribute combination ratio as shown in **Figure A5.1**. The FB-CC strategy is able to outcompete the FB-CB strategy across all company scales, because the higher risk score is countered by the higher significance placed on the lower E factor ratings. The remaining relationships with the ATF-CB able to offer superior ranking as the importance of the economic benefits is maintained for the medium and small sized companies.

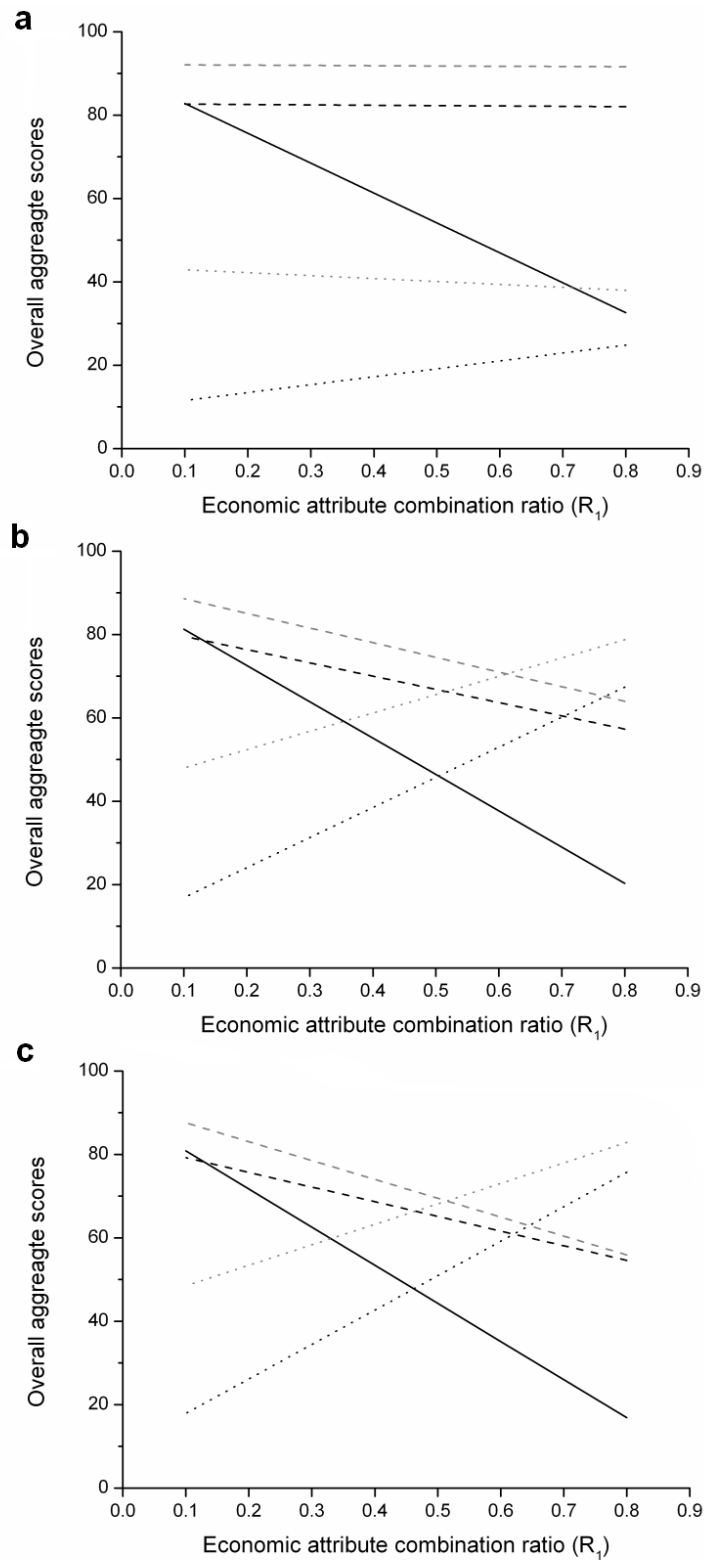


Figure 5.9. Sensitivity plots portraying the effect of the economic attribute combination ratio (R_1) in the overall aggregate scores when the environmental combination ratio is constant, for a) the large-sized company, b) medium-sized company and c) small-sized company, for the base case (solid black line), FB-CB (grey dashed line), ATF-CB (grey dotted line), FB-CC (black dashed line) and ATF-CC (black dotted line).

5.4 Conclusion

This chapter has evaluated the feasibility of continuous biopharmaceutical manufacturing strategies utilising perfusion cell culture and semi-continuous chromatography throughout the product life cycle from Pre-Clinical to Commercial manufacture. The decision-support framework was configured to cope with the continuous nature of the manufacturing strategies. The framework was used to provide an in-depth analysis of the potential of mAb manufacturing facilities based on the standard batch platform compared to the alternate continuous manufacturing strategies across a range of manufacturing and company scales so as to represent scenarios of relevance to industry. The analysis highlighted the underlying cost drivers for each strategy and evaluated the robustness of each strategy via a risk score. The derivation of environmental indices not only provided useful benchmarks of E factors for continuous processes but also enabled the economic, environmental and operational outputs to be assessed simultaneously. The tool predicts that the complete continuous strategy (ATF-CC) struggles to compete on economic, environmental and robustness fronts for Commercial manufacture, but offers saving during product development (Pre-Clinical, PoC, Phase III). In contrast the hybrid batch and continuous strategies (FB-CB & ATF-CB) outperform the continuous strategy for all manufacturing and company scales. The FB-CB strategy was shown to be the most consistent strategy offering savings at all manufacturing and company scales and is always the preferred manufacturing strategy for the large sized company. The ATF-CB strategy is predicted to offer superior economic benefits during product development that outweigh its lower robustness and increased Commercial manufacturing costs for the medium and small sized companies. However the analysis highlighted that if the operational feasibility is considered more important than the economic benefits the hybrid FB-CB strategy is found to be the preferred strategy for all company scales. The simulation framework therefore acts as a valuable test bed for assessing the potential of novel continuous strategies to cope with different scales of operation and decisional drivers.

6 Process Validation: Principles & Practices

6.1 A Paradigm Shift in Process Validation

Over the last two decades the biopharmaceutical industry has changed dramatically, with a growth rate outstripping pharmaceuticals sales, the establishment of a number of biological blockbusters and more recently the emergence of biosimilars (Aggarwal 2011). In contrast the United States Food and Drug Administration (FDA) has been supporting the same guidance document on process validation for the biopharmaceutical industry since 1987. However in January 2011, it released its first major update to its original 1987 guidance document. The original 1987 guidance titled “Guideline on General Principles of Process Validation” centred on instrument testing and qualification, and placed significant emphasis on collecting large amounts of data from a number of validation batches to demonstrate process robustness and repeatability. In contrast the latest guidance document “Guidance for Industry – Process Validation: General Principles and Practices” is a significant shift in process validation strategy with the guidance concentrating on risk management, quality by design (QbD) and the implementation of a continuous improvement process (PharmOut 2011; Scott 2011). The new guidance has been the principle driver in global drug registration in recent years and as a result has directly contributed to a number of quality guidance’s from the International Conference on Harmonisation Technical Requirements for Registration of Pharmaceuticals for Human Use (ICH) (PharmOut 2011; Scott 2011). The ICH brings together multiple regulatory authorities and industrial representatives in Europe, the US and Japan to harmonise scientific and technical aspects of drug registration.

The ICHs quality guidelines form the basis for of all drug registrations in Europe, the US and Japan, with process validation covered in a number of key quality guidance documents: ICH Q7 (Good Manufacturing Practice), ICH Q8 (Pharmaceutical development), ICH Q9 (quality risk management), ICH Q10 (pharmaceutical quality system) and ICH Q11 (Development and

Manufacturing of Drug Substances). These guidelines are directly referenced in the new FDA guidance document and highlight the shift from data driven process validation to a more holistic risk management derived process validation (PharmOut 2011). The new holistic guideline approach is centred on the `Products Lifecycle` and as a result can be defined as a three-stage approach to process validation: from process design, to process qualification followed by continued process verification. This new paradigm is a significant shift from the 1987 FDA guidelines, which promoted validation as a one-off event prior to product commercialisation. The FDA is keen to stress to companies that this thinking is no longer acceptable and states accordingly:

“Focusing exclusively on qualification efforts without also understanding the manufacturing process and associated variations may not lead to adequate assurance of quality. After establishing and confirming the process, manufacturers must maintain the process in a state of control over the life of the process, even as materials, equipment, production environment, personnel, and manufacturing procedures change.”

This new stance has triggered significant debate within the industry as it comes to terms with the long-term impact of the new guidelines. **Table 6.1** highlights the activities a company is now expected to fulfil over the lifecycle of the product and process.

Table 6.1. Validation stages and expected activities

Stage	Intent	Typical Activities
Process Design	<p>To define the commercial process on knowledge gained through development and scale up activities.</p> <p>The outcome is the design of a process suitable for routine manufacture that will consistently deliver product that meets its critical quality attributes.</p>	<ul style="list-style-type: none">• A combination of product and process design (QbD)• Product development activities• Experiments to determine process parameters, variability and necessary controls• Risk assessments• Other activities required to define the commercial process• Design of experiment testing
Process Qualification	<p>To confirm the process design as capable of reproducible commercial manufacturing.</p>	<ul style="list-style-type: none">• Equipment & utilities qualification• Process Performance Qualification (PPQ)• Strong emphasis on the use of statistical analysis of process data to understand process consistency and performance
Continued Process Validation	<p>To provide ongoing assurance that the process remains in a state of control during routine production through quality procedures and continuous improvement initiatives.</p>	<ul style="list-style-type: none">• Procedural data collection from every batch.• Data trending and statistical analysis• Equipment and facility maintenance calibration• Management review and production staff feedback• Improvement initiatives through process experience

Adapted from PharmOut 2011.

The new validation paradigm places significant emphasis on non-qualification activities (traditional IQ, OQ, PQ activities) such as product development and procedural monitoring for on-going process verification (PharmOut 2011). This new approach has been described as the “four Ds”: Design (for standard requirements & control), Demonstration (by experimentation & verification), Documentation (employing Good Manufacturing Practices & sound scientific rigour) and Determination (on-going process monitoring) (PharmOut 2011). This approach requires an increasing knowledge of statistics and risk management to realise the required linkages between risk management and QbD into process validation activities. **Figure 6.1** demonstrates how these new approaches and requirements will impact a products lifecycle, from early development to commercial manufacture. The core risk management theme highlighted in **Figure 6.1**, starts with definition of the products Critical Quality Attributes (CQA) in early development. An initial risk assessment then ranks the process parameters with respect to potential impact on the products CQA. The high-risk parameters are then studied in process characterisation (PC) studies and can feedback into the process design. After PC a further risk assessment is carried out to evaluate the findings from the PC work and re-rank the process parameters and confirm expected linkages to product CQA. The top parameters are then classified as critical process parameters (CPP) to highlight the level of control required to maintain product quality and process robustness. The CPP and their controls are documented in the process Control Strategy Document (CSD), which also includes the required future process monitoring strategy of the product CQA and CPP to demonstrate Continuous Process Verification (CPV). The expectation for CPV is the continued monitoring and statistical trending of CQA and CPP over time. This should allow companies to discover trend shifts, which will highlight future problems earlier ideally preventing process failures, product losses, regulatory issues and expensive mistakes (Scott 2011). The generic development and lifecycle approach shown in **Figure 6.1**, will not always be the same between companies due to their differences in risk management and the level of QbD principles they maybe adopting in their products registration filing.

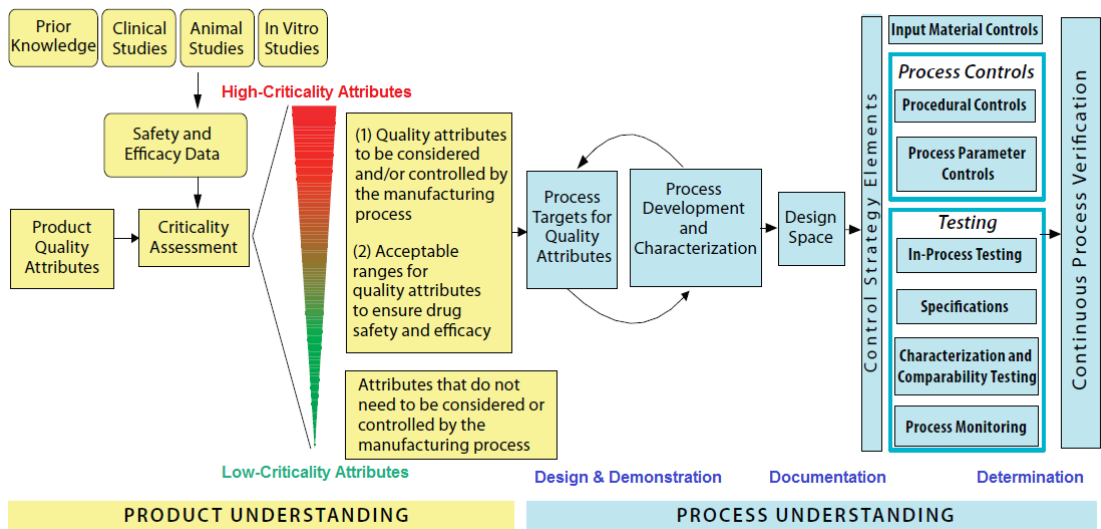


Figure 6.1. Validation activities throughout a products lifecycle. Adapted from Scott 2011.

6.2 Validation Concerns for Continuous Processes

The current drug registration quality guidance regulations are surprising silent on designating or even promoting a preference to the mode of manufacturing to be used, with respect to batch and continuous processing. One the most common concerns cited with continuous processing is the regulatory impact of batch/lot definition. The ICH Q7 quality guidance document defines a batch/lot as follows:

“A specific quantity of material produced in a process or series of processes so that it is expected to be homogeneous within specified limits. In the case of continuous production, a batch may correspond to a defined fraction of the production. The batch size can be defined either by a fixed quantity or by the amount produced in a fixed time interval.”

The ICH definition demonstrates that the current regulatory definition for both batch and lot are applicable to a continuous process. This definition is aligned within all ICH supporters and also in US law, with an analogous definition cited in the Code of Federal Regulations (CFR).

While the regulatory agencies looked primed to accept the idea of a complete continuous manufacturing process for biopharmaceutical product registration, there are still a number of concerns with validating the individual continuous and semi-continuous unit operations employed. For example continuous perfusion cell culture unit operations have one principle difference to batch cell cultures, which is the longer operating time. The longer operating times will raise the risk of genetic or production drift in the cell line, bioburden contamination and a higher risk for the introduction and growth of viruses (Kozlowski 2013). These regulatory concerns have been answered for a number of products in recent years, however these product registrations were filed using the 1987 FDA guidance document and as a result no continuous perfusion based process has been successfully registered under the new regulations. Continuous perfusion cell culture processes are unlikely to cause significant regulatory concerns under the new regulations, due to historic acceptance by multiple manufactures and products.

In contrast continuous chromatographic unit operations, which are widely seen in the food and chemical industries, have yet to appear in the manufacture of a registered biopharmaceutical product. Similarly, the principal validation concern for continuous chromatographic unit operations is the longer operating time and how it impacts the separation power of the step with respect to contaminants and product quality (Kozlowski 2013). Another key area of concern is how to validate the viral clearance of a continuous chromatography step (Kozlowski 2013). **Chapter 4** of this thesis demonstrated that in principle the separation power of a protein A continuous chromatography unit operation is representative with fresh resin and by leveraging a single column lifetime study can demonstrate robust separation power for the lifetime of the resin. The use of small-scale cycle studies followed by supporting manufacturing scale verification is a widely accepted

principle for batch chromatographic operations and therefore should be acceptable for continuous chromatographic unit operations as well. Validation of the continuous chromatography's viral clearance will be more of a challenge and is likely to be one of the key hurdles for this technology to overcome if it is to be utilised in biopharmaceutical manufacture. Viral clearance for batch chromatography systems is established by experimentally deriving the Log clearance and the partitioning of the viral panel. Due to the wealth of information available to mAb manufacturers due to the use of platform manufacturing strategies (constant resin section and operating conditions), the likely Log clearance and fraction location of partitioned virus can be predicted. However the impact of recycling flow-through and wash volumes over a new column with low product concentration may significantly alter how the virus is fractionated over the system and therefore the viral log clearance of that step. To date there is no official guidance or published data on the impact of viral clearance across a continuous chromatographic system.

There appears to be no significant regulatory roadblocks towards the adoption of continuous biopharmaceutical manufacturing, with the concepts in ICH Q7, Q8, Q9, Q10 and Q11 all being applicable to continuous processing (Kozłowski 2013). There are however, some unit operation dependant validation concerns (viral clearance in a continuous chromatographic system) that still need to be addressed before the technology is widely adopted. To date continuous perfusion cell cultures are the only continuous technology to feature in a manufacturing process of a successfully registered biopharmaceutical product. Until a more developed continuous manufacturing process is successfully registered under ICH guidelines there will always remain a degree of uncertainty around continuous processing in biopharmaceutical manufacturing. However the FDA and EMEA stress in any public disclosure that dialog is always encouraged around any regulatory issues, suggesting there is a clear path forward to answer any regulatory compliance concerns around continuous technologies.

7 Conclusions & Future Work

Biopharmaceutical manufactures currently find themselves in very challenging environment, with increasing competition, lower reimbursement levels and the loss of patent exclusivity for a number of blockbusters. To remain competitive in such an environment companies are looking to reduce R&D and manufacturing costs by improving their manufacturing platform processes whilst maintaining flexibility and product quality. As a result companies are now exploring whether they should choose conventional batch technologies or invest in novel continuous technologies, which may lead to lower production costs. Currently the only way to explore these technologies is with proof of concept laboratory scale evaluations, which are highly resource intensive. In the last decade, the potential impacts on clinical and commercial manufacturing of new technologies has been routinely assessed with decision-support tools. However, to date the publication of any decision-support tools capable of capturing multiple continuous unit operations, or even a continuous biopharmaceutical manufacturing process has not been seen. This chapter summarises the efforts made in this thesis to create such a dynamic tool as part of a decision-support framework that is capable of simulating and optimising continuous monoclonal antibody (mAb) manufacturing in this challenging environment. It also points out a number of future developments that will increase the understanding of the potential benefits and pitfalls of continuous processing in the biopharmaceutical sector.

7.1 Overall Conclusions

The primary aim of this the thesis has been the design and development of a decision-support framework that is capable of simulating and optimising continuous mAb manufacturing processes in the challenging environment biopharmaceutical manufactures find themselves. The resulting tool described throughout this thesis is capable of facilitating more informed decision-making when evaluating continuous and semi-continuous

manufacturing strategies, with respect to their economic, environmental and operational feasibility. The aim of this body of work was realised through a number of objectives that formed the basis of each of the preceding chapters. These chapters clearly demonstrate that the framework is a powerful test bed for assessing the potential of novel continuous technologies and manufacturing strategies to cope with future titres, multiple scales of operation and key decisional drivers.

Chapter 2 details the development approach adopted in the establishment of the resulting decision-support framework. The framework was built to tackle the complex problem domain found in biopharmaceutical manufacturing. This was achieved through the utilisation of deterministic discrete-event simulation, Multi-Attribute Decision Making and Monte Carlo simulation techniques. Hence, the framework is capable of describing a large number of scenarios within the industry, highlighting the key economic, environmental and operational metrics of the facilities, processes and technologies investigated under uncertainty. This was made possible by the hierarchal nature of the framework, which simulates the manufacturing scenarios of interest on a number of levels of detail ranging from high-level process performance metrics to low-level ancillary task estimates. This approach made the resource-demand profiles for tasks more realistic, allowing the constraining nature of facility resources to be modelled more accurately in both deterministic and stochastic simulations. The hierarchal approach adopted also aided the development of semi-continuous unit operation process models with the addition of a sixth hierarchal layer (sub-batches) making it possible to track the merging and splitting of batches. This allowed the framework to fulfil the primary aim of this work, namely assisting decision-making in the evaluation of alternative manufacturing strategies employing semi-continuous unit operations. The framework's ability to capture the impact of a number of individual semi-continuous unit operations and manufacturing strategies linking multiple semi-continuous unit operations has been demonstrated in **Chapters 3, 4 & 5**.

Chapter 3 presents the utilisation of the framework to assist in cost-effective bioprocess design in the presence of uncertainty and multiple conflicting outputs relating to economic, environmental and operational feasibility. The tool was configured to cope with the continuous nature of perfusion cultures, the consequences of failures as well as the use of single-use bioreactors and bags when the scale was appropriate. The tool was used to provide an in-depth analysis of the potential of mAb facilities based on fed-batch cell culture systems compared to 1st (spin-filter) and 2nd (alternating tangential flow; ATF) generation perfusion systems across a range of titres and scales of operation so as to represent different possible scenarios of relevance to industry. The analysis highlighted the underlying cost drivers for each process and identified the robustness of each strategy along with the root causes for the differences. The derivation of environmental indices not only provided useful benchmarks of E factors for fed-batch and perfusion processes but also enabled the economic, environmental and operational outputs to be assessed simultaneously. This was achieved using a multi-attribute decision-making technique that provided a more holistic approach to managing conflicting outputs. The tool's predictions that the spin-filter perfusion strategy struggles to compete on economic, environmental, operational and robustness fronts at most titres and scales provides insight into its limited use in industrial processes. In contrast, the ATF perfusion strategy is predicted to offer economic benefits that outweigh its lower robustness (versus traditional fed-batch cell culture), even when it achieves cell densities that are only 3 fold higher than fed-batch strategies for typical titre and demand levels. However, the analysis highlighted that if environmental or operational feasibility (e.g. ease of operation and validation) are considered more important than process economics savings then the fed-batch strategy is found to be preferred.

In **Chapter 4** the framework's capability to simulate multiple downstream purification manufacturing strategies was demonstrated by assessing the impact of semi-continuous chromatography for product capture across a product's lifecycle from Proof-of-Concept to Commercial manufacture. Semi-continuous chromatography is a new technology and as such there were no

dedicated design and optimisation protocols. Therefore a novel approach was adopted linking small-scale single-column experimental studies to the framework. The experimental work was key to determining the critical design parameters for the periodic counter current system (PCC) investigated, through the derivation of mass balance, scale-up and scheduling equations. The integrated techno-economic evaluation presented in the chapter predicts that semi-continuous chromatography has the ability to offer manufacturing cost savings in early clinical phase material generation, which can be significant due to the high attrition rates of early phase projects. The analysis also demonstrated the obstacles to using such a technology at commercial scale and the importance in the selection of the protein A resin employed. The framework was then employed to determine the semi-continuous system specification required to operate with similar costs to a standard batch process while a process change application is pursued for a theoretical transition from semi-continuous chromatography in early development to a conventional batch chromatography system in commercial manufacture.

Chapter 5 demonstrates the fulfilment of the primary thesis aim, by presenting a feasibility evaluation of multiple continuous biopharmaceutical manufacturing strategies utilising perfusion cell culture and semi-continuous chromatography throughout the product life cycle from Pre-Clinical to Commercial manufacture. The framework was used to provide an in-depth analysis of the potential of mAb manufacturing facilities based on the standard batch platform compared to the alternate continuous manufacturing strategies across a range of manufacturing and company scales so as to represent scenarios of relevance to industry. The analysis highlighted the underlying cost drivers for each strategy and evaluated the robustness of each strategy via a risk score. The derivation of environmental indices not only provided useful benchmarks of E factors for continuous manufacturing strategies but also enabled the economic, environmental and operational outputs to be assessed simultaneously. The tool predicts that the complete continuous strategy (ATF perfusion linked to continuous purification train) struggles to compete on economic, environmental and robustness fronts for Commercial manufacture, but offers saving during product development (Pre-

Clinical, Proof-of-Concept & Phase III). In contrast the hybrid batch and continuous strategies (fed-batch or ATF perfusion linked to a continuous capture step, followed by batch polishing steps; FB-CB & ATF-CB) outperform the continuous strategy for all manufacturing and company scales investigated. The FB-CB strategy was shown to be the most consistent strategy offering savings at all manufacturing and company scales and is always the preferred manufacturing strategy for the large sized company (targeting 2 product launches a year). The ATF-CB strategy is predicted to offer superior economic benefits during product development that outweigh its lower robustness and increased Commercial manufacturing costs for the medium and small sized companies (targeting one product launch every year or every two years, respectively). However the analysis highlighted that if the operational feasibility is considered more important than the economic benefits the hybrid FB-CB strategy is found to be the preferred strategy for all company scales.

In addition to the techno-economic evaluations presented in **Chapters 3, 4 & 5**, it was recognized that the potential benefits of the new or alternative technologies needed to be balanced against any regulatory concerns. **Chapter 6** addresses the current state of drug registration and assesses the regulatory impact of new continuous technologies and continuous manufacturing in general. The chapter highlights that there appears to be no significant regulatory roadblocks towards the adoption of continuous biopharmaceutical manufacturing, with the concepts in ICH Q7, Q8, Q9, Q10 and Q11 all being applicable to continuous processing. There are however, some unit operation dependant validation concerns (viral clearance in a continuous chromatographic system) that still need to be addressed before the technology is widely adopted. To date continuous perfusion cell cultures are the only continuous technology to feature in a manufacturing process of a successfully registered biopharmaceutical product. Until a more developed continuous manufacturing process is successfully registered under ICH guidelines, there will always remain a degree of uncertainty around continuous processing in biopharmaceutical manufacturing. However the FDA and EMEA stress in any public disclosure that dialog is always

encouraged around any regulatory issues, suggesting there is strong path forward to answer any regulatory compliance concerns around continuous technologies.

7.2 Future Work

The objective of this body of work has been the design and development of a decision-support framework that is capable of simulating and optimising continuous mAb manufacturing processes. The preceding chapters have demonstrated how the framework has successfully fulfilled this objective. The framework is clearly a powerful test bed for assessing the potential of novel continuous technologies and manufacturing strategies, and can therefore act as a strong foundation from which future work can build; several examples are highlighted and discussed below.

In addition to the continuous unit operations assessed in this thesis there are a further number of new and existing unit operations that could also be assessed. A number of alternative continuous cell culture systems exist that may not achieve the high cell densities offered by the ATF system, but still offer competitive cell densities with potentially lower system failure rates. These include gravity settlers, hydrocyclones and centrifugal cell retention devices, which do not employ filters to retain cells and therefore are not as prone to fouling related failure events (Voisard et al. 2003). Concentrated fed-batch cell culture is a new hybrid cell culture technology, which employs batch and continuous cell-culture techniques (Clincke et al. 2013a; Clincke et al. 2013b). A concentrated fed-batch cell culture is operated in a batch manner but is continuously fed fresh media to promote ultra-high cell densities and product concentrations. Unlike perfusion cell culture both the cells and product are retained in the bioreactor for a similar duration to a typical fed-batch culture (12-14 days), resulting in viable cell densities in the 100s of millions (10^8) of cells per ml and mAb yields 6 times higher than a typical fed-batch culture (Clincke et al. 2013a; Clincke et al. 2013b).

The latest continuous unit operations are not just confined to cell culture systems, with single pass tangential flow filtration (TFF) (Dizon-Maspat et al. 2012), continuous precipitation (Jaquez et al. 2010) and multicolumn counter current solvent gradient purification (MCSGP) to name a few (Müller-Späth et al. 2008). Single pass TFF allows continuous concentration or conductivity reduction of a product stream, offering a continuous replacement to batch ultrafiltration (Dizon-Maspat et al. 2012). Another technology showing a lot of potential is continuous precipitation, which builds on a historical knowledge base of batch precipitation seen in early mAb manufacturing and transforms this existing technology into a scalable continuous purification approach. Biogen Idec has recently realised this potential by demonstrating how continuous precipitation can be successfully integrated into a continuous purification train consisting of precipitate isolation, precipitate storage, and downstream purification through two flow-through chromatography steps (Jaquez et al. 2010). MCSGP builds on the recent influx of semi-continuous chromatography systems, but instead concentrates on the polishing chromatographic operations instead of the initial product capture. The system employs multiple ion-exchange columns (3-6) to divide closely related charge variants of a continuous mAb product stream into separate product pools, replacing low-throughput batch gradient elution chromatographic steps (Müller-Späth et al. 2008). All the prescribed technologies have the potential to significantly impact the way mAbs are manufactured in the future, and the framework could act as test bed for these technologies and be used to visualize their impact in future hybrid and continuous manufacturing strategies.

Chapter 5 highlighted how manufacturing strategies with varied combinations of batch and continuous technologies offer different levels of economic benefits depending on the scale of production and the company's size. These findings are also supported by conclusions in **Chapter 4**, which highlights the economic benefits of using continuous capture in early clinical development to reduce resin costs, but the disadvantage of using such a technology during commercial manufacturing. This suggests that a company can realise significant economic benefits by adopting various levels of

continuous manufacturing technologies throughout their pipeline portfolio. For example, the most economical way of producing a new mAb product would be to use a hybrid early phase clinical facility employing ATF perfusion cell culture linked to a continuous capture step. Before transferring to a large-scale commercial facility (contract manufacturer or in-house) for late stage clinical and commercial manufacturing employing hybrid (fed-batch cell culture linked to continuous capture) or conventional batch technologies. To establish what the optimal configuration of manufacturing sites and the technologies they should employ is currently outside the reach of this version of the framework presented in this thesis. However, by adding additional hierarchical layers the framework would be able to tackle the next key decisional domain of the biopharmaceutical industry; portfolio management. A number of tools exist that have demonstrated their ability to optimise a company's product portfolio with respect to site management, contract manufacturing and partnering decisions. These approaches can be readily combined into this framework to take the current short-term techno-economic evaluations presented in this work into long-term capacity planning and portfolio management.

In conclusion, the future work that has been outlined looks to increase the scope of continuous technologies the framework can simulate and also broaden the level of analysis possible, by building on the existing frameworks methods and approaches discussed in this thesis. Over the next decade continuous technologies are expected to become more prevalent in biopharmaceutical manufacturing, a paradigm shift of this magnitude has not been seen since chromatography became a platform technology in the 1970s. Due the high number of technologies and hybrid manufacturing strategies a framework that is capable of relating proof-of-concept technology evaluations to portfolio optimisation, will have a significant impact on the rate of uptake of continuous technologies.

8 References

- Aggarwal S. 2011. What's fueling the biotech engine[mdash]2010 to 2011. *Nat Biotech* 29(12):1083-1089.
- Anderson HL. 1986. Metropolis, Monte Carlo, and the MANIAC. *Los Alamos Science*(Fall).
- Banks J. 1998. *Handbook of simulation*: Wiley Online Library.
- Bennett S, McRobb S, Farmer R. 2010. *Object-oriented systems analysis and design using UML*. London; Boston; Madrid: McGraw-Hill Education.
- Bisschops M, Frick L, Fulton S, Ransohoff T. 2009a. Single-Use, Continuous-Countercurrent, Multicolumn Chromatography. *BioProcess Int* 7(6).
- Biwer A, Griffith S, Cooney C. 2005. Uncertainty analysis of penicillin V production using Monte Carlo simulation. *Biotechnology and bioengineering* 90(2):167-179.
- Bogdan B, Villiger R. 2010. *Valuation in Life Sciences. Valuation in Life Sciences: A Practical Guide, Third Edition*:67-303.
- Borge D. 2002. *The book of risk*: Wiley.
- Bosch P, Lundgren B, Kaisermayer C. 2008. How to Construct a Monoclonal Antibody Factory: A Comparison of Production Costs in Fed Batch and Perfusion Culture with Microcarriers - Part Two. *Bioprocessing Journal* 7(2):30-43.
- Brower M. Surpassing productivity limitations of traditional mAb manufacture - a continuous processing case study; 2013; Cambridge, UK.
- Burnouf T. 2007. Modern plasma fractionation. *Transfus Med Rev* 21(2):101-17.
- Cacciuttolo M. 2007. Perfusion or Fed-Batch? A matter of perspective. In: Butler M, editor. *Cell Culture & Upstream Processing*: Taylor Francis Group, London, UK. p 173-184.
- Carstens JN, Clarke HRG, Jensen JP. 2009. Perfusion! Jeopardy or the ultimate advantage? *Bioprocess International, Webinar*, October.
- Cartwright ME, Cohen S, Fleishaker JC, Madani S, McLeod JF, Musser B, Williams SA. 2010. Proof of Concept: A PhRMA Position Paper With Recommendations for Best Practice. *Clinical Pharmacology & Therapeutics* 87(3):278-285.
- Centocor ILA. 2006. http://www.epa.ie/licences/lic_eDMS/090151b2800c1411.pdf (accessed 2011).
- Chapman K, Pullen N, Coney L, Dempster M, Andrews L, Bajramovic J, Baldrick P, Buckley L, Jacobs A, Hale G and others. 2009. Preclinical development of monoclonal antibodies Considerations for the use of non-human primates. *Mabs* 1(5):505-516.
- Clincke M-F, Mölleryd C, Samani PK, Lindskog E, Fäldt E, Walsh K, Chotteau V. 2013a. Very high density of Chinese hamster ovary cells in perfusion by alternating tangential flow or tangential flow filtration in WAVE bioreactor™—part II: Applications for antibody production and cryopreservation. *Biotechnology Progress* 29(3):768-777.

- Clincke MF, Molleryd C, Zhang Y, Lindskog E, Walsh K, Chotteau V. 2013b. Very high density of CHO cells in perfusion by ATF or TFF in WAVE bioreactor. Part I. Effect of the cell density on the process. *Biotechnol Prog* 29(3):754-67.
- Cohen J. 2009 Market access in the wake of NICE: Biopharma's friend or foe? *European Biopharmaceutical Review*:8-12.
- Cohn E, Strong LE, Hughes W, Mulford D, Ashworth J, Melin M, Taylor H. 1946. Preparation and Properties of Serum and Plasma Proteins. IV. A System for the Separation into Fractions of the Protein and Lipoprotein Components of Biological Tissues and Fluids^{1a, b, c, d}. *Journal of the American Chemical Society* 68(3):459-475.
- Crowley J, Wubben M, Coco Martin JM; 2008. Process For Cell Culturing by Continuous Perfusion and Alternating Tangential Flow patent 20080131934.
- Curling J. 2009. The development of antibody purification technology. In: Gottschalk U, editor. *Process scale purification of antibodies*: Wiley.
- Deb K. 2008. *Multi-objective Optimization using Evolutionary Algorithms*: John Wiley & Sons, Ltd.
- Deo YM, Mahadevan MD, Fuchs R. 1996. Practical considerations in operation and scale-up of spin-filter based bioreactors for monoclonal antibody production. *Biotechnol.Prog.* 12(1):57-64.
- DiMasi JA, Feldman L, Seckler A, Wilson A. 2010. Trends in Risks Associated With New Drug Development: Success Rates for Investigational Drugs. *Clinical Pharmacology & Therapeutics* 87(3):272-277.
- DiMasi JA, Grabowski HG. 2007. The cost of biopharmaceutical R&D: is biotech different? *Managerial and Decision Economics* 28(4-5):469-479.
- DiMasi JA, Hansen RW, Grabowski HG. 2003. The price of innovation: new estimates of drug development costs. *J Health Econ* 22(2):151-85.
- Dizon-Maspat J, Bourret J, D'Agostini A, Li F. 2012. Single pass tangential flow filtration to debottleneck downstream processing for therapeutic antibody production. *Biotechnol Bioeng* 109(4):962-70.
- Evans ST, Huang X, Cramer SM. 2010. Using Aspen to Teach Chromatographic Bioprocessing: A Case Study in Weak Partitioning Chromatography for Biotechnology Applications. *Chemical Engineering Education* 44(3):198-207.
- Farid SS. 2006. Established bioprocesses for producing antibodies as a basis for future planning. *Cell Culture Engineering* 101:1-42.
- Farid SS. 2007. Process economics of industrial monoclonal antibody manufacture. *Journal of Chromatography B-Analytical Technologies in the Biomedical and Life Sciences* 848(1):8-18.
- Farid SS. 2009a. Economic Drivers and Trade-Offs in Antibody Purification Processes. *BioPharm International*:October: S38-S42.
- Farid SS. 2009b. Process Economics Drivers in Industrial Monoclonal Antibody Manufacture. In: Gottschalk U, editor. *Process Scale Purification of Antibodies*: John Wiley & Sons, Inc. p 239-262.
- Farid SS. 2012. Evaluating and Visualizing the Cost-Effectiveness and Robustness of Biopharmaceutical Manufacturing Strategies.

- Biopharmaceutical Production Technology: Wiley-VCH Verlag GmbH & Co. KGaA. p 717-741.
- Farid SS, Washbrook J, Titchener-Hooker NJ. 2005. Decision-support tool for assessing biomanufacturing strategies under uncertainty: Stainless steel versus disposable equipment for clinical trial material preparation. *Biotechnology Progress* 21(2):486-497.
- Farid SS, Washbrook J, Titchener-Hooker NJ. 2007. Modelling biopharmaceutical manufacture: Design and implementation of SimBiopharma. *Computers & Chemical Engineering* 31(9):1141-1158.
- Fishburn PC. 1967. Letter to the Editor—Additive Utilities with Incomplete Product Sets: Application to Priorities and Assignments. *Operations Research* 15(3):537-542.
- Gagnon P. 2012. Technology trends in antibody purification. *J Chromatogr A* 1221:57-70.
- George ED, Farid SS. 2008a. Stochastic Combinatorial Optimization Approach to Biopharmaceutical Portfolio Management. *Industrial & Engineering Chemistry Research* 47(22):8762-8774.
- George ED, Farid SS. 2008b. Strategic Biopharmaceutical Portfolio Development: An Analysis of Constraint-Induced Implications. *Biotechnology Progress* 24(3):698-713.
- Ghose S, Nagrath D, Hubbard B, Brooks C, Cramer SM. 2004. Use and Optimization of a Dual-Flowrate Loading Strategy To Maximize Throughput in Protein-A Affinity Chromatography. *Biotechnology Progress* 20(3):830-840.
- Godawat R, Brower K, Jain S, Konstantinov K, Riske F, Warikoo V. 2012. Periodic counter-current chromatography -- design and operational considerations for integrated and continuous purification of proteins. *Biotechnol J* 7(12):1496-508.
- Gosling I. 2005. Process simulation and modeling for industrial bioprocessing: tools and techniques. *Industrial Biotechnology* 1(2):106-109.
- Haekler S, Stretch K, Zaino T. 2010 *Biotech Production: Planning, Scheduling and Throughput Analysis with a Combined Theory of Constraints, Lean and Simulation Approach*. PharmaManufacturing.
- Hahn R, Bauerhansl P, Shimahara K, Wizniewski C, Tscheliessnig A, Jungbauer A. 2005. Comparison of protein A affinity sorbents II. Mass transfer properties. *Journal of Chromatography A* 1093(1-2):98-110.
- Hahn R, Schlegel R, Jungbauer A. 2003. Comparison of protein A affinity sorbents. *Journal of Chromatography B* 790(1-2):35-51.
- Hassan I. 2009. A techno-economic framework for assessing manufacturing process changes in the biopharmaceutical industry: University College London.
- Heflin DL, Harrell CR. *Simulation modeling and optimization using ProModel*; 1998. IEEE Computer Society Press. p 191-198.
- Helfferrich FG, Carr PW. 1993. Non-linear waves in chromatography: I. Waves, shocks, and shapes. *Journal of Chromatography A* 629(2):97-122.
- Ho SV, McLaughlin JM, Pollock J, Farid SS. 2011. Toward Greener Therapeutic Proteins. In: Tao J, Kazlazuskas R, editors. *Biocatalysis*

- for Green Chemistry and Chemical Process Development. New Jersey: John Wiley & Sons. p 197-219.
- Holzer M, Osuna-Sanchez H, David L. 2008. Multicolumn chromatography; A new approach to relieving capacity bottlenecks for downstream processing efficiency. *BioProcess International*.
- Hou Y. Implementation of membrane chromatography into continuous antibody purification process; 2012; San Diego, CA.
- Irabien Á, Aldaco R, Dominguez-Ramos A. 2009. Environmental Sustainability Normalization of Industrial Processes. In: Jacek J, Jan T, editors. *Computer Aided Chemical Engineering*: Elsevier. p 1105-1109.
- Jaquez OA, Gronke RS, Przybycien TM. Design of a scalable continuous precipitation process for the high throughput capture and purification of high titre monoclonal antibodies; 2010; Salt Lake City.
- Juza M, Mazzotti M, Morbidelli M. 2000. Simulated moving-bed chromatography and its application to chirotechnology. *Trends in Biotechnology* 18(3):108-118.
- Kahn D, Plapp R, Modi A. 2001. Modeling a multi-step protein synthesis and purification process: A case study of a CAPE application in the pharmaceutical industry. *Computer Aided Chemical Engineering* 9:419-426.
- Kamarck ME. 2006. Building biomanufacturing capacity - the chapter and verse. *Nature Biotechnology* 24(5):503-505.
- Kelley B. 2009. Industrialization of mAb production technology The bioprocessing industry at a crossroads. *Mabs* 1(5):443-452.
- Kelley B, Blank G, Lee A. 2009. Downstream processing of monoclonal antibodies: current practices and future opportunities. In: Gottschalk U, editor. *Process scale purification of antibodies*: Wiley.
- Kelley BD. 2007. Very large scale monoclonal antibody purification: The case for conventional unit operations. *Biotechnology Progress* 23(5):995-1008.
- Kelley BD, Tobler SA, Brown P, Coffman JL, Godavarti R, Iskra T, Switzer M, Vunnum S. 2008. Weak partitioning chromatography for anion exchange purification of monoclonal antibodies. *Biotechnology and Bioengineering* 101(3):553-566.
- Kelton WD, Law AM. 2000. *Simulation modeling and analysis*: McGraw Hill Boston, MA.
- Kozlowski S. 2013. *Pharmaceutical Manufacturing: Quality of Biotechnology Products*. NIPTE Research Conference. Rockville, MD.
- Łacki KM. 2012. High-throughput process development of chromatography steps: Advantages and limitations of different formats used. *Biotechnology Journal*:n/a-n/a.
- Lakhdar K, Savery J, Papageorgiou LG, Farid SS. 2007. Multiobjective long-term planning of biopharmaceutical manufacturing facilities. *Biotechnol Prog* 23(6):1383-93.
- Lang HJ. 1948. Simplified Approach to Preliminary Cost Estimates. *Chemical Engineering* 55(112).
- Langer E. 2012 CMOs and biodevelopers taking different approaches to DSP problems: CMOs get serious about new technologies. *Pharmaceutical Outsourcing*.

- Langmuir I. 1916. THE CONSTITUTION AND FUNDAMENTAL PROPERTIES OF SOLIDS AND LIQUIDS. PART I. SOLIDS. *Journal of the American Chemical Society* 38(11):2221-2295.
- Langmuir I. 1918. THE ADSORPTION OF GASES ON PLANE SURFACES OF GLASS, MICA AND PLATINUM. *Journal of the American Chemical Society* 40(9):1361-1403.
- Leigh SR. 1996. Evolution of human growth spurts. *American Journal of Physical Anthropology* 101(4):455-474.
- Li Y, Kahn D, W., Galperina O, Blatter E, Luo R, Wu Y, Zhang G. 2009. Development of a platform process for the purification of therapeutic monoclonal antibodies. In: Gottschalk U, editor. *Process scale purification of antibodies*: Wiley.
- Lim AC, Washbrook J, Titchener-Hooker NJ, Farid SS. 2006. A computer-aided approach to compare the production economics of fed-batch and perfusion culture under uncertainty. *Biotechnology and Bioengineering* 93(4):687-697.
- Lim AC, Zhou YH, Washbrook J, Sinclair A, Fish B, Francis R, Titchener-Hooker NJ, Farid SS. 2005. Application of a decision-support tool to assess pooling strategies in perfusion culture processes under uncertainty. *Biotechnology Progress* 21(4):1231-1242.
- Liu HF, Ma J, Winter C, Bayer R. 2010. Recovery and purification process development for monoclonal antibody production. *Mabs* 2(5).
- Mahajan E, George A, Wolk B. 2012. Improving affinity chromatography resin efficiency using semi-continuous chromatography. *Journal of Chromatography A* 1227:154-162.
- Maria A. 1997. Introduction to modeling and simulation. *Proceedings of the 29th conference on Winter simulation*. Atlanta, Georgia, USA: IEEE Computer Society. p 7-13.
- Marichal-Gallardo PA, Álvarez MM. 2012. State-of-the-art in downstream processing of monoclonal antibodies: Process trends in design and validation. *Biotechnology Progress* 28(4):899-916.
- Merie L. 2013. Blockbuster biologics 2012. *Pipeline Review*.
- Miller DW, Starr MK. 1960. *Executive decisions and operations research*. Englewood Cliffs, N.J.: Prentice-Hall. 446 p. p.
- Mitchell P. 2005. Next-generation monoclonals less profitable than trailblazers? *Nature Biotechnology* 23(8):906-906.
- Mollan MJ, Lodaya M. 2004 *Continuous Processing in Pharmaceutical Manufacturing*. PharmaManufacturing.
- Morgan S, Grootendorst P, Lexchin J, Cunningham C, Greyson D. 2011. The cost of drug development: a systematic review. *Health Policy* 100(1):4-17.
- Müller-Späth T, Aumann L, Melter L, Ströhlein G, Morbidelli M. 2008. Chromatographic separation of three monoclonal antibody variants using multicolumn countercurrent solvent gradient purification (MCSGP). *Biotechnology and Bioengineering* 100(6):1166-1177.
- Mustafa M, Washbrook J, Titchener-Hooker N, Farid S. 2006. Retrofit decisions within the biopharmaceutical industry: an EBA case study. *Food and bioproducts processing* 84(1):84-89.

- Nicholas M, Arianna WR, Marshall NR, Augusta HT, Edward T. 1953. Equation of State Calculations by Fast Computing Machines. The Journal of Chemical Physics.
- Novais JL, Titchener-Hooker NJ, Hoare M. 2001. Economic comparison between conventional and disposables-based technology for the production of biopharmaceuticals. *Biotechnology and Bioengineering* 75(2):143-153.
- O'Hagan P, Farkas C. 2009. Bringing pharma R&D back to health. Bain & Company.
- Ogden CL, Fryar CD, Carroll MD, Flegal KM. 2004. Mean body weight, and body mass index, United States 1960-2002. In: *Surveys DoHaNE*, editor: CDC.
- Palmer E. 2013 19th February GSK Commits to continuous processing. FiercePharma Manufacturing.
- Papavasileiou V, Koulouris A, Siletti C, Petrides D. 2007. Optimize manufacturing of pharmaceutical products with process simulation and production scheduling tools. *Chemical Engineering Research and Design* 85(7):1086-1097.
- Papavasileiou V, Siletti C, Koulouris A, Petrides D. 2009. Bioprocess Design, Computer-Aided. *Encyclopedia of Industrial Biotechnology: Bioprocess, Bioseparation, and Cell Technology*.
- Paul SM, Mytelka DS, Dunwiddie CT, Persinger CC, Munos BH, Lindborg SR, Schacht AL. 2010. How to improve R&D productivity: the pharmaceutical industry's grand challenge. *Nat Rev Drug Discov* 9(3):203-214.
- Pavlotsky RV. 2004 Approximating facilities costs. *Solid State Technology*.
- Paz A, Puich M. 2004. Simulations Improve Production Capacity. *BioPharm International*.
- Pellek A, Arnum PV. 2008 Continuous Processing: Moving with or against the Manufacturing Flow. *PharmTech*:52-58.
- Peters MS, Timmerhaus KD, West RE. 2006. Plant design and economics for chemical engineers. Boston [u.a.]: McGraw-Hill.
- Petrides DP, Calandris J, Cooney CL. 1996 Bioprocess optimization via CAPD and simulation for product commercialization. *Genetic Engineering News*:24-60.
- Petrides DP, Koulouris A, Lagonikos PT. 2002. The role of process simulation in pharmaceutical process development and product commercialization. *Pharmaceutical Engineering* 22(1):56-65.
- PharmOut. 2011. FDA Guidance for Industry Update - Process Validation. www.pharmaout.net.
- PhRMA. 2004. 2004 Survey: Medicines in Development: Biotechnology. Pharmaceutical Research and Manufacturers Association.
- PhRMA. 2006. 2006 Report: Medicines in Development: Biotechnology. Pharmaceutical Research and Manufacturers Association.
- PhRMA. 2008. 2008 Report: Medicines in Development: Biotechnology. Pharmaceutical Research and Manufacturers Association.
- PhRMA. 2011. 2011 Report: Medicines in Development: Biotechnology. Pharmaceutical Research and Manufacturers Association.
- Pollock J, Bolton G, Coffman J, Ho SV, Bracewell DG, Farid SS. 2013a. Optimising the design and operation of semi-continuous affinity

- chromatography for clinical and commercial manufacture. *J Chromatogr A* 1284:17-27.
- Pollock J, Ho SV, Farid SS. 2012. Computer-aided design and evaluation of batch and continuous multi-mode biopharmaceutical manufacturing processes. 22nd European Symposium on Computer Aided Process Engineering. p 487-491.
- Pollock J, Ho SV, Farid SS. 2013b. Fed-batch and perfusion culture processes: Economic, environmental, and operational feasibility under uncertainty. *Biotechnology and Bioengineering* 110(1):206-219.
- Pyne D, Ehrenstein M, Morris V. 2002. The therapeutic uses of intravenous immunoglobulins in autoimmune rheumatic diseases. *Rheumatology (Oxford)* 41(4):367-74.
- Rajapakse A, Titchener-Hooker NJ, Farid SS. 2005. Modelling of the biopharmaceutical drug development pathway and portfolio management. *Computers & Chemical Engineering* 29(6):1357-1368.
- Rajapakse A, Titchener-Hooker NJ, Farid SS. 2006. Integrated approach to improving the value potential of biopharmaceutical R&D portfolios while mitigating risk. *Journal of Chemical Technology & Biotechnology* 81(10):1705-1714.
- Reichart JM. 2009. Probabilities of success for antibody therapeutics. *mAbs* 1(4):387-389.
- Reichart JM. 2013. Therapeutic monoclonal antibodies approved or in review in the European Union or United States. The Antibody Society.
- Remer DS, Idrovo JH. 1991. Cost-estimating factors for biopharmaceutical process equipment. *Pharmaceutical Technology International* 36.
- Rodrigues ME, Costa AR, Henriques M, Azeredo J, Oliveira R. 2010. Technological Progresses in Monoclonal Antibody Production Systems. *Biotechnology Progress* 26(2):332-351.
- Saaty TL. 1980. The analytic hierarchy process. New York: McGraw-Hill International.
- Schaber SD, Gerogiorgis DI, Ramachandran R, Evans JMB, Barton PI, Trout BL. 2011. Economic Analysis of Integrated Continuous and Batch Pharmaceutical Manufacturing: A Case Study. *Industrial & Engineering Chemistry Research* 50(17):10083-10092.
- Scott C. 2011 Quality By Design and the New Process Validation Guidance *Bioprocess International*:14-21.
- Shanklin T, Roper K, Yegneswaran PK, Marten MR. 2001. Selection of bioprocess simulation software for industrial applications. *Biotechnology and Bioengineering* 72(4):483-489.
- Sheldon RA. 1994. Consider the environmental quotient. *Journal Name: CHEMTECH; (United States); Journal Volume: 24:3:Medium: X; Size: Pages: 38-46.*
- Sheldon RA. 1997. Catalysis: The Key to Waste Minimization. *Journal of Chemical Technology & Biotechnology* 68(4):381-388.
- Sheldon RA. 2007. The E factor: fifteen years on. *Green Chemistry* 9(12):1273-1283.
- Shevitz J; 2000. Fluid Filtration System patent 6544424.
- Shukla AA, Hubbard B, Tressel T, Guhan S, Low D. 2007. Downstream processing of monoclonal antibodies--application of platform

- approaches. *J Chromatogr B Analyt Technol Biomed Life Sci* 848(1):28-39.
- Simaria A, Gao Y, Turner R, Farid S. Designing multi-product biopharmaceutical facilities using evolutionary algorithms; 2011. Elsevier. p 286.
- Sinclair A. 2008. How to evaluate the cost impact of using disposables in biomanufacturing. *BioPharm International* 21(6).
- Sinnott RK, Coulson JM, Richardson JF. 2005. Coulson & Richardson's chemical engineering. Vol. 6, Chemical engineering design. Oxford: Elsevier Butterworth-Heinemann.
- Siu S, Baldascini H, Hearle D, Hoare M, Titchener-Hooker N. 2006. Effect of fouling on the capacity and breakthrough characteristics of a packed bed ion exchange chromatography column. *Bioprocess and Biosystems Engineering* 28(6):405-414.
- Steuer RE, Na P. 2003. Multiple criteria decision making combined with finance: A categorized bibliographic study. *European Journal of operational research* 150(3):496-515.
- Stonier A, Pain D, Westlake A, Hutchinson N, Thornhill N, Farid S. 2011. Integration of stochastic simulation with advanced multivariate and visualisation analyses for rapid prediction of facility fit issues in biopharmaceutical processes.
- Stonier A, Pain D, Westlake A, Hutchinson N, Thornhill NF, Farid SS. 2013. Integration of stochastic simulation with multivariate analysis: Short-term facility fit prediction. *Biotechnology Progress* 29(2):368-377.
- Stonier A, Simaria AS, Smith M, Farid SS. 2012. Decisional tool to assess current and future process robustness in an antibody purification facility. *Biotechnology Progress*:n/a-n/a.
- Stonier A, Smith M, Hutchinson N, Farid SS. Dynamic Simulation Framework for Design of Lean Biopharmaceutical Manufacturing Operations. In: Gani R, editor. *Computer-Aided Chemical Engineering Series*; 2009. Amsterdam: Elsevier B. V. Ltd. p 1069-1074.
- Strohl WR. 2009. Therapeutic Monoclonal Antibodies: Past, Present, and Future. *Therapeutic Monoclonal Antibodies*: John Wiley & Sons, Inc. p 1-50.
- Strohlein G, Aumann L, Muller-Spath T, Tarafder A, Morbidelli M. 2007. Continuous Processing: The Multicolumn Countercurrent Solvent Gradient Purification Process. *BioPharm International*.
- Toumi A, Jürgens C, Jungo C, Maier BA, Papavasileiou V, Petrides DP. 2010. Design and optimization of a large scale biopharmaceutical facility using process simulation and scheduling tools. *Pharmaceutical Engineering*.
- Triantaphyllou E. 2000. Multi-criteria decision making methods: A comparative study. Netherlands: Kluwer Academic Publishers.
- Vallez-Chetreau F, Ferreira LGF, Rabe R, von Stockar U, Marison IW. 2007. An on-line method for the reduction of fouling of spin-filters for animal cell perfusion cultures. *Journal of Biotechnology* 130(3):265-273.
- Velayudhan A, Menon MK. 2007. Modeling of purification operations in biotechnology: enabling process development, optimization, and scale-up. *Biotechnol Prog* 23(1):68-73.











- Vester A. Towards a fully continuous production line for monoclonal antibodies; 2013; World biopharma forum, Continuous processing in biopharmaceutical manufacturing. Cambridge, UK.
- Voisard D, Meuwly F, Ruffieux PA, Baer G, Kadouri A. 2003. Potential of cell retention techniques for large-scale high-density perfusion culture of suspended mammalian cells. *Biotechnol Bioeng* 82(7):751-65.
- Wang XL, Das TK, Singh SK, Kumar S. 2009. Potential aggregation prone regions in biotherapeutics A survey of commercial monoclonal antibodies. *Mabs* 1(3):254-267.
- Warikoo V, Godawat R, Brower K, Jain S, Cummings D, Simons E, Johnson T, Walther J, Yu M, Wright B and others. 2012. Integrated continuous production of recombinant therapeutic proteins. *Biotechnology and Bioengineering*:n/a-n/a.
- Werner RG. 2004. Economic aspects of commercial manufacture of biopharmaceuticals. *J Biotechnol* 113(1-3):171-82.
- Williams JR. 1947. Six-tenths Factor Aids in Approximating Costs. *Chemical Engineering* 54:112-114.
- Wojciechowski PW, Smit HI, Myers MM, Voronko PJ, Laverty T, Ramelmeier RA, Siegel RC. 2007. Making Changes to a Biopharmaceutical Process during Development and Commercial Manufacturing: The REMICADE Story. In: Shukla AA, Etzel MR, Gadam S, editors. *Process Scale Bioseparations for the Biopharmaceutical Industry*: Taylor Francis Group, London, UK. p 507-523.
- Yabannavar VM, Singh V, Connelly NV. 1992. Mammalian cell retention in a spinfilter perfusion bioreactor. *Biotechnol Bioeng* 40(8):925-33.
- Yamane-Ohnuki N, Satoh M. 2009. Production of therapeutic antibodies with controlled fucosylation. *Mabs* 1(3):230-236.

9 Appendices

9.1 Chapter 2 Appendix

9.1.1 Tables

Table A2.1. Block Types Employed Within the Simulation Framework

Block Source	Block	Function
<i>Pre-fabricated</i>		
	Executive	Manages event scheduling, providing simulation control, item allocation and attribute management.
	Item Generation	Creates default items with no attribute values.
	Set Attribute Value	Sets the attribute properties of an item passing through the block.
	Get Attribute Value	Displays and outputs the attribute properties of an item passing through the block.
	Item Queue	Queues items and release them based on a user selected algorithm. (e.g. first in first out, first in last out etc.)
	Item Activity	Holds one or more items and release them based on a delay time from an attribute.
	Item Exit	Passes items out of the simulation.
	Interchange (Item & Flow)	Acts as a tank interfacing between flow and times
	Tank (Flow)	Acts as a source, storage or sink for flow.
	Valve (Flow)	Controls, monitors and transfers flow.


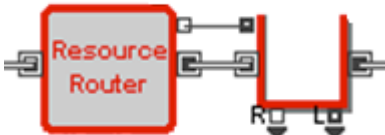
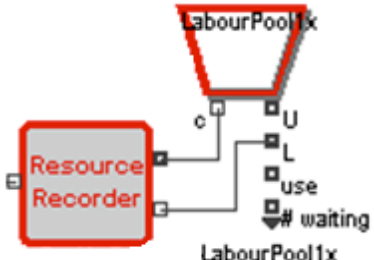



Block Source	Block	Function
Customised		
	Item Routing	Directs item to specific block based upon attribute or database value.
	Resource Router & Queue	Checks if a resource is available and record its use or holds item until resource is available.
	Resource Recorder & Pool	Records contents of pool and signals with resource queue when a resource is available.
Bespoke		
	Passing Block	Executes bespoke algorithms and equations specified in ModL on item arrival, sets attribute and database values.
	Remote Generation Block	On remote signal or time trigger from executive block. Executes bespoke algorithms and equations specified in ModL and generates a new item and sets attribute and database values.
	Remote Signalling Block	On remote signal or time trigger from executive block. Executes bespoke algorithms and equations specified in ModL updates database values and can send remote signals to other blocks.

Table A2.2. Equipment size, cost and exponential scaling coefficients

Equipment	Size _{Low}	Size _{High}	Size _{Base}	Cost _{Base} (USD)	Coefficient
Stainless Steel Vessel (m ³)	0.01	1	0.01	31807	0.137
	1	5	1	61119	0.0681
	5	80	5	73207	0.6254
Stainless Steel Bioreactor (m ³)	0.01	0.03	0.02	104000	0
	0.03	0.3	0.1	728000	0
	0.3	0.8	0.1	800000	0
	0.8	20	0.1	54505	0.1882
Single Use Bioreactor Skid (m ³)	0.002	0.2	0.2	88000	0
	0.2	0.5	0.5	98000	0
	0.5	1	1	110000	0
	1	2	2	174614	0
Spin-filter (L)	0	2000	N/A	35000	0
	1	3	N/A	20000	0
	4	20	N/A	30000	0
	20	100	N/A	90000	0
	100	200	N/A	130000	0
	200	800	N/A	180000	0
	800	1600	N/A	360000	0
Centrifuge (L/hr)	100	16000	1800	757500	1.105
DF Skid (m ²)	2	400	5	7500	0.7565
Chromatography Skid (L)	1	10	50	677174	0
	10	100	50	677174	0
	100	3000	100	677174	0.3133
VRF Skid (m ²)	0.01	1	1	257420	0
	1	50	1	257420	0.2216
UFDF Skid (m ²)	0.1	2	1	103250	0
	2	100	2	142971	0.4696

The cost models shown were primarily sourced from the projects industrial sponsor (Sa V Ho, Pfizer R&D Global Biologics, MA, USA). Other cost models were derived from discussions with Morten Munk, Christoffer Bro and Jacob Jensen (CMC biologics, Copenhagen, Denmark) and Karol Lacki and Roger Nordberg (GE Healthcare, Uppsala, Sweden).

Table A2.3. Consumables costs

Consumable	Description	Size	Unit Cost (USD)	Reuses
Filter Membranes	Depth Filter	0.2	250	1
	Viral Retention Filter	0.2	3250	1
	50 kDa UF Filter	0.2	250	30
Chromatographic Resins	Protein A	1	8000	200
	Anion Exchange Resin	1	1500	100
	Cation Exchange Resin	1	1500	100
Disposable Bags	500L	500	453	1
	200L	200	324	1
	100L	100	360	1
	50L	50	52	1
Single Use Bioreactors	50L Wave	25	210	1
	100L Wave	50	420	1
	200L Wave	100	462	1
	200L SUB	200	4200	1
	500L SUB	500	5460	1
	1000L SUB	1000	8260	1
	2000L SUB	2000	9800	1

Table A2.4. Raw material costs

Buffer Name	Cost (USD per litre)
Fermentation Media	3.133
Fermentation Feed	13.070
Fermentation Flush Buffer	0.044
Chromatography Packing Buffer	0.376
Protein A - Equilibrium Buffer	0.842
Protein A - Wash Buffer	0.067
Protein A - Elution Buffer	0.067
Protein A - Regeneration Buffer	0.257
Protein A - Storage Buffer	2.699
Protein A - Cleaning Buffer	0.064
2.0M Acetic Acid	0.440
2.0M Tris Base	6.763
CEX - Cleaning Buffer	0.615
CEX - Equilibrium Buffer	0.072
CEX - Wash Buffer	0.032
CEX - Elution Buffer	0.104
CEX - Regeneration Buffer	0.626
CEX - Storage Buffer	0.630
AEX - Cleaning Buffer	0.672
AEX - Equilibrium Buffer	0.265
AEX - Wash Buffer	0.044
AEX - Regeneration Buffer	0.625
AEX - Storage	0.620
Nano Virus Flush Buffer	0.065
Nano Virus CIP Flush Buffer	0.064
Diafiltration Buffer	0.044
Final Diafiltration Buffer	0.122
Caustic Rinse	0.192
Acid Rinse - 3% w/v Phosphoric acid	0.120
WFI	0.020

Table A2.5. Consumable unit masses

Consumable	Mass per Unit (kg)	Unit
Chromatography Resin	1.5	litre of resin
Depth Filter	2	m ² of filter
Viral Retention Filter	4	m ² of filter
UFDF Filter	2	m ² of filter
50L Wave	2	bioreactor bag
100L Wave	2	bioreactor bag
200L Wave	2	bioreactor bag
200L SUB	2.8	bioreactor bag
500L SUB	3.2	bioreactor bag
1000L SUB	7	bioreactor bag
2000L SUB	7	bioreactor bag
500L Disposable Bag	3.4	bag
200L Disposable Bag	2.6	bag
100L Disposable Bag	1.8	bag
50L Disposable Bag	1.7	bag

9.1.2 Equations

9.1.2.1 Centrifugation

$$M_{pOut} = M_{pIn} * Yield \quad (A2.1)$$

$$Vol_{Out} = \frac{M_{pOut}}{\left(\frac{M_{pIn}}{Vol_{In}}\right)} \quad (A2.2)$$

$$Vol_{Waste} = Vol_{In} - Vol_{Out} \quad (A2.3)$$

$$Conc_{Out} = \frac{M_{pOut}}{Vol_{Out}} \quad (A2.4)$$

9.1.2.2 Depth Filtration

$$Vol_{Out} = Vol_{In} + (Area_{DF} * Flush_{DF}) \quad (A2.5)$$

$$t_{process} = \frac{Vol_{Out}}{(J_{DF} * Area_{DF})} \quad (A2.6)$$

$$Conc_{Out} = \frac{Conc_{In} * Vol_{In} * Yield}{Vol_{Out}} \quad (A2.7)$$

9.1.2.3 Viral Retention Filtration

$$Vol_{Out} = Vol_{In} + (Area_{VRF} * Flush_{VRF}) \quad (A2.8)$$

$$t_{Process} = \frac{Vol_{In}}{J_{VRF} * Area_{VRF}} \quad (A2.9)$$

$$Conc_{Out} = \frac{Conc_{In} * Vol_{In} * Yield}{Vol_{Out}} \quad (A2.10)$$

9.1.2.4 Concentration and Diafiltration

$$t_{Process} = t_{concentration} + t_{DF} + t_{Final} \quad (A2.11)$$

$$Vol_{Out} = Vol_{Retentate} * Yield \quad (A2.12)$$

$$Conc_{Out} = Conc_{Final} \quad (A2.13)$$

9.1.2.5 Chromatography

$$Col_{Area} = \pi * \left(\frac{Col_{Dia}^2}{2} \right) \quad (A2.14)$$

$$Col_{Volume} = Col_{Area} * Col_{Height} \quad (A2.15)$$

$$Q_{In} = v * Col_{Area} \quad (A2.16)$$

$$t_{Process} = \frac{Vol_{Buffer}}{Q_{In}} \quad (A2.17)$$

$$M_{Cycle} = \frac{M_{In} * Yield}{N_{Cycles}} \quad (A2.18)$$

$$Conc_{Out} = \frac{N_{Cycles} * M_{Cycle}}{Vol_{Out}} \quad (A2.19)$$

9.1.2.6 Viral Inactivation

$$Vol_{Out} = Vol_{Acid} + Vol_{Base} + Vol_{In} \quad (A2.20)$$

$$Conc_{Out} = \frac{Conc_{In} * Vol_{In} * Yield}{Vol_{Out}} \quad (A2.21)$$

9.2 Chapter 3 Appendix

9.2.1 Tables

Table A3.1. Uncompleted qualitative factor questionnaire

Qualitative factors	Rank of factor (1 – 5, 1 = most important & 5 = least important)	Rating (1 = Low, 2 = Medium, 3 = High)		
		FB	SPIN	ATF
<i>Example Factor</i>		2	3	3
Ease of control / operation				
Ease of validation (time / effort)				
Ease of development (time / effort)				
Operational flexibility				
Batch-to-batch variability				

1. Please rank the qualitative factors in order of importance, where 1 = the most important factor and 5 = the least important factor.
2. Then rate the impact of each factor, where 1 = low impact, 2 = medium impact and 3 = high impact, for each cell culture option (*see example factor*).

Table A3.2. Completed qualitative factor questionnaire – Respondent #1

Qualitative factors	Rank of factor (1 – 5, 1 = most important & 5 = least important)	Rating (1 = Low, 2 = Medium, 3 = High)		
		FB	SPIN	ATF
<i>Example Factor</i>		2	3	3
Ease of control / operation	1	1	3	3
Ease of validation (time / effort)	3	1	3	3
Ease of development (time / effort)	2	1	3	3
Operational flexibility	5	1	3	3
Batch-to-batch variability	4	1	3	3

Table A3.3. Completed qualitative factor questionnaire – Respondent #2

Qualitative factors	Rank of factor (1 – 5, 1 = most important & 5 = least important)	Rating (1 = Low, 2 = Medium, 3 = High)		
		FB	SPIN	ATF
<i>Example Factor</i>		2	3	3
Ease of control / operation	3	3	1	3
Ease of validation (time / effort)	4	3	1	2
Ease of development (time / effort)	5	3	1	2
Operational flexibility	2	3	1	2
Batch-to-batch variability	1	2	1	3

Table A3.4. Completed qualitative factor questionnaire – Respondent #3

Qualitative factors	Rank of factor (1 – 5, 1 = most important & 5 = least important)	Rating (1 = Low, 2 = Medium, 3 = High)		
		FB	SPIN	ATF
<i>Example Factor</i>		2	3	3
Ease of control / operation	3	1	3	1
Ease of validation (time / effort)	4	1	3	2
Ease of development (time / effort)	5	1	3	2
Operational flexibility	2	1	3	2
Batch-to-batch variability	1	2	3	1

Table A3.5. A comparison of the key economic metrics

Titre (g/L)	Demand (kg/year)	Number and size of fermenters (L)			Capital investment (million RMU)			COG/g (RMU/g)		
		FB	SPIN	ATF	FB	SPIN*	ATF*	FB	SPIN*	ATF*
2	100	1 x 2800	1 x 1440	1 x 430 ⁺	63	-25%	-40%	127	0 %	-22%
	500	2 x 6720	4 x 1800	2 x 1080 ⁺	102	-6%	-45%	51	+43%	-21%
	1000	2 x 13430	8 x 1800	3 x 1440 ⁺	119	+39%	-42%	34	+97%	-11%
5	100	1 x 1150 ⁺	1 x 580	1 x 180 ⁺	48	-7%	-25%	100	+12%	-12%
	500	1 x 5620	2 x 1440	1 x 860 ⁺	88	-23%	-46%	39	+17%	-20%
	1000	2 x 5380	3 x 1920	2 x 860 ⁺	104	-14%	-41%	29	+20%	-19%
10	100	1 x 570 ⁺	1 x 290	1 x 90 ⁺	43	+2%	-19%	92	+16%	-9%
	500	1 x 2810	1 x 1440	1 x 430 ⁺	79	-30%	-42%	35	-2%	-19%
	1000	1 x 5620	2 x 1440	1 x 860 ⁺	102	-27%	-46%	25	+7%	-22%

* Percentage change relative to the fed-batch process

+ Disposable bioreactor (maximum volume 2000 Litres)

9.2.2 Figures

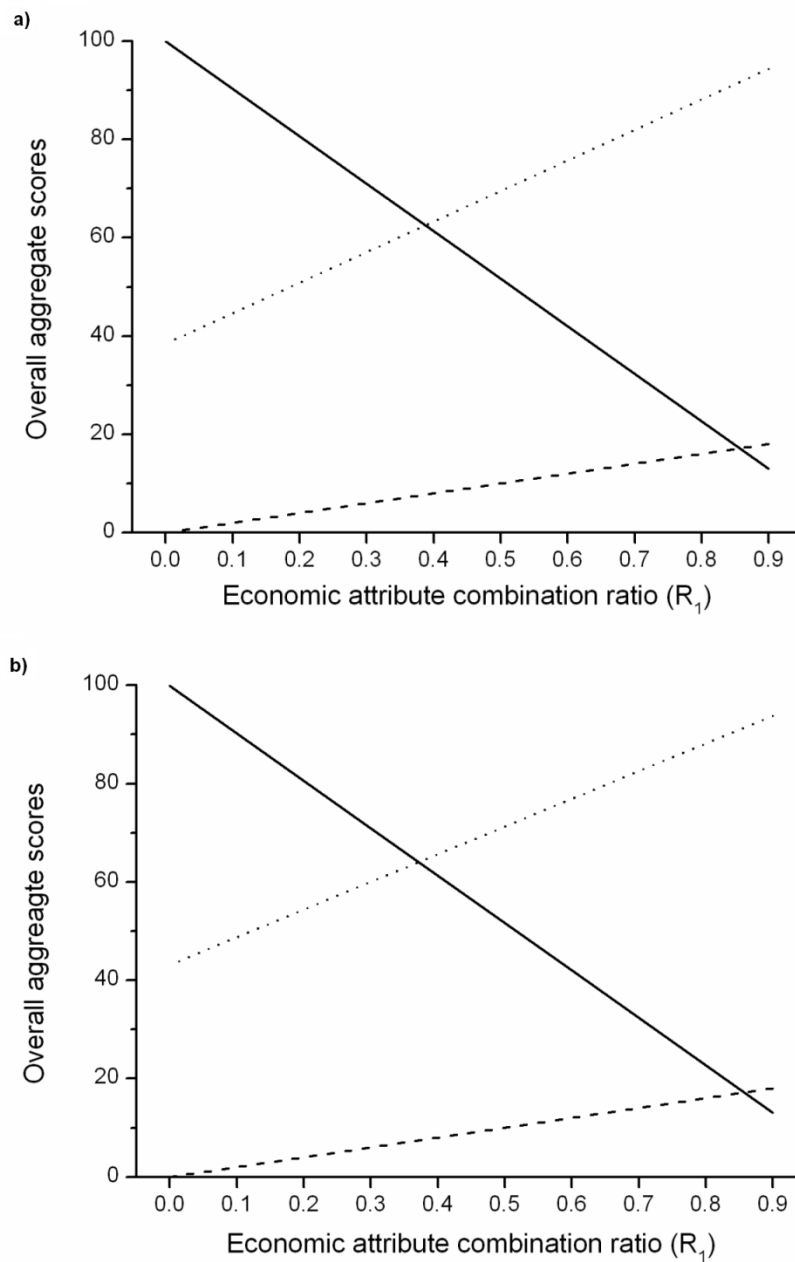


Figure A3.1. Sensitivity plots showing the effect of the economic attribute combination ratio (R_1) on the overall aggregate scores when (a) the operational attribute combination ratio is constant and (b) the environmental attribute combination ratio is constant. For the fed-batch (solid line), spin-filter (dashed line), and ATF (dotted line) processes, for 100 kg/year scale of production and equivalent titre of 5 g/L.

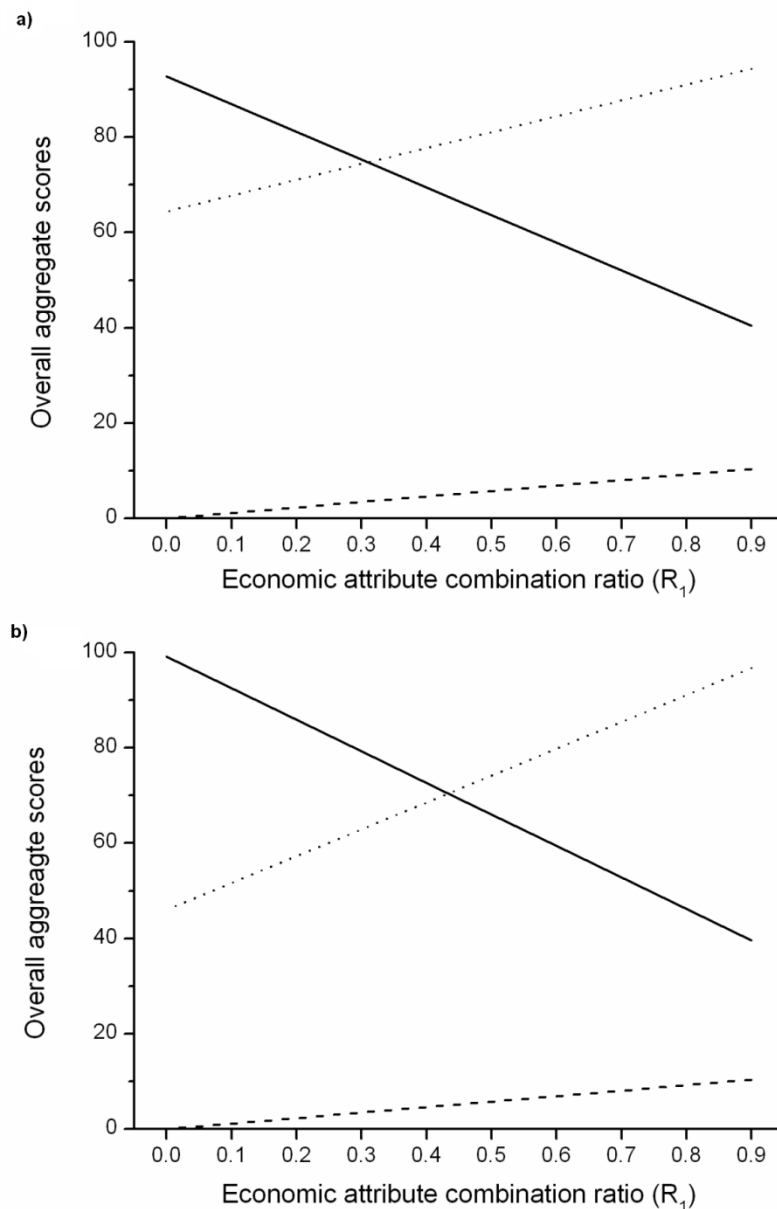


Figure A3.2. Sensitivity plots showing the effect of the economic attribute combination ratio (R_1) on the overall aggregate scores when (a) the operational attribute combination ratio is constant and (b) the environmental attribute combination ratio is constant. For the fed-batch (solid line), spin-filter (dashed line), and ATF (dotted line) processes, for 1000 kg/year scale of production and equivalent titre of 5 g/L.

9.3 Chapter 4 Appendix

9.3.1 Tables

Table A4.1. Scenario Equipment Scales

Mode	Clinical scale	Number of Batches	Batch size (kg)	Number of fermenter	Fermenter scale (L)	Protein A Scale (L)	Number of Cycles	TMAE Scale (L)	Number of Cycles	VRF Scale (m ²)	UFDF Scale (m ²)
STD	PoC	1	4	1	1820	31.4	5	10.6	3	2.8	2.8
STD	PhaseIII	4	10	1	2280	49.1	7	29.5	3	6.2	6.2
STD	Corn	20	10	1	2280	49.1	7	29.5	3	6.2	6.2
3C-PCC	PoC	1	4	1	1820	4.9	17	10.6	3	1.8	2.2
3C-PCC	PhaseIII	4	10	1	2280	12.6	16	23.9	3	4	5.2
3C-PCC	Corn	20	10	1	2280	12.6	16	23.9	3	4	5.2
4C-PCC	PoC	1	4	1	1820	3.1	26	10.6	3	1.8	2.2
4C-PCC	PhaseIII	4	10	1	2280	7.1	29	23.9	3	4	5.2
4C-PCC	Corn	20	10	1	2280	7.1	29	23.9	3	4	5.2

Table A4.2. Batch Uptake Experimental Data for the New Resin Sample

NEW	Eppendorf #1				Eppendorf #2				Eppendorf #3			
	Time (Seconds)	Mobile Phase (mg)	Stationary Phase (mg)	Binding Capacity (mg/mL)	C/Co	Mobile Phase (mg)	Stationary Phase (mg)	Binding Capacity (mg/mL)	C/Co	Mobile Phase (mg)	Stationary Phase (mg)	Binding Capacity (mg/mL)
0	0	4.67	0	1	0	4.67	0	1	0	4.67	0	1
120	0.49	4.19	12.15	0.9	0.49	4.19	12.21	0.9	0.4	4.28	9.9	0.92
240	0.68	3.99	17	0.86	0.8	3.88	19.77	0.84	0.66	4.02	16.39	0.87
360	0.89	3.79	22.04	0.82	1.1	3.58	27.42	0.77	0.91	3.77	22.51	0.81
480	1.08	3.6	26.97	0.77	1.15	3.53	28.62	0.76	0.98	3.7	24.46	0.8
600	1.17	3.51	29.23	0.75	1.33	3.35	33.16	0.72	1.17	3.51	29.09	0.76
720	1.26	3.41	31.49	0.74	1.41	3.27	35.17	0.7	1.24	3.44	30.91	0.74
840	1.46	3.22	36.26	0.69	1.5	3.18	37.37	0.68	1.43	3.25	35.55	0.7
960	1.57	3.11	39.16	0.67	1.59	3.09	39.63	0.67	1.53	3.15	38.12	0.68
1080	1.69	2.99	42.22	0.64	1.69	2.99	42.1	0.64	1.59	3.09	39.73	0.67
1200	1.62	3.06	40.47	0.66	1.72	2.96	42.9	0.64	1.69	2.98	42.24	0.64
2400	n/a	n/a	n/a	n/a	2.18	2.5	54.47	0.54	2.18	2.5	54.45	0.54
3600	n/a	n/a	n/a	n/a	2.44	2.24	60.76	0.48	2.44	2.24	60.88	0.48
5400	2.36	2.32	58.82	0.5	2.54	2.14	63.33	0.46	2.61	2.07	65.12	0.45
7200	2.51	2.17	62.64	0.47	2.7	1.98	67.44	0.43	2.69	1.99	67.18	0.43
9000	2.56	2.11	64	0.46	2.78	1.9	69.46	0.41	2.76	1.92	68.86	0.42
10800	2.6	2.08	64.91	0.45	2.77	1.9	69.24	0.41	2.76	1.92	68.88	0.42

Table A4.3. Batch Uptake Experimental Data for the Cycled Resin Sample

Cycled	Eppendorf #1				Eppendorf #2				Eppendorf #3			
	Time (Seconds)	Mobile Phase (mg)	Stationary Phase (mg)	Binding Capacity (mg/mL)	C/Co	Mobile Phase (mg)	Stationary Phase (mg)	Binding Capacity (mg/mL)	C/Co	Mobile Phase (mg)	Stationary Phase (mg)	Binding Capacity (mg/mL)
0	0	4.62	1.44	1	0	4.62	0	1	0	4.62	0	1
120	0.64	3.98	17.3	0.87	0.49	4.13	13.6	0.9	-0.3	4.92	-6.09	1.07
240	0.67	3.95	18.09	0.86	0.4	4.22	11.36	0.92	0.11	4.51	4.03	0.98
360	0.64	3.98	17.41	0.87	0.37	4.25	10.62	0.93	0.27	4.36	7.97	0.95
480	0.91	3.71	24.05	0.81	0.75	3.87	20.02	0.84	0.47	4.15	13.15	0.9
600	0.91	3.71	24.1	0.81	0.66	3.97	17.73	0.86	0.55	4.07	15.17	0.89
720	1.05	3.57	27.53	0.78	0.85	3.77	22.57	0.82	0.66	3.96	17.9	0.86
840	1.1	3.53	28.73	0.77	0.83	3.8	21.98	0.83	0.75	3.88	19.97	0.84
960	1.15	3.47	30.09	0.76	0.96	3.66	25.28	0.8	0.85	3.77	22.66	0.82
1080	1.2	3.42	31.28	0.75	0.95	3.67	25.19	0.8	0.88	3.74	23.4	0.81
1200	1.33	3.29	34.59	0.72	0.99	3.63	26	0.79	0.9	3.72	23.79	0.81
2400	1.5	3.12	38.83	0.68	1.3	3.32	33.94	0.72	1.22	3.4	31.79	0.74
3600	1.6	3.02	41.35	0.66	1.4	3.22	36.43	0.7	1.36	3.27	35.23	0.71
5400	1.69	2.93	43.61	0.64	1.52	3.1	39.39	0.68	1.49	3.14	38.48	0.68
7200	1.61	3.02	41.46	0.66	1.6	3.02	41.31	0.66	1.57	3.05	40.54	0.67
9000	1.69	2.93	43.61	0.64	1.58	3.04	40.85	0.66	1.64	2.98	42.39	0.65
10800	1.74	2.88	44.94	0.63	1.66	2.96	42.88	0.65	1.67	2.95	43.08	0.64

Table A4.4. Batch Uptake Experimental Data for the NaOH Cycled Resin Sample

NaOH	Eppendorf #1				Eppendorf #2				Eppendorf #3			
	Time (Seconds)	Mobile Phase (mg)	Stationary Phase (mg)	Binding Capacity (mg/mL)	C/Co	Mobile Phase (mg)	Stationary Phase (mg)	Binding Capacity (mg/mL)	C/Co	Mobile Phase (mg)	Stationary Phase (mg)	Binding Capacity (mg/mL)
0	0	4.73	0	1	0	4.73	0	1	0	4.73	0	1
120	0.46	4.28	9.92	0.91	0.4	4.34	8.43	0.92	0.08	4.65	0.64	0.99
240	0.72	4.01	16.5	0.85	0.53	4.2	11.76	0.89	0.12	4.61	1.51	0.98
360	1.01	3.73	23.73	0.79	0.65	4.08	14.85	0.87	0.54	4.2	11.92	0.89
480	1.21	3.52	28.89	0.75	0.9	3.83	21.07	0.82	0.79	3.95	18.23	0.84
600	1.19	3.54	28.4	0.75	1.01	3.72	23.8	0.79	0.82	3.91	19.11	0.83
720	1.33	3.41	31.71	0.73	1.17	3.57	27.71	0.76	0.99	3.74	23.34	0.8
840	1.38	3.35	33.07	0.71	1.23	3.5	29.28	0.75	0.99	3.74	23.31	0.8
960	1.53	3.2	36.79	0.68	1.36	3.38	32.46	0.72	1.23	3.5	29.4	0.74
1080	1.57	3.17	37.66	0.67	1.4	3.34	33.46	0.71	1.25	3.48	29.89	0.74
1200	1.64	3.1	39.46	0.66	1.48	3.25	35.63	0.69	1.34	3.39	32.07	0.72
2400	2.05	2.69	49.67	0.57	1.95	2.78	47.34	0.59	1.82	2.91	44.08	0.62
3600	2.27	2.46	55.31	0.53	2.16	2.58	52.43	0.55	2.07	2.67	50.21	0.57
5400	2.35	2.38	57.31	0.51	2.32	2.41	56.59	0.51	2.28	2.45	55.55	0.52
7200	2.45	2.29	59.67	0.49	2.3	2.43	56.11	0.52	2.39	2.34	58.25	0.5
9000	2.53	2.2	61.76	0.47	2.38	2.35	58.08	0.5	2.42	2.31	59.02	0.49
10800	2.48	2.25	60.5	0.48	2.41	2.32	58.87	0.5	2.44	2.29	59.53	0.49

Table A4.5. Isotherm Experimental Data for the New Resin Sample

NEW	Experiment #1			Experiment #2			Experiment #3		
	Challenge Load (mg)	Mobile Phase (mg)	Stationary Phase (mg)	Binding Capacity (mg/mL)	Mobile Phase (mg)	Stationary Phase (mg)	Binding Capacity (mg/mL)	Mobile Phase (mg)	Stationary Phase (mg)
0.23	0	0.23	9.03	0.01	0.23	8.81	0	0.23	9.2
0.44	0	0.45	17.94	0	0.44	17.41	0	0.43	17.12
0.66	0	0.7	27.88	0.01	0.71	28.31	0	0.65	25.67
0.88	0.01	0.9	35.69	0.01	0.93	37.1	0.01	0.83	33.02
1.09	0.01	1.14	45.27	0.01	1.16	46.29	0.01	1.14	45.39
1.28	0.04	1.32	52.66	0.02	1.37	54.72	0.01	1.25	49.88
1.47	0.09	1.48	58.92	0.07	1.56	62.18	0.08	1.53	60.87
1.76	0.22	1.53	60.82	0.18	1.65	65.65	0.22	1.65	65.61
1.96	0.37	1.63	65.12	0.32	1.69	67.4	0.39	1.65	65.87
2.2	0.55	1.66	66.33	0.51	1.69	67.52	0.57	1.76	70.06
2.42	0.85	1.57	62.51	0.72	1.74	69.32	0.76	1.72	68.59
2.65	0.99	1.64	65.58	0.95	1.7	67.97	1.04	1.73	68.98

Table A4.6. Isotherm Experimental Data for the Cycled Resin Sample

Cycled	Experiment #1			Experiment #2			Experiment #3		
Challenge Load (mg)	Mobile Phase (mg)	Stationary Phase (mg)	Binding Capacity (mg/mL)	Mobile Phase (mg)	Stationary Phase (mg)	Binding Capacity (mg/mL)	Mobile Phase (mg)	Stationary Phase (mg)	Binding Capacity (mg/mL)
0.24	0	0.22	10.1	0	0.23	10.52	0	0.21	9.49
0.49	0	0.46	20.91	0	0.48	21.67	0	0.4	18.2
0.66	0.02	0.61	28.03	0.02	0.57	26.14	0.01	0.63	28.66
0.87	0.03	0.79	36.03	0.04	0.77	35.42	0.04	0.8	36.52
1.09	0.19	0.9	41.11	0.15	0.89	40.62	0.19	0.88	40.03
1.29	0.36	0.92	42.32	0.35	0.88	40.22	0.36	0.91	41.61
1.47	0.57	0.92	42.18	0.56	0.91	41.42	0.57	0.92	42.03
1.74	0.77	0.96	43.81	0.76	0.93	42.34	0.8	0.94	43.2
1.97	1	0.92	41.93	1	0.9	41.35	0.95	0.94	42.84
2.17	1.12	0.99	45.5	1.1	0.99	45.3	1.05	0.99	45.19
2.41	1.27	0.98	44.92	1.3	0.98	44.88	1.33	0.98	44.89
2.65	1.47	0.98	44.74	1.46	0.99	45.35	1.18	0.96	43.71

Table A4.7. Isotherm Experimental Data for the NaOH Cycled Resin Sample

NaOH	Experiment #1			Experiment #2			Experiment #3		
Challenge Load (mg)	Mobile Phase (mg)	Stationary Phase (mg)	Binding Capacity (mg/mL)	Mobile Phase (mg)	Stationary Phase (mg)	Binding Capacity (mg/mL)	Mobile Phase (mg)	Stationary Phase (mg)	Binding Capacity (mg/mL)
0.23	0	0.21	9.66	0	0.21	9.65	0	0.2	8.78
0.49	0	0.42	19.29	0	0.46	20.87	0	0.45	20.46
0.67	0.02	0.61	27.84	0.01	0.63	28.7	0.01	0.61	27.95
0.89	0.03	0.81	36.86	0.02	0.85	38.94	0.01	0.83	38.03
1.1	0.06	0.98	45.06	0.04	1.19	54.54	0.01	1.05	48.05
1.29	0.09	1.16	53.18	0.07	1.23	56.22	0.04	1.28	58.71
1.47	0.21	1.26	57.86	0.24	1.28	58.86	0.11	1.36	62.32
1.63	0.4	1.27	58.41	0.47	1.28	58.5	0.15	1.15	52.85
1.97	0.6	1.31	60.15	0.66	1.28	58.76	0.62	1.27	58.19
2.17	0.73	1.37	62.89	0.88	1.28	58.83	0.71	1.32	60.3
2.4	0.98	1.36	62.15	1.1	1.3	59.53	0.86	1.25	57.2
2.64	1.23	1.35	62.02	1.27	1.33	61	1.14	1.16	53.13

9.3.2 Figures

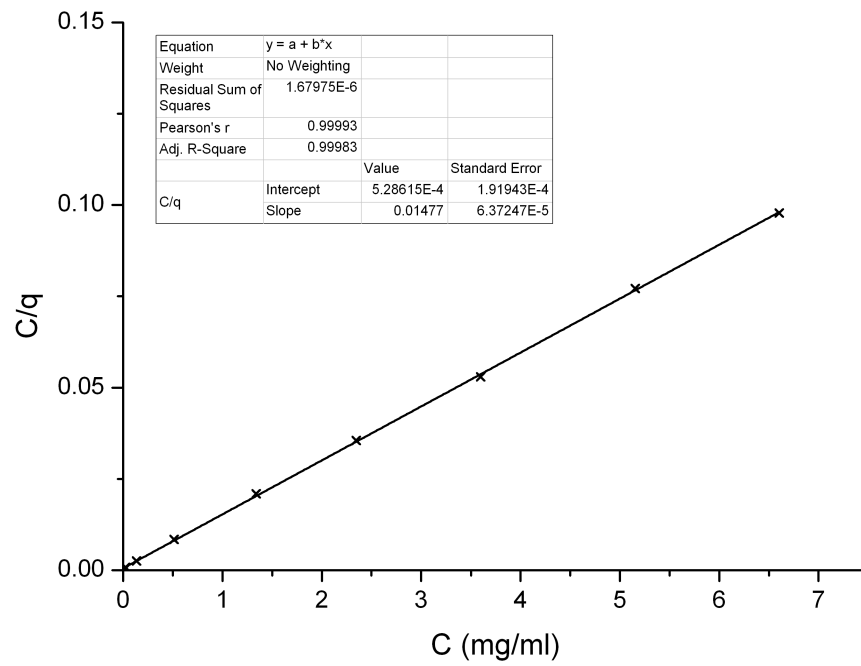


Figure A4.1. Langmuir regression plots for the new resin sample.

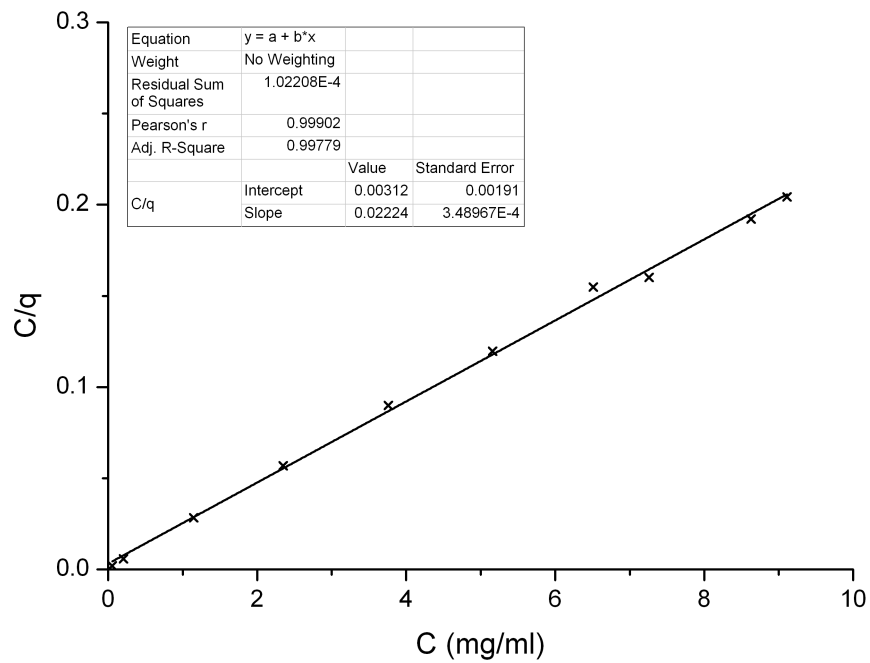


Figure A4.2. Langmuir regression plots for the cycled resin sample

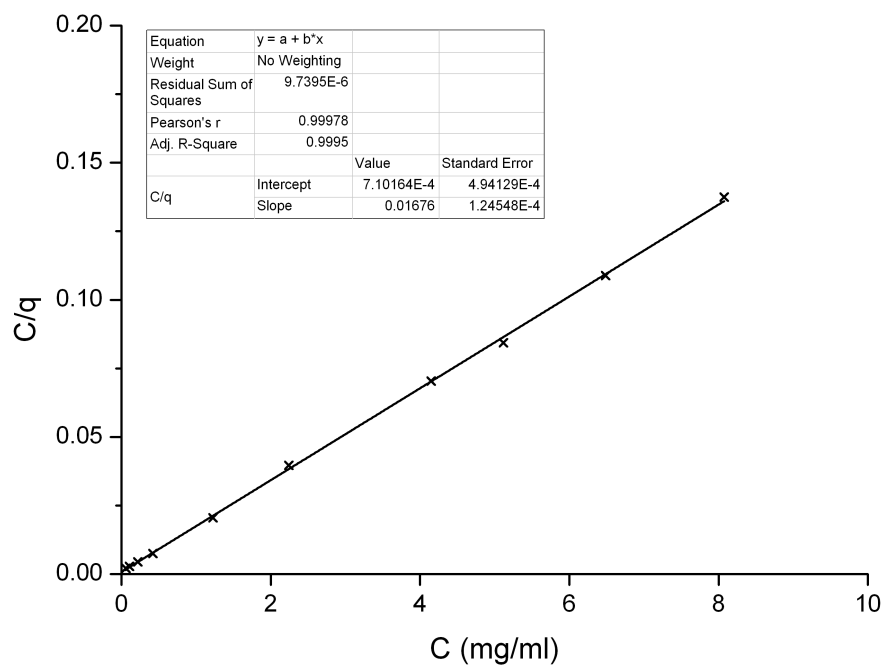


Figure A4.3. Langmuir regression plots for the NaOH cycled resin sample

9.4 Chapter 5 Appendix

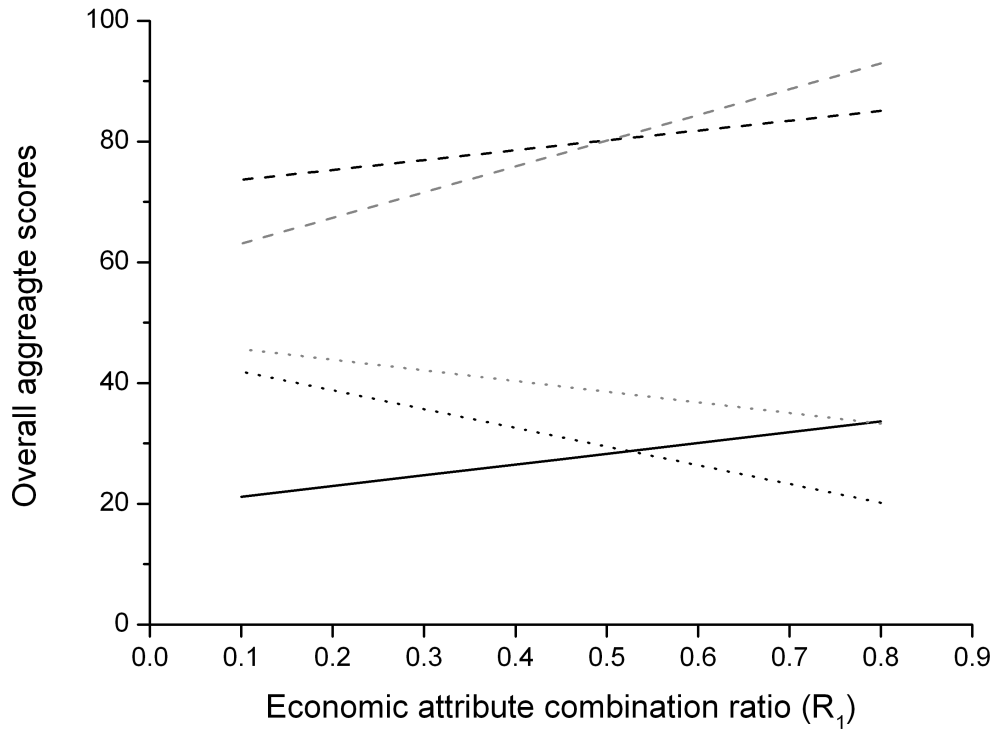
9.4.1 Tables

Table A5.1. Scenario Equipment Scales

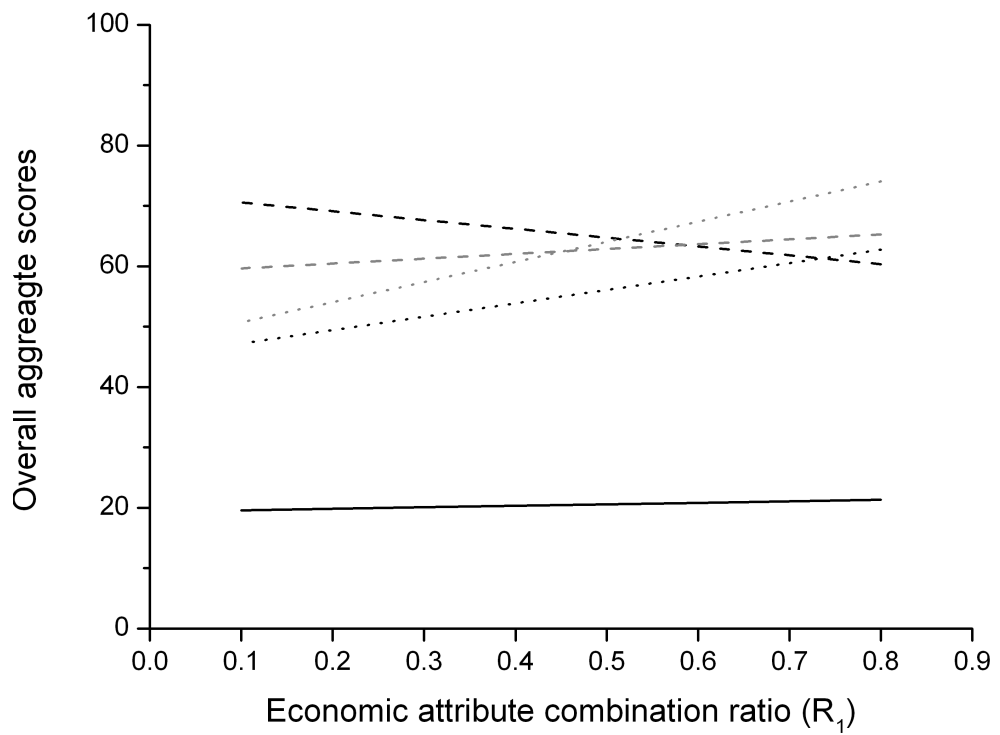
Mode	Clinical scale	Batch size (kg)	Fermenter scale (L)	Number of Columns	Protein A Scale (L)	Number of Cycles	TMAE Scale (L)	Number of Cycles	VRF Scale (m ²)	UFDF Scale (m ²)
STD	Pre-clinical	0.5	230	1	3.85	5	1.18	3	0.4	0.4
STD	PoC	4	1820	1	31.42	5	10.60	3	2.8	2.6
STD	PhaseIII	10	2280	1	49.09	7	23.86	3	6	6
STD	Commercial	10	2280	1	49.09	7	23.86	3	6	6
FB-CB	Pre-clinical	0.5	230	3	0.79	13	1.18	3	0.4	0.4
FB-CB	PoC	4	1820	3	4.91	17	10.60	3	1.8	2.2
FB-CB	PhaseIII	10	2280	3	9.62	21	23.86	3	4	5.2
FB-CB	Commercial	10	2280	3	9.62	21	23.86	3	4	5.2
ATF-CB	Pre-clinical	0.5	25	3	0.20	66	1.18	2	0.2	0.4
ATF-CB	PoC	4	170	3	1.54	57	2.31	3	0.6	2.4
ATF-CB	PhaseIII	10	215	3	1.54	145	4.71	2	0.6	5.6
ATF-CB	Commercial	10	215	3	1.54	145	4.71	2	0.6	5.6
FB-CC	Pre-clinical	0.5	230	3	0.79	13	1.18	1	0.2	0.4
FB-CC	PoC	4	1820	3	4.91	17	4.71	1	1.4	2.2
FB-CC	PhaseIII	10	2280	3	9.62	21	10.60	1	3.4	5.6
FB-CC	Commercial	10	2280	3	9.62	21	10.60	1	3.4	5.6
ATF-CC	Pre-clinical	0.5	25	3	0.20	66	1.18	1	0.2	0.4
ATF-CC	PoC	4	170	3	1.54	57	2.31	1	0.6	2.4
ATF-CC	PhaseIII	10	215	3	1.54	145	2.31	1	0.6	5.8
ATF-CC	Commercial	10	215	3	1.54	145	2.31	1	0.6	5.8

6.1.1. Figures

a)



b)



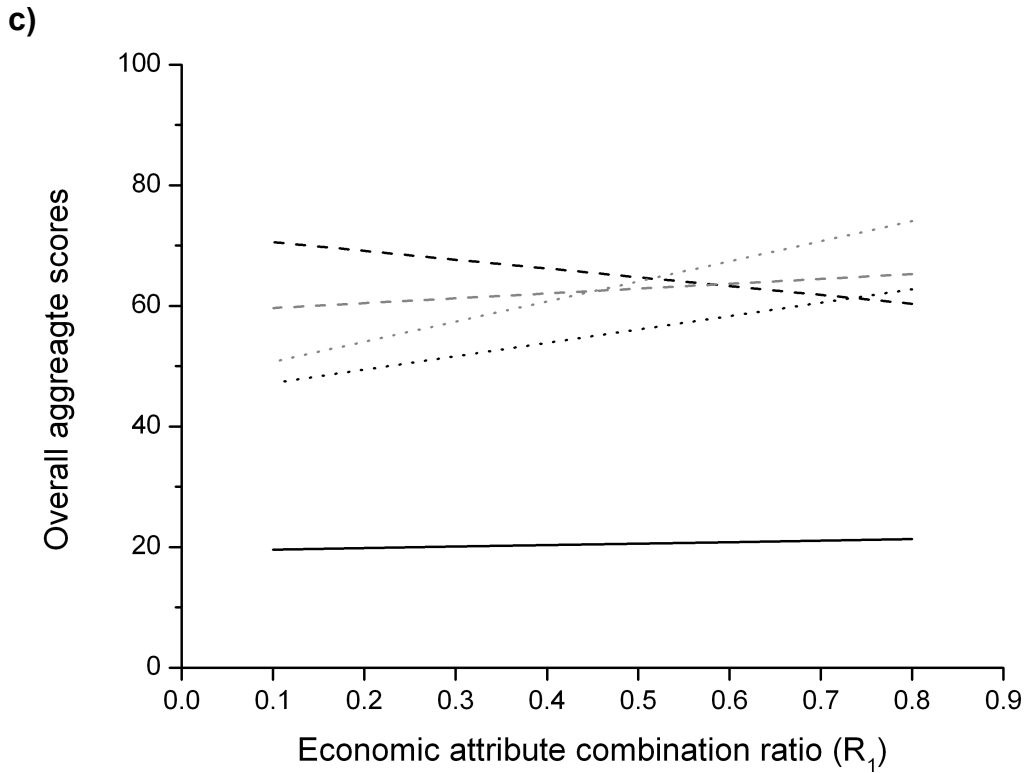


Figure A5.1. Sensitivity plots portraying the effect of the economic attribute combination ratio (R_1) in the overall aggregate scores when the environmental combination rate is constant, for a) the large-sized company, b) medium-sized company and c) small-sized company, for the base case (solid black line), FB-CB (grey dashed line), ATF-CB (grey dotted line), FB-CC (black dashed line) and ATF-CC (black dotted line).

9.5 Papers by the Author

The following papers are included in this appendix are listed below.

Pollock J, Ho SV, Farid SS (2012) Computer-Aided Design and Evaluation of Batch and Continuous Multi-Mode Biopharmaceutical Manufacturing Processes 22 EUROPEAN SYMPOSIUM ON COMPUTER AIDED PROCESS ENGINEERING, 30, 487 - 491.

Pollock J, Ho SV, Farid SS (2013) Fed-batch and perfusion culture processes: economic, environmental, and operational feasibility under uncertainty. *Biotechnol Bioeng*, 110(1), 206 - 219. [10.1002/bit.24608](https://doi.org/10.1002/bit.24608).

Pollock J, Bolton G, Coffman J, Ho SV, Bracewell DG, Farid SS (2013) Optimising the design and operation of semi-continuous affinity chromatography for clinical and commercial manufacture. *J Chromatogr A*, 1284, 17 - 27. [10.1016/j.chroma.2013.01.082](https://doi.org/10.1016/j.chroma.2013.01.082).